

AD-A019 044

THE DEVELOPMENT OF AN ADVANCED ANTI-ICING/DEICING  
CAPABILITY FOR U. S. ARMY HELICOPTERS. VOLUME 1,  
DESIGN CRITERIA AND TECHNOLOGY CONSIDERATIONS

J. B. Werner

Lockheed-California Company

Prepared for:

Army Air Mobility Research and Development Laboratory

November 1975

DISTRIBUTED BY:

**NTIS**

National Technical Information Service  
U. S. DEPARTMENT OF COMMERCE

## KEEP UP TO DATE

Between the time you ordered this report—which is only one of the hundreds of thousands in the NTIS information collection available to you—and the time you are reading this message, several *new* reports relevant to your interests probably have entered the collection.

Subscribe to the **Weekly Government Abstracts** series that will bring you summaries of new reports as soon as they are received by NTIS from the originators of the research. The WGA's are an NTIS weekly newsletter service covering the most recent research findings in 25 areas of industrial, technological, and sociological interest—invaluable information for executives and professionals who must keep up to date.

The executive and professional information service provided by NTIS in the **Weekly Government Abstracts** newsletters will give you thorough and comprehensive coverage of government-conducted or sponsored re-

search activities. And you'll get this important information within two weeks of the time it's released by originating agencies.

WGA newsletters are computer produced and electronically photocomposed to slash the time gap between the release of a report and its availability. You can learn about technical innovations immediately—and use them in the most meaningful and productive ways possible for your organization. Please request NTIS-PR-205/PCW for more information.

The weekly newsletter series will keep you current. But *learn what you have missed in the past* by ordering a computer **NTISearch** of all the research reports in your area of interest, dating as far back as 1964, if you wish. Please request NTIS-PR-186/PCN for more information.

WRITE: Managing Editor  
5285 Port Royal Road  
Springfield, VA 22161

## Keep Up To Date With SRIM

SRIM (Selected Research in Microfiche) provides you with regular, automatic distribution of the complete texts of NTIS research reports *only* in the subject areas you select. SRIM covers almost all Government research reports by subject area and/or the originating Federal or local government agency. You may subscribe by any category or subcategory of our WGA (**Weekly Government Abstracts**) or **Government Reports Announcements and Index** categories, or to the reports issued by a particular agency such as the Department of Defense, Federal Energy Administration, or Environmental Protection Agency. Other options that will give you greater selectivity are available on request.

The cost of SRIM service is only 45¢ domestic (60¢ foreign) for each complete

microfiche report. Your SRIM service begins as soon as your order is received and processed and you will receive biweekly shipments thereafter. If you wish, your service will be backdated to furnish you microfiche of reports issued earlier.

Because of contractual arrangements with several Special Technology Groups, not all NTIS reports are distributed in the SRIM program. You will receive a notice in your microfiche shipments identifying the exceptionally priced reports not available through SRIM.

A deposit account with NTIS is required before this service can be initiated. If you have specific questions concerning this service, please call (703) 451-1558, or write NTIS, attention SRIM Product Manager.

This information product distributed by

**NTIS**

U.S. DEPARTMENT OF COMMERCE  
National Technical Information Service  
5285 Port Royal Road  
Springfield, Virginia 22161

013077  
USAAMRDL-TR-75-34A



**THE DEVELOPMENT OF AN ADVANCED ANTI-ICING/DEICING  
CAPABILITY FOR U. S. ARMY HELICOPTERS**  
**Volume 1 - Design Criteria and Technology Considerations**

Lockheed-California Company  
Box 511  
Burbank, Calif. 91520

November 1975

Final Report for Period 30 June 1973 - 30 June 1975

Approved for public release:  
distribution unlimited.

Prepared for

**EUSTIS DIRECTORATE  
U. S. ARMY AIR MOBILITY RESEARCH AND DEVELOPMENT LABORATORY  
Fort Eustis, Va. 23604**

Reproduced by  
**NATIONAL TECHNICAL  
INFORMATION SERVICE**  
U.S. Department of Commerce  
Springfield, VA. 22151

ADAO19044

### EUSTIS DIRECTORATE POSITION STATEMENT

This Directorate concurs in the findings presented in this report and recommends use of the information contained herein to enhance the design and development of ice protection systems for rotary-wing aircraft.

The main thrust of this effort was to accurately quantify design criteria for helicopter ice protection systems and to identify and evaluate the most promising rotor blade ice protection concept. Various concepts were analyzed, and the cyclic-electrothermal concept was identified as the most promising for application to future and existing Army helicopters.

Although the cyclic-electrothermal blade deicing concept appears to be the most feasible for application to helicopter rotor blades in the near future, the penalties for ice protection are significant. Additionally, this deicing concept has been subjected only to limited simulated icing tests. Although this flight testing was adequate to demonstrate concept feasibility, additional simulated and natural ice testing is mandatory to finalize system control parameters and to resolve problem areas identified to date.

This directorate will continue investigations of ice protection concepts that show promise of minimizing system penalties.

The Project Engineer for this effort was Richard I. Adams of the Military Operations Technology Division.

#### DISCLAIMERS

The findings in this report are not to be construed as an official Department of the Army position unless so designated by other authorized documents.

When Government drawings, specifications, or other data are used for any purpose other than in connection with a definitely related Government procurement operation, the United States Government thereby incurs no responsibility nor any obligation whatsoever; and the fact that the Government may have formulated, furnished, or in any way supplied the said drawings, specifications, or other data is not to be regarded by implication or otherwise as in any manner licensing the holder or any other person or corporation, or conveying any rights or permission, to manufacture, use, or sell any patented invention that may in any way be related thereto.

Trade names cited in this report do not constitute an official endorsement or approval of the use of such commercial hardware or software.

#### DISPOSITION INSTRUCTIONS

Destroy this report when no longer needed. Do not return it to the originator.



Unclassified

SECURITY CLASSIFICATION OF THIS PAGE (When Data Entered)

REPORT DOCUMENTATION PAGE		READ INSTRUCTIONS BEFORE COMPLETING FORM
1. REPORT NUMBER USAAMRDL-TR-75-34A	2. GOVT ACCESSION NO.	3. RECIPIENT'S CATALOG NUMBER
4. TITLE (and Subtitle) THE DEVELOPMENT OF AN ADVANCED ANTI-ICING/ DEICING CAPABILITY FOR U. S. ARMY HELICOPTERS, Volume I - Design Criteria and Technology Considerations		5. TYPE OF REPORT & PERIOD COVERED Final Report for Period 30 June 1973 to 30 June 1975
7. AUTHOR(s) J. B. Werner		6. PERFORMING ORG. REPORT NUMBER LR 27180
9. PERFORMING ORGANIZATION NAME AND ADDRESS Lockheed-California Company Box 511 Burbank, Calif. 91520		8. CONTRACT OR GRANT NUMBER(s) DAAJ02-73-C-0107
11. CONTROLLING OFFICE NAME AND ADDRESS Eustis Directorate U. S. Army Air Mobility R&D Laboratory Fort Eustis, Va. 23604		10. PROGRAM ELEMENT, PROJECT, TASK AREA & WORK UNIT NUMBERS 62209A 1F262209AH76 00 002 EK
14. MONITORING AGENCY NAME & ADDRESS (if different from Controlling Office)		12. REPORT DATE November 1975
		13. NUMBER OF PAGES 253
		15. SECURITY CLASS. (of this report) Unclassified
16. DISTRIBUTION STATEMENT (of this Report) Approved for public release; distribution unlimited.		15a. DECLASSIFICATION/DOWNGRADING SCHEDULE
17. DISTRIBUTION STATEMENT (of the abstract entered in Block 20, if different from Report)  <b>PRICES SUBJECT TO CHANGE</b>		
18. SUPPLEMENTARY NOTES  Volume I of a 2-volume report.		
19. KEY WORDS (Continue on reverse side if necessary and identify by block number) Ice Electrothermal Deicing Snow Protection Deicing System Ice Prevention Advanced Rotary Wing Aircraft Freezing Point Depressant UH-1H		
20. ABSTRACT (Continue on reverse side if necessary and identify by block number) The work which has been accomplished under this program is reported in two volumes. Volume I discusses (1) icing severity level analysis and recommended design criteria, (2) adverse weather protection technology, (3) a trade-off comparison of different types of ice protection systems for various categories of helicopters, and (4) a technology development program for an advanced electrothermal deicing system. Volume II, Ice Protection System Application to the UH-1H Helicopter, describes the application of the recommended electrothermal deicing system to a UH-1H test aircraft. It provides a detailed description of the modifications to the basic aircraft		

Unclassified

SECURITY CLASSIFICATION OF THIS PAGE(When Data Entered)

Block 20. Abstract - continued.

(including the flight test instrumentation) and the results of the ground and flight test program for that aircraft conducted in the winter of 1974-75.

2a

Unclassified

SECURITY CLASSIFICATION OF THIS PAGE(When Data Entered)

## SUMMARY

The work which has been accomplished under this program is reported in two volumes. Volume I discusses (1) icing severity level analysis and recommended design criteria, (2) adverse weather protection technology, (3) a trade-off comparison of different types of ice protection systems for various categories of helicopters, and (4) a technology development program for an advanced electrothermal deicing system. Volume II, Ice Protection System Application to the UH-1H Helicopter, describes the application of the recommended electrothermal deicing system to a UH-1H test aircraft. It provides a detailed description of the modifications to the basic aircraft (including the flight test instrumentation) and the results of the ground and flight test program for that aircraft conducted in the winter of 1974-75.

Meteorological design criteria are provided for freezing rain and drizzle, snow, and supercooled droplets (icing). It is shown that the minimum (99th percentile criterion) temperature for freezing rain is  $14^{\circ}$  F, that the liquid water content does not exceed 0.32 gram per cubic meter, and that the droplet diameter ranges from 400 to 1200 microns. The 99th percentile snowfall criterion ranges from 1.6 grams per cubic meter at  $15^{\circ}$  F to 2.1 grams per cubic meter at  $35^{\circ}$  F. It is recommended that the existing FAA (and equivalent military specification) be used for the severity of supercooled droplets under continuous maximum icing conditions and that the 99th percentile severity be used for intermittent maximum conditions.

The technology review focuses upon protection against supercooled clouds, the normal icing problem. It is shown that protection against freezing rain is not justified and that snow can be accommodated by proper basic design with negligible penalty. The principal emphasis in technology is on main and tail rotor blade protection. It is concluded that electrothermal cyclic deicing offers the best solution for

existing and future helicopters and that the same basic design is suitable for both all-metal and composite blade construction. It is shown that the most critical problem with the electrothermal system is obtaining a reliable blade heater assembly, and this has been identified as the key development task. The timer/controller/power distribution subsystem recommended for use with the cyclic deicing system is a hybrid solid-state/electromechanical design incorporating extensive electrical fault sensing and protection.

Protection requirements for engine inlets, windshields, radomes, flight probes, and weapons and sensors are also discussed, and the state of the art of ice detectors and severity level instrumentation is defined. Engine inlet protection is highly dependent upon the inlet design, and it is shown that several existing designs apparently do not require a protection system. Windshield protection utilizing electrical anti-icing by a transparent conductive film is recommended. The need for radome ice protection depends upon the type of radar employed and its location on the aircraft, and often the radar performance penalties associated with an ice protection system exceed the penalties due to ice. Flight probe anti-icing designs are currently more than satisfactory. The need for weapon system ice protection needs to be experimentally evaluated as there is no available information. Sensor windows, e.g. those on cameras, IR sights, and weapon sights, need protection when they are subject to icing, but it is shown that the only feasible method of protection is a cover door or an engine bleed air heating system.

A trade-off has been performed for windshield ice protection, and the results show that the electrical system is superior.

The trade-off analysis compares five systems of rotor blade ice protection systems for seven helicopter types. The five systems are: the electrothermal cyclic deicing system, the chemical freezing point depressant (alcohol) system, and three variations of circulating liquid

loop anti-icing utilizing engine exhaust gas heat. Weight, performance penalties, reliability, and production, operating and maintenance costs have been developed. In addition, system weight and performance penalties have been evaluated for the systems for freezing rain requirements as well as supercooled droplets, and the electrothermal and chemical system requirements have also been evaluated as a function of icing severity. The results show that based upon year around penalties and an icing encounter duration of 1 hour, the chemical freezing point depressant system is the lightest and cheapest system for all but the two heaviest helicopter types (with electrothermal system second or first). If, however, maximum mission time is used as the basis for calculating year around system weight and penalties, the electrothermal deicing system is shown to have less penalty for helicopters with a TOGW in excess of 16,000 lb. Based upon performance and logistics considerations, however, the electrothermal system is recommended for all types of helicopters.

The materials, processes, quality controls and structural criteria and properties are described for main and tail rotor deicer heater blankets. Recommended materials are described, and it is shown that the resulting structural properties are satisfactory. Electroformed nickel is recommended for the erosion shield, and a stainless steel etched foil design is recommended for the heating element. The through-scan ultrasonic inspection technique is recommended for bonding verification on the rotor blade as the last production step.

The electrothermal deicing system which has been developed and demonstrated on the UH-1H helicopter (Volume II) requires 13.4 kilowatts for the main rotor blades (two) and 4 kilowatts for the tail rotor. The main rotor blade is divided into six spanwise sections for cyclic deicing, with the heating sequence from the tip to blade root. Power density varies from 12 watts/in<sup>2</sup> at the tip to 26 watts/in<sup>2</sup> at the root. The entire tail rotor is deiced at 20 watts/in<sup>2</sup>. The main rotor gyro stabilizer bar and tip weight is anti-iced (continuously heated

during icing conditions) at 5 watts/in<sup>2</sup> and requires 2 kw. The windshields are also anti-iced with electric heat (using a tin oxide coating) and require 5.4 kw. A new ac electrical system is installed using a 20/30 kva generator. This system also has the capability of providing a variable voltage in accordance with icing severity: 160 volts (line-to-line) for light icing, 200 volts (the nominal value) for moderate icing, and 230 volts for heavy icing.

The helicopter underwent 15 hours of airworthiness and electrical systems flight testing at Edwards Air Force Base, California, and 15 hours at Moses Lake, Washington, behind the CH-47 Helicopter Icing Spray System (HISS). A total of 35 flight hours and 19 ground operating hours were obtained on the aircraft. All structural loads measured were found to be within limits, and aircraft handling qualities were better than those for the basic aircraft (reduced main rotor boost-off control force requirements).

Icing tests behind the tanker were made at ambient temperatures as low as -4° F and at liquid water contents up to 0.75 gram per cubic meter (equivalent to over 1 g/m<sup>3</sup> of natural icing). Complete shedding of the ice from the main rotor blade was observed at temperatures down to +5° F, but shedding was reported to be incomplete inboard of station 83 (where the doublers start) at an ambient of -4° F. No tail rotor icing was observed. Windshield and stabilizer anti-icing power appeared to be adequate. It is recommended that further flight testing be conducted to achieve a greater variety of conditions: hover behind the Canadian National Research Council Spray Rig at Ottawa, Ontario, behind the HISS, and in natural icing.

## PREFACE

This program to determine adverse weather protection requirements was conducted by the Lockheed-California Company under Contract DAAJ02-73-C-0107 to the Eustis Directorate, US Army Air Mobility Research and Development Laboratory (USAAMRDL) Fort Eustis, Virginia.

The program was performed during the period 30 June 1973 through 30 June 1975. Technical monitor of the project for USAAMRDL was Richard I. Adams.

The Lockheed program was under the technical direction of J. B. Werner, Senior Research and Development Engineer. Additional Lockheed personnel making major technical contributions to the program included J. T. Alpern, W. A. Anderson, H. Carr, R. H. Cotton, M. J. Cronin, A. M. James, R. M. Johnston, J. E. Rhodes, G. M. Ryan, J. Schmidt, K. K. Schmidt, V. S. Sorenson, and J. H. Van Wijk.

Simulated icing tests were conducted by the US Army Aviation Engineering Flight Activity (USAAEFA), Edwards Air Force Base, California. Major technical contributions were made by Maj. Robert K. Merrill, Project Officer and Engineering Test Pilot, Capt. Louis Kronenberger, Flight Test Engineer, and Capt. Lenoard Hanks, chase plane pilot and icing test consultant.

## TABLE OF CONTENTS

	Page
SUMMARY . . . . .	3
PREFACE . . . . .	7
LIST OF ILLUSTRATIONS . . . . .	12
LIST OF TABLES . . . . .	16
1 INTRODUCTION . . . . .	18
2 ICING SEVERITY LEVEL ANALYSIS . . . . .	20
2.1 Types of Adverse Weather . . . . .	20
2.1.1 Freezing Rain and Drizzle . . . . .	21
2.1.2 Snow . . . . .	24
2.1.3 Supercooled Water Droplets . . . . .	24
2.1.4 Freezing Fog . . . . .	26
2.2 Recommended Design Criteria . . . . .	26
2.2.1 Approach . . . . .	26
2.2.2 Freezing Rain and Drizzle . . . . .	28
2.2.3 Snow . . . . .	32
2.2.4 Supercooled Clouds . . . . .	36
2.2.5 Freezing Fog . . . . .	45
3 ADVERSE WEATHER PROTECTION TECHNOLOGY REVIEW . . . . .	46
3.1 Components Requiring Protection . . . . .	46
3.2 Candidate Concepts for Rotor Blades . . . . .	49
3.2.1 Electrothermal Cycling Deicing . . . . .	51
3.2.2 Chemical Freezing Point Depressant . . . . .	102
3.2.3 Fluid Thermal Anti-Icing . . . . .	106
3.2.4 System Characteristics . . . . .	112
3.3 Engine Inlet Protection . . . . .	112
3.3.1 Design Criteria . . . . .	112
3.4 Windshield Protection . . . . .	119
3.5 Fuselage Nose and Radome Protection . . . . .	125
3.6 Flight Probe Protection . . . . .	130
3.7 Weapons and Sensors . . . . .	132

**Preceding page blank**



	Page
3.8 Icing Instrumentation . . . . .	134
3.8.1 Simple "Hot Rod" . . . . .	135
3.8.2 Ultrasonic System . . . . .	136
3.8.3 Hot Wire System . . . . .	136
3.8.4 Radioisotope System . . . . .	136
3.8.5 Differential Pressure System . . . . .	137
3.8.6 Infrared System . . . . .	137
3.8.7 Evaluation . . . . .	137
3.8.8 Determination of Droplet Size . . . . .	139
4 SYSTEM TRADE-OFF ANALYSIS . . . . .	143
4.1 Objectives . . . . .	143
4.2 Postulated Advanced Helicopters and their Missions . . . . .	144
4.3 Systems Analyzed . . . . .	145
4.3.1 Rotor Blades . . . . .	145
4.3.2 Windshield . . . . .	150
4.4 Results - Rotor Blades . . . . .	153
4.4.1 Evaluation of Systems . . . . .	153
4.4.2 Weight and Vehicle Performance Penalties . . . . .	172
4.4.3 Cost Comparisons . . . . .	181
4.4.4 Reliability and Maintainability Comparison . . . . .	191
4.4.5 Effect of Icing Severity on System Design Requirements. . . . .	194
4.4.6 Trade-off Study Conclusions and Recommendations . . . . .	199
5 ADVANCED ELECTROTHERMAL DEICING SYSTEM DEVELOPMENT . . . . .	204
5.1 Heater Development . . . . .	204
5.2 Development Test Results . . . . .	215
5.2.1 Preliminary Screening . . . . .	215
5.2.2 "Dogbone" Tension Cycling and Fatigue Tests . . . . .	215
5.2.3 Coupon Tests From Rotor Blade . . . . .	219
5.2.4 Further Dogbone Tests . . . . .	223
5.2.5 Bonding Strength Analysis . . . . .	224
5.3 Material and Processes . . . . .	234

	Page
5.3.1 Non Destructive Test Methods - Conclusions and Recommendations . . . . .	247
6 PROGRAM CONCLUSIONS AND RECOMMENDATIONS . . . . .	250
7 REFERENCES . . . . .	252

# LIST OF ILLUSTRATIONS

Figure		Page
1	Typical Temperature Profiles During the Occurrence of Supercooled Precipitation at the Ground . . . . .	23
2	Cross Section Through a Warm Front During the Occurrence of Freezing Rain . . . . .	25
3	Freezing Rain and Drizzle . . . . .	29
4	Freezing Rain Severity Levels - 99th Percentile Condition. . . . .	30
5	Snow Probability . . . . .	33
6	Cumulative Probability Distribution for Snow at Various Temperatures . . . . .	35
7	Worldwide Maximum Snowfall Liquid Water Criteria - 99th Percentile Condition . . . . .	37
8	Ambient Air Temperature Exceedance Probability . . . . .	38
9	Liquid Water Content Exceedance Probability in Stratiform Clouds . . . . .	39
10	Icing Severity Levels for a Probability of Exceedance = 0.01, Stratiform Clouds . . . . .	41
11	Icing Severity Levels in Supercooled Stratiform Clouds for 99th Percentile Criteria . . . . .	42
12	Recommended Atmospheric Icing Criterion . . . . .	43
13	Spanwise Elements for Chordwise Shedding . . . . .	52
14	Chordwise Elements for Spanwise Shedding . . . . .	52
15	Four Blade Rotor Deicing Sequence . . . . .	53
16	Deicing Control - Simplified Block Diagram . . . . .	54
17	Recommended Blade Heater Design . . . . .	55
18	Conceptual UH-1H Main Rotor Composite Blade Design . . . . .	73
19	Coefficient of Thermal Expansion for Laminate Family . . . . .	75
20	Fatigue Behavior of Blade Materials at $10^6$ Load Cycles . . . . .	79
21	Platter Slipring Design . . . . .	83

Figure		Page
22	Stacked Slipring Assembly . . . . .	84
23	Cylindrical Slipring Assembly . . . . .	85
24	A Possible Configuration for a Rotary Transformer . . . . .	88
25	Hybrid Sequential Power Switch . . . . .	91
26	Solid-State Sequential Power Switch . . . . .	91
27	Electromechanical Rotor Stepping Switch . . . . .	94
28	Close-Up of Power Contactors and Contacts . . . . .	94
29	Comparison of Electrothermal Rotor Deicing System Weight Hybrid Versus Solid-State Sequential Switching System . .	96
30	Power Modulation Methods . . . . .	98
31	Deicer Controller - Schematic of Hybrid System . . . . .	99
32	Schematic of Chemical Freezing Point Depressant Ice Protection System . . . . .	103
33	Required Theoretical Freezing Point Depressant Fluid Expulsion Rate for UH-1 Main Rotor Blades . . . . .	105
34	Liquid Rotary Seal for Water-Glycol Rotor Blade Anti-Icing . . . . .	107
35	Rotating Heat Exchanger System for Rotor Blade Anti-Icing . . . . .	108
36	Rotor Anti-Icing/Transmission Lube Oil Cooling - Return Oil Seal . . . . .	109
37	Typical Blade Leading-Edge Cross Section of Four Passage System . . . . .	111
38	Electrical Anti-Icing Requirements for an Engine Inlet Duct . . . . .	115
39	Anti-Icing Requirements of Engine Inlet Duct Using Engine Bleed Air . . . . .	116
40	Maximum Heat Required Vs Airspeed and OAT for Windshield Anti-Icing . . . . .	120
41	Ice Buildup After 15 Minutes on 1/6 Scale Icing Tunnel Model of C-5A Nose Radome - Test 2 . . . . .	126
42	Ice Buildup After 28 Minutes on 1/6 Scale Icing Tunnel Model of C-5A Nose Radome - Test 2 . . . . .	126
43	Impingement Limits on Fuselage Nose for Various Droplet Diameters . . . . .	127

Figure		Page
44	Comparison of Required and Available Anti-Ice Power Intensities for Typical Pitot-Static Tube Heater . . . . .	131
45	Water Droplet Collection Device . . . . .	140
46	Water Droplet Photomicrograph . . . . .	141
47	Variation of Engine SFC at Partial Power . . . . .	149
48	Chemical Freezing Point Depressant System Penalty for Two Sets of Icing Criteria . . . . .	155
49	Chemical Freezing Point Depressant Fluid Quantity Required for Rotor Blade Ice Protection as a Function of Ambient Temperature - MIL-E-38453 Criterion . . . . .	157
50	Chemical Freezing Point Depressant Fluid Quantity Required for Rotor Blade Ice Protection - 99th Percentile Icing Criterion . . . . .	158
51	Freezing Rain Protection Penalty (Fixed Weight and Fuel) for Chemical Freezing Point Depressant Deicing System - 1 Hour . . . . .	160
52	Total Weight and SHP Penalties for Electrothermal Deicing System During Flight Through Icing for 1 Hour . . . . .	164
53	Comparison of Power Extraction Requirements for Electrothermal Ice Protection . . . . .	167
54	Ambient Icing Design Temperatures and Liquid Water Content - Fully Evaporative Performance . . . . .	170
55	Liquid-Heated Skin Evaporative Anti-Icing System Penalty for Various Icing Criteria . . . . .	171
56	Comparison of Weight Penalties for 1-Hour Flight Through Icing - MIL-E-38453 Criteria . . . . .	174
57	Comparison of SHP Requirements for Flight Through Icing . . . . .	175
58	Comparison of Weight Penalties for 1-Hour Flight Through Freezing Rain . . . . .	176
59	Comparison of SHP Requirements for Flight Through Freezing Rain . . . . .	177
60	Comparison of Weighted Average Penalties for Flight Through Icing . . . . .	180
61	MMH/FH Vs Total Heater Element Area, Main and Tail Rotor Blades . . . . .	193
62	Weight and SHP Penalty Change With Temperature for the Electrothermal System . . . . .	197

Figure		Page
63	Weighted Average Total Penalty With LWC for the Chemical Freezing Point Depressant System . . . . .	198
64	Flight Through Icing Weight Penalty Vs Ice Encounter Duration . . . . .	200
65	Average Weight Penalties for Year-Round Operation . . . .	201
66	Main and Tail Rotor Blade Deicing Installation for UH-1H . . . . .	206
67	Photo of Rotor Blade Deicer Laminate . . . . .	210
68	Tension Cycling Test Specimen . . . . .	213
69	Fatigue Test Specimen . . . . .	214
70	UH-1H Blade Cross-Section Showing Installed Deicer Boot .	220
71	Bond Delamination Progression . . . . .	225
72	Rotor Blade Shear Transfer . . . . .	227
73	Location of Main Rotor Conductors . . . . .	233
74	Rotor Blade Shear Transfer Area . . . . .	233
75	Main Rotor Blade Deicer Blanket . . . . .	243
76	Main Rotor Deicer Bonding Tool . . . . .	243
77	Blade Contour Check With Template . . . . .	245
78	Main Rotor Blade Balance Weight Rework . . . . .	245
79	"C" Scan Test Signature . . . . .	248

# LIST OF TABLES

Table		Page
1	Value of Constants A, B, C, and F in Equations (1) and (2) . . . . .	28
2	Problem Summary Electrical Deicer Systems . . . . .	58
3	Rain Erosion Resistance of Metallic Materials . . . . .	61
4	Sand Erosion Resistance of Metallic Materials (Sandblast Test) . . . . .	62
5	Sand Erosion Resistance of Metallic Materials (Whirling Arm Test) . . . . .	63
6	Typical Aircraft Applications of Electrothermal Deicing Systems . . . . .	67
7	Comparison of Heating Element Characteristics . . . . .	70
8	Structural Properties of Selected Composite Materials . .	72
9	Rotor Blade Dynamic Loads at UH-1H R.S. 150.0 . . . . .	77
10	Stress Levels in Basic Blade at R.S. 150.0 . . . . .	78
11	Reliability and Maintainability Summary, Subsystem Totals, and Application of Rotary Wing Predictions . . . .	95
12	Rotor Ice Protection Concepts . . . . .	113
13	Thermal Windshield Anti-Icing Requirements . . . . .	121
14	Summary of C-5A Model Radome Icing/Radar Test Results . .	129
15	Characteristics of Future Helicopters . . . . .	148
16	Estimated Penalties for Windshield Anti-Icing Chemical Freezing Point Depressant System . . . . .	151
17	Estimated Penalties for Windshield Anti-Icing Electrically Heated System . . . . .	152
18	Estimated Weight and SHP Penalties for Flight Through Icing - Chemical Freezing Point Depressant System for MIL-E-38453 Criteria - 1 Hour . . . . .	154
19	Rotor Configuration and Electrothermal Deicing System Data for OAT = -4° F . . . . .	162
20	Estimated Weight and SHP for Flight Through Icing Electrothermal Deicing System - 1 Hour . . . . .	163
21	Rotor Electrothermal Freezing Rain Deicing System Data . .	166
22	Estimated Weight and SHP for Freezing Rain Protection - Electrothermal Deicing for 1 Hour . . . . .	169

## Table

## Page

23	Estimated Weight and SHP Penalties for Flight Through Icing - Integrated Transmission Lub Oil/Anti-Icing System - Evaporative Performance for MIL-E-38453 Criteria for 1 Hour . . . . .	173
24	Weighted Average Penalties for MIL-E-38453 Icing Criteria.	179
25	Cost Summary - 200 Aircraft Program . . . . .	182
26	Cost Breakdown by Percentage - 200 Aircraft Program . . .	184
27	Anti-Icing/Deicing Total Cost Summary - Systems by Aircraft Type and Production Quantities . . . . .	185
28	Major Component Group Cost Ranking . . . . .	187
29	Anti-Icing/Deicing System, Electrothermal (includes generator) Cost Summary - Aircraft Type and Production Quantities . . . . .	189
30	Maintenance Man-Hours Per Flight Hours (touch time) for Anti-Icing/Deicing System . . . . .	192
31	Rotor Ice Protection - Reliability Comparison . . . . .	195
32	Summary of Tests - Deicer Boot Configuration . . . . .	207
33	Data Summary-Tests of Heater Boot Configurations . . . . .	211
34	Deicer Boot Development Test Results . . . . .	216
35	Heater Blanket Stress Distribution Based on Strain Gage Measurements . . . . .	217
36	Shear Strength of Coupons Cut From Main Rotor Test Blade .	221
37	Flatwise Tensile Strength of Coupons Cut From Main Rotor Test Blade . . . . .	221
38	Rotor Blade Deicer Boot Production Coupon Test . . . . .	222
39	Material Configuration Selections . . . . .	235



## SECTION 1

### INTRODUCTION

The widespread use of Army rotary-wing aircraft and the increased emphasis now being placed on all-weather, round-the-clock operation of such aircraft have made reliable operation in adverse weather conditions an urgent safety-of-flight requirement for all instrument-certified rotary-wing aircraft. For helicopters to be capable of completing assigned military airmobile missions under adverse environmental conditions, it is necessary that the criteria used in the design specification be at least as severe as the conditions reasonably expected to be encountered. In particular, all-weather aircraft must be designed to ensure safe flight in icing conditions and yet not burden overall aircraft performance with unnecessary penalties due to the ice protection system. Future-generation Army aircraft must possess adequate capability in at least moderate icing conditions. These requirements will be reflected in the systems specifications for future Army aircraft systems as they are developed.

Reference<sup>(1)</sup> reviewed icing design criteria and ice protection technology for advanced rotary wing aircraft. In this study it was determined that existing design criteria and technology can be applied to all parts of the helicopter except the rotor blade system to allow safe flight through clouds with supercooled water droplets. The rotor blade system imposes unique protection requirements which have not been adequately treated during the evolution of ice protection technology. As a result,

---

(1) Werner, J. B., ICE PROTECTION INVESTIGATION FOR ADVANCED ROTARY-WING AIRCRAFT, Lockheed-California Company, USAAMRDL Technical Report 73-38, Eustis Directorate, US Army Air Mobility Research and Development Laboratory, Fort Eustis, Virginia, August 1973, AD 769062

the state of the art for rotor blade protection was deemed inadequate to meet the demands of stringent ice protection requirements. This gap in the rotor blade deicing technology must be closed by development of a lightweight system that is functionally efficient, mechanically and electrically reliable, maintainable, and cost effective.

Even though helicopter engine flameouts due to snow ingestion have proven to be a serious problem, the near-total lack of specific snow ingestion criteria or specifications also became apparent during the Reference (1) study. Accordingly, there was a requirement for the development of snow design criteria and snow abatement or protection techniques. In addition, there are other aspects of adverse-weather, such as freezing drizzle and rain, which should be considered in rotary-wing vehicle design.

The primary objectives of this program, therefore, are to assure that accurate design and test criteria exist for future-generation Army helicopter ice protection systems and that technology will be available to satisfy those requirements in a cost-effective manner. A secondary objective of the program is to provide information and technology which has a high probability of being directly applicable to the current fleet.

This volume of the final report discusses meteorological criteria to be used for adverse-weather system design, the technology available to provide ice protection for the various critical helicopter components, the trade-offs comparing different types of rotor blade ice protection system for a spectrum of helicopter designs, and the development program which has been conducted for the critical state of the art component. Volume II describes the application of an advanced technology rotor blade ice protection system to a UH-1H helicopter and the airworthiness and systems ground and flight test program that was conducted.

## SECTION 2

### ICING SEVERITY LEVEL ANALYSIS

The effects of snow and ice on helicopter performance and handling qualities must be assessed and balanced against the cost of providing and maintaining a system capable of ice removal or prevention. Meteorological criteria affect the design of ice protection systems. Certain design parameters such as liquid water content, droplet diameter, and ambient temperature influence heavily the type and size of ice protection systems.

Of primary significance in this task were the meteorological conditions that cause helicopter surface ice formations which detrimental / alter the aerodynamic and handling qualities, rotor balance, engine operation, and structural integrity.

The trade-off studies discussed in Section 4 show that the recommended meteorological design criteria shown in this section are based upon a consideration for the penalties of the severity chosen. Depending upon the ice protection technique, the penalties are a function of either:

- (1) The ambient temperature (e.g., electrothermal cyclic deicing of rotor blades and running-wet thermal anti-icing of the engine inlets, or
- (2) the combination of ambient temperature and icing severity (e.g., chemical deicing and evaporative thermal anti-icing of the rotor blades).

In addition, particle diameter influences the required area which must be protected. Thus, in establishing recommended severity levels, it is necessary to balance the penalties for protection against the likelihood of occurrence.

#### 2.1 TYPES OF ADVERSE WEATHER

Adverse weather is generally taken to mean those extremes which occur at the colder end of the ambient temperature range, rather than extremes associated with elevated temperatures. Adverse weather consists of rain,

freezing rain and drizzle, snow, supercooled water droplets, and freezing fog. Rain, however, does not present the safety-of-flight hazards of the other conditions, and existing design provisions for rain protection and/or removal are generally accepted as adequate.

#### 2.1.1 Freezing Rain and Drizzle

Freezing rain and drizzle are particularly critical to helicopter operation because of the formation of a coating known as glaze<sup>(2)</sup> upon exposed surfaces, which can result in various degrees of performance degradation. Glaze\* is related to two other forms of ice, rime and hoarfrost, but differs from them chiefly by its greater specific gravity (0.9 or greater). The high density of glaze results from the fact that the drops of precipitation responsible for its formation are large enough and freeze slowly enough to enable them to flow together before freezing, thus occluding almost all air from the formation (the specific gravity of solid ice is 0.92). Also, glaze is more likely to be transparent and highly amorphous in structure, whereas rime and hoarfrosts are generally opaque or translucent and have highly developed crystal structure. Hoarfrost usually has the lowest specific gravity and is generally composed of delicate, feathery masses of crystals laced together into such a loose network of ice that most of the volume occupied by the formation consists of air spaces. Rime is primarily the product of the freezing of cloud or fog droplets which are very small in size and are more capable of freezing before they have had an opportunity to coalesce; rime contains a large percentage of air held in interstices between the masses of ice, and is associated with a low surface equilibrium temperature (below 10° F).

---

(2) Bennett, I., GLAZE, ITS METEOROLOGY AND CLIMATOLOGY, GEOGRAPHICAL DISTRIBUTION, AND ECONOMIC EFFECTS, Technical Report EP-105, US Army Quartermaster Research and Engineering Center, Natick, Massachusetts, March 1959.

\* Glaze is also a term which is used to describe a type of ice accretion occurring from small supercooled droplets. In this context glaze is also described as a relatively smooth clear ice coating and is formed at temperatures just below freezing.

Glaze clings more tenaciously to surfaces on which it forms than do either rime or hoarfrost because more particles are in contact with the surface and because it adheres closely to the form of the object<sup>(3)</sup>. The type of ice formed (hoarfrost, rime, glaze, or a combination of these) depends upon the speed with which freezing occurs, the size of the drops, the rate of drop impingement, and the degree of supercooling. Slow rate of freezing, large drop size, rapid rate of impingement, and slight supercooling (surface equilibrium temperature just below 32° F) favor glaze formation. Since glaze results from liquid precipitation, an appropriate range of droplet diameters is 150 microns for the smallest drizzle droplets to 2,500 microns for rain droplets.

Basically, supercooled rain and drizzle are associated with the following atmospheric temperature structure: (1) a relatively warm layer of air aloft (temperatures above freezing) which is of sufficient thickness so that precipitation originating as snow at higher altitudes is melted by passage through this warm layer, and (2) a relatively cold layer (temperatures below freezing) which is of sufficient thickness to supercool liquid precipitation droplets falling through it. Two profiles illustrating typical atmospheric temperature structure during the worldwide occurrence of supercooled rain and drizzle are presented in Figure 1. The Nashville profile indicates that supercooling occurs in a layer characterized by a temperature inversion (temperature increasing with increasing altitude), whereas the San Antonio profile indicates that supercooling occurs in a multiple structured layer composed of an inversion aloft and a well mixed adiabatic layer near the ground in which the temperature decreases with increasing altitude. In terms of relating the occurrence of freezing rain aloft to its occurrence at the ground, the structure of these profiles is of critical importance. For the Nashville case, when the lower limit of the inversion layer is at the ground, there exists an altitude within the inversion layer

---

(3) Byers, H. R., GENERAL METEOROLOGY, McGraw-Hill, New York, New York 1944.

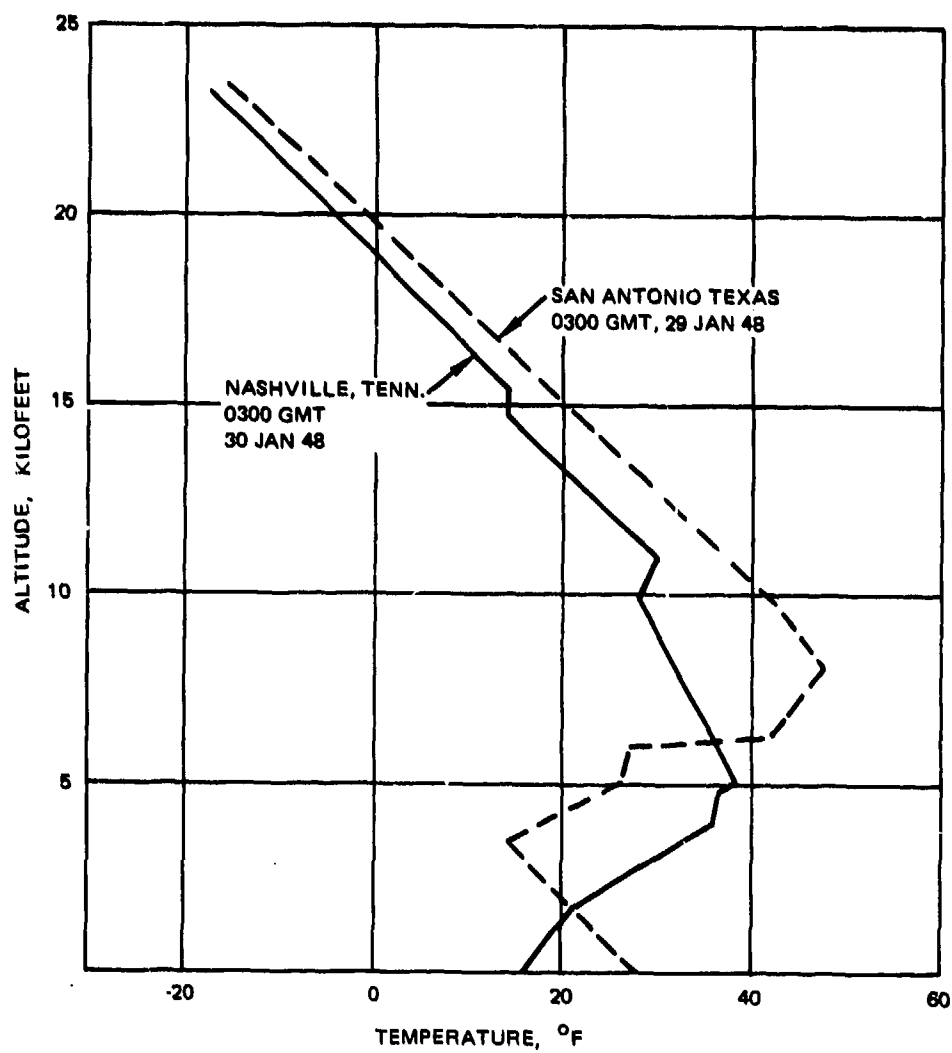


Figure 1. Typical Temperature Profiles During the Occurrence of Supercooled Precipitation at the Ground.

above which liquid precipitation has not yet become supercooled. This altitude is related to the time required for the liquid droplets to become supercooled, which in turn is related to the size and terminal velocity of the droplets and the humidity of the air.

The area affected by supercooled precipitation can be as small as a few square miles, but the average storm covers an elongated area 200 to 600 miles long.

As illustrated in Figure 2, supercooled precipitation occurs in conjunction with a wide variety of other forms of precipitation. Although a majority of occurrences of glaze occur in the cold air ahead of an advancing warm front, it also frequently occurs with cold fronts in the Southern Great Plains, or stationary fronts in the Northern Great Plains.

#### 2.1.2 Snow

In certain configurations, helicopter engine plenum chambers can be the source of large ice formations which, if ingested, could result in an engine flameout. The ice formation is attributable to snow, which, upon entering the plenum chamber, impinges on the back of the warm firewall and melts; the water runs down to the cold plenum floor, where it freezes. In order that the possibility of such an occurrence in future Army helicopters be eliminated, it is necessary to develop severity criteria for the pertinent physical parameters of snow, namely liquid water content (i.e., mass of melted snow per cubic meter of ingested air and associated temperature). Recommended severity criteria for snow and the methodology for their development are given in Paragraph 2.2.

#### 2.1.3 Supercooled Water Droplets

The occurrence of supercooled water in clouds has been a subject of diminishing interest since the advent of turbojet aircraft that have the capability of cruising above areas of critical icing. Most of the work done on icing was completed in the 40's and 50's by the NASA Lewis Group. The severity criterion developed forms the basis for severity

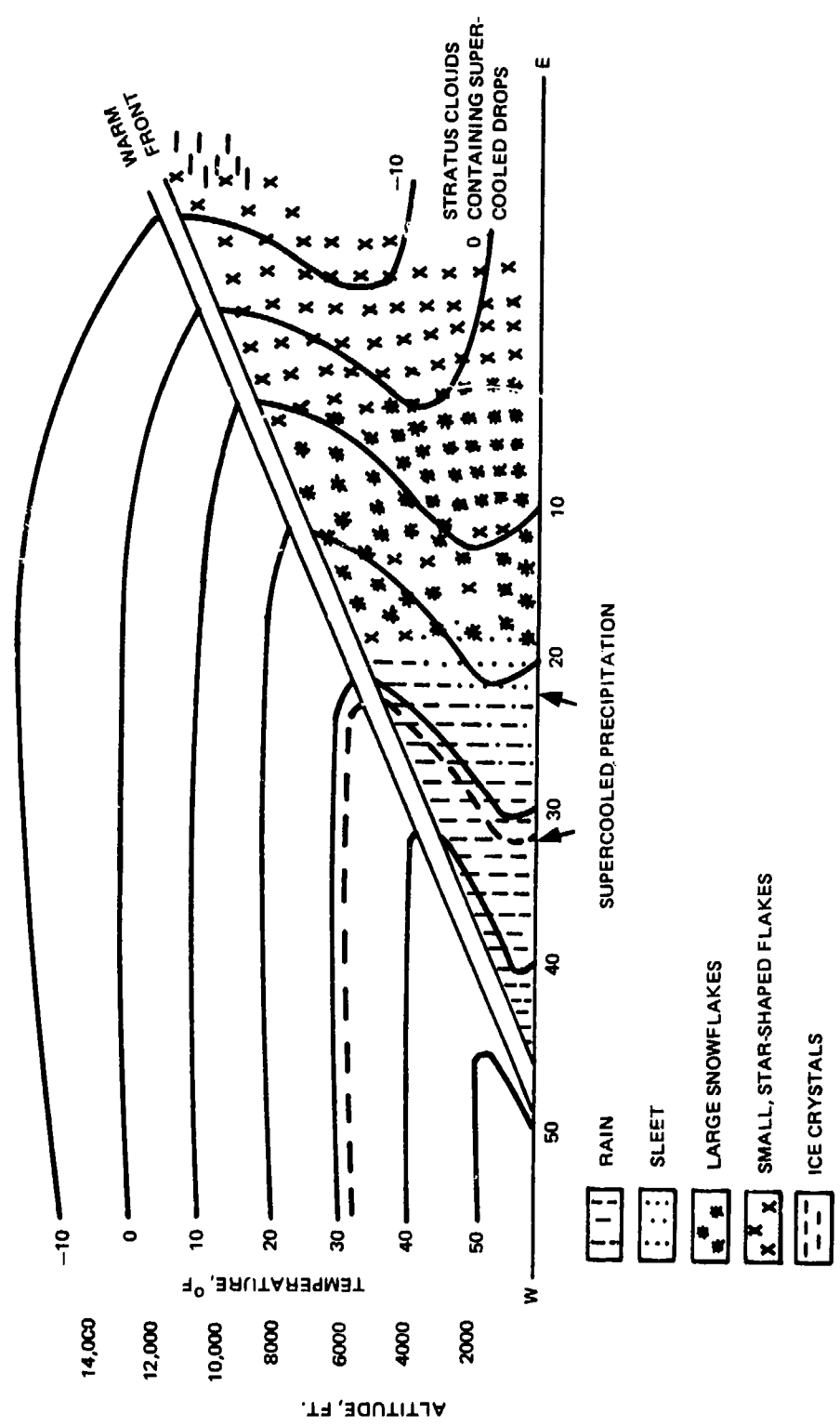


Figure 2. Cross Section Through a Warm Front During the Occurrence of Freezing Rain (From Reference 3).



criteria contained in Federal Aviation Regulation 25<sup>(4)</sup> and its equivalent military counterpart MIL-E-38453<sup>(5)</sup>. A discussion of how these existing criteria may be used for helicopter design is given in Paragraph 2.2.

#### 2.1.4 Freezing Fog

Freezing fog is a supercooled cloud which is near or in contact with the ground. Therefore, it is reasonable to assume that the physical characteristics of freezing fog are comparable with supercooled clouds at the same temperature. For the purpose of developing icing severity criteria in the present study, a conservative approach is taken by assuming that clear and/or rime icing is associated with freezing fog to the same degree it is associated with supercooled clouds, and that criteria applicable to supercooled clouds are also applicable to freezing fog.

### 2.2 RECOMMENDED DESIGN CRITERIA

#### 2.2.1 Approach

According to regulation AR-70-38<sup>(6)</sup>, Army material must be designed to withstand extreme conditions that are exceeded only 1 percent of the time in the most extreme month in the most extreme areas of the world. To assure that future Army helicopters can be designed to satisfy this requirement, design criteria for the severity of the various types of adverse weather described in Paragraph 2.1 have been developed under this study.

---

(4) Federal Aviation Regulation Part 25: AIRWORTHINESS STANDARDS; Transport Category Airplane Appendix C

(5) MIL-E-38453 (USAF) Amendment 1, ENVIRONMENTAL CONTROL, ENVIRONMENTAL PROTECTION, AND ENGINE BLEED AIR SYSTEMS, AIRCRAFT AND AIRCRAFT LAUNCHED MISSILES, GENERAL SPECIFICATION FOR dated 4 May 1967.

(6) ARMY AVIATION - GENERAL PROVISIONS, AR 70-38 (Army Regulations), 12 September 1969.

Severity levels are defined in terms of critical icing parameters including liquid water content (LWC), volume median effective droplet size (D), and temperature (T), that are exceeded 1 percent of the time (exceedance probability,  $P_e$ , equal to 0.01). The term extreme icing describes conditions for  $P_e \leq 0.01$ . This severity is then compared to other existing criteria (References 4 and 5) for supercooled droplets.

Whenever possible, existing measurements and analyses of critical icing parameters are used in the derivation of severity criteria. Thus, earlier NACA studies are used in the development of criteria for supercooled water droplets in stratiform clouds. As discussed in paragraph 2.1.4, freezing fog criteria are synonymous with those developed for supercooled stratiform clouds. Since insufficient direct measurements exist of the liquid water content and effective drop size of snow, freezing rain and drizzle, it is necessary to estimate their extreme values indirectly. To do this it is assumed that the physical relationship ordinarily developed in radar meteorology between liquid water content, effective drop size, and precipitation accumulation rate at the ground, R (melted), is applicable. Thus LWC (liquid water content) and D can be calculated from R according to

$$LWC = AR^B \quad (1)$$

$$D = CR^F \quad (2)$$

The constants for freezing rain and drizzle and snow (melted) are given in Table 1, where D is in cm, R is in mm/hr and LWC is in  $g/m^3$ .

Given a long record (5-10 years) of hourly surface weather observations, the cumulative probability distribution (exceedance probability equals 1 minus cumulative probability) of R for snow or freezing rain and drizzle can be determined. For specified exceedance probability, the value of R is known, and LWC and D are calculated from Equations (1) and (2), respectively.

TABLE 1. VALUES OF CONSTANTS A, B, C, AND F IN EQUATIONS (1) and (2)		
	Freezing Rain and Drizzle (Marshall and Palmer, Ref.(7))	Snow (Sekhon and Srivastova, Ref.(8))
A	0.09	0.25
B	0.84	0.86
C	0.09	0.14
F	0.21	0.45

#### 2.2.2 Freezing Rain and Drizzle

Following the approach outlined in Paragraph 2.2.1, the cumulative probability distributions of hourly precipitation rate, R, (melted) for freezing rain and drizzle were calculated from data obtained at Albany, New York, and Caribou, Maine (Jan-Apr, Oct-Dec 1954-64), and Flint, Michigan (Jan-Apr, Oct-Dec 1958-64). These distributions are compared with a distribution derived by Lewis and Perkins<sup>(9)</sup> for freezing rain over New England. Additional abscissa scales given in Figure 3 were calculated from Equations (1) and (2) by substitution of the constants for freezing rain and drizzle given in Table 1. The distribution given by Lewis and Perkins is in most cases generally the most severe except that it is less severe than at Albany for cumulative probabilities greater than 98 percent. It can be seen from Figure 4 that the Lewis and Perkins data (NACA TN 4220) follows a smooth continuous curve, while the two Albany data points that show a greater freezing rain severity for a probability greater

(7) Marshall, J. S. and Palmer, W., THE DISTRIBUTION OF RAINDROPS WITH SIZE, J. Meteor., 1948, pp. 165 - 166.

(8) Sekhon, R. S. and Srivastova, R. C., SNOW SIZE SPECTRA AND RADAR REFLECTIVITY, J. Atmos. Sci., 27, March 1970, pp. 299 - 307.

(9) Lewis, W. and Perkins, P. J., A FLIGHT EVALUATION AND ANALYSIS OF THE EFFECT OF ICING CONDITIONS ON THE ZPG-2 AIRSHIP, NACA Technical Note 4220, Washington, D. C., April 1958.

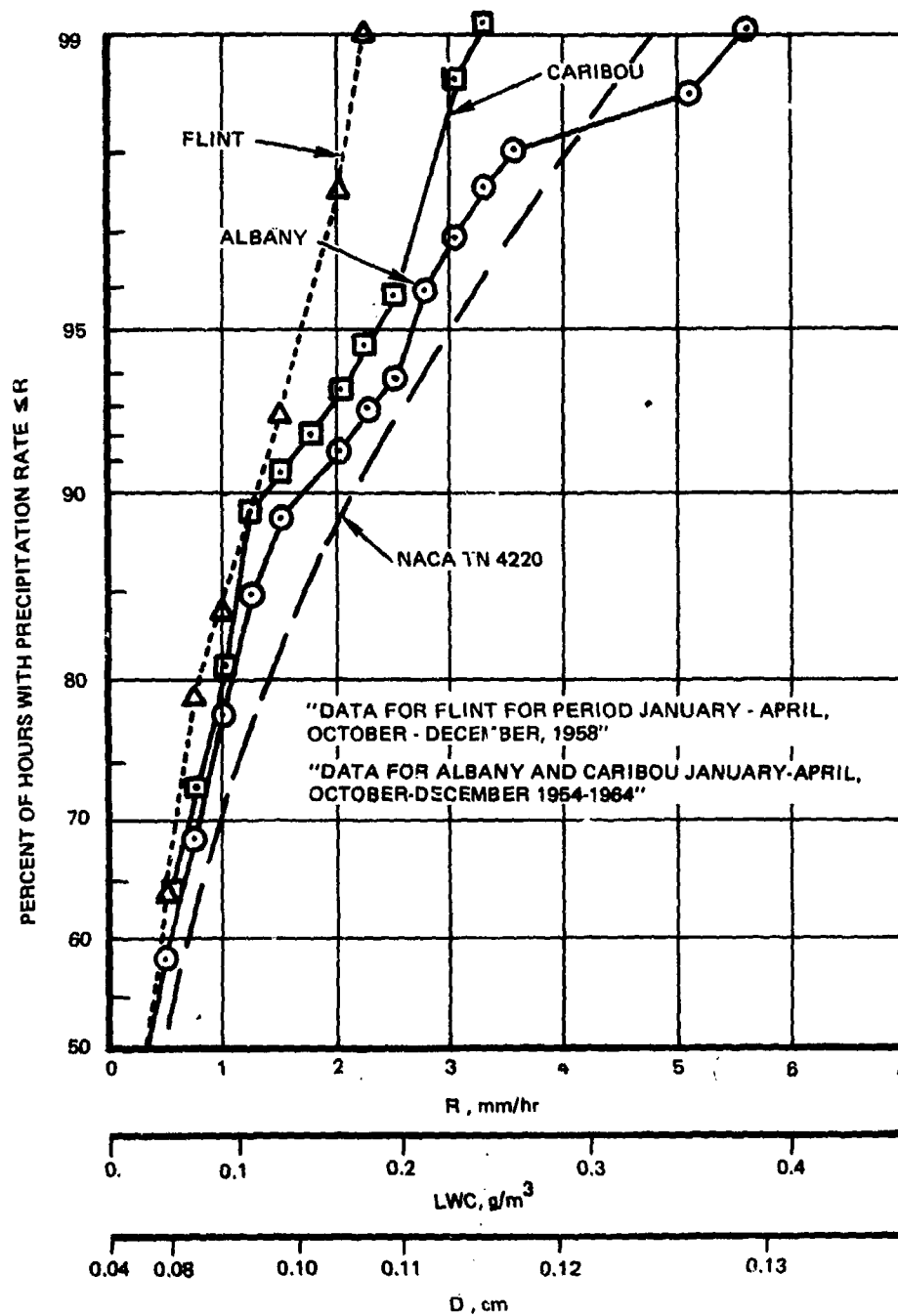


Figure 3. Freezing Rain and Drizzle.

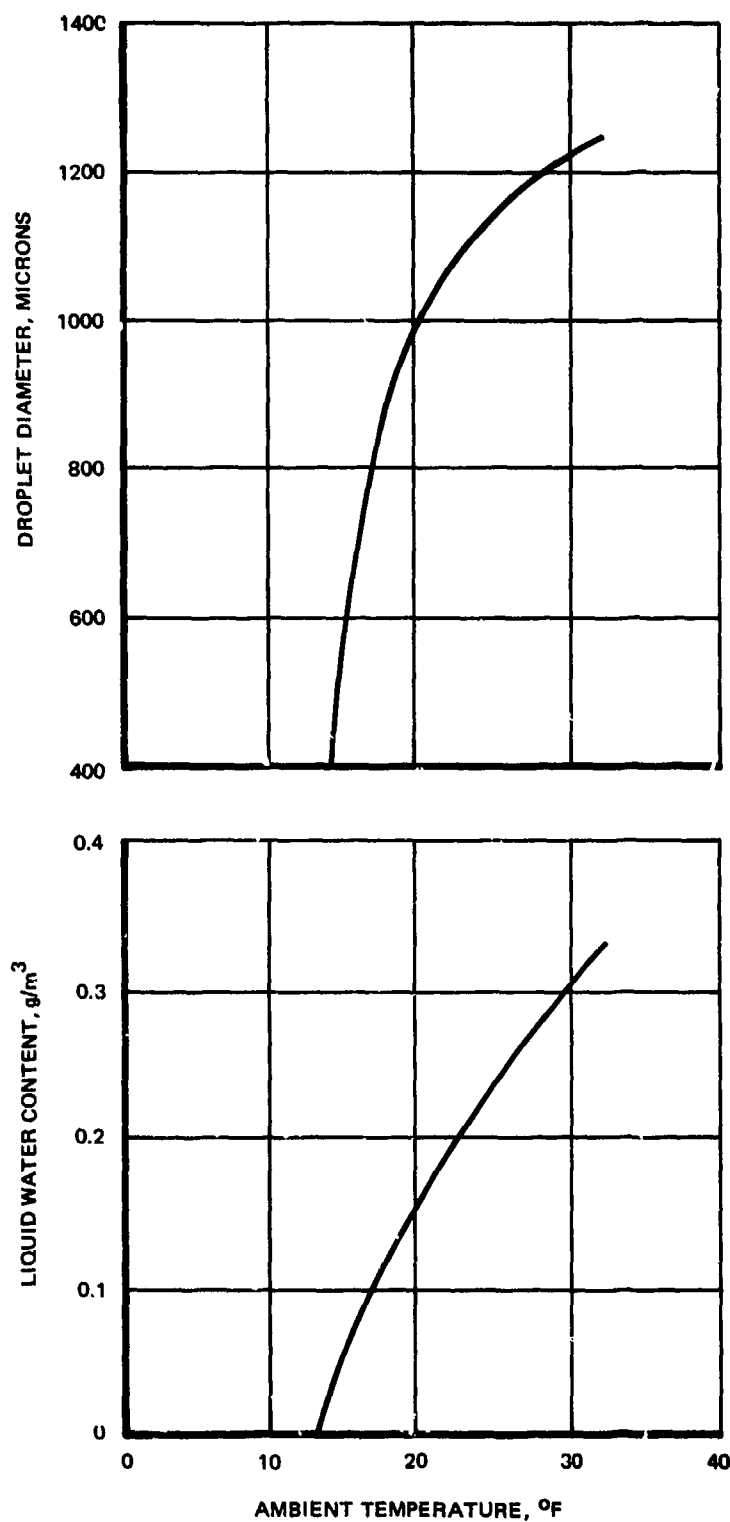


Figure 4. Freezing Rain Severity Levels-99th Percentile Conditions.

than 98 percent appear to be out of line with the general data trend. It appears that the two Albany data points in question represent an anomaly due to lack of broad statistical data. Therefore, the Lewis and Perkins data in conjunction with Equations (1) and (2) are used as the baseline for determining the 99th percentile envelope. It is noted that existing design standards for freezing rain were calculated for a rainfall rate of 0.1 inch per hour with drops 1 mm in diameter<sup>(10)</sup> and this is considerably less severe than the baseline data adopted herein.

According to Reference (2), though glaze is fairly common in parts of Europe, frequencies are nowhere as high as in the major portion of the glaze belt of the Central and Eastern United States. Glaze storms are weather phenomena most typically associated with North America. They are products of the "optimum" conditions in the eastern two-thirds of the North American continent for clash between cold dry polar air and warm moist tropical air. In addition, the two air masses need to be relatively "fresh" from their source regions. Most of Europe does not experience the extremes of winter climate resulting from the frequent clash of continental polar and maritime tropical air common in North America. In the southern hemisphere, there is little chance for a meeting of these air masses, primarily because of the absence of cold polar air. Air from the Antarctic is cold enough when it leaves the source region, but by the time it reaches Africa, Australia, or South America, it has travelled a long distance over open water so that the possibility of its temperature being below 32° F is relatively small. Apart from the eastern part of North America, the best area for frequent contact between polar and moist tropical air is found along the eastern coast of Asia, particularly the coasts of China and Japan. However, whereas in North America the moist tropical air often penetrates far inland during the winter, the pronounced anticyclonic

---

(10) Anonymous: HYDROMETEOROLOGICAL LOG OF THE CENTRAL SIERRA SNOW LABORATORY, Department of Army, Corps of Engineers, 1946-47 to 1951-52.

circulation that dominates Asia in winter limits such invasions to rare occasions. The strength and persistence of the anticyclone results in the almost continual winter-long dominance of cold dry air over the entire area from eastern Europe to the Siberian and Chinese coasts. Conditions prevailing in Japan are similar to those found along the eastern coast of the United States. Thus, there is no evidence that severity of freezing rain and drizzle are more severe at any location outside North America.

Therefore, the recommended 99th percentile liquid water content and associated effective drop size for freezing rain and drizzle are those shown in Figure 4. The precise size of freezing rain drops is of trivial importance because for the large drops involved (in excess of 400 microns) the flight surface catch efficiency approaches 100 percent and affects the entire surface.

In the United States freezing rain is encountered in the northeastern region more often than in other areas. Statistics on rainfall rate and temperature in freezing rain accumulated over a 3-year period over land areas in the Northeastern United States indicate that freezing rain occurs in this geographical area only about three to five storms per year. Severe freezing rain ( $>0.22 \text{ g/m}^3$ ) occurs in from 1 to 5 percent of the freezing rain occurrences Reference (9).

### 2.2.3 Snow

The most critical parameters associated with snow are liquid water content and ambient temperature. These parameters would establish the energy intensity levels for an in-flight snow removal system, if one were required. Following the approach outlined in Paragraph 2.2.1, the cumulative probability distributions of hourly snow accumulation rate,  $R$ , (melted) were calculated from data obtained at the Sierra Snow Laboratory Reference (10) during six winters (1946-47 to 1951-52), Flint, Michigan, and Juneau, Alaska (Jan-Apr, Oct-Dec 1958-64), and Albany, New York, and Caribou, Maine (Jan-Apr, Oct-Dec 1954-64); these distributions are illustrated in Figure 5. Additional abscissa scales given in Figure 5

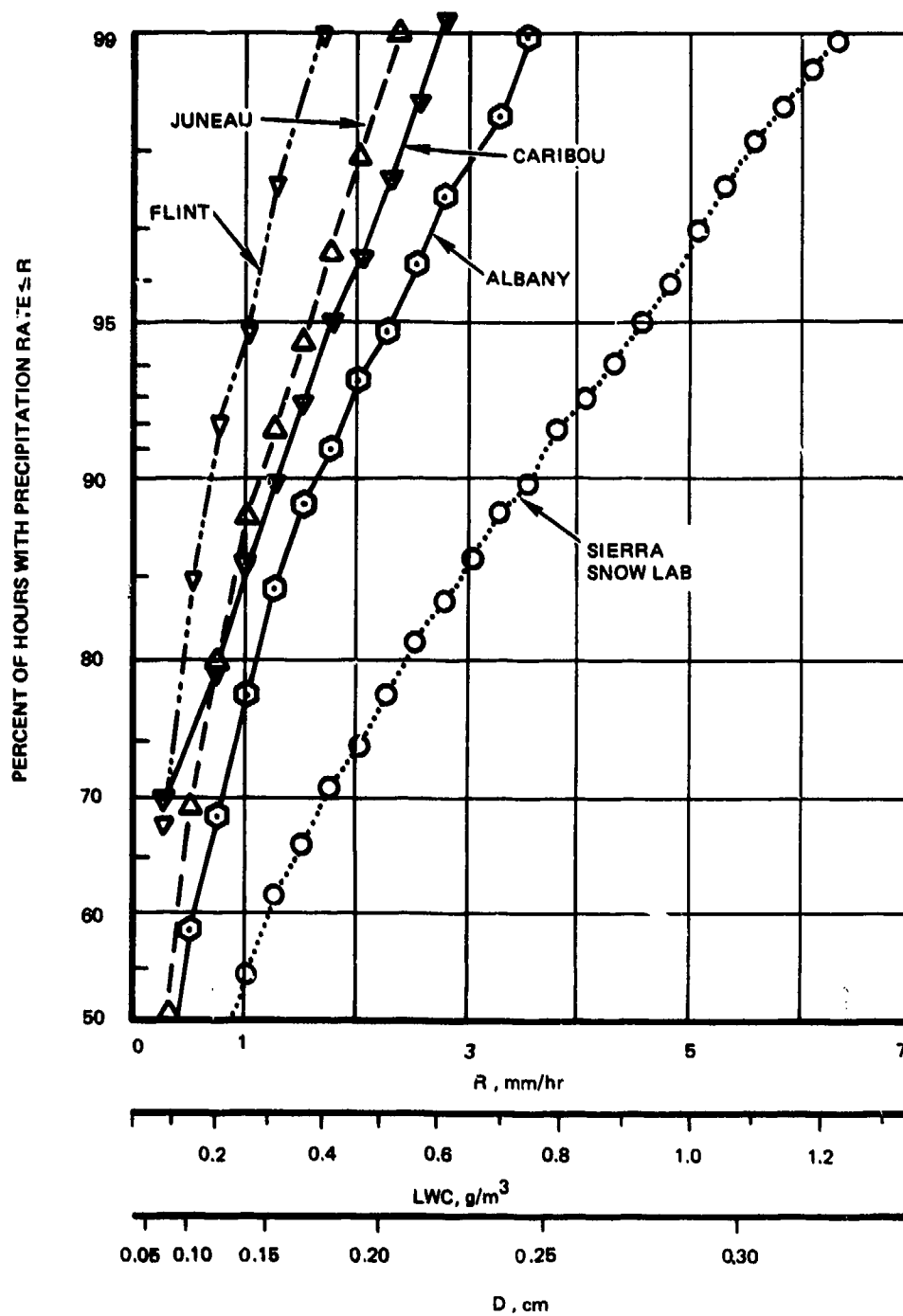


Figure 5. Snow Probability.



were calculated from Equations (1) and (2) by substitution of the constants for snow given in Table 1. The distribution of R for snow is shown to be strongly dependent on location, with the Sierra Snow Laboratory indicating the most extreme snowfall rates.

Additional data obtained from the Sierra Snow Laboratory are presented in Figure 6. These data show the precipitation rate (mm/hr) percentile for snowfall as a function of temperature. For example, the 99th percentile occurs at precipitation rates of 5.2, 6.35, and 7.1 mm/hr for the temperatures of 15°, 25°, and 35° F, respectively.

By converting the precipitation rate to mm/hr and substituting into Equation (1), the liquid water content can be obtained. For the 99th percentile the associated liquid water content at 15°, 25°, and 35° F are 1.26, 1.49, and 1.64 g/m<sup>3</sup>, respectively.

One may question whether the extreme conditions of the Sierra Laboratory data are representative of worldwide conditions for the establishment of severity criteria for Army helicopters. The selection of the particular stations was based upon the availability of data. With respect to snow, it is known that the severity levels at the Sierra locations are exceeded in Washington Cascades, in the Colorado Rockies, and in the area of Thompson Pass in Alaska; however, hourly data for long periods at the latter stations are not available. A comparison of extreme 24-hour snowfall in the Sierra with similar occurrences at the other more extreme locations has been used to establish a correction factor for the Sierra severity levels.

Based upon the above approach, the observed 99th percentile 1-hour snow accumulation rate at the Sierra Snow Laboratory can be used to approximate the 1-hour 99th percentile at a more extreme location where hourly data are not available.

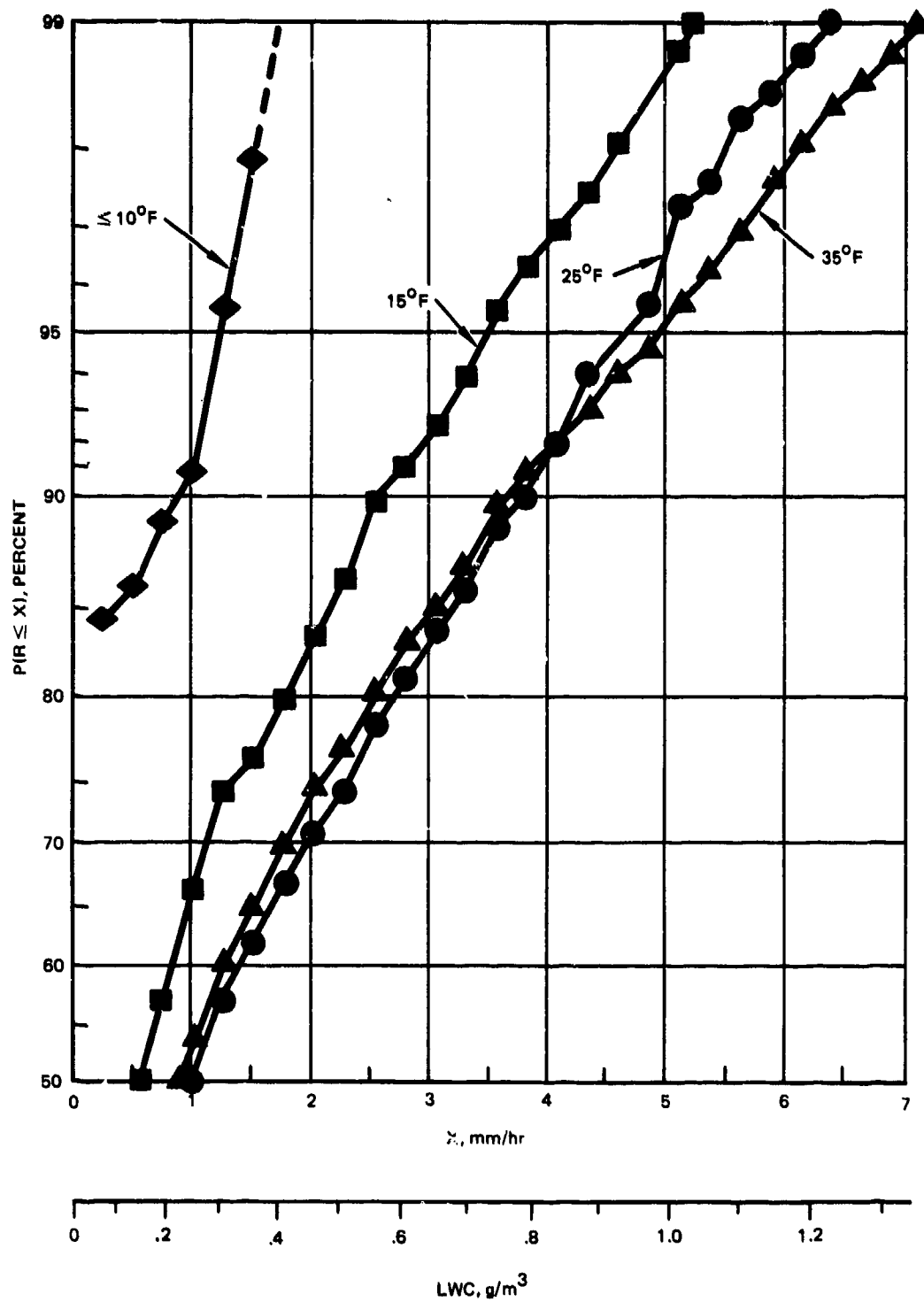


Figure 6. Cumulative Probability Distribution for Snow at Various Temperatures.

Riordan's data<sup>(11)</sup> indicate that the record 24-hour snowfall is 193 cm at Silver Lake, Colorado, compared to 152 cm in the Sierras. The 1-hour 99th percentile for the world is thus obtained by multiplying the value of R obtained at the Sierra Snow Laboratory (6.4 mm/hr from Figure 5) by a factor of 193/152 to obtain 8.1 mm/hr. Application of this factor to the Sierra snow data yields the worldwide recommended 99th percentile liquid water content of snow as a function of ambient temperature. For temperatures of 15°, 25°, and 35° F the recommended snow liquid water contents are 1.59, 1.88, and 2.07 g/m<sup>3</sup>, respectively, a plot of which is shown as Figure 7.

#### 2.2.4 Supercooled Clouds

The most critical parameters associated with icing due to encounters with supercooled clouds are droplet diameter, liquid water content, and ambient temperature. The droplet diameter determines how far back the droplets will impinge on a surface (hence the size and weight of the protected surface). Liquid water content establishes the amount of ice which will accumulate (hence the energy requirements for certain types of anti-icing systems), while ambient temperature also strongly influences the energy requirement. Thus, these parameters size an ice protection system's geometry and weight, and determine its power requirements and operating penalties. In order for an estimate to be made of severity levels associated with extreme icing, data must be available on extremes of ambient temperature and liquid water content. Figures 8 and 9 show independent probability of icing temperature and liquid water content below 10,000 feet.

An estimate of severity levels associated with extreme icing in stratiform clouds based on NACA data is given by Lewis and Bergrun<sup>(12)</sup>.

(11) Riordan, P., EXTREME 24-HOUR SNOWFALLS IN THE UNITED STATES: ACCUMULATION, DISTRIBUTION, AND FREQUENCY, Special Report ETL-SR-73-4, US Army Engineers Topographic Laboratories, Fort Belvoir, Virginia, January 1973.

(12) Lewis, W. and Bergrun, R., A PROBABILITY ANALYSIS OF THE METEOROLOGICAL FACTORS CONDUCTIVE TO AIRCRAFT ICING IN THE US, NACA Technical Note 2738, Washington, D. C., July 1952

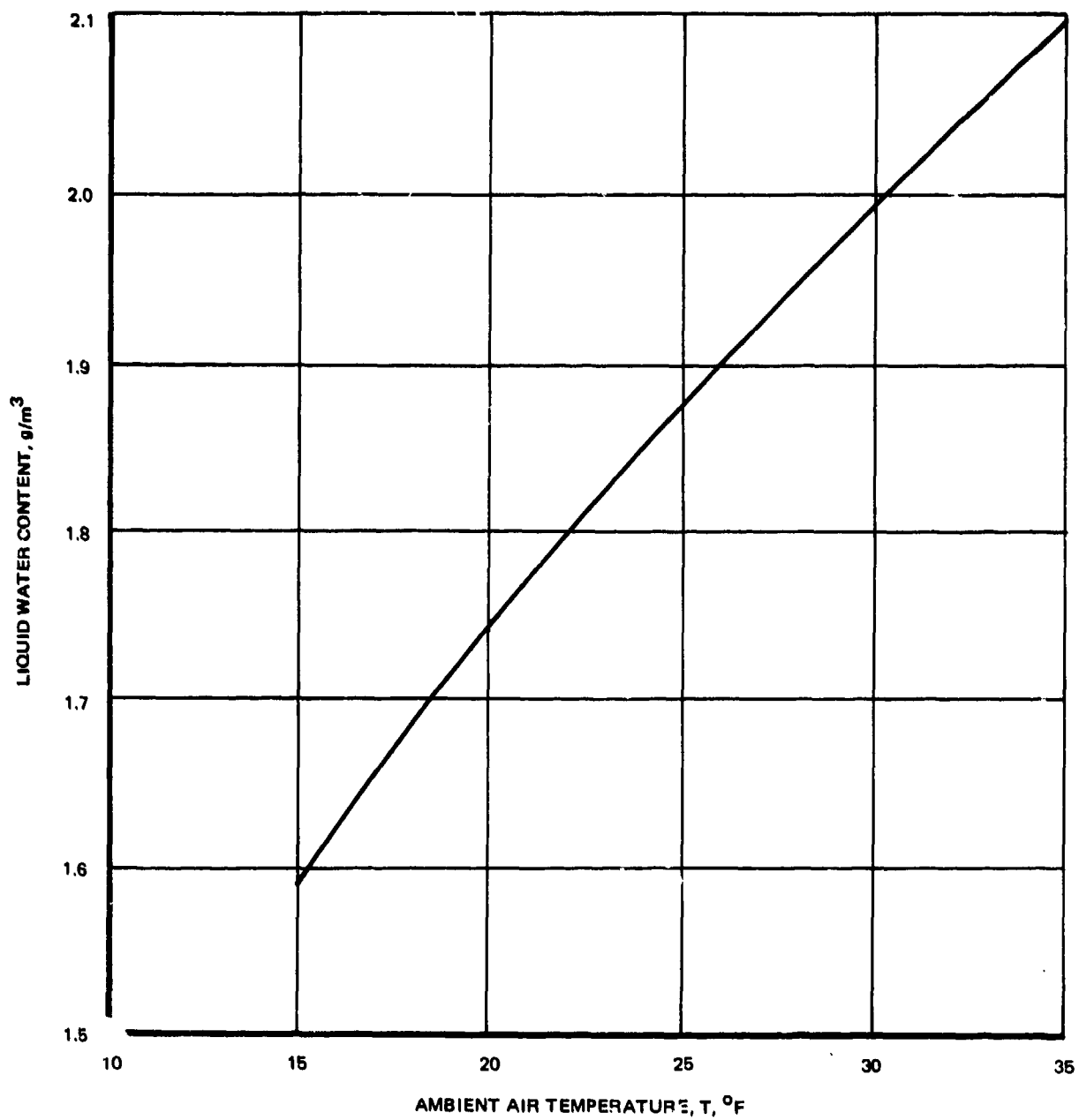


Figure 7. Worldwide Maximum Snowfall Liquid Water Criteria - 99th Percentile Conditions.

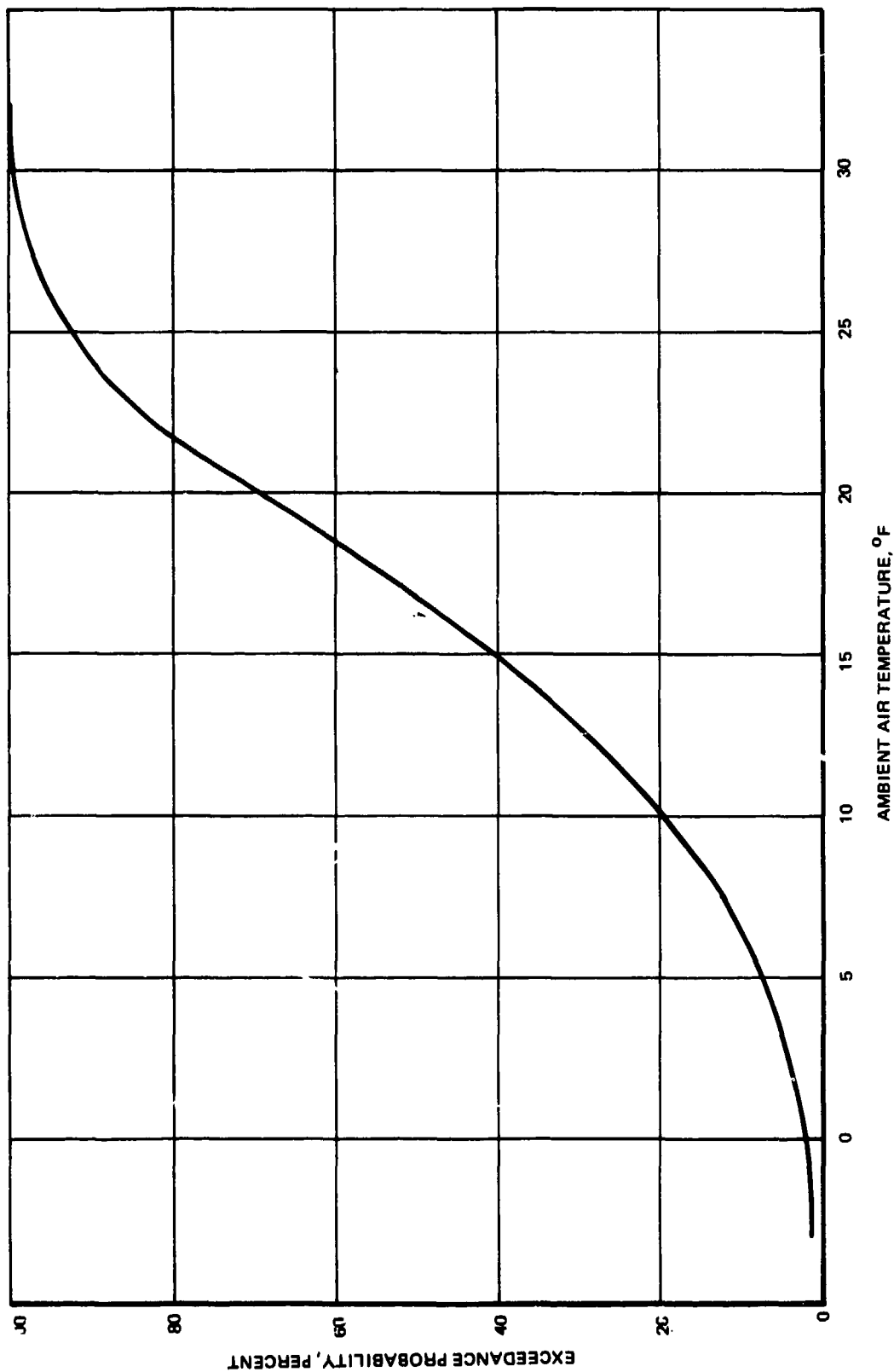


Figure 8. Ambient Air Temperature Exceedance Probability.

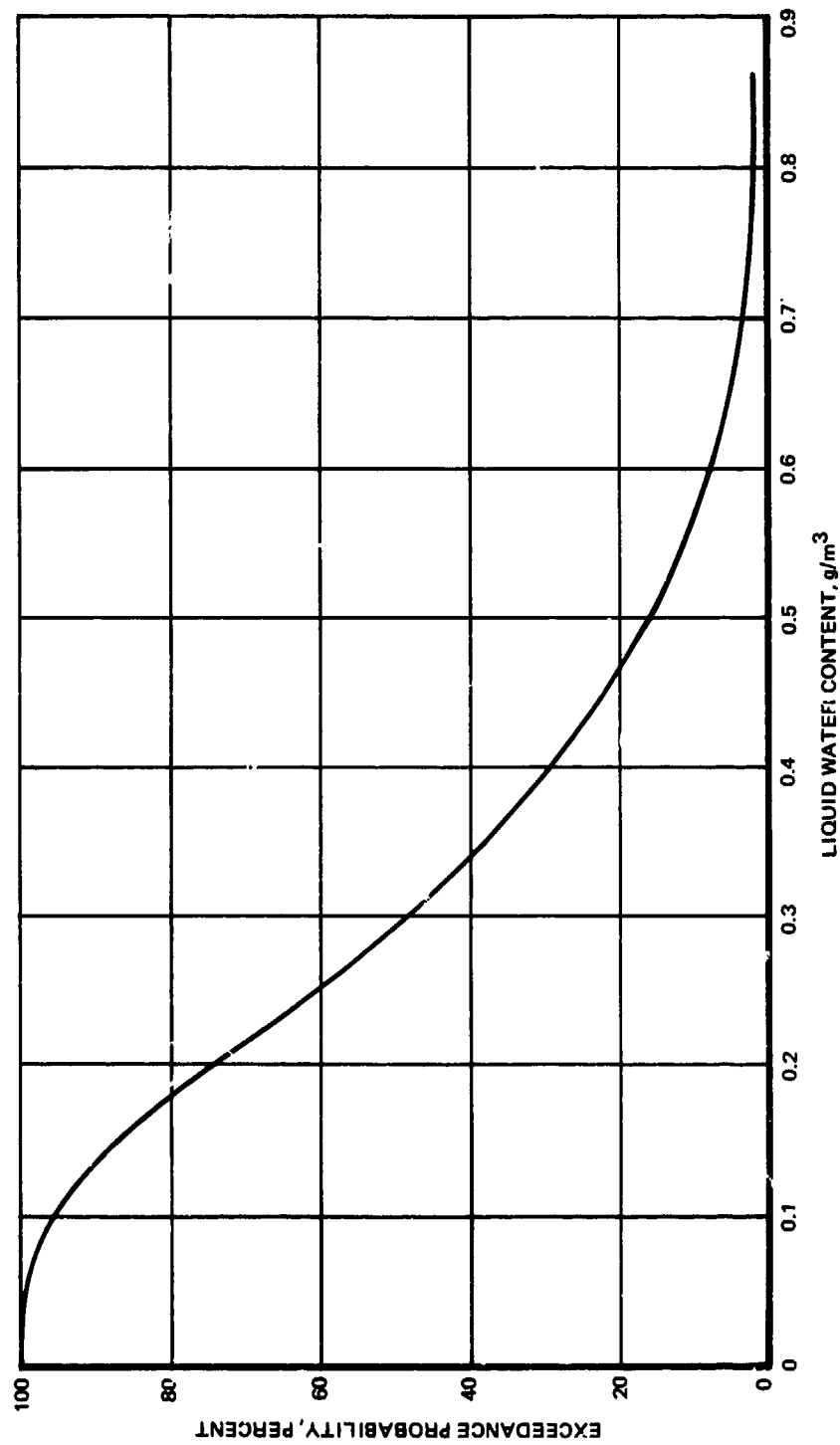


Figure 9. Liquid Water Content Exceedance Probability in Stratiform Clouds.

This estimate is compared in Figure 10 with existing criteria for continuous maximum conditions specified in FAR-25 (MIL-E-38453). The original NACA data were originally analyzed according to geographic areas of the United States. The comparison was accomplished by taking a weighted average of liquid water content for an exceedance probability,  $P_e$ , equal to 0.01 at various temperatures according to the number of observations in each geographic area (171 over the Pacific Coast, 119 over the Plateau, and 404 over the Eastern United States).

Figure 10 shows that, based on Reference (12) data, the extreme location for supercooled clouds is the Pacific Coast; and the data for this location have been used to prepare the 99th percentile as presented in Figure 11. Before the start of this investigation, it was believed that the criteria given in FAR-25 for liquid water content as a function of median effective drop size (Figure 12a) represented moderate icing. In the present study the goal is to define extreme icing in terms of conditions that have exceedance probability  $\leq 0.01$ . It has been found that the FAR-25 criteria (previously considered moderate) are, in general, more severe than the 99th percentile extreme conditions indicated by NACA data. There is no documentation relating to the ground rules upon which the FAR-25 criteria were established in the early 50's. However, informal contact with FAA Western Region personnel revealed that the FAR-25 criteria were believed to represent the 99.9 percentile severity levels.

The foregoing data for continuous maximum conditions are based upon measurements throughout the altitude range from sea level to 22,000 feet and it is not known how the statistics might be biased at the lower altitudes of primary interest for helicopter operation. Most of the data were taken during routine airline operation and thus are more representative of altitudes associated with normal DC-6, Constellation, and Convairliner cruise. Of the 443 data points reviewed, however, approximately 1 percent represent temperatures colder than  $-4^{\circ}\text{F}$  at altitudes below 10,000 feet. Therefore, it is recommended that a lower design

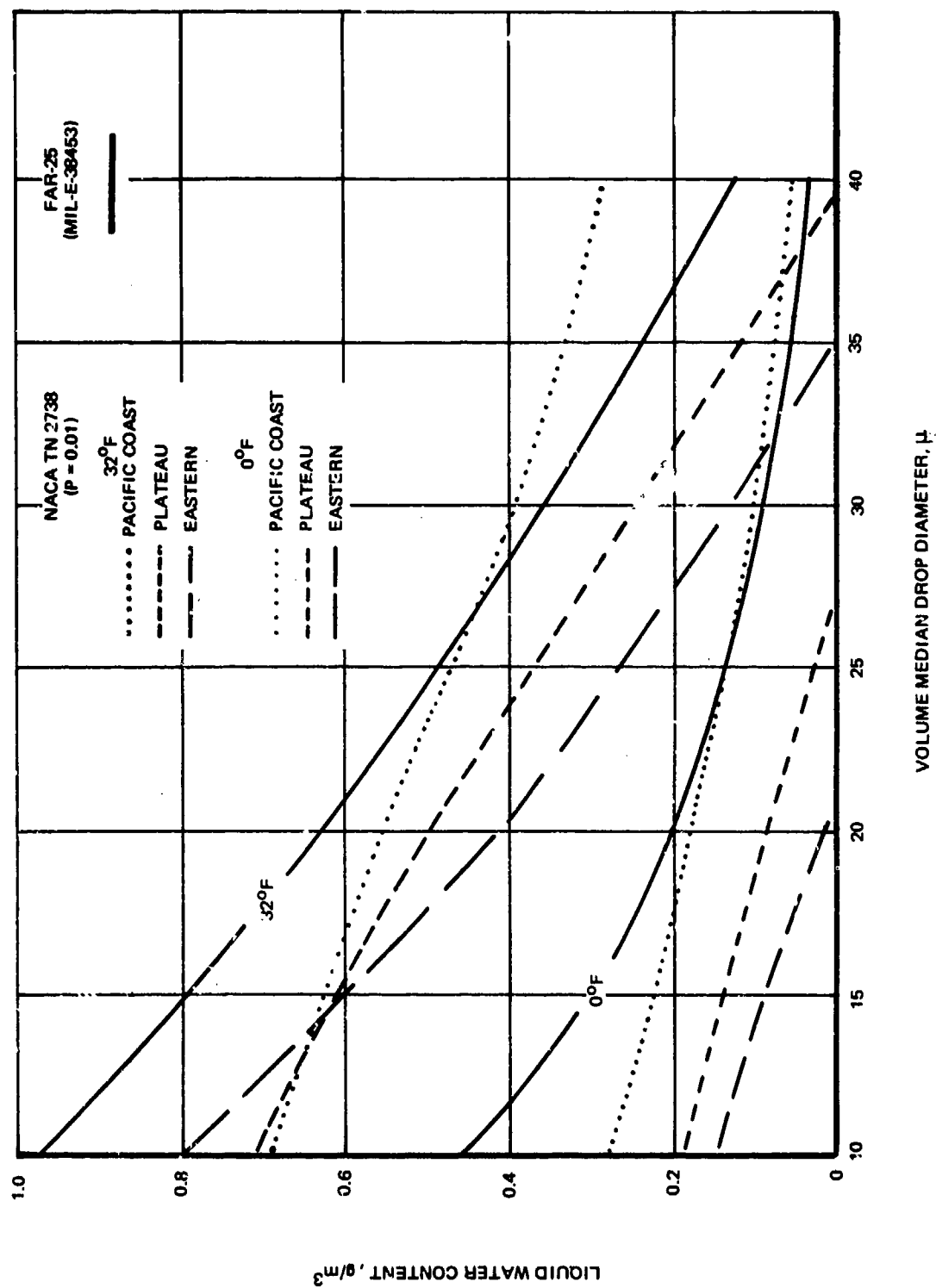


Figure 10. Icing Severity Levels for a Probability of Exceedance = 0.01, Stratiform Clouds.



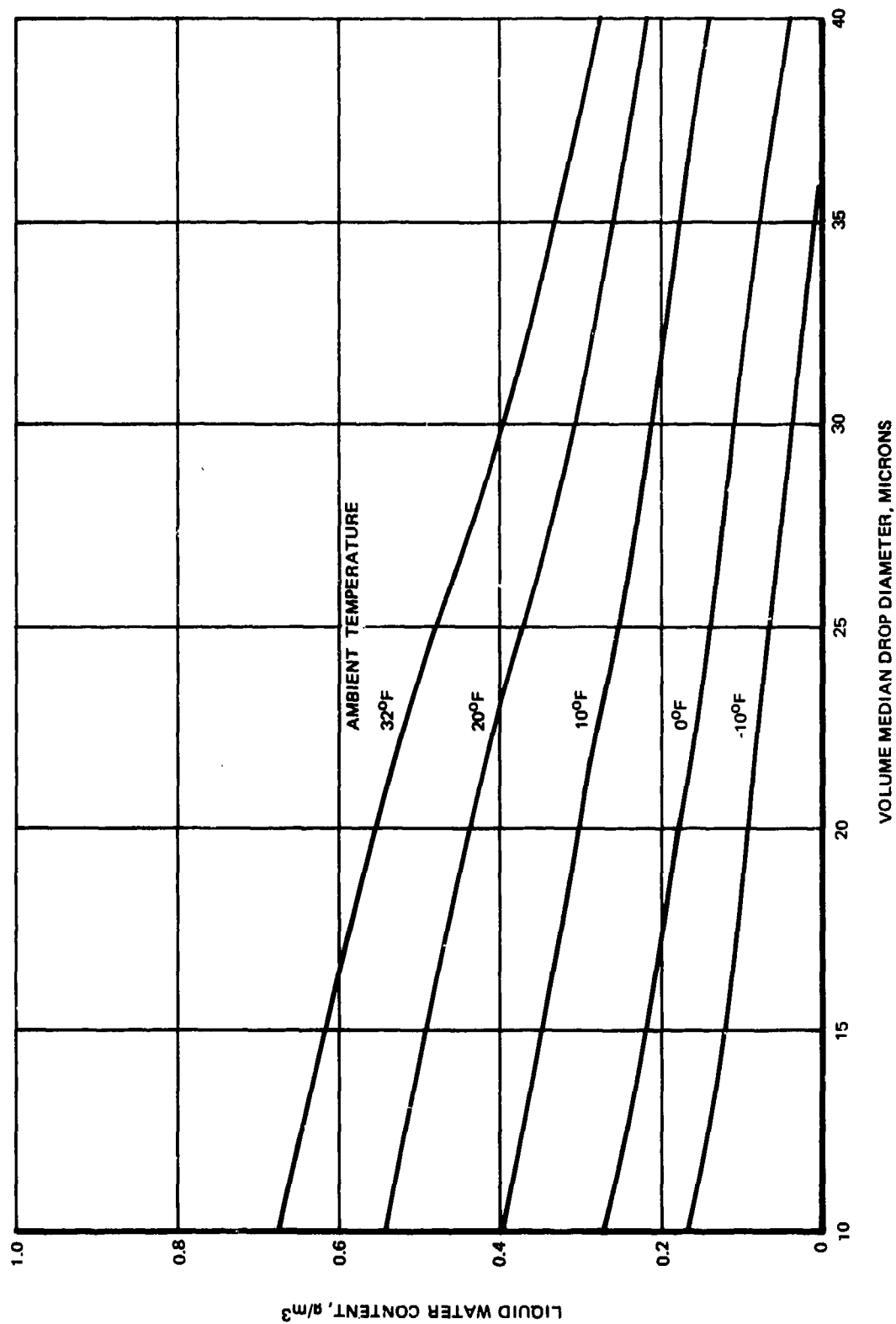


Figure 11. Icing Severity Levels in Supercooled Stratiform Clouds for 99th Percentile Criterion.

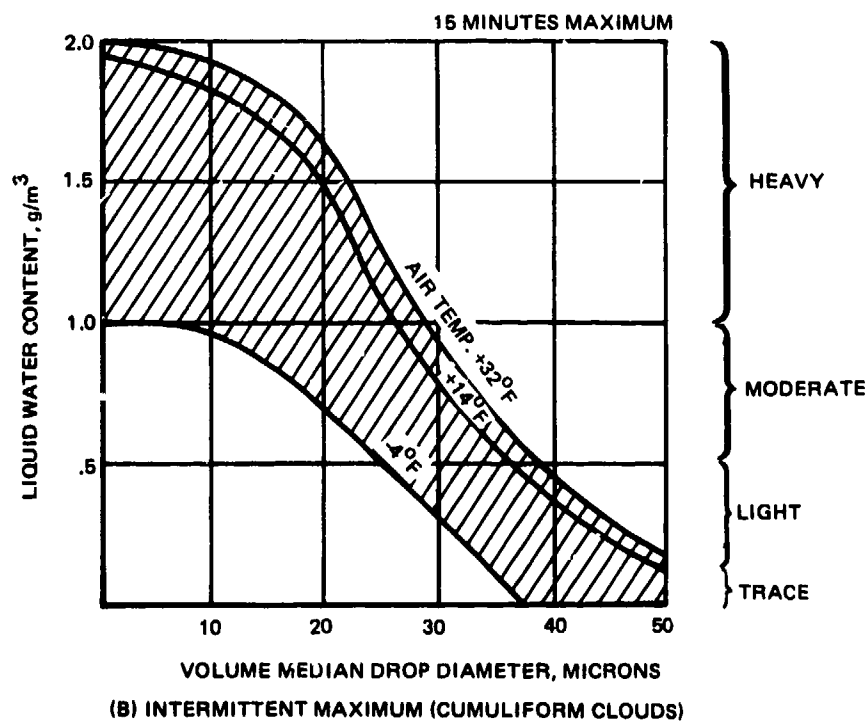
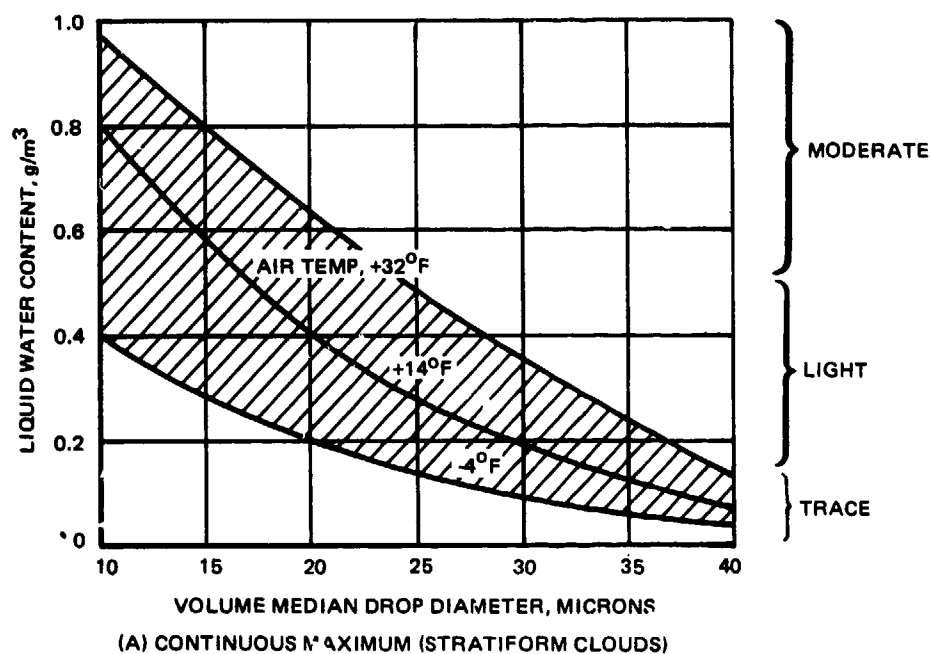


Figure 12. Recommended Atmospheric Icing Criterion.

temperature limit of  $-4^{\circ}$  F be used for helicopters. It is also recommended that a droplet size of  $40\mu$  be used in calculating impingement limits since it is slightly conservative relative to the data in Reference (12) which suggests a 35 micron maximum cloud droplet size for a 1% exceedance probability and agrees with the data in NACA TN 1424 for a 1% exceedance probability. This recommendation is consistent with AV-E-8593, and as noted in Section 4, the design penalty for this temperature compared to  $0^{\circ}$  F recommended in Reference (1) is relatively small (less than 2 percent total weight penalty increment for electrothermal deicing).

When using criteria such as shown in Figures 12a, 12b, the engineer must design the aircraft (and its ice protection systems) for any and all points within the shaded areas. It is thus necessary to examine a number of meteorological combinations to determine the critical design conditions. The maximum water catch on airfoils, for example, has been found to occur for liquid water contents corresponding to a volume median droplet diameter in the range of 15 to 20 microns (for the continuous maximum criterion). For smaller droplet diameters, the decrease in catch efficiency on the airfoil more than offsets the higher liquid water content shown in Figure 12a; and, for larger droplet diameters, the increased catch efficiency does not offset the decrease in liquid water content. (The recommended 40 micron droplet diameter for impingement limit calculations "correlates" with the 20 micron diameter for water catch calculations since a useful rule-of-thumb for natural icing is a maximum discernible cloud droplet diameter of two times the volume median diameter.)

The recommendation for the intermittent maximum icing condition (cumulus clouds) is shown in Figure 12b. This, however, is for the 99th percentile condition and was also obtained from the data in Reference (12). This criterion is well below that used in MIL-E-38453 and FAR-25. That requirement was taken from the recommendation made in NACA TN 1855 in 1949, before any statistical data were available and were based upon an assumption that a "reasonable" intermittent maximum would be 1/2 the theoretical instantaneous maximum and that a reasonable horizontal extent

would be 6 times the instantaneous value of 1/2 mile. In general, the existing intermittent maximum corresponds to a 99.9th percentile condition. It is also to be noted that TN 1855 pointed out that the maximum liquid water content would occur near the top of the cumulous clouds and suggested an altitude range of 8,000 to 30,000 feet for application at these high liquid water contents.

#### 2.2.5 Freezing Fog

Criteria pertaining to continuous icing in supercooled stratiform clouds are applicable to freezing fog because freezing fog is nothing but a supercooled cloud near or in contact with the ground. Clear and/or rime icing is associated with freezing fog to the same degree as it is associated with other supercooled stratiform clouds. The problems associated with freezing fog have not generated sufficient interest in comparison to the problems associated with other forms of icing because it occurs less frequently, and when it does occur it represents a lesser hazard because of the small size of droplets involved (less than 10 microns).

### SECTION 3

#### ADVERSE WEATHER PROTECTION TECHNOLOGY REVIEW

Reference (1) contained a broad ice protection system technology review encompassing a consideration of many types of systems. It was concluded from the study that the electrothermal cyclic deicing system offered the best possibility of being incorporated for the main and tail rotor blades. However, it was not possible to study in depth all the technology problems for the various components of the system and to quantitatively verify that the electrothermal concept is indeed the best system choice. Therefore, an in-depth review of the state of the art of ice protection technology has been performed in order to:

1. Establish suitable concepts which might be considered for rotor blade ice protection (later used in an optimization trade-off).
2. Determine the reliability of critical system components to establish development requirements and to assist in selecting the best approach for system application.

While emphasis has been placed on main and tail rotor system protection, the application of various concepts to the needs of other critical concepts such as engine inlets and particle separators, windshields, radomes, weapons, and weapon system sensors is also discussed. In addition, an evaluation of ice detectors and icing severity instrumentation is included.

This section starts with a discussion of the components requiring ice protection, proceeds to a discussion of candidate protection concepts, then the application of the concepts, and concludes with a discussion of component development requirements.

#### 3.1 COMPONENTS REQUIRING PROTECTION

Reference (1) stated that the critical components requiring ice protection generally consisted of the engine and its induction system, the windshield,

the main and tail rotor systems, and the pitot static air speed system. Engine and induction system protection are required to prevent loss in engine power, flameout, and engine damage. Windshield protection is required to assure landing and in-flight visibility, and rotor ice protection is required to prevent vehicle damage from uncontrolled self-shedding, serious vibrations resulting from asymmetrical shedding, and excessive power increases and loss in autorotational capability due to ice buildup on the blades. Pitot static protection, of course, is required to assure correct airspeed indication to the pilot for vehicle management and navigation.

Other components on a helicopter might require protection depending upon their location, functional requirements, and mission need during flight in or subsequent to an icing encounter. These include auxiliary air inlets and miscellaneous vents, guns and rockets, radar systems, infrared sensors, and cameras and other optical systems.

Cooling air inlets (e.g., oil coolers) are generally sized to provide the relatively high airflow required for hot day operation ( $125^{\circ}$  F). Therefore, a substantial blockage of the inlet can occur during icing conditions without adversely affecting the reduced (cold day) cooling requirement. Because of this, generally, it is not necessary to provide ice protection for system cooling air inlets. If, nevertheless, ice protection of auxiliary inlets becomes necessary, the engine induction system protection technology is applicable. Vent outlets normally exhaust aft and are thus not subject to direct impingement. In addition, there is an area close to the fuselage which is in a shadow zone where the water droplets are deflected away from the surface due to the airflow field around the vehicle. Because of this phenomenon, short vents (extending less than 1-1/2 inches) which are not near the nose are not likely to suffer direct impingement. Thus, these components must be examined on individual installation basis as to their vulnerability to icing. The need for protecting the other potentially sensitive components which are listed above are discussed in Sections 3.3 through 3.8.

Effective protection against the adverse hazards of freezing rain is, perhaps, the most difficult, if not an insurmountable protection technology problem. Freezing rain is encountered on considerably fewer occasions than supercooled clouds; however, on the few occasions when it is encountered, freezing rain may represent a great hazard. As a result, helicopters have not been deliberately flown in either simulated or natural freezing rain conditions.

It is important to recognize the basic characteristics of freezing rain ice formations as distinguished from those resulting from supercooled stratus clouds encounters. Review of the effects of freezing rain icing on helicopters leads to the following conclusions:

1. On aircraft exposed to freezing rain while parked on the ground, all upward facing surfaces, including those of the fuselage, rotors, canopy and windshield, and antennas, may be covered with ice deposits, the thickness of which would depend on the severity of the precipitation and the exposure duration. Coupled with severe side winds, freezing rain may even cause icing over filters, screens, and other surfaces normally not affected by this phenomenon. While holding on the ground, with the engines running in idle, freezing rain would also cause icing of the forward engine elements, if the latter are not heated. Unless there is a ground deicing spray facility available for ice clearing (using a hot water-glycol solution, such as employed by commercial airlines) it appears that use of a shelter or cover is the only means to cope with the freezing rain phenomenon on the ground.
2. Icing due to freezing rain occurs at high ambient subfreezing temperatures, with severe icing occurring only above 25° F, and virtually no freezing rain occurring below 15° F.
3. The in-flight catch efficiency of the large droplets (in excess of 400 microns) associated with freezing rain is 100 percent. Thus, theoretically, the droplet impingement limit would reach the station of maximum body thickness on the fuselage, rotors, and other affected surfaces.
4. At high angles-of-attack, in excess of 6.5 degrees, the entire lower surface of the rotor blades would be covered with ice.

5. The high subfreezing ambient temperature associated with freezing rain and the large drop sizes involved cause considerable runback in the aft direction (low freezing fraction), which may extend the ice formation to the blade trailing edge even on the upper surface.
6. To permit shedding of ice accumulated on the ground and in flight, freezing rain protection for rotor blades must be considered for the entire upper and lower rotor blade surfaces, from the leading to the trailing edge.
7. The maximum water catch rate (per foot span) due to freezing rain on an unprotected rotor blade is of the same order of magnitude as the corresponding catch rate caused by supercooled water droplets.
8. Icing, due to freezing rain, is limited to not more than 70 percent of the rotor blade span. Inboard of the 15-percent rotor span station the slow tangential velocity causes very little icing, and outboard of the 70-percent rotor span station the ram air temperature rise due to the high tangential velocity is sufficiently high to prevent icing.
9. The high subfreezing temperature of freezing rain represents a mitigating factor as far as the hazard is concerned. Rotor self-shedding of freezing rain deposits is enhanced due to the longer dwell time of the catch, in liquid form, on the surface. This facilitates the blowoff of the larger portion of catch by aerodynamic and centrifugal forces. Once frozen, the ice may shed before a significant buildup by centrifugal forces. The adhesive strength of the ice bond to the blade is relatively low at high subfreezing ambient temperatures (Figure 3 of Reference 1). Experience in supercooled cloud encounters has shown that the lower the ambient temperature the more serious the hazard. High temperature icing generally represents very little hazard because it is conducive to self-shedding. However, to establish conclusively the degree of self-shedding of ice in freezing rain, and hence the feasibility of flying under these conditions a flight test program is mandatory.

### 3.2 CANDIDATE CONCEPTS FOR ROTOR BLADES

Ice protection concepts are broadly divided into two classes: anti-icing systems, which maintain the critical surface free of ice at all times, or deicing systems, which remove ice after it is formed, either periodically or possibly at the end of an encounter. Some systems may actually be used for either mode of operation, such as thermal systems or chemical freezing point depressant systems. Thermal anti-icing can



be of either the evaporative type, wherein the entire water catch is evaporated within a discrete area determined by the droplet impingement limits, or of the running-wet type, wherein the entire affected surface is maintained at a temperature slightly above the 32° F freezing point.

Propulsion systems, windshields, and pitot static systems are always protected with anti-icing systems since the presence of any ice at any time is generally not tolerable. Aerodynamic surfaces, such as the rotor system, wings, empennage, or propellers may be safely operated with some degree of ice, and hence, deicing is an acceptable alternate for these surfaces.

Reference (1) established two systems which can be considered as technically feasible for rotor blade ice protection, either as anti-icing systems or as deicing systems. These are electrothermal and chemical freezing point depressant systems. In addition, work under the present contract has identified the possibility of using engine exhaust gas heat transferred to a heat transfer liquid circulating through the rotor blade for either evaporative anti-icing or deicing. These three basic types of systems, therefore, have been examined in depth for a determination of their application for main and tail rotor ice protection against super-cooled icing clouds and freezing rain and drizzle (Section 4).

It should be noted that Reference 1 also identified those ice protection components which are either inappropriate for rotor ice protection or have in fact been proven to have no merit. These are: pneumatic boots, which are periodically inflated to cause a major deformation of the airfoil to break the ice bond but impose unacceptable aerodynamic effects; ice phobic tapes, which are claimed to reduce the shear strength of the ice bond below the centrifugal forces but do not accomplish this because impact freezing of water droplets results in keying of the ice to the porous surface and in erosion of the tape surface; and use of bleed air for thermal anti-icing or deicing, which is in fact not available in the required quantities based upon engine manufacturers' allowance. Changing the allowable bleed quantities in existing engine designs is not feasible

because of the required bleed port redesign, great mismatch between compressor and turbine airflow, the effect on the fuel control system, and the limitation on maximum shaft power (see Section 5.3 of Reference 1). While a new engine could be designed to accommodate 10-15 percent bleed airflows, the associated power penalties (i.e., 30-35 percent loss in maximum power) would be found to be unacceptable.

### 3.2.1 Electrothermal Cyclic Deicing

With the electrothermal cyclic deicing system concept, the rotor system is allowed to build up a small amount of ice which is then removed periodically by energizing electrical heaters to heat the blade surface to 32° F. The main rotor system heaters are divided into a number of sections which are energized sequentially in order to conserve electrical power. Two ways have been explored for dividing up the heated area: chordwise shedding and spanwise shedding. In chordwise shedding, the heating elements run spanwise from root to tip, and the blade heater is divided into chordwise segments (Figure 13). In spanwise shedding, the blade heaters are divided into a number of segments spanwise (with deicing running from tip to root) and there is only one element chordwise around the blade (Figure 14). A simplified representation for a four-blade main rotor with six sections is shown in Figure 15. The insert table shows a possible heater sequence, with allowance for the tail rotor being energized twice as often as the main rotor. The corresponding schematic for the electrical system is shown in Figure 16. The tail rotor may be considered as equivalent to one segment of the main rotor.

Reference (1) identified the heater element design as a critical factor for successful system operation. The timer/controller/power distribution subsystem was also identified as a key component of a successful electrothermal deicing system. The heater element assembly is shown schematically in Figure 17. It consists of a metallic erosion shield, a dielectric material, the heater element itself, and a rear dielectric material and adhesive for attachment to the blade.

TIP END

ROOT END

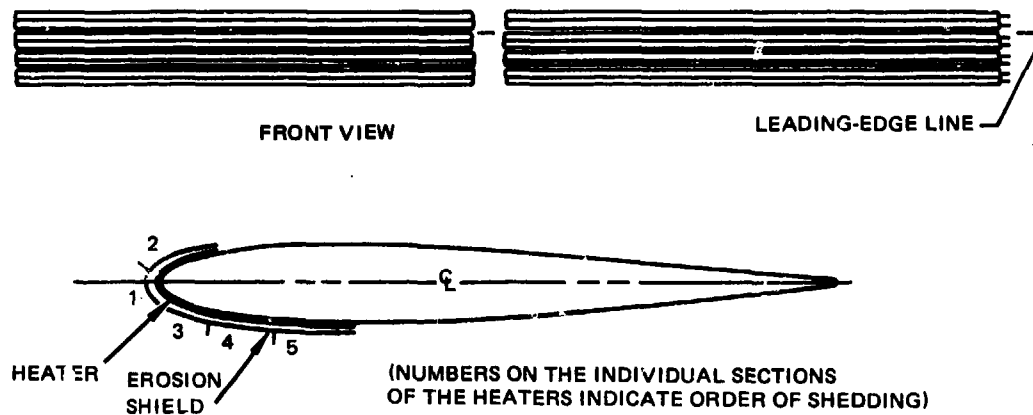


Figure 13. Spanwise Elements for Chordwise Shedding.

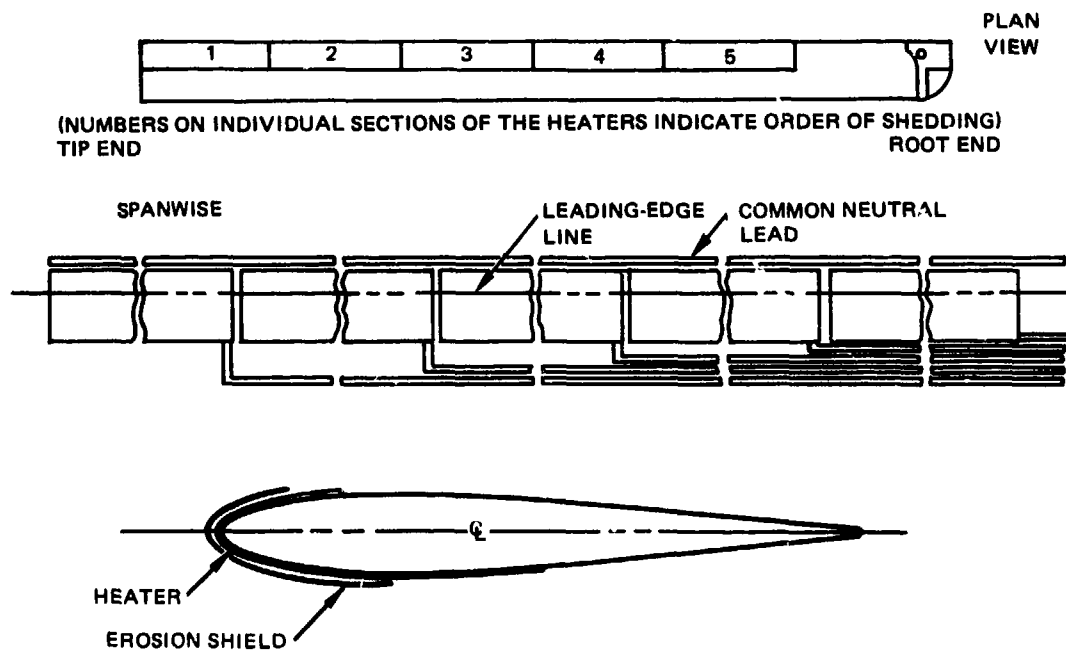
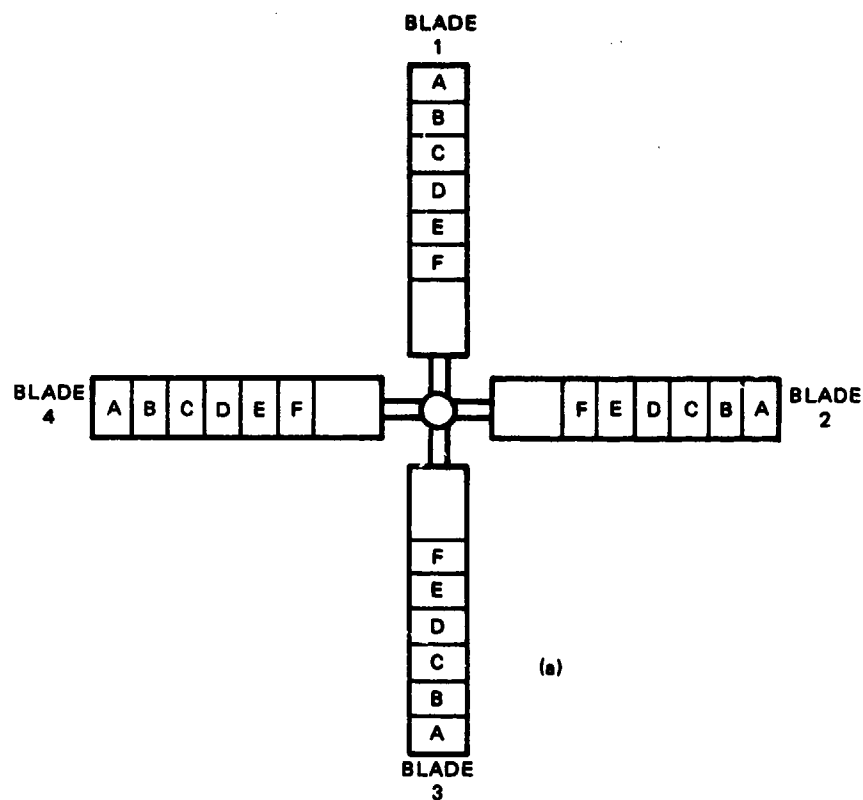


Figure 14. Chordwise Elements for Spanwise Shedding.



HEAT SEQUENCE OR PERIOD	BLADES				
	1	2	3	4	
1					TAIL
2	1A	2A	3A	(4A)	
3	1B	(2B)	3B	4A	
4	1C	2B	(3B)	4B	
5	(1D)	2C	3C	4C	TAIL
6					
7	1D	2D	3D	(4D)	
8	1E	(2E)	3E	4D	
9	1F	2E	(3E)	4E	
10	(1F)	2F	3F	4F	

(b)

Figure 15. Four Blade Rotor Deicing Sequence.

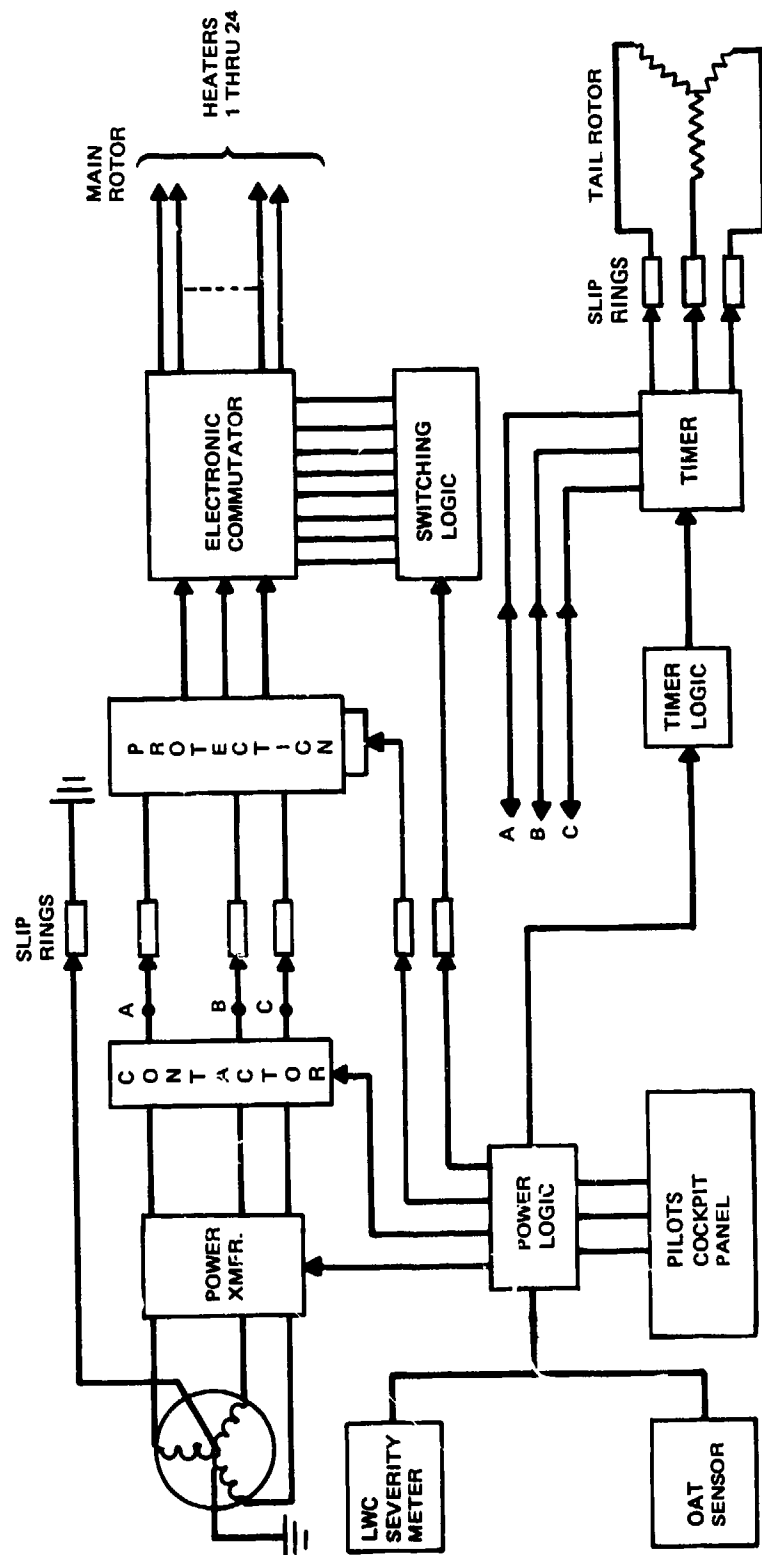
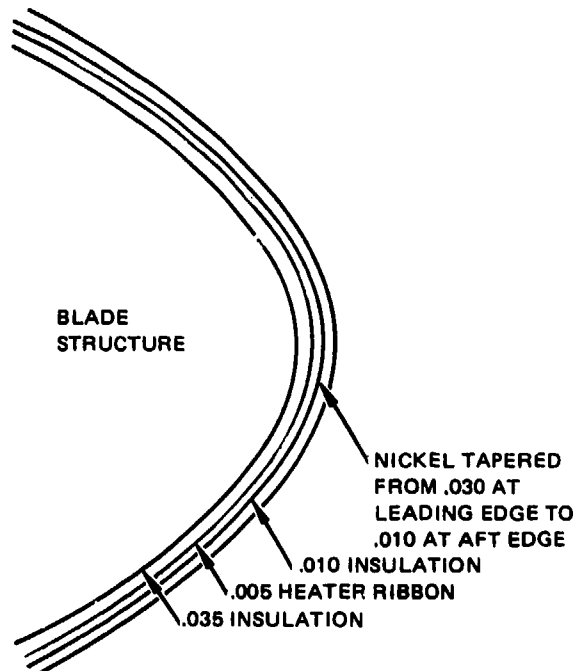
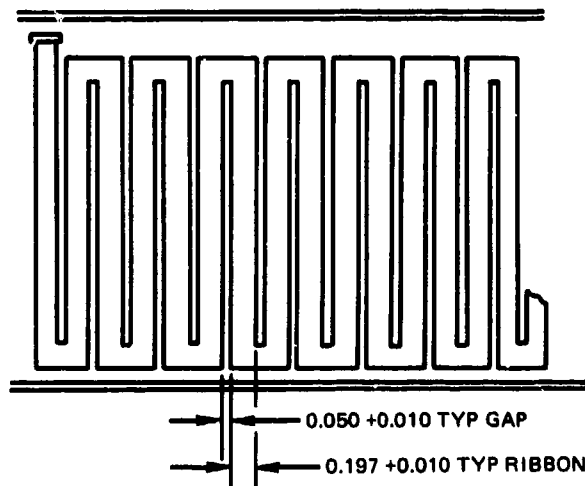


Figure 16. Deicing Control-Simplified Block Diagram.



NOTE: ALL DIMENSIONS IN INCHES.



INSTALLATION PATTERN HEATER RIBBON

Figure 17. Recommended Blade Heater Design.

Since deicing power intensities can range from 12 to 30 watts/inch<sup>2</sup>, it is necessary to use a very thin dielectric between the heater element and the surface and to use as plane a heating element as possible (along with a good thermal conductor for the erosion shield to minimize thermal gradients along the surface). As detailed in the following subsection, there are a number of structural constraints which also must be considered in the design of a successful rotor blade heater assembly, and this component has thus been identified as being the most critical item from a technology standpoint. The most critical factor in achieving successful heater assembly hardware is control of bonding and assembly processes. This involves another field of technology covering fabrication and control procedures applicable to adhesive bonded structure and fiber/resin composites. Latest techniques in this area are discussed in Paragraph 3.2.1.1.

As noted above, the timer/controller/power distribution subsystem was also identified as a component where careful design and advanced technology are a requirement. The timer/controller portion may be required to modulate the system in accordance with meteorological conditions (ambient temperature and liquid water content) and to sense all types of failure (short circuits and open circuits as well as a failure of itself). The power distributor portion must be located on the rotor hub in order to minimize the number of sliprings and wiring weight and is thus located in a very unfavorable environment, both from a weather and vibration point of view. Considerations involved in the timer/controller design are discussed in Paragraph 3.2.1.2.

#### 3.2.1.1 Blade Heater Design

The design, manufacture, and quality control of an electrothermal deicing system is actually quite complex. For production of successful hardware, careful attention must be devoted to minute details in the design and manufacture of each element of the system, including erosion shields, electrical heater elements, heater insulation, electrical sensing and control devices, and the electrical distribution system.

A review of the service record of some electrothermal deicing systems on both fixed- and rotary-wing aircraft indicates that, in general, the reliability of most of them is very poor. A majority of the service failures can be traced to poor design and selection of materials or components for the heater assembly coupled with faulty processing resulting from use of unreliable fabrication methods and lack of process control. Some of the problems which have been encountered in service relative to meeting basic design requirements are summarized in Table 2.

As a result of this experience, a detailed review of all aspects of heater design, fabrication, and assembly has been performed. As noted earlier, the heater assembly consists of an erosion shield, dielectrics, and heater element. The technology associated with each of these components and their assembly is discussed in this section.

Survey of Erosion Shield Materials - In a heater boot installation, the erosion shield material, in addition to exhibiting maximum resistance to snow, rain, and sand, must provide maximum heat transfer in a relatively short time. Therefore, in such installations a metallic shield is mandatory. The leading candidates for erosion shield metallic materials are:

Nickel - Rolled Sheet

Nickel - Electroformed - Hard

Nickel - Electroformed - Soft

Stainless Steel

Titanium.

To determine the eligible candidate erosion shield materials, a state-of-the-art survey concerning erosion shield materials was initiated. The objective of this survey was to investigate material erosion shield materials in sufficient depth to:



TABLE 2. PROBLEM SUMMARY ELECTRICAL DEICER SYSTEMS

Design or Performance Requirement	Potential Service Problems	Probable Causes
Heat uniformity	Hot spots, cold spots	<p>Variability in heating element resistance</p> <p>Voids in adhesive bondlines and insulation laminates. May occur in fabrication or by delamination in service.</p> <p>Variation in thickness of adhesive bond lines and insulation laminates.</p>
Prevent malfunction of heaters	<p>Broken element</p> <p>Short circuit in element</p> <p>Short circuit-element to erosion shield or structure</p>	<p>Thermal stress fatigue, applied stress fatigue, low strain capability, and ductility of element.</p> <p>Stress fatigue of bondlines and insulation causing voids and delamination in conjunction with moisture entry and displacement of elements under dynamic loading.</p> <p>Undetected fabrication flaws or marginal bond strength in laminates may be contributing factors.</p>
Damage tolerance and ease of repair	Damaged element or insulation	Physical damage or electrical supply malfunction.

1. Evaluate the relative durability of candidate materials in resisting rain and sand erosion.
2. Develop a bank of data sources covering configuration, structural behavior, producibility, and cost. Data concerning thickness, tapering, forming, preparation for adhesive bonding, etc., was obtained.

To be effective, an erosion shield must resist rain erosion coupled with sand and dust erosion. Also, one of the purposes of the erosion shield is to meet the tree-cutting requirement. The latter must be met without compromising the structural integrity of the blades so that no safety hazard is imposed on the aircraft. However, blade repair due to local damage of the rotor blade surface heating system may be required. In this respect the electrothermal cyclic deicing system is considerably less vulnerable than the chemical system or the liquid-heated system. With the electrothermal deicing system, damage, if any, would be confined to only one heating segment and this can be repaired relatively easily; while, with the other techniques the entire system may be lost due to loss of fluid. For the same reasons, the electrothermal system is also less vulnerable to battle damage incurred by bullets or shell fragments.

The erosion resistance of materials as reported in the literature has been determined both by suitable laboratory tests and by flight testing of materials mounted on fixed- and rotary-wing aircraft. In general, laboratory test methods are not standardized; therefore, there is no direct basis for comparison of materials from various data sources. In addition, materials which are optimum according to rain erosion tests may or may not perform satisfactorily in sand erosion tests. The rain erosion test most generally used currently employs the Air Force Materials Laboratory whirling arm tester. In this test, water drops of specified size are hurled at the test specimen at a specified velocity and angle of impingement. These variables are set to simulate a given rain condition. The erosion effects on test samples may be assessed by various methods including weight loss, area loss, and time of erosion. Sand erosion tests employ a whirling arm apparatus similar to the rain erosion apparatus described above. Alternate methods employ sand blasting

by air pressure jets. Assessment methods are essentially the same as those used for rain erosion tests. In flight testing on aircraft, material specimens are bonded to the leading edges of airfoil surfaces. Results are assessed by visual examination after various periods of exposure in flight.

In the course of this survey, it was noted that both test methods and methods for quantitatively assessing the degree of erosion vary considerably in reported investigations. In addition, the material form, method of application, the substrate on which it is applied, and material thickness all affect erosion rates. As a result, evaluation of material performance on a common basis utilizing all available data is impractical. Therefore, the data presented in this report were selected to show relative performance of materials through the use of similar test conditions, assessment methods, and thickness for a standard basis of comparison. As a result of this survey, it appears that some correlation has been established between laboratory erosion tests and flight tests in comparing relative erosion resistance of materials. However, it is evident that laboratory testing cannot be used to predict the life of erosion shields on an absolute basis. A 0.020 inch thickness has been commonly used for rotor blade application.

Selected data showing relative erosion resistance of candidate materials are presented in Tables 3, 4, and 5. These data were selected as being the most applicable to this program. Further, the test conditions were sufficiently similar to provide some basis for comparison. Examination of Table 3 covering rain erosion tests indicates that results are not too conclusive since thickness and substrate are not identified for stainless steel; and, in some cases, tests were not run to failure. The data shows, however, that by using the same assessment method, the time required to pit nickel is at least six times longer than to pit 302 stainless steel, and 13 times longer than to pit 308 stainless.

TABLE 3. RAIN EROSION RESISTANCE OF METALLIC MATERIALS

Material	Material Type	Data Source (Ref No)	Rain Erosion Resistance Standard Test Method and Test Conditions Unless Otherwise Noted: 500 mph, 1 in./hr Rainfall - Approximately 2-1/4mm Dia Droplets				Remarks
			Material Thickness (Minimum)	Substrate	Test Conditions	Test Time and Result	Other Failure Criteria
Electroformed or Electroplated Nickel	Hard	13	10 Mils	Glass/Epoxy Graphite/Epoxy Boron/Epoxy	Standard	3 hrs No Failure	
	Unidentified	14	15 Mils	Steel	Standard		Time to Pitting: 39 hrs
	Hard	15	9 Mils	Glass/Epoxy Graphite/Epoxy Boron/Epoxy	Standard	3 hrs No Failure	
	Soft	15	9 Mils	Glass/Epoxy Graphite/Epoxy Boron/Epoxy	Standard	3 hrs No Failure	
	Hard	16	10 Mils	Glass/Epoxy	Standard	1-1/2 hrs to Failure	
	Hard	16	14 Mils	Glass/Epoxy	Standard	4-1/2 hrs to Failure	
Stainless Steel Sheet	301 Full Hard	17			Rain Condition 3-1/2 in./hr	1 hr No Failure	
	302	14					Time to Pitting 5-6 hrs
	308	14					Time to Pitting 3 hrs

- (13) Schmitt, George F., Jr., RAIN EROSION BEHAVIOR OF GRAPHITE AND BORON FIBER REINFORCED EPOXY COMPOSITE MATERIALS, AFML-TR-70-316, March 1971.  
 (14) Lapp, R. R., et al., A STUDY OF THE RAIN EROSION OF PLASTICS AND METALS, WADC-TR-185, Part II, May 1955.  
 (15) Weaver, James H., ELECTRODEPOSITED NICKEL COATINGS FOR EROSION PROTECTION, AFML-TR-70-11, July 1970.  
 (16) Weaver, J. H., ELECTROPLATED NICKEL RAIN EROSION RESISTANT COATING, AFML-TR-67-356, January 1968.  
 (17) U. S. Army Report TC REC-TR-62-111, HELICOPTER ROTOR BLADE EROSION PROTECTIVE MATERIALS, December 1968.

TABLE 4. SAND EROSION RESISTANCE OF METALLIC MATERIALS (SANDBLAST TEST)				
Material	Sand Erosion Resistance Standard AFML Dry Sand Blast Test 30 PSIG Air Pressure 3-1/3 Lb/Min Sand Flow			
	Data Source (Ref No)	Material Thickness (Minimum)	Subs rate	Test Results Erosion Time Minutes Per 0.001 In
Nickel Plate - Hard	17	2 Mils	4130 Steel	0.70
Nickel Plate - Sulfuric	17	2 Mils	4130 Steel	1.00
Nickel Plate - Electroless	17	5 Mils	4130 Steel	0.10 to 0.20
Nickel - Electroformed	17	13 Mils	4130 Steel	0.80 to 0.96
301 Stainless Steel Annealed	17	5 Mils	4130 Steel	0.30
301 Stainless Steel 1/4 Hard	17	10 Mils	4130 Steel	0.45 to 0.55
301 Stainless Steel 1/2 Hard	17	10 Mils	4130 Steel	0.60 to 0.70
301 Stainless Steel Full Hard	17	10 Mils	4130 Steel	0.60 to 0.70
Titanium 6 AL-4V	17	9 Mils	4130 Steel	0.47
Titanium 13V-11 Cr-3AL	17	10 Mils	4130 Steel	0.55 to 0.65

TABLE 5. SAND EROSION RESISTANCE OF METALLIC MATERIALS (WHIRLING ARM TEST)									
Sand Erosion Resistance - Whirling Arm Tester Varying Conditions as Individually Noted									
Material	Data Source (Ref No.)	Material Thickness	Substrate	Test Conditions			Test Results		
				Air Blast Speed	Specimen Speed	Sand Rate	Time to Failure	Erosion Rate Mr./cm <sup>2</sup> 5 Min	
Electroplated Nickel (Hard)	15	12 Mils	Aluminum		530 MPH	0.75 Lb/Min	8 Min		
Electroplated Nickel (Hard)	15	12 Mils	Glass/Epoxy		530 MPH	0.75 Lb/Min	5 Min		
Electroplated Nickel (Soft)	15	12 Mils	Glass/Epoxy		530 MPH	0.75 Lb/Min	1 Min		
Electroformed Nickel	17	11 Mils	4130 Steel		600 Ft/Sec	2 Lb/Min	26 Min		1.87
301 Stainless Steel (All Hardnesses Equivalent)	17	9 Mils	4130 Steel		600 Ft/Sec	2 Lb/Min	7 Min		2.20
Nickel Plate	18	20 Mils	Graphite/Epoxy	660 Ft/Sec	1100 Ft/Sec	2 Lb/Min			2.33
Ti 6 AL - 4 V	18	-	-	660 Ft/Sec	1100 Ft/Sec	2 Lb/Min			1.91
Ti 6-2-4-2	18	-	-	660 Ft/Sec	1100 Ft/Sec	2 Lb/Min			
Ti 8-1-1 Duplex Annealed	18	-	-	660 Ft/Sec	1100 Ft/Sec	2 Lb/Min			
(18) Morris, J. S. and Wahl, M. J., SUPERSONIC RAIN AND SAND EROSION RESEARCH: EROSION CHARACTERISTICS OF AEROSPACE MATERIALS, AFML-TR-70-265, November 1970.									

Table 4 covers sand erosion tests of nickel, stainless steel, and titanium which use a sand blast method. These results show that electroformed nickel or sulfuric nickel plate are superior to all the other materials listed.

Table 5 covers sand erosion tests which use the whirling arm method and shows that electroformed nickel is superior to other forms of nickel and is approximately four-times better than 301 stainless steel, by using time to failure as the criterion. Other tests using erosion rate as the criterion show that nickel plate has a slight edge over three titanium alloys.

In summary, the predominant trend of these data indicates that nickel and especially electroformed nickel is superior to stainless steel and titanium alloys in erosion resistance.

Since electroformed nickel and 301-1/2 hard stainless steel sheet appeared to be the prime candidates for erosion shields from a performance standpoint, a brief study was made to compare producibility and cost aspects of these materials. A production cost estimate was made for fabricating and installing heater boots of both materials. The UH-1 blade was used as a model to provide a basis for comparison. Costs (for either main or tail rotors) were as follows:

- Electroformed nickel shield - \$150.00 per foot of formed heater boot
- Stainless steel shield - \$100.00 per foot of formed heater boot

Although the electroformed nickel costs more than mechanically formed stainless steel sheet, the nickel offers some advantages relative to fabrication. These are:

1. Electroformed nickel can be formed into a more complex shape than stainless steel.
2. Electroformed nickel is easily tapered in the electroforming process. It is impractical to taper stainless steel sheet in the thickness range of 0.020-inch planned for heater boot erosion shields.

These fabrication advantages could affect the design of heater boots in at least two ways:

1. By using electroformed nickel, the erosion shield could be formed in one piece, including the area over blade root end doublers, whereas stainless steel would probably be of two-piece construction to overcome forming problems due to change in contour in the doubler area.
2. By using nickel, the erosion shield could be tapered from the leading edge to the trailing edge of the boots. A suggested taper is from 0.030 inch at the airfoil zero percent line to 0.005 or 0.010 inch at the trailing edge of the erosion shield. Since thickness affects the life of erosion shields, it is readily apparent that nickel shields could be optimized by using an increased thickness at the leading edge where rain, sand, and dust erosion rate is maximum. Since it is impractical to taper stainless steel sheets, increasing thickness to increase erosion life would introduce weight, balance, and aerodynamic fairing problems.

Since electroformed nickel offers considerable promise for use in erosion shields, current industry practice relative to processes used, fabrication methods, and characteristics of materials produced have been reviewed:

1. Nickel deposited from a sulfuric acid bath produces a material having the most desirable prospects for erosion shields when compared to other nickel plating processes.
2. The fabrication method basically consists of placing a metal pattern in a tank of electrolyte. Special electrodes are then strategically placed next to the metal pattern. The nickel is deposited on the pattern at current densities determined to be optimum depending upon the type and quality of metal desired and deposition rate. Tapering of deposited nickel may be accomplished primarily by varying location and distance of electrodes relative to the part.
3. Two types of nickel have been standardized which are produced by the sulfuric acid electroforming process: (1) a hard nickel having an elastic modulus of  $30 \times 10^6$  psi and (2) a soft nickel with a modulus of  $20 \times 10^6$  psi. The hard nickel has a slightly better erosion resistance than the soft nickel (by approximately 10 percent). However, the soft nickel is believed to be optimum for both composite and aluminum helicopter blade erosion shields because of the lower modulus coupled with higher total strain capability (6-12 percent elongation vs 3-6 percent for hard nickel). In addition to these two types of nickel, an intermediate modulus nickel can be obtained with some development.



Based on the above, the soft type of nickel was selected for heater development described in Section 5.

Survey of Heating Element Configurations - There are five prominent types of electrical resistance heating elements which have been used for deicing systems on airfoils and have some service history. These are:

1. Etched metal foil grid
2. Sprayed metal grid
3. Knitted metal wire/glass fabric
4. Pierced, expanded metal grid
5. Wires embedded in rubber

The etched metal foil grid most commonly employs stainless steel foil. The element is fabricated by bonding the foil to a backing of glass fabric/resin laminate and then etching the metal to form a pattern of continuous conductor ribbons by using a masking technique (Figure 17). The sprayed metal grid is usually formed from a copper-manganese aluminum alloy. It is fabricated by spraying melted metal on a glass fabric/resin laminate backing to form a pattern of conductor ribbons again using a masking technique. The knitted fabric type incorporates nichrome wire interleaved (in one direction) with glass yarn to form a fabric with a prescribed electrical resistance. The pierced, expanded metal grid usually is constructed of inconel sheet. This is fabricated by using standard expanded metal techniques. The sheet metal is pierced in the required pattern; the metal is then mechanically stretched to expand the sheet size and form an open grid of ribbon conductors of the prescribed density.

In all types, except the wires in rubber, the metallic conductor element is sandwiched between plies of glass-fabric-reinforced plastic to form an electrically insulated heating element.

Typical aircraft employing electrothermal deicing together with the specific application and types of heating elements used are listed in Table 6.

Service experience with the five types of heating elements is summarized as follows:

Etched Metal Grid - This type has been in service on the P-3 airplane for over 15 years; the reliability record is outstanding and service problems are minimal.

TABLE 6. TYPICAL AIRCRAFT APPLICATIONS OF ELECTROTHERMAL DEICING SYSTEMS		
Aircraft	Application	Type of Heating Element
CH-46 Helicopter	Main Rotor Blades	Sprayed Metal Grid and <sup>(1)</sup> Knitted Wire/Glass Fabric
UH-2 Helicopter	Rotor Blades	Wire Embedded in Rubber
F-104	Engine Inlet	Sprayed Metal Grid
C-141 Transport	Empennage	Expanded Metal Grid
P-3 ASW Patrol	Empennage	Etched Metal Grid
(1) Both types used on different serial aircraft since two different contractors were involved in heater fabrication.		

Sprayed Metal Grid - This element has been used for cyclic deicing on the British Bristol Britannia and Vickers Vanguard fixed-wing aircraft (but without metal erosion shields) for a number of years. Rotary-wing experience has been on experimental Wessex aircraft, an experimental Bolkow BO-105 and the CH-46. The best information available concerning the performance of this element type on CH-46 helicopter blades indicates that all installed deicing systems are inoperative and abandoned because of frequent short circuits and burned-out heaters. The cause of this condition has been identified as cracked nickel plated stainless steel erosion shields.

Expanded Metal Grid - This element type is performing satisfactorily on C-141 aircraft and is reported to have an MTBF of 171,000 hours.

Knitted Wire/Glass Fabric - This type of element has been used for deicing on Beech models 65 and 80 business aircraft. is just entering production on the Canadian CH-S' 2 helicopter, and was on half of the CH-46 aircraft. As noted above, the CH-46 system has been deactivated. There has been no way to distinguish reliability differences between the sprayed metal and the knitted wire design since the deicer problems are attributed to the basic boot construction.

Wire Imbedded in Rubber - Use of this element has given rise to numerous short circuits to blade and erosion shield. The general problem of burnouts is due to extreme wire temperature causing charring of the rubber.

Rationale for Selection of Type of Heater Element - The heating element performance goals are:

1. Uniform Heating - The electrical resistance of the heating element must be controlled within close limits throughout the element. This is a function of dimensional control of conductor cross section and variability in the resistance of conductor material. The conductor material must also be stable with little change in resistance with time in service.
2. Thermal Efficiency - the configuration of the heating element must be such as to allow the closest possible placement to the erosion shield. It should also provide the closest approximation to a uniform source (i.e., a continuous film would be ideal).
3. Durability - This is primarily a function of resistance to static and dynamic loading transferred to the element from blade structure or loading induced by differential thermal expansion. To resist these loads, the base conductor material and the element configuration must have sufficient fatigue resistance to preclude premature fracture cause by cyclic thermal and applied stress.
4. Damage Tolerance - Damage is normally conceived as being deformation caused by impact of foreign objects, hail, ground vehicles, etc. To resist this type of damage, the heater element material and configuration must have high ductility or strain capability and resilience (toughness) associated with high energy absorption under impact loading.
5. Repairability - To satisfy this design goal, the element material and configuration must be such that broken conductors and heating elements may be easily exposed and spliced by soldering techniques.
6. Adaptability to Advanced Rotor Blade Configurations - In general, advanced rotor blades being considered will be constructed of fiber/resin composites such as glass/epoxy, graphite/epoxy, or Kevlar 49/epoxy. These blades will generally be characterized by lower stiffness than metal blades. The characteristic of a heater element required for compatibility with composite blades is high strain capability (elongation) discussed above for resisting static and dynamic loading.

Due to time and economic constraints it was impractical to conduct an experimental evaluation of heater element types in this program. Therefore, the approach employed was to select the type of heating element based on industry and the contractor's experience. This decision was considered necessary in order to concentrate on optimizing one type of construction for rotor blades in the preliminary development work discussed in Section 5.

Deactivation of the electrothermal cyclic deicers on the rotor blades of the CH-46 was prompted by short circuits due to water entering the assembly because of numerous cracks in the nickel plated stainless steel erosion shield. The CH-46 blades featured sprayed metal grid heaters on one half of the fleet and knitted wire/glass fabric heaters on the other half. There is no known difference in the service record of one method over the other, and the fundamental reliability problem was due to the structural incompatibility of the erosion shield with the basic blade. In any survey of service experience it is very difficult to pinpoint causes of failure because of lack of detailed data. This contractor's early experience indicates that service failures can also be traced to defects stemming from inadequate quality control of fabrication processes as opposed to inadequate features inherent in the design. There is, of course, an interplay between design and practical fabrication control. Therefore, in addition to the survey of experience, an analysis of the merits of each type of heating element relative to performance goals was made to further assure selection of the optimum type for this program.

With the requirements and desired characteristics in mind as discussed above, a comparison of candidate heating elements is made in Table 7. Based on this comparison and on operational experience records, the etched metal foil grid element was selected as optimum to meet performance goals of this program.

Application of Heater Blanket to Composite Rotor Blades - The application of electrothermal deicing concepts to advanced composite rotor blade designs was investigated to determine the structural compatibility.

TABLE 7. COMPARISON OF HEATING ELEMENT CHARACTERISTICS

Characteristic	Type of Heating Element				
	Etched Metal Foil Grid	Sprayed Metal Grid	Wire	Pierced Expanded Metal	
Conductor material (conventional)	302 stainless steel	Copper-manganese-aluminum alloy	Nichrome wire	Inconel	
Conductor shape	Ribbon	Ribbon	Round wire	Intersecting ribbons-deformed	
Dimensional control of conductor cross-section (electrical resistance control)	Foil thickness tolerance rigidly controlled in rolling process. Ribbon width controlled by accurate photo-chemical masking process.	Thickness control depends on skill of operator plus frequent testing. Ribbon width controlled by paper or tape masks.	Wire can be procured with close tolerance	Grid density subject to considerable variation in expanding process.	
Ductility and strain capability (resistance to thermal stress plus static and dynamic loading)	Stainless steel is a structural sheet material with high ductility and strain capability.	The sprayed alloy is a weak, cast material with very low max. elongation and low ductility.	Nichrome wire is not normally used structurally. Has low max elongation and low ductility.	Inconel is a structural sheet material with high ductility and strain capability.	
Fatigue resistance	Stainless steel sheet - very good.	Cast brittle metal -	Brittle material -	Inconel sheet - very good.	
Damage tolerance	Stainless steel is very impact resistance due to high ductility.	Cast metal is brittle with very little impact resistance.	Elongation of nichrome is low, fracture on impact can be expected.	Inconel is very impact resistant due to high ductility.	
Amenability to repair	Flat element ribbons can be exposed and spliced by soldering foil across break.	Flat element ribbons can be exposed. Material is difficult to solder and match resistance with foil splice resulting in high resistance splice.	Difficult to expose broken wires. Use of foil to splice wires - difficult to solder and may result in high resistance joint.	Deformed ribbons difficult to expose. Also difficult to splice deformed element with flat foil resulting in high resistance joint.	
Adaptability to advanced fibrous composite rotor blades	High ductility and strain capability make adaptability very possible.	Low ductility and strain capability make probability of success low.	Low ductility and strain capability make probability of success low.	High ductility and strain capability make adaptability very possible.	
Thermal efficiency	Flat conductors and wide ribbon allow uniform heating and close approach to surface.	Uniform heating possible, but production process not amenable to thin dielectric next to erosion shield.	Use of 40-50 wires/inch allows uniform heating, but wires require substantial distance from erosion shield. Wire laid in rubber generally 10-15 wires/inch and large thermal gradients result.	Similar to etched foil.	

Advanced composite designs consist of unidirectional fibers oriented to provide optimum rotor blade characteristics. Of the fiber reinforcements currently available, three materials in particular offer the greatest potential for use on rotor blades when mechanical properties and economic factors are considered. These materials include: 'S' Glass, Kevlar 49, and Thornel 300. The mechanical and physical properties of unidirectional laminates constructed of these materials are given in Table 8.

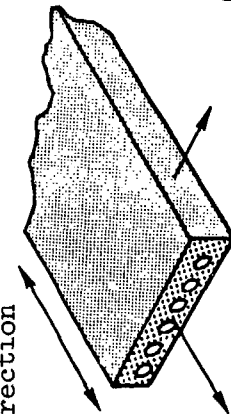
The rotor blade selected for design utilizing advanced composite materials is the UH-1H main rotor blade, since it is the blade being utilized in the deicer blade flight test program. The design criteria established for the composite blade specifies matching the mass and stiffness distributions (with the deicer boot installed) with that of the existing metallic blade design. This criterion guarantees no changes in the dynamic response of the main rotor and therefore permits the use of rotor loads from the metallic design. The rotor blade design criteria dictate the requirement for high longitudinal and high torsional stiffnesses in the basic blade. The use of laminates which contain appropriate proportions of 0-degree laminae and +45 degree laminae will satisfy this requirement and will provide a composite design sufficiently optimum for preliminary design purposes.

A number of blade configurations were developed for evaluation, and the configuration selected is shown in Figure 18; it utilizes all the advanced composite materials shown in Table 8. This design satisfies the design criteria by providing the required mass and stiffness with the addition of the deicer boot assembly.

The results of the design analysis indicate that there are two areas of concern in association with the electrothermal deicing concept currently under consideration. These areas are directed to the use of a continuous metallic erosion shield and include:

- Residual stresses due to thermal expansion incompatibilities
- Operating stresses for strain compatibility (cyclic fatigue)

TABLE 8. STRUCTURAL PROPERTIES OF SELECTED COMPOSITE MATERIALS

Fiber Direction		Units	Interm. Mod. Graphite/ Epoxy $V_F = 60\%$	FRD 49/ Epoxy $V_F = 60\%$	S-Glass/ Epoxy $V_F = 63\%$
Longitudinal	Transverse				
Tension Modulus, Longitudinal		million psi	17.2	11.91	7.99
Tension Modulus, Transverse		million psi	1.21	0.64	2.69
Poisson's Ratio, Longitudinal		-	0.21	0.325	0.25
Shear Modulus, In-Plane		million psi	0.63	0.40	0.80
Tensile Strength, Longitudinal		thousand psi	225.4	171.6	276
Tensile Strength, Transverse		thousand psi	7.3	1.58	9
Compressive Strength, Longitudinal		thousand psi	159.1	38.98	100
Compressive Strength, Transverse		thousand psi	35.3	9.36	29.3
Shear Strength, In-Plane		thousand psi	17.9	11.87	13.4
Density		lb/in. <sup>3</sup>	0.055	0.048	0.071
Coeff. of Thermal Expan., Long.		in./in./°F°	0.3	-1.6	3.6
Coeff. of Thermal Expan., Trans.		in./in./°F°	14.4	18	12.1

Note:  $V_F$  = Percentage of fiber in composite, by volume

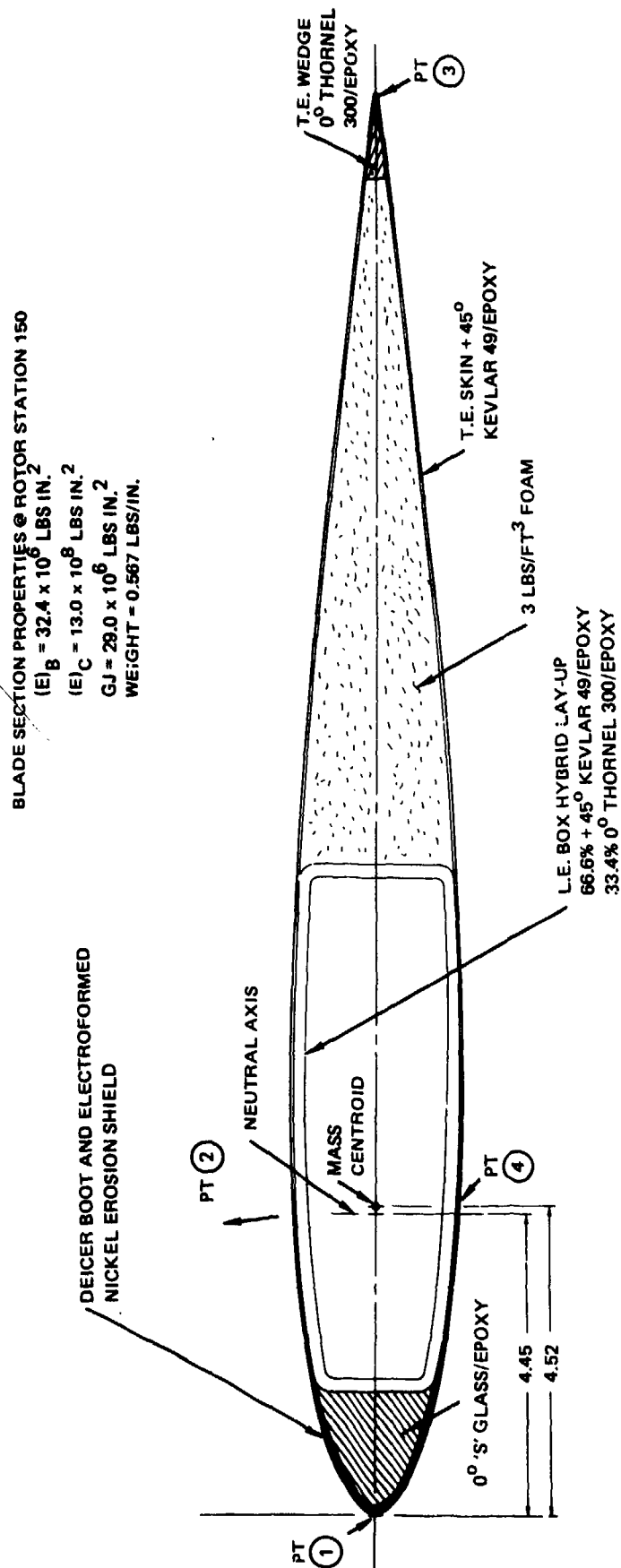


Figure 18. Conceptual UH-1H Main Rotor Composite Blade Design.



The analysis further indicates that the electrothermal deicing element itself is compatible with advanced composite rotor blade designs.

The residual stresses are due to the differences in the thermal coefficients of expansion of the erosion shield material and the composite laminate material, and are developed during the bonding of the deicer/erosion shield to the composite blade. The thermal coefficient of expansion associated with advanced composite laminates is shown in Figure 19 in conjunction with values associated with candidate erosion shield materials. As shown in this figure, the thermal coefficients of composite materials are considerably lower than the erosion shield material values. This will lead to residual tensile stresses in the erosion shield due to the elevated temperature cure cycle and compressive stresses in the composite material. The magnitude of the residual stress levels depends on each of the following parameters:

- Bonding temperature of the assembly
- Operating temperature of the blade
- Relative amounts of composite and metallic materials
- Lamina orientation of the composite.

A thermal stress analysis performed on the blade design shown in Figure 18 indicates a residual tensile stress in the nickel erosion shield of 23,800 psi. The analysis assumed a curing temperature of 250° F with bonding occurring at 180° F, and a blade operating temperature of 70° F.

As mentioned previously, another area of concern has to do with the magnitude of the operating stresses in the erosion shield due to differences in moduli of elasticities. Since the modulus of the composite lamina is lower than the modulus of the erosion shield material, the erosion shield will be subjected to higher stress levels than the composite materials. In order to maintain strain compatibility, the stress levels will be directly proportionate to the modulus of the materials.

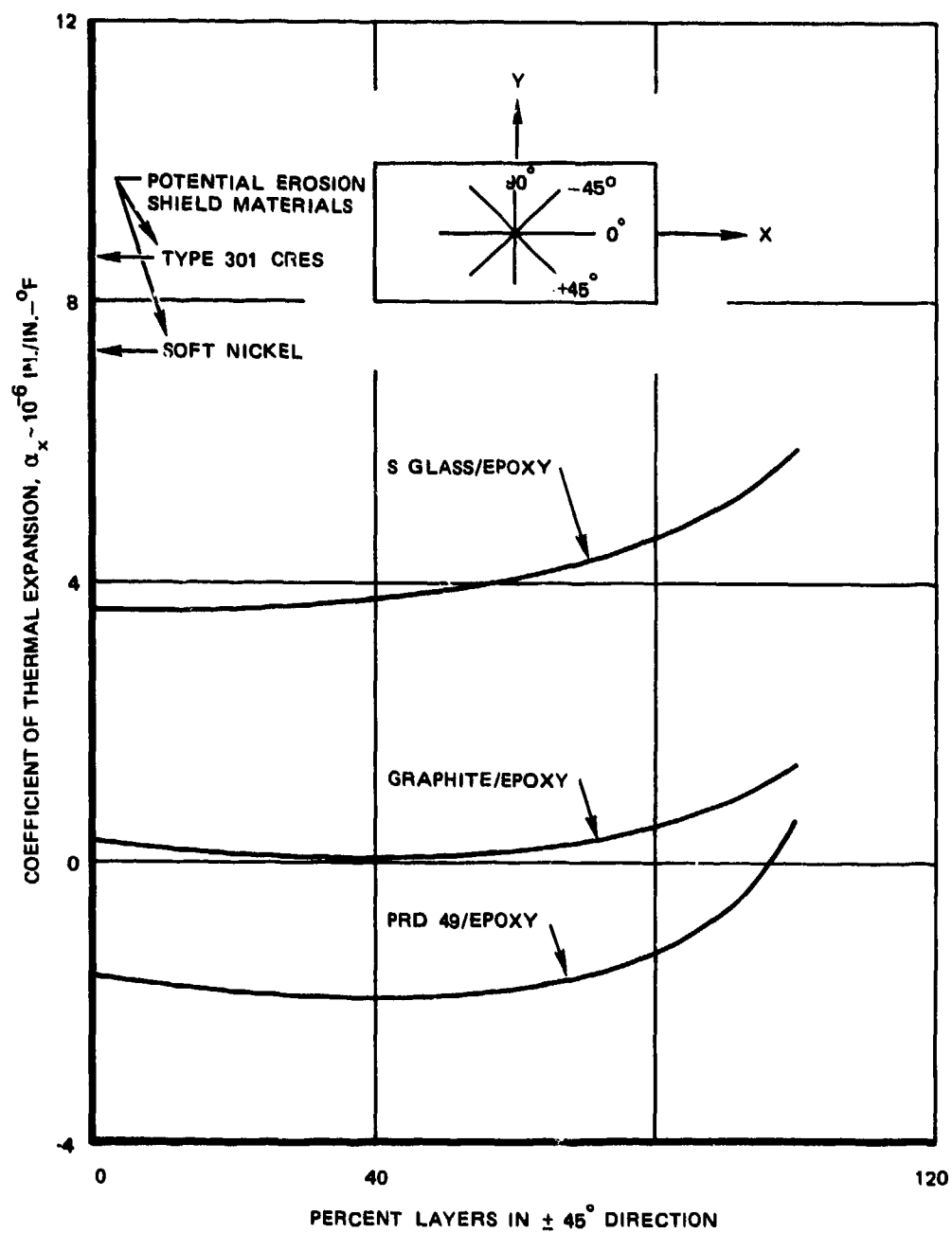


Figure 19. Coefficient of Thermal Expansion for Laminate Family.

Since composite materials generally exhibit fatigue characteristics superior to metals, and since metals operate at higher stress levels due to the differences in moduli (and due to thermal expansion effects), the erosion shield becomes the critical element in the assembly. However, the actual effect on fatigue life can be assessed only for a given rotor blade design and blade operating stress levels. To this end, a stress analysis of the advanced composite rotor blade design shown in Figure 18 at Rotor Station 150 (UH-1H Blade Station) was conducted by utilizing the fatigue loadings shown in Table 9. These spectra of fatigue loadings are representative of loadings experienced by the UH-1H rotor system for both 1-g symmetrical flight conditions and transient maneuver conditions (See References (19) and (20)). The stress levels at various locations on the blade section (see Figure 18 for locations) for these loadings are given in Table 10. A comparison of these stress levels with fatigue allowables associated with the materials used in the blade design (see Figure 20) indicate fatigue life well in excess of that indicated for the existing metallic blade design. Therefore, by proper blade design the electrothermal deicer concept currently being considered will be structurally compatible with all-composite rotor blade designs as it is with the all-metal blade configurations.

#### Manufacturing Process Control and Quality Assurance of Heater Assembly -

Examination of Table 2 indicates that many of the service problems encountered in the past regardless of the heater design are traceable to faulty laminating processes and fabrication procedures used in producing heater-assemblies, in addition to poor design. Inadequate control of processes employed for adhesive bonding and laminating of the glass fabric/resin insulation results in voids, porosity, and delamination occurring either during processing or under service conditions. Prevention of such flaws is very critical in the development of a successful

- 
- (19) J. R. Garrison, "Load Level Test of UH-1D Helicopter in 48 Foot Diameter Main Rotor Configuration" Bell Report 205-099-049, April 27, 1964, Volumes I-IV.
  - (20) J. R. Garrison, "Structural Demonstration of 48 Foot Diameter Rotor on a UH-1D Helicopter" Bell Report 205-099-058, May 13, 1964, Volumes I-IV.

TABLE 9. ROTOR BLADE DYNAMIC LOADS @ UH-1H R.S. 150.0

Cond No	Centrifugal Force	Beam Bending Moment		Chord Bending Moment	
		Steady	Cyclic	Steady	Cyclic
	lb	in.-lb			
1	63,000	-898	11,139	4,669	115,997
2	63,000	-43	9,235	14,840	126,494
3	63,000	1,659	9,319	27,966	149,618
4	63,000	-3,000	9,000	31,000	39,000
<p>Conditions 1, 2 and 3 are transient maneuver conditions</p> <p>Condition No. 4 is a 1-g symmetrical Flight condition</p>					

TABLE 10 STRESS LEVELS IN BASIC BLADE @ R.S. 150.0

Load Cond	Point ①		Point ②				Point ③		Point ④			
	$f_1$ ksi	$f_2$ ksi	$f_1$ ksi	$f_3$ ksi	$f_4$ ksi	$f_4$ ksi	$f_3$ ksi	$f_4$ ksi	$f_1$ ksi	$f_3$ ksi	$f_4$ ksi	$f_4$ ksi
1	46.2± 8.6	9.0±3.2	46.6±8.3	22.8±8.3	1.6±0.6	1.6±0.6	20.8±29.6	1.5±2.1	45.2±8.3	21.4±8.3	1.5±0.6	
2	46.8± 8.7	9.2±3.5	46.0±6.8	22.2±6.8	1.6±0.5	1.6±0.5	18.3±32.2	1.3±2.3	45.8±6.8	22.0±6.8	1.6±0.5	
3	47.8±10.2	9.6±4.1	44.7±6.9	20.9±6.9	1.5±0.5	1.5±0.5	15.0±38.0	1.1±2.7	47.1±6.9	23.3±6.9	1.7±0.5	
4	48.0± 2.7	9.7±1.1	48.1±6.4	24.3±6.4	1.7±0.5	1.7±0.5	14.2± 9.9	1.0±0.7	43.7±6.4	19.9±6.4	1.4±0.5	
Stress levels shown are $f_{steady} \pm f_{vary}$												
$f_1$ - Stress in Nickel - Steady stress includes thermal residual stress of 23,800 psi												
$f_2$ - Stress in O'S Glass Epoxy												
$f_3$ - Stress in 0° Thornel 300 Epoxy												
$f_4$ - Stress in ±45° Kevlar 49 Epoxy												

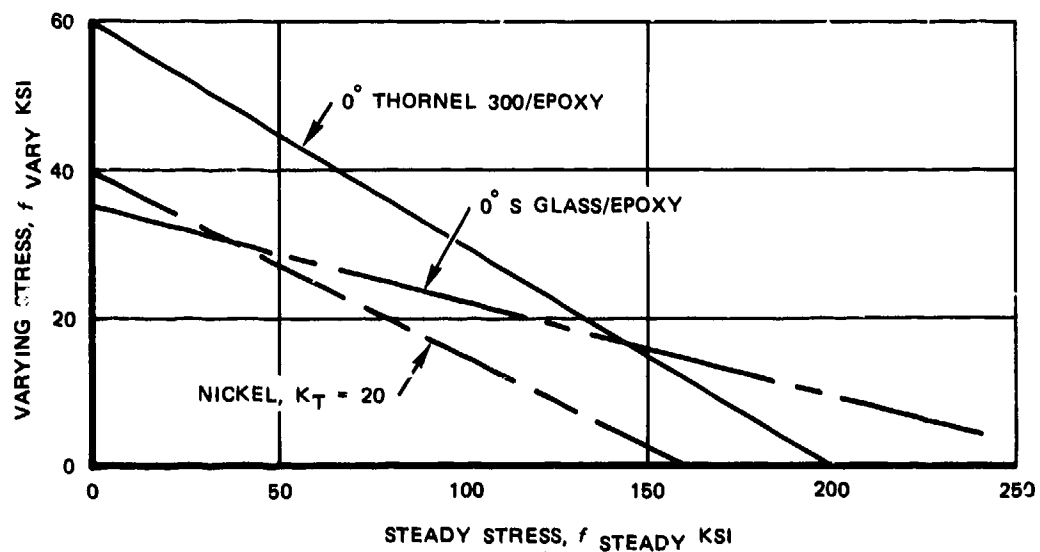
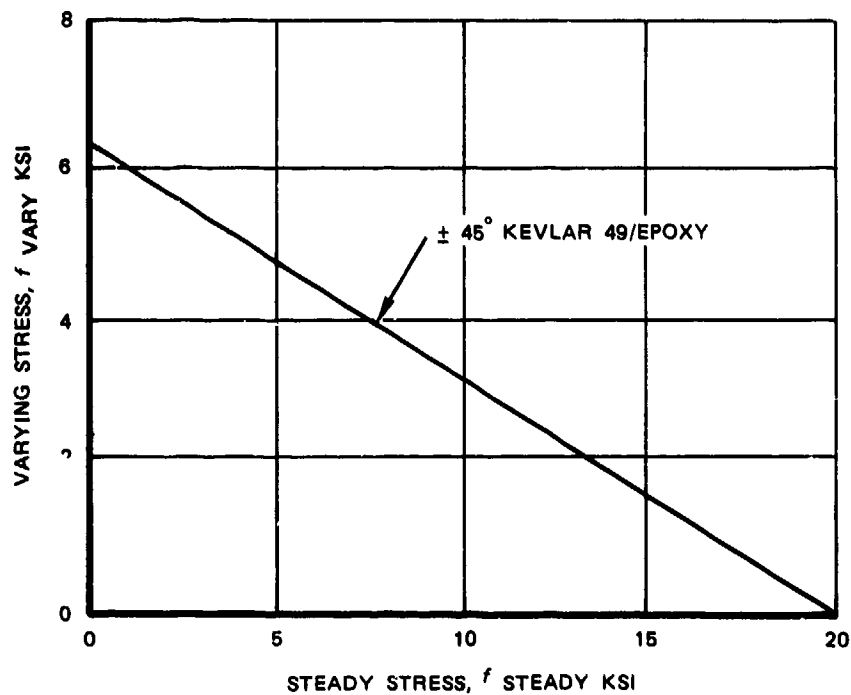


Figure 20. Fatigue Behavior of Blade Materials @  $10^6$  Load Cycles.

electrothermal deicing system meeting performance and reliability goals above. Therefore, it is necessary that fabrication of hardware should include all of the latest controls and procedures used in related adhesive bonding and composite structure technology. These are:

Material Control - All adhesive and prepreg materials must be tested for conformance to established requirements. These perishable materials must be stored in refrigerators until used and retested before use if storage life limits are exceeded.

Equipment and Facilities Control - All chemical solutions used for preparation of surfaces for bonding must be periodically tested for concentration and proper temperature. Semiclean rooms for lay-up of laminates and application of adhesives must be checked periodically to assure required temperature and humidity. All ovens and autoclaves used for processing must be checked for heat uniformity and accuracy of instrumentation.

Cure Cycles - All cure cycles used for adhesive bonding or laminating of parts, including time, temperature, vacuum, and pressure, must be recorded and checked before part acceptance.

Surveillance - All processing operations performed by personnel must be monitored to prevent deviation from established procedures. Tag and coupons should be utilized to verify bonding integrity.

Acceptance testing must also include provisions for verifying thermal efficiency (done by measuring speed of response of the surface to a heat pulse by the heating element), dielectric strength between the heating element and the erosion shield, proper electrical resistance of the heating element, the absence of voids, and proper conformance to blade contour. These procedures are described in Section 5.

#### 3.2.1.2 Heater Power Supply and Control

The elements of the electrical system required for accomplishing electrothermal cyclic deicing are:

1. Electric power generation
2. Method of power transmission to the rotors
3. Method of sequential switching of power to the different heaters
4. Controller/timer logic functions

The present-day deicing systems on both fixed- and rotary-wing aircraft apply a fixed heater power intensity to the blades regardless of the severity of the icing encounter; also, these systems are designed to supply sufficient power to meet the worst level of icing conditions. Therefore, in light or moderate icing, the same power is applied regardless of the fact that it would be possible to conserve electrical power at these conditions.

In an advanced deicing system, it is possible to incorporate modulation of the power intensity to the heater elements as a function of icing severity encountered. With this approach, a more steady and lower level of power may be supplied by the generator system. It is estimated that this modulation will increase the overall cost of ownership by 10-15 percent.

Electric Power Generation - The magnitude of power demand by an electro-thermal deicing system requires special consideration of the electric generator system. Power requirements for helicopter deicing systems vary from 15 kw for the smaller vehicles to 75 kw for the largest. Typical 28-volt dc generators on vehicles in use today are limited to 6-9 kw. Higher voltage dc generators (120 to 250 volts, dc) are a possibility; but in view of the predominance of three-phases, 115/200 volts, 400-Hz generators available in the required capacity, ac power stands as the logical choice. These higher power ac generators will be found in some of the Army's future generation helicopters. From a weight standpoint, it is preferable to use the 8000-12,000 rpm generators which are currently available, with the weight decreasing as generator speed increases.



Transmission of Power to the Rotors - Three methods of deicing power transmission to the rotating blades are typically applicable: conventional sliprings, hub-generators and rotating transformers. Sliprings have been used almost exclusively in transmitting the electrical power from the fuselage to the rotors, but problems have been occasioned by the rings operating in a dirty and oil-contaminated environment. As a result of the dust/oil contamination, arcing and shorting between rings have occurred.

Selection of the proper ring/brush combinations is also important, as is brush contact pressure to minimize brush wear. Similarly, a shrouding or well-designed and sealed environmental enclosure can eliminate outside contamination such as dust, sand, water, etc., but it adds weight and increases maintenance activity.

There are three basic types of sliprings: platter (radial) type, stacked type, and cylindrical. Figures 21 and 22 display platter and stacked rings, and Figure 23 describes a cylindrical configuration. Self-cleaning designs should be a goal in all applications, and in this regard, centrifugal force is usually the best cleaning medium; also it is more effective on radial rather than disk or platter rings. Some disadvantages of platter rings are:

1. Foreign particles are forced outwardly passing from ring to ring causing further wear and providing arc paths.
2. Ring speed varies and results in uneven brush wear.
3. The electrical rings are bonded into the platter, increasing maintenance and material costs for ring replacement (with stacked rings, only one need be changed).
4. Platter rings are usually heavier because of higher strengths required to overcome centrifugal loads.
5. Flatness is harder to obtain, and lack of flatness results in brush bounce and then damage to the brush and ring.

There are distinct advantages with the stacked and cylindrical rings that overcome the platter ring disadvantages:

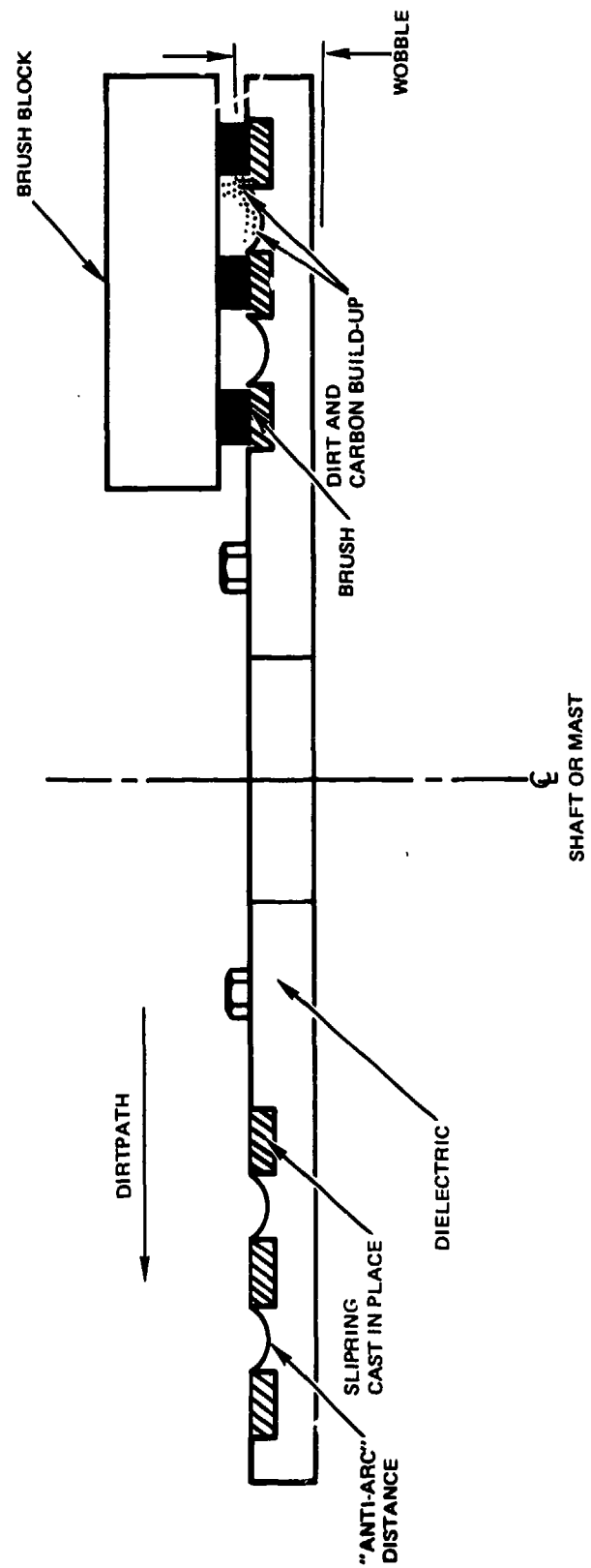


Figure 21. Platter Slipring Design.

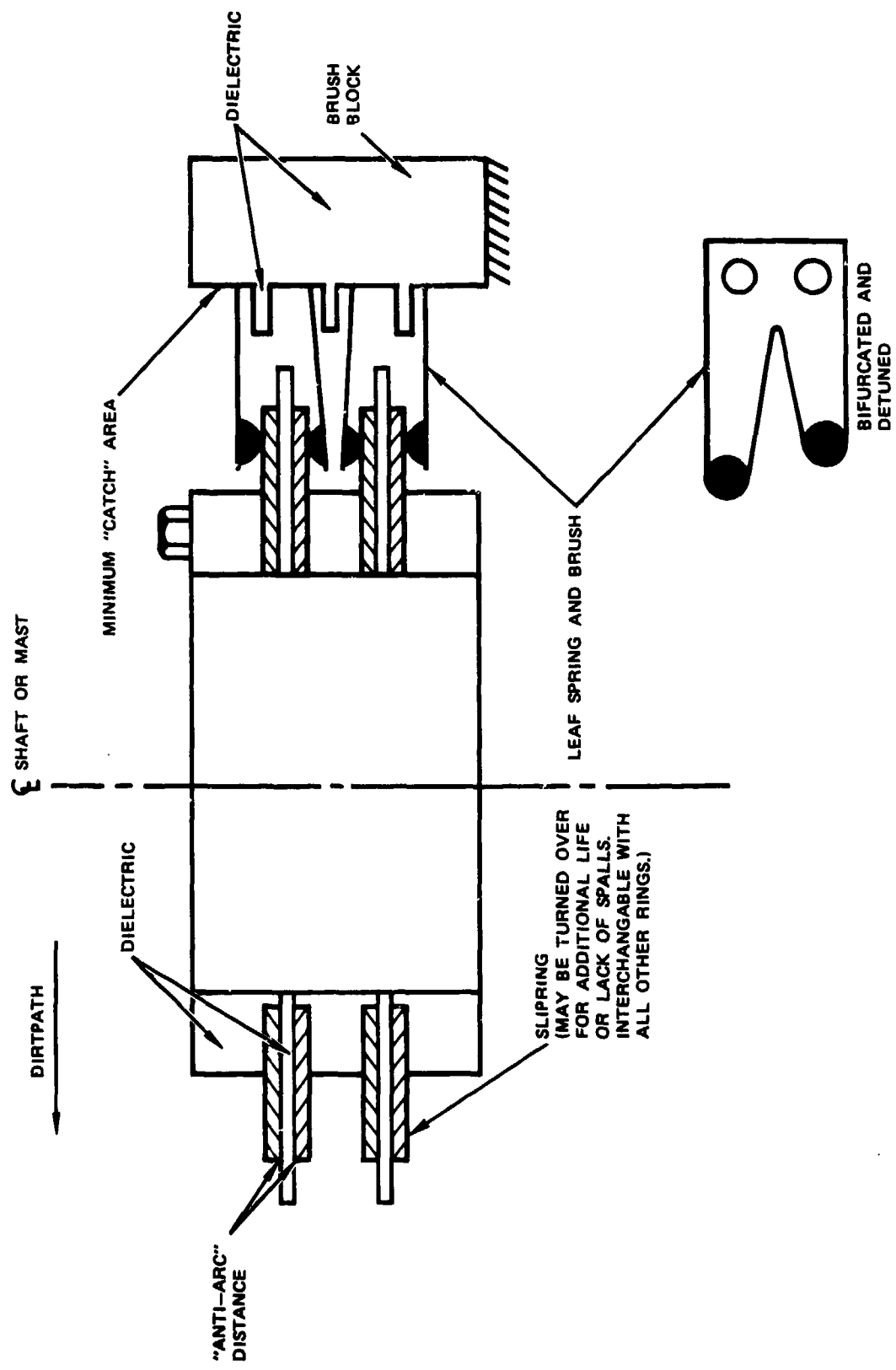


Figure 22. Stacked Slipring Assembly.

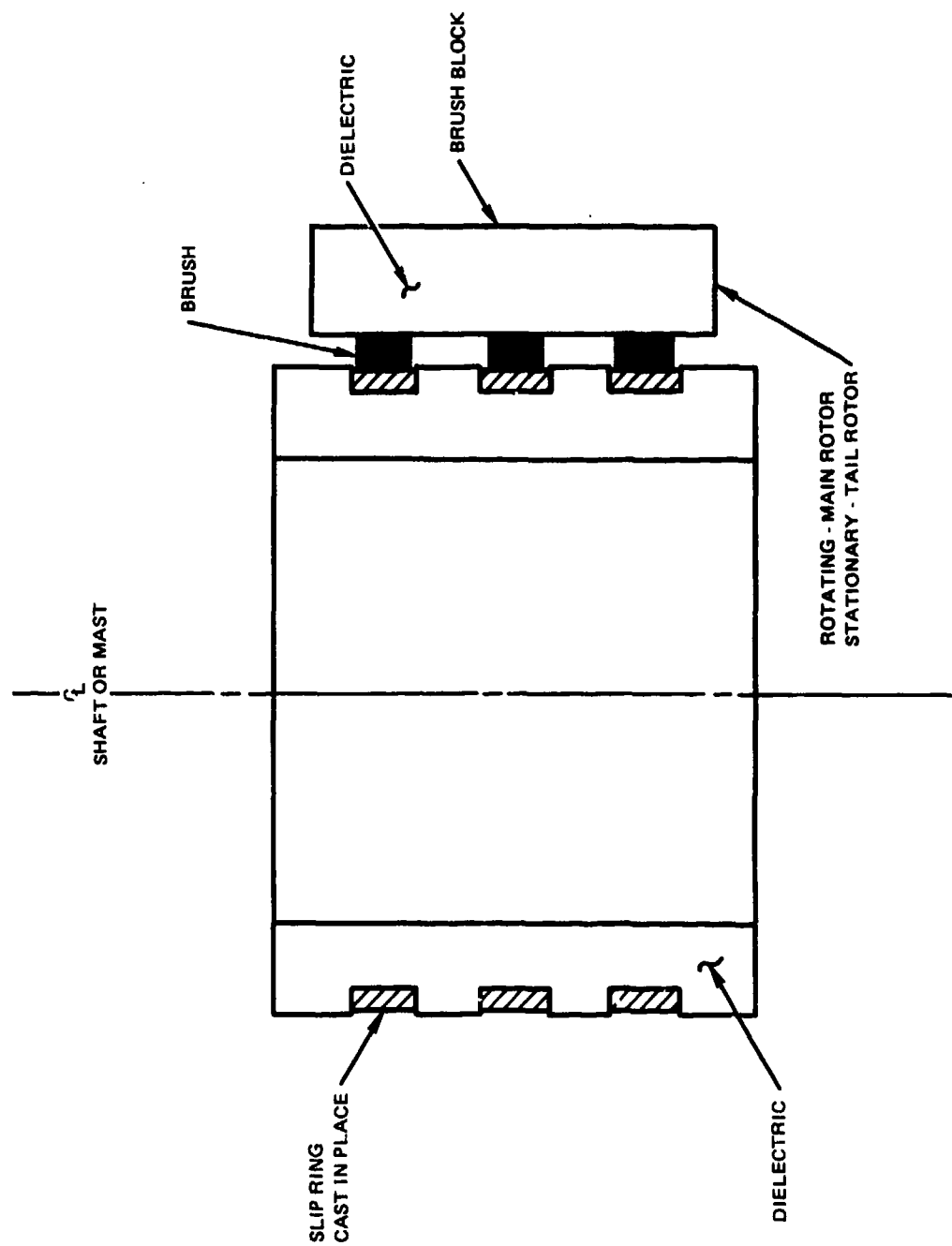


Figure 23. Cylindrical Slipring Assembly.

1. Self-cleaning by centrifugal force. Arcing is prevented by extended inserts in both the ring and block.
2. Brush block presents small catch areas. Foreign material is not accumulated at the brush contact point.
3. Brushes can be easily cleaned and inspected since they do not fall behind one another.
4. Brushes can be bifurcated (on stacked rings) and detuned to prevent bounce through harmonics.
5. Stacked rings are replaceable and interchangeable (one ring can be changed); their servicable parts need not be scrapped.
6. Wobble is minimal or nonexistent.
7. All ring surface speeds are equal; brush wear by friction is equal - maintenance task frequencies may be planned.
8. Reduction in brush wear may eliminate the need for brush lifters.

Ring materials available are hard coin silver or copper. Brush material is silver graphite, with the mixture ratio being determined by current density and rubbing speed. Brushes can be either leaf-spring type (spring material being beryllium copper) or plunger type.

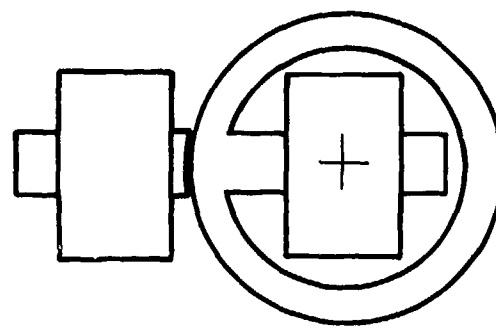
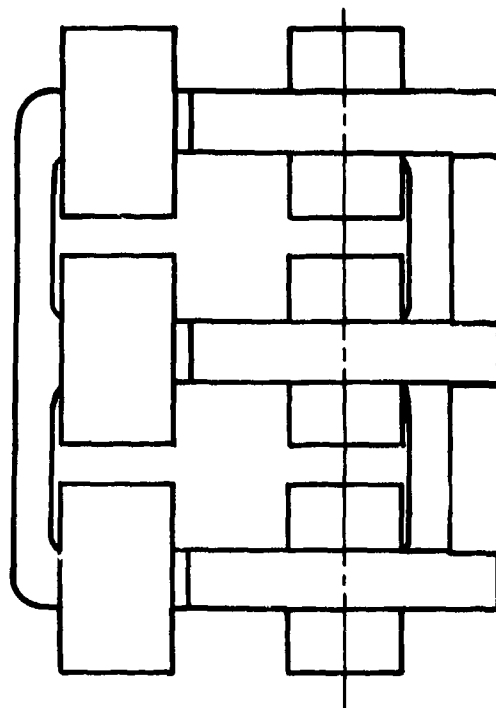
Experience with propeller deicing on modern turboprop installation results in favoring a series of axial-type rings of equal diameter spaced axially along the shaft and bolted together with spacers and barriers. For most cases, the brushes have been leaf-spring type bolted together with spacers. Individual rings can be turned over or replaced in the field, and they can be tuned to have different mechanical frequency response. Brush blocks can be replaced or rebuilt quite easily. Lockheed has experienced only six propeller removals, for slipring replacement, over a 7-year period covering some several million flight hours ( $MTBF = 1.53 \times 10^5$  hr). This indicates that this design approach can yield a highly reliable design. Cylindrical rings can also provide a satisfactory design. The choice will ultimately depend on the availability of space: the stacked ring design will be shorter but fatter than the cylindrical configuration.

A review of typical control systems indicates that a minimum of four rings (three power, one control with the control circuit referenced to ground or one of the power phases) and a maximum of seven rings (three ac power, two dc power, and two control) would meet the requirements of an advanced deicer control system.

As a means of minimizing brush wear, it would be beneficial to provide a means of retracting the brushes during any protracted period when the system is not in use but this engenders undesirable complications and is not recommended even though a number of pneumatic and solenoid lift-designs are available.

Rotating Transformer - As an alternative for eliminating sliprings completely there is the possibility of transferring energy from the structure to the rotor via a transformer. This can be done by using a hub-mounted generator, but a low rotational speed would necessitate either a very high flux density and/or a very large number of conductors to keep the weight/size to reasonable proportions. Also the regulator would have to be built into the rotor with the attendant difficulty of controlling the flux density from the rotating side, or coupling the voltage sensing circuit back to the stationary side. In effect, this would be equivalent to a brushless generator, built inside out but, as stated, the weight and size would be prohibitive.

Figure 24 is another possibility using a special design of a rotating transformer, in which a circular magnetic flux path is provided for the secondary. As a starting point for the discussion, a weight of 16 lb is assumed for a standard 16-kva transformer with approximately 50 percent of this weight assigned to the core and 50 percent to the windings for the core. Adding frame and structure would increase this to 18 lb. Core losses (hysteresis and eddy current) are proportional to core weight so that they are more than doubled. The air gap also affects the size and increases the core reluctance. Further, because of the high leakage reactance incident upon the design, the increase in magnetizing current (due to increased core losses and reluctance) would entail a 10-percent



STATIONARY  
PRIMARY

ROTATING  
SECONDARY

SUPPORTS AND BEARINGS  
NOT SHOWN

Figure 24. A Possible Configuration for a Rotary Transformer.

increase in primary copper. This in turn affects the secondary voltage loss and would require an approximate 10-percent increase in the turns ratio, bringing the transformer weight to 32 lb (including 5 lb for bearing and bearing support). This weight compares unfavorably with a slipring weight of 10 pounds.

Another problem is that transformers can experience a high inrush current. This is usually not important with continuous loads, but if load sequencing is done by switching in the primary side and the load is cyclic, it may be of consequence. Any transformer that is switched on when the voltage wave is passing through zero draws a magnetizing current which can be many times full load current. Residual magnetism in one direction decreases this effect and increases it in the other. One mitigating factor is the primary leakage reactance which would probably be high enough to reduce the effect to acceptable limits.

A rotor-mounted controller must sense power interruption as a command signal. Thus, additional rotary transformers or sliprings would be necessary for this function.

The efficiency of a conventional transformer of the required size would be approximately 90 percent. However, with the addition losses incident upon rotary transformer construction, the 90-percent efficiency would drop to approximately 80-85 percent.

Because of the technical and practical design difficulties for rotary transformers, the slipring approach is the more practical system for the present and future helicopters. Slipring vendors are willing to guarantee a life of 3,000 hours.

Sequential Switching of Power to the Cyclic Zones - Electromechanical, solid-state, and hybrid combinations of electromechanical and solid state were investigated for the sequential switching of power to the cyclic zones of electrothermal deicing systems. Proposals for switching systems applicable for helicopter electrothermal cyclic deicing were solicited from companies active in icing and control technology. Fully solid-state and hybrid systems were the only ones considered since the



pure electromechanical concept has inherent deficiencies such as poor reliability due to required mechanical contacts to apply and remove power and attendant EMI problems due to inability to apply and remove power at zero voltage. A schematic diagram of the hybrid concept is shown in Figure 25, and the fully solid-state concept is shown in Figure 26.

In the case of the hybrid system, cyclic control of the main rotor heater elements is accomplished by means of an electromechanical stepping switch. An electromechanical power contractor is inserted ahead of the stepping unit, and its purpose is to handle the making and breaking of the current to the various heater elements. Further, as a refinement which eliminates or minimizes radio frequency (rf) interference problems, the electrical contacts of the power relay are shunted by a full wave silicon controlled rectifier (triac), or three phase full-wave solid-state switch. This circuit arrangement, as shown in Figure 25, to a large extent combines the best features of an electromechanical and fully solid-state system, since the triac of the hybrid system is designed to close some 30 milliseconds before the main power contractor, and to open some 30 milliseconds afterwards. This eliminates the rf radiation noise problem incident upon arcing contacts, and gating (turn-on/turn-off) of the triac is effected at the zero crossover points. With this type of control, the current to each heater element is made and broken only as the ac current wave passes through zero. The other important advantage inherent in this approach is the fact that, when the power contractor closes, the 1.0- to 1.5-volt drop of the triac is reduced to approximately 0.04 volt. This means that the high power dissipation of approximately 50 watts per triac, or 150-watt total for the three-phase, is reduced to only 6 watts.

In the fully solid-state system the power stepper switch is replaced by three full-wave, back-to-back, silicon controlled rectifiers (SCR's). A single SCR unit conducts in one direction only and generates half a wave. Therefore, either two (back-to-back) SCR units or an equivalent single

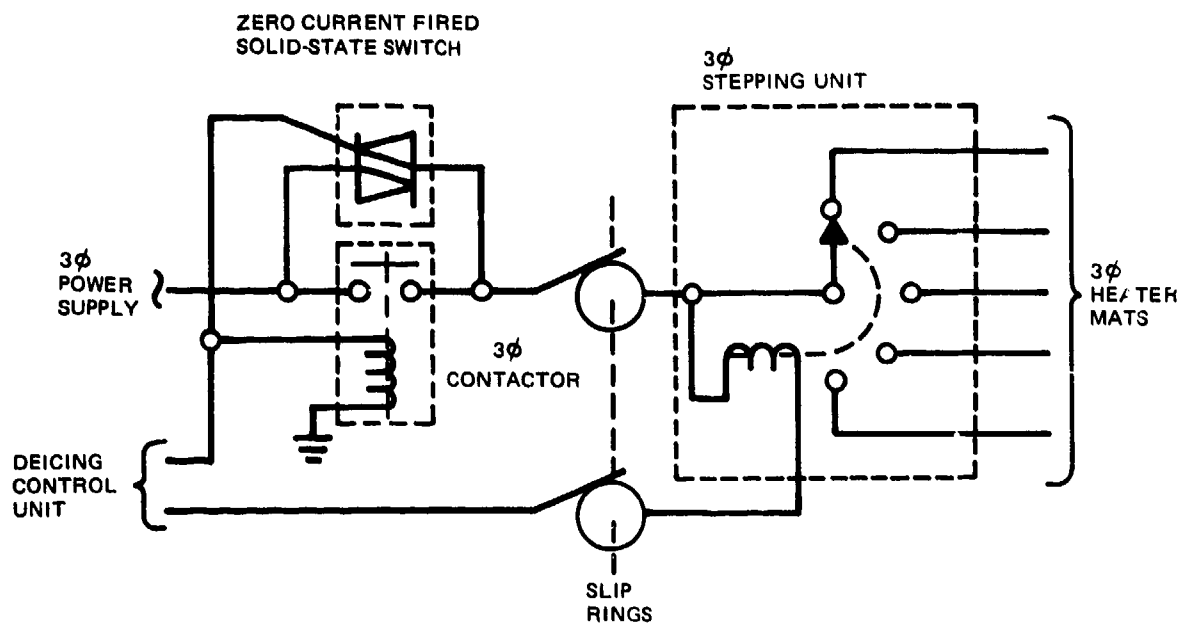


Figure 25. Hybrid Sequential Power Switch.

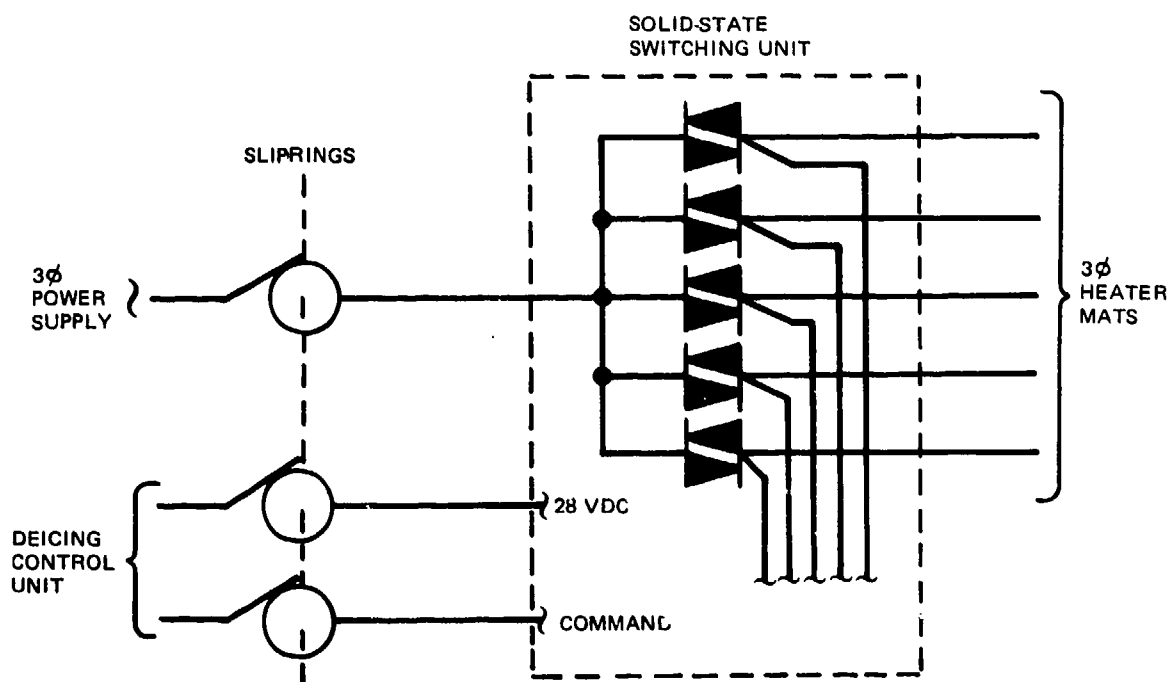


Figure 26. Solid-State Sequential Power Switch.

unit (triac) is required for generating a full wave. Since the solid-state switching requires that there be one such set of three-phase triacs per heater zone, the individual groups must be closed in correct sequence, by command logic from the controller which is located on the fuselage side of the rotor mast. Also, a heat dissipation of approximately 150 watts continuously must be managed by the heat sink on which the triacs are mounted.

Another approach is to use high voltage dc (260 volts) obtained from rectified ac (using thyristors). This reduces the complexity and quantity of wiring since only two leads (plus that required for control) need go into the rotor head. The disadvantages of this system are the EMI associated with the current pulses (no zero voltage switching is possible with dc) and the increased generator size and shaft power loss due to ac-dc conversion inefficiency. A detailed analysis would need to be performed for a candidate aircraft in order to establish the relative merits of an ac or dc system.

An analysis of the advantages and disadvantages and estimated reliability of the all-solid-state and hybrid control concepts proposed has been made. The main problem normally associated with the electromechanical stepping switch is a susceptibility to hang-up and binding, particularly under the vibration environment of the rotor system. However, some improved designs have been developed to overcome this apparent weakness.

The advantages of stepping switches are that they offer: (1) Small size, (2) low power dissipation, (3) light weight, and (4) low cost. In comparison, solid-state switches are (1) sensitive to transients, (2) subject to gating by stray pickup, (3) dependent on finned-type dissipators as heat sinks, (4) unable to withstand the surge currents of a heater element short circuit, (5) not available to the JAN (Joint Army-Navy) specification in the current ratings required for deicing power, and (6) relatively costly. The primary advantage of solid-state switches is that they are less sensitive to a vibration/shock and nonclean environment.

One type of electromechanical stepping switch which has been developed for helicopters uses a long cylindrical drum (driven by an electromagnetic ratchet) which rotates raised lands on the cylinder to lift metal-leaf or blade-type contacts connected to the various heater zones. Figures 27 and 28 are photographs of a typical unit capable of controlling up to eighteen 20-kw heater zones. This design concept has been substantiated by three million step operations in a helicopter-induced vibration environment and is projected by its manufacturer to have an MTBF record of 4,000 hours.

Some typical reliability and maintainability data, comparing an all-solid-state system and a hybrid system, are listed in Table 11. A weight estimate of an all-solid-state deicing system and a hybrid deicing system is plotted in Figure 29 as a function of number of cyclic zones (for a light helicopter). This shows that when the number of heater zones are few (one to three) the power demand reflected to the generator is increased, so the weight of the generator is increased. For instance, a 60-kw generator would be required if there were only one heater zone per blade, and this generator, depending on its speed, would weigh 75 to 115 lb. For a greater number of heater elements, the demand decreases to 20 kw for five zones. For some helicopters, the generator capacity may be fixed and limited so that in such instances it may be necessary to use a much larger number of zones. However, a legacy of a larger number of zones is that the volume requirements for a solid-state system increases almost proportionately with the number of heater zones. In fact, for the solid-state system, the heat dissipator volume for, say, eight to ten zones would be more than three times the volume of a stepper switch and would be a limiting factor. (More zones, of course, also implies more wiring to the blades.)

Controller Time - The controller timer can be designed to adjust the zone "on" time as a function of OAT and the "off" time as an inverse function of LWC. Another alternative is to adjust the "on" time as a function of OAT, and the power intensity to the blade can be controlled

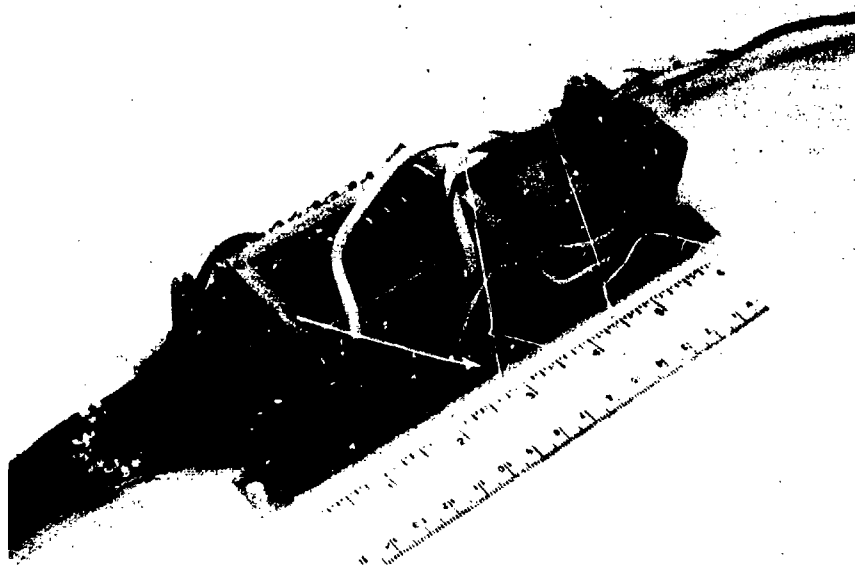


Figure 27. Electromechanical Rotor Stepping Switch.



Figure 28. Close-Up of Power Contactors and Contacts.

TABLE 11. RELIABILITY AND MAINTAINABILITY SUMMARY,  
SUBSYSTEM TOTALS AND APPLICATION OF  
ROTARY WING PREDICTIONS

System	MIMA (A) hr	MTUR (B) hr	MTEF (C) hr	MMH/FH (D)
Electrothermal Cycling, Deicing				
Including Generator and Supervisory Panel				
All Solid State System	388	1279	2740	0.0081
Hybrid System	451	1375	2932	0.0079
Excluding Generator and Supervisory Panel				
All Solid State System	546	2127	4115	0.0066
Hybrid System	659	2347	4484	0.0066
(A) Mean time between maintenance actions (B) Mean time between unscheduled removals (C) Mean time between failures (D) Maintenance man-hours per flight hour				

as function of LWC. To accomplish the latter, some form of power modulation is required.

Power modulation may be accomplished by pulse-width modulation, phase-angle control, or voltage amplitude modulation. When, however, there is a dedicated generator for deicing, a far simpler technique is to use voltage amplitude modulation which can be effected directly through the generator's regulator system. On the other hand, with an existing generator system which supplies loads other than deicing, the technique of pulse-width modulation by means of "gating" a number of cycles as a

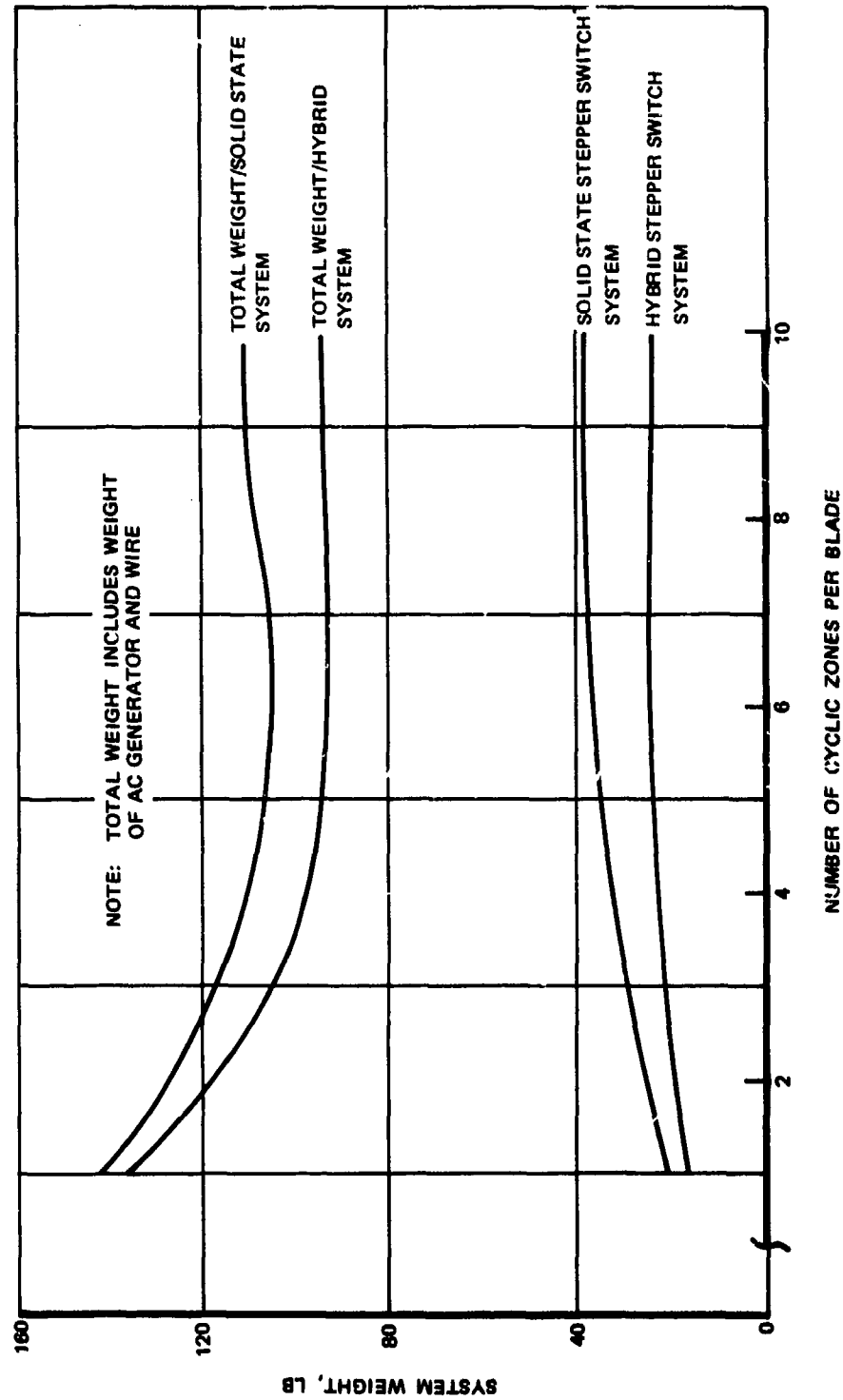


Figure 29. Comparison of Electrothermal Rotor Deicing System Weight/Hybrid Versus Solid-State Sequential Switching System.

function of the required power intensity can be used (Figure 30). Another method would be to use an autotransformer with a number of voltage taps which could be selected to change the effective voltage. The technique of phase-angle control, shown in Figure 30, is not recommended because of EMI generation problems since zero voltage switching is inherently not possible (pulse-width modulation can employ zero voltage switching, Figure 30). For a typical application of voltage (power) modulation, three levels of power intensity could be applied to the heater elements and these would correspond to light, moderate, and heavy icing conditions. To achieve a 50-percent power increase going from light to moderate, voltage change from 160 volts ac to 200 volts ac would be necessary; Similarly, another 50-percent increase going from "moderate" to "heavy" would require a voltage increase to 230 volts. As power intensity increases, the rate of temperature rise at the blade skin also increases, so less "on" time is required at the highest voltage. By using this technique, the controller timer can be made to shorten the "on" time schedule as a function of icing severity level.

A number of controller designs were evaluated as far as they were applicable to the advanced deicing system concept. The primary differences were in the timing logic; typical systems used capacitor discharge comparators for OAT control, and three voltage levels were used to signal generator voltage changes in response to LWC changes. Figure 31 is a schematic of a controller timer which utilized the electromechanical stepping switch described earlier. Protection is shown to prevent potentially destructive faults and to preclude damage to rotor blades or control system. Detection of heater element short circuits, open circuits, and faults to structure is included. The purpose of the protection is to isolate destructive or unsafe failures without disturbing the remainder of the deicing system.

One of the potentially hazardous problems in many past electrothermal deicing systems has been the prospect of insulation breakdown and failures of the heater elements resulting in high destructive fault currents.



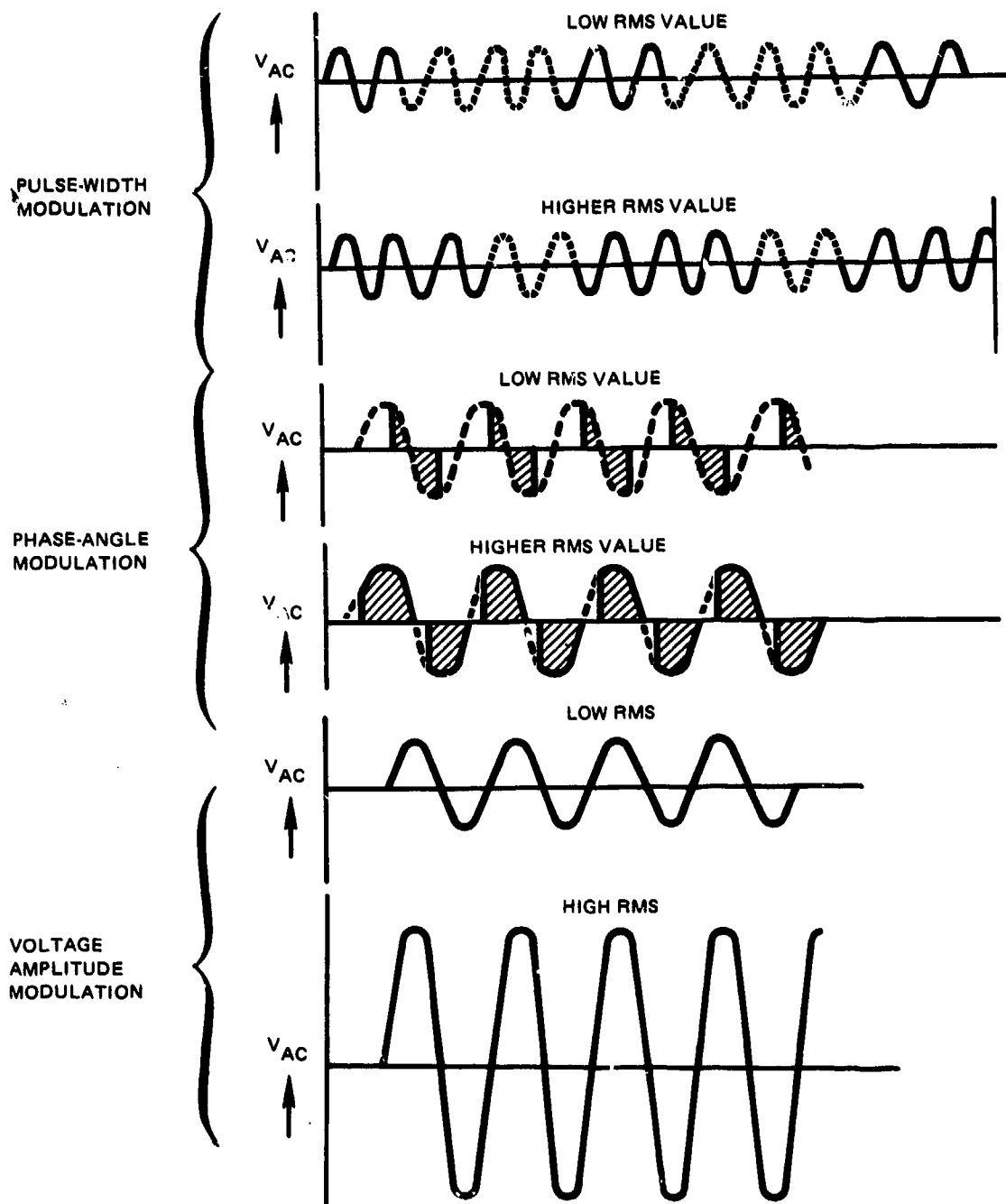


Figure 30. Power Modulation Methods.

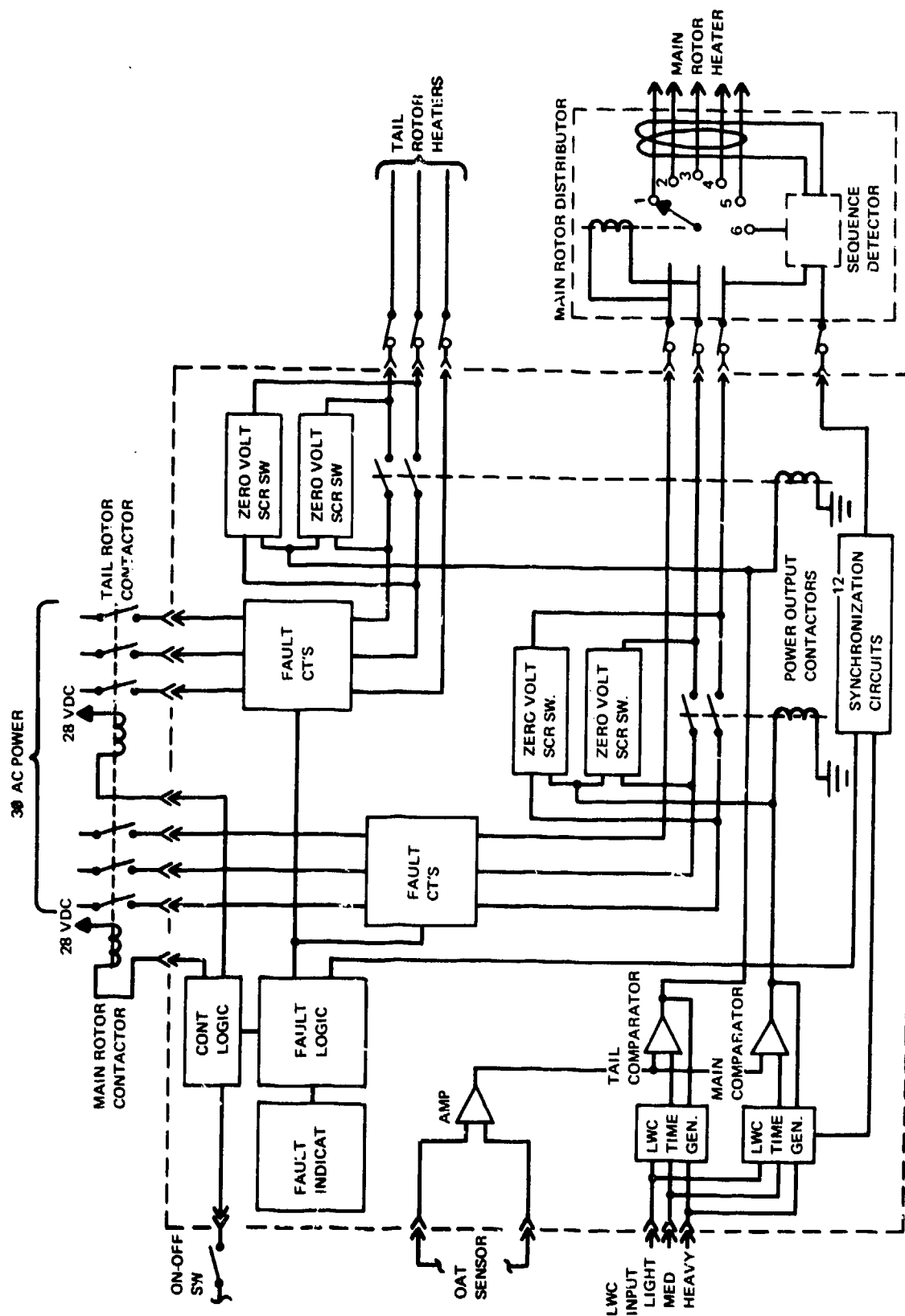


Figure 31. Deicer Controller - Schematic of Hybrid System.

Many times, when such failures have occurred, the result has been not only a damaged heater element but structural damage to the blades. Corrective action then usually requires removal of the blade and repair (if possible) of the heater element. To avoid this hazard, the neutral of the three-phase generator can be ungrounded and a sensing circuit connected between the neutral point and ground so as to detect any inadvertent ground faults. Current limiting is an associated feature of this protection, and if a line-to-ground fault occurs (in the wiring or one of the blade heater elements) the fault current is limited to milliamperes, and a "ground" light is illuminated on the pilot's control panel. Using an ungrounded neutral system makes it necessary to isolate grounds that are normally found in some components. While this rewiring is an inconvenience, the advantages are significant. It is implicit in such grounded neutral designs that once a ground warning is received the ground should be isolated and removed. However, this does not create an emergency condition, (since detection can occur at 50 milliamps) and there is no problem in continuing the mission. A serious fault can be handled by system overcurrent protection which would shut the system down with a 25 percent overcurrent. The ground fault can actually be removed at the next scheduled maintenance period.

Since currents are normally balanced in the rotor systems, current transformers (CT) can be used to detect any unbalance between the three-phase currents, as would be the case with a line-to-line fault or an open-phase fault condition. Discrimination between these two faults is dependent on the fact that a line-to-line fault will normally be associated with an overcurrent. If this occurs, the circuit logic can trip the faulty rotor system and latch out the main rotor or tail rotor contactor.

If the problem is an open circuit or open-phase fault, there is no overcurrent but the fault can produce unequal heating over the heater blade surface. If the open circuit is in the supply lines then it will affect all heater zones, but if it is a heater element failure, then it will

affect only the one heater. In the latter event, it is necessary that the symmetrically opposite heater also be deactivated to avoid any out of balance moments due to failure to deice on one blade.

In designing protective circuits, consideration must be given to the fact that the timer can "stall" in one position - due to either a mechanical binding seizure or an open circuit in the control line to the stepping device. If this happens, three-phase power would be applied continuously to one set of heater elements and there would be no over-current, open phase, or current unbalance to detect it. As a result of this possible problem the design must incorporate logic to recognize a stalled timer. Small current transformers can be located in the rotor head assembly to monitor the currents to successive heater elements. These units would be connected with opposite polarity, and the wiring to the alternate groups of heater elements would be such that if the stepping device is operating normally, the control logic will receive alternate positive and negative signals. If the stepper is stalled, the successive power pulses will hit the same heater elements;-also the current will pulse through the same current transformer causing the control logic to detect successive pulses of one polarity. The logic can recognize this event and interrupt the power to the main rotor by opening the ac line contactor. This logic will prevent overheat due to stalled timer.

The timing functions can be accomplished statically by RC (resistance-capacity) circuits within the controller/processor. Under normal circumstances, the functioning of the timing circuits would be assumed to be of high integrity and to be in correspondence with the system demand. However, since faulty timer logic could result in excessively long power "on" times, the controller should have logic to limit the maximum allowable power "on" time per zone.

Conclusion - In view of the higher technical risk involved in development of an all-solid-state system, the need for careful thermal management, and the volume and weight considerations, the hybrid approach is

recommended since it has the best potential for minimum weight, lowest production cost, best reliability, and is virtually state of the art.

### 3.2.2 Chemical Freezing Point Depressant

The chemical freezing depressant system uses a fluid which lowers the freezing point when mixed with water impinging on the surface. The fluid, such as an alcohol (ethyl, methyl, or isopropyl) or glycol solution, is expelled at the stagnation line by means of holes, nozzles, or a porous panel. The system is composed of a fluid supply, a pump, a distribution arrangement at the point of icing, switches, control valves, and instruments, as shown typically in Figure 32 for the prototype system installed and tested on a UH-1 helicopter in 1960-61. A slinger ring is used to transfer the fluid from a fixed nozzle to the rotating blade (Figure 32). The fluid is supplied to the blade by centrifugal force resulting from the rotational velocity of the slinger ring. Leading edge grooves distribute fluid to the holes in the stainless steel leading edge. The size and location of the injection holes in the leading edge are critical, and, to achieve satisfactory deicing performance separate development and testing, are required for each application to obtain a distribution system (whether it be orifices, nozzles, or porous panels). A sensitive ice detector is required to ensure that the fluid depressant is turned on as soon as possible because the fluid may not be able to cope with a 2-minute ice buildup in heavy icing. Such a buildup may prevent uniform fluid distribution and may cause rivulets with a continued buildup between rivulets, thus increasing the profile drag and causing excessive vibration due to asymmetric shedding.

Army helicopters, particularly in the lighter weight range, are designed to operate in a battle environment remote from the major supply base; thus, the logistic problem of maintaining a deicing fluid supply in forward areas for on-board replenishment as required represents a major liability of the chemical system. Another important point relating to the application of a freezing point depressant deicing system to combat helicopters concerns the vulnerability of the system to battle damage.

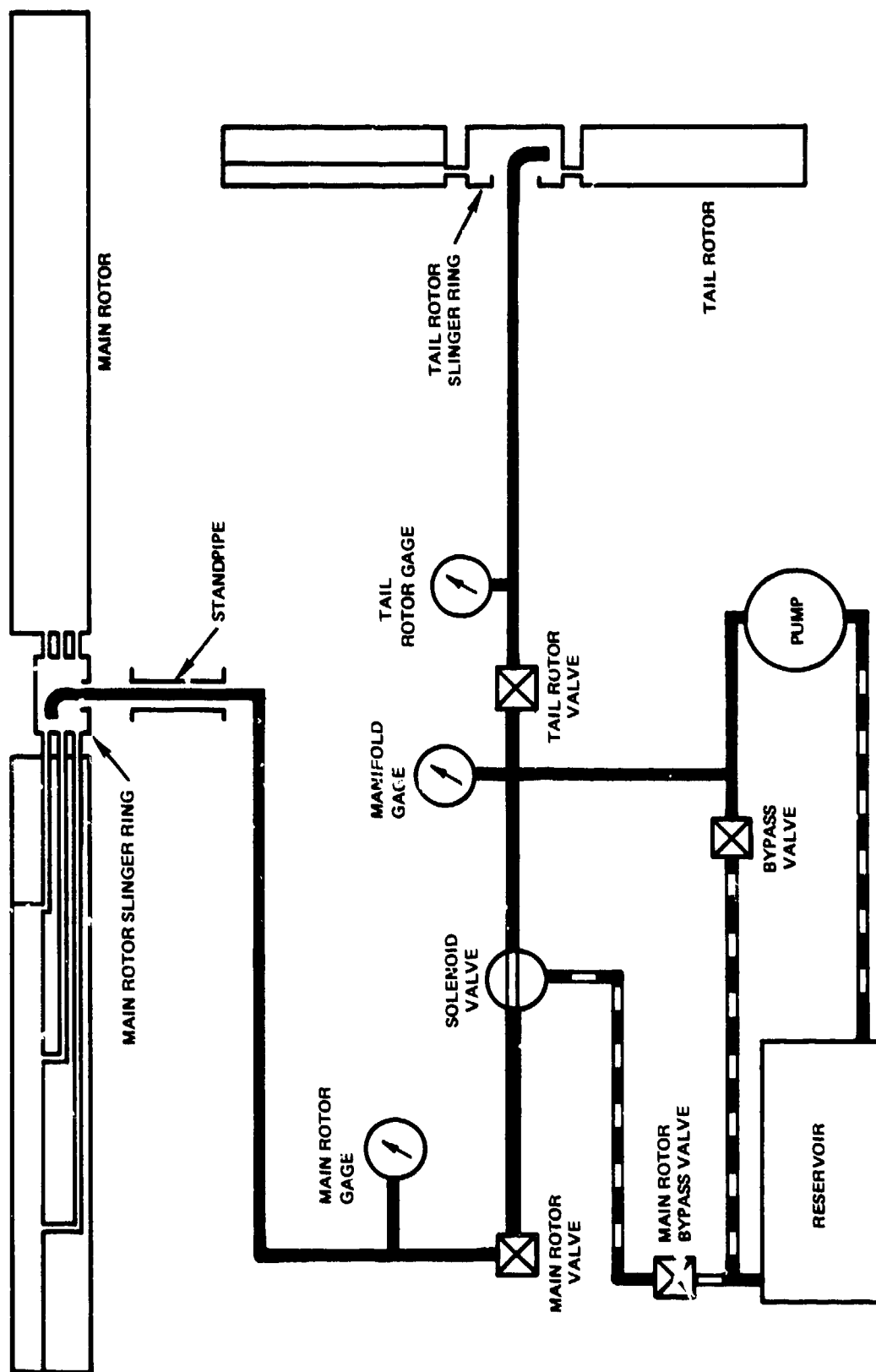


Figure 32. Schematic of Chemical Freezing Point Depressant Ice Protection System.

Puncture of the fluid reservoir or fluid feed lines by bullets or shell fragments would cause loss of the entire system. In this respect, the freezing point depressant system is the more vulnerable than the electrothermal concept because of its extension over a large space.

The theoretical value for the required rate of fluid expulsion can be easily computed (p 216 of Reference 1). Basically this theoretical value is a function of the type of fluid and its strength in the applied solution, of the ambient temperature and airspeed, and of the water catch rate. Figure 33 shows that of the two extremes of the continuous maximum icing envelope, the maximum catch rate extreme (maximum LWC's) associated with a skin equilibrium temperature of  $32^{\circ}\text{F}^*$  and the minimum ambient temperature extreme associated with an OAT of  $-4^{\circ}\text{F}$  (minimum catch rate), it is the latter that imposes more severe requirements. It is also seen that a 50-percent ethylene glycol-water solution is considerably less effective than the ethyl alcohol-glycerine mixture used in the Bell UH-1 experimental program. The ethylene glycol mixture, however, has been a common choice since it has several advantages: It is commercially available in large quantities, has a low volatility, and is not a fire hazard.

The UH-1 test data revealed that the actual total required fluid quantity was 64 lb/hr, which, in terms of the average expulsion rate per unit span length of the main and tail rotors amounts to 1.32 lb/hr/ft span. This experimental value is higher than the maximum 60-percent span theoretical value of 0.88 lb/hr/ft span (Figure 33). The difference is due to the fact that in practice an ideal distribution of the fluid film cannot be achieved; thus, for the actual required average expulsion

\* The (unheated) equilibrium temperature is determined by an energy balance between aerodynamic heating on the surface and evaporation of a water film. The ambient temperature associated with this balance decreases towards the blade tip due to the increased kinetic heating and hence the "design" liquid water content (from Figure 12) varies spanwise. Since the water catch is proportional to the velocity and the liquid water content, the total catch is a maximum at some mid-span station.

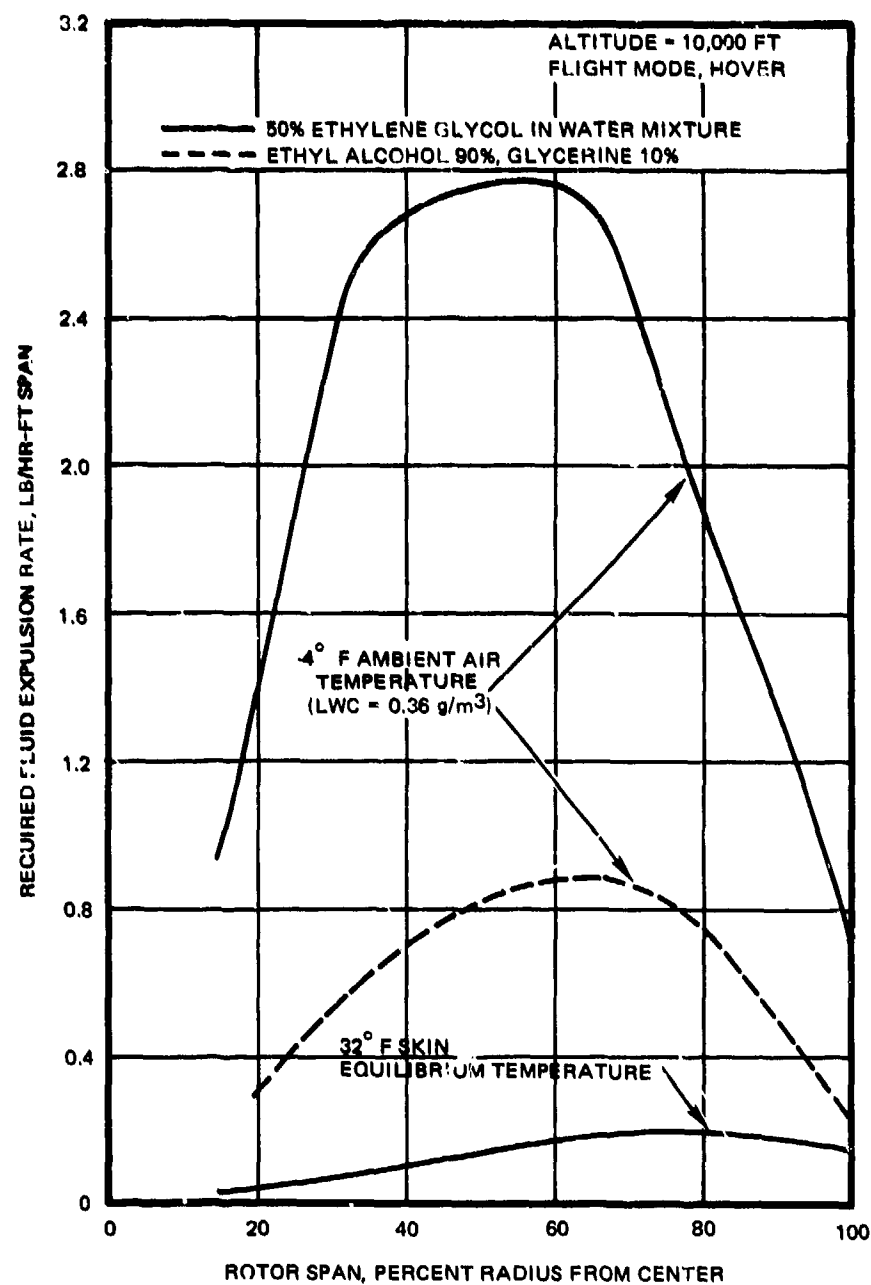


Figure 33. Required Theoretical Freezing Point Depressant Fluid Expulsion Rate for UH-1 Main Rotor Blades.



rate, it is necessary to apply a factor of 1.5 to the theoretically computed local maximum rate occurring at the 60-percent span station.

### 3.2.3 Fluid Thermal Anti-Icing

The basic feature of the concept is the reclamation, with little or no penalty, of normally wasted engine exhaust heat and/or engine transmission oil heat. The system, wherein these heat sources are utilized to heat a suitable liquid which is pump circulated in a closed loop through the rotor blades and heat exchanger(s), has been analyzed because it shows a potential of being the only system capable of fully evaporative performance at a reasonable weight penalty. The problem associated with the rotational transfer of a heating fluid into and from the helicopter rotor is the most critical aspect of the entire concept. Three approaches for solution of this problem have been investigated:

1. Airframe Mounted Stationary Heat Exchanger - A small portion of the engine exhaust gas flow is diverted to heat the closed loop water-glycol solution via a heat exchanger. Water-glycol has been studied because of its low-freezing and high-boiling temperatures. Also, its high specific heat minimizes the heat exchanger size. The pump-circulated liquid is supplied to the rotor by means of a rotating seal (Figure 34). After giving off its heating energy for rotor blade anti-icing, the cool liquid is returned to the airframe heat exchanger via a second rotary seal similar in construction to the liquid supply seal.
2. Rotating Heat Exchanger System - Elimination of the rotating liquid seals and confinement of the liquid loop to the rotor alone can be achieved by a system wherein the water glycol-to-exhaust gas heat exchanger, liquid pump, and reservoir are mounted on the hub and rotate with the blades (Figure 35). As can be seen, engine exhaust gas is ducted to the rotating heat exchanger via a gas seal.
3. Integration of Rotor Anti-Icing With Transmission Lubrication and Cooling - In this scheme, the engine transmission oil would be routed into the rotor blades for oil cooling and rotor blade anti-icing (Figure 36). Since transmission heating of the oil is not sufficient by itself for rotor blade anti-icing, a large portion of the oil would be heated in an exhaust gas heat exchanger. The hot oil from the transmission and heat exchanger is introduced into a tube in the rotor shaft by a ball joint seal at the shaft base. Return oil

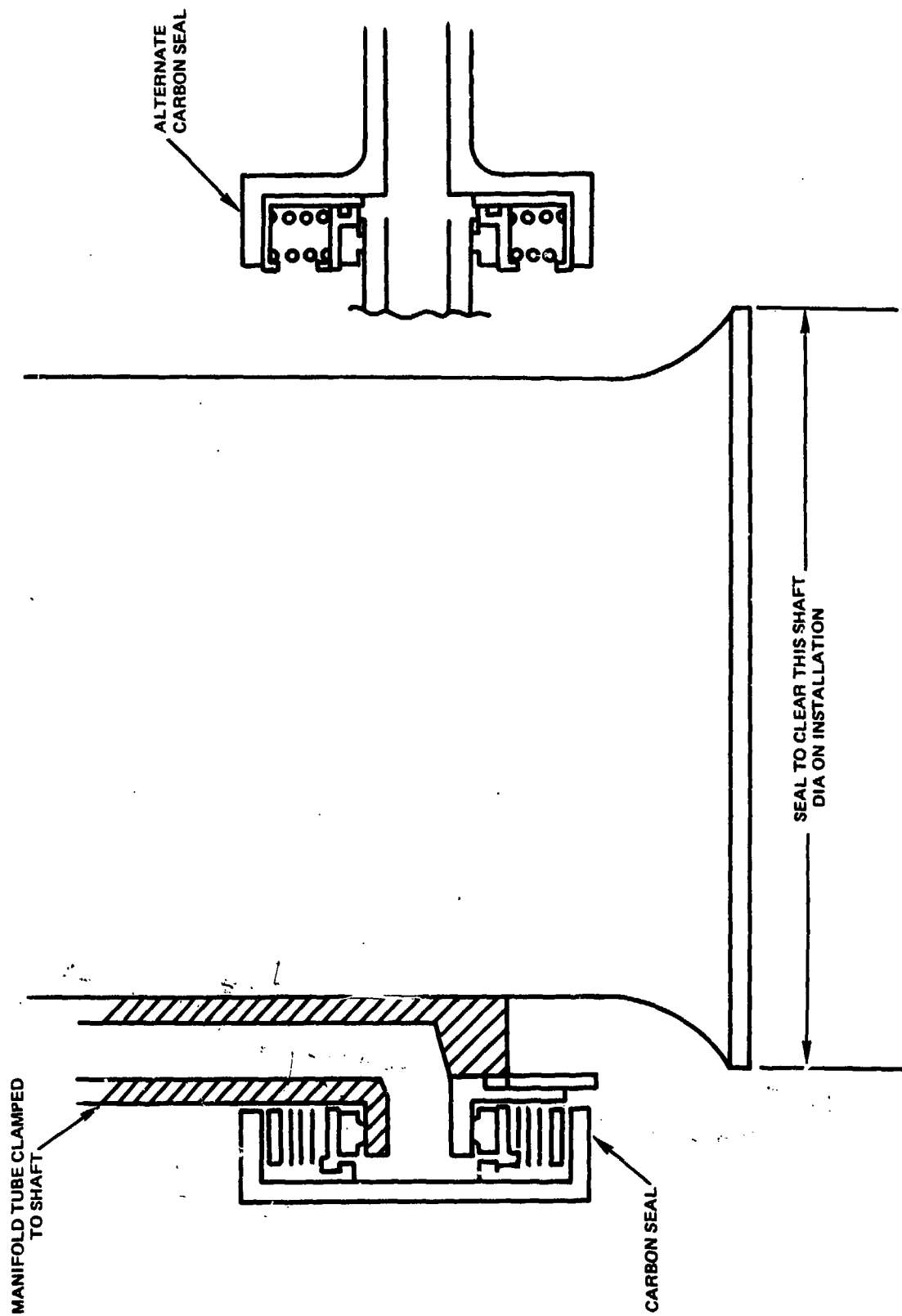


Figure 34. Liquid Rotary Seal for Water-Glycol Rotor Blade Anti-Icing.

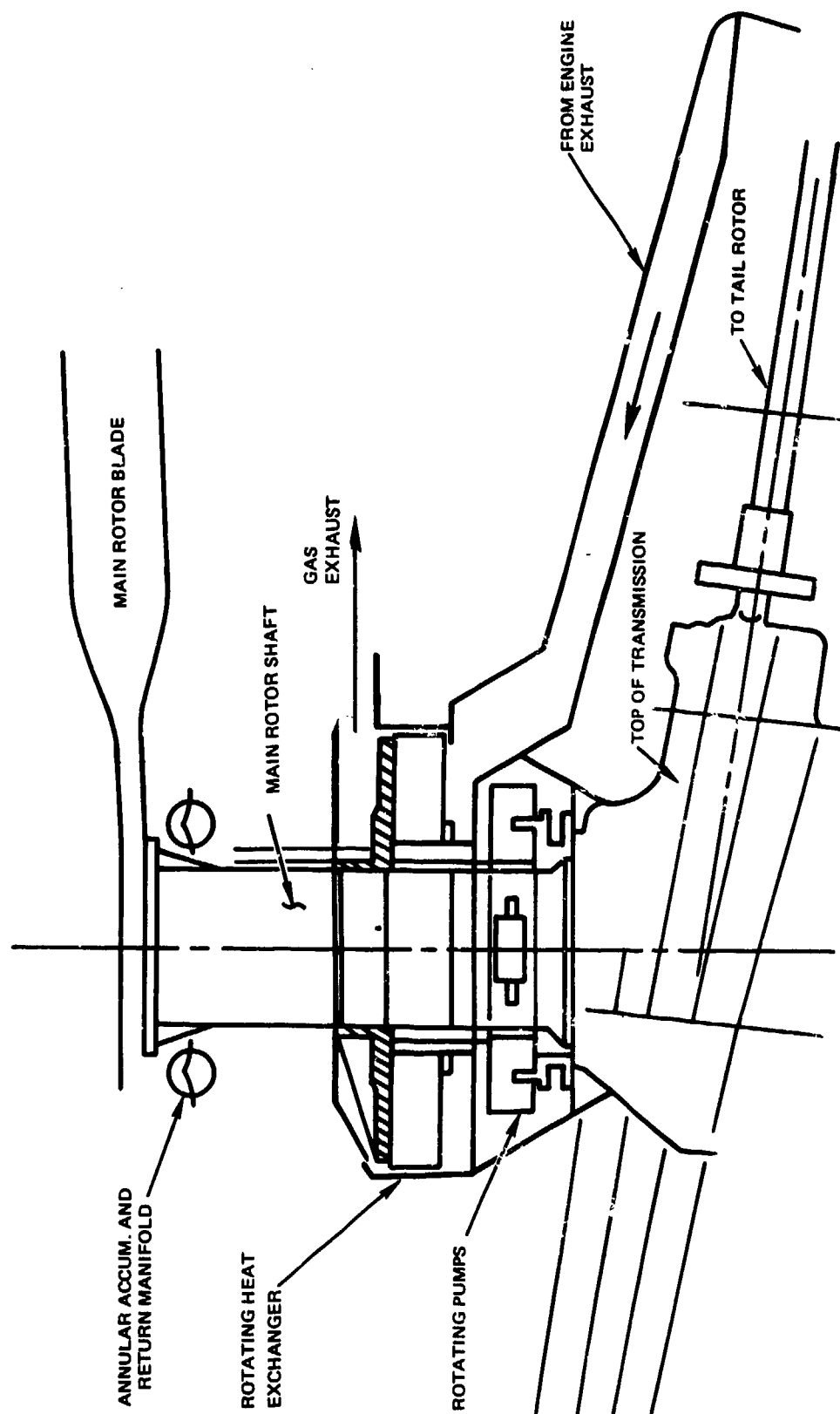


Figure 35. Rotating Heat Exchanger System for Rotor Blade Anti-Icing.

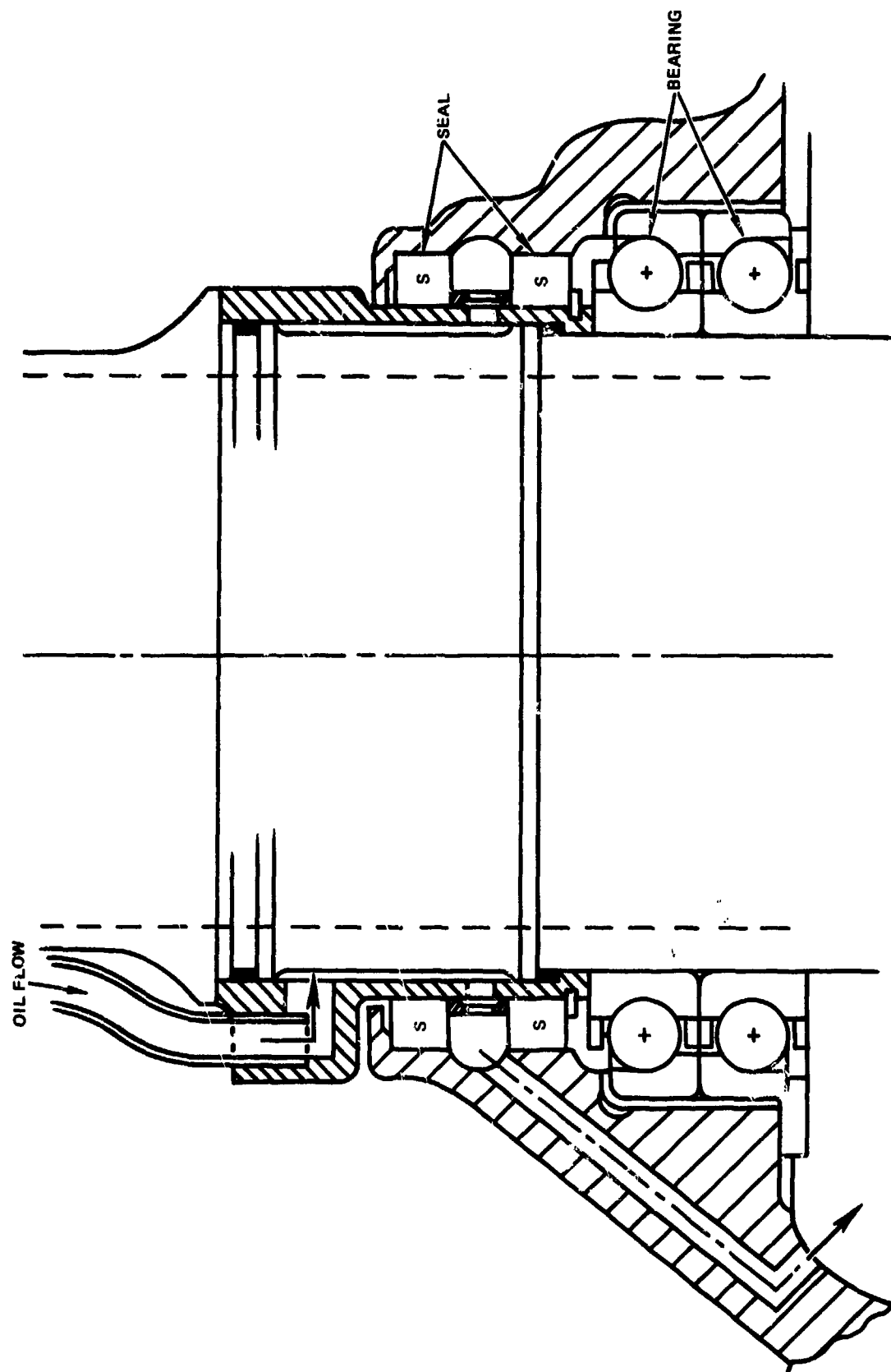


Figure 36. Rotor Anti-Icing/Transmission Lube Oil Cooling-Return Oil Seal.

from the blades flows into the transmission case through a seal concentric to the rotor shaft.

A typical airfoil cross section and tube configuration is shown in Figure 37. The stainless steel skin of the lower surface between the balance bar and the spar is covered by a 0.050-inch-thick aluminum fin which holds the tubes in place and equalizes the heat flux and surface temperature in the chord-wise direction. For an all-stainless-steel configuration, six tubes would be required (instead of four) to compensate for the lower conductivity of steel.

Of the three approaches considered herein, System 3 is the lightest and most reliable because: (1) It eliminates the transmission oil cooler, (2) it does not require a special liquid pump since the normally required oil pump is replaced with one of increased capacity, (3) the high pressure (200 psi) supply oil is brought into the rotor shaft via a compact ball joint seal proven in service, (4) oil is returned to the transmission case by a seal which is subject to pressures only slightly higher than ambient, and (5) the continuous oil flow through the rotor supply and return seals in non-icing weather enhances the life of these seals. On the debit side, the extension of the transmission oil system over a larger area, made necessary by combining it with anti-icing, severely compromises the integrity of the oil system and makes it unacceptably vulnerable to battle damage. Excessive liquid leakage may represent a problem even during normal operation. Furthermore, there is a high degree of vulnerability and the potential loss of the entire system that is associated with a tree-cutting incident.

Compared to other systems (e.g., chemical and electrothermal), the most significant feature of the indirect liquid anti-icing system is the fact that it offers the only practical possibility of achieving evaporative anti-icing for the rotor blades with a competitive weight penalty. For example, evaporative anti-icing of a UH-1H rotor blade would require 68.5 kw of electric power, or if using engine bleed air, 11 percent of engine airflow (compared to an allowable of 4-percent bleed). However, there are also several important drawbacks to the liquid-heated system:

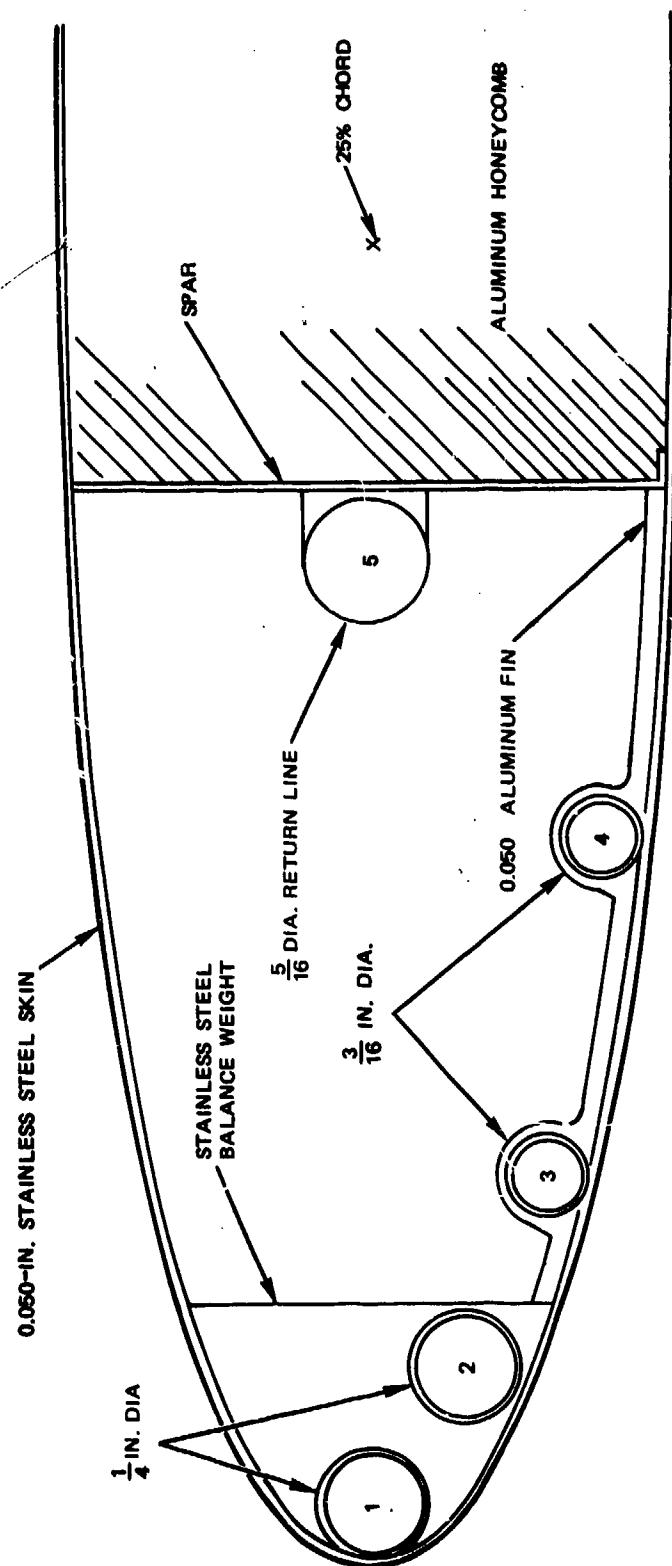


Figure 37. Typical Blade Leading-Edge Cross Section of Four-Passage System.

(1) it requires extensive development and testing; (2) it can be applied to metal blades only and is not compatible with a composite blade structure due to the need for a direct metal conduction path from the tubes to the skin; (3) the life of the engine exhaust heat exchanger would be limited by the corrosive-conductive environment; (4) potential tube leakage may compromise the blade flutter and balance requirements and thus affect the safety of the vehicle.

#### 3.2.4 System Characteristics

A summary of the various ice protection concepts including major advantages and drawbacks is shown in Table 12. Some of the techniques mentioned in this table are not practical for helicopter blade application because of mechanical or structural considerations (e.g., pneumatic boots), or because of inherent engine limitations (e.g., bleed air), or because of excessive energy requirements, such as a running-wet anti-icing system. This would require heating the entire vehicle, and for the UH-1H would take 71 kw of electric power. Not mentioned in this table are the icephobic and polymer coatings which have proven, so far, of no practical value. The principle of operation of these coatings is based on a low ice adhesion strength to the surface and/or achievement of a deformable resilient surface layer conducive to ice crack propagation and shedding. Also not mentioned in the table is the electroimpulse concept because there is not sufficient design data to perform a trade-off.

### 3.3 ENGINE INLET PROTECTION

#### 3.3.1 Design Criteria

Prevention of engine damage from ingested ice and/or snow, and prevention of performance deterioration due to inlet blockage can be achieved by either: (1) a special ice protection system wherein sufficient thermal energy is supplied to the critical surfaces to prevent ice from forming, (2) induction system design features that eliminate or minimize the icing and snow hazard, or (3) a combination of the two above mentioned techniques. Icing design criteria for the engine and engine inlet are specified in Tables 9 and 10 of AV-E-8593. Two basic conditions are

TABLE 12. ROTOR ICE PROTECTION CONCEPTS

Alternative	Mechanism	Advantages	Disadvantages
Chemical Freezing Point Depressant	Suitable fluid such as alcohol-glycerin mix is injected through holes, nozzles or porous leading edge panels - depressing freezing point - preventing or removing ice	<ul style="list-style-type: none"> <li>• Low dry weight penalty</li> <li>• Low fair weather drag</li> <li>• Simple control system</li> <li>• Low cost</li> </ul>	<ul style="list-style-type: none"> <li>• Fire hazard of stored alcohol</li> <li>• Blade imbalance and vibration due to faulty liquid distribution cause discomfort and reduce operating life</li> <li>• High vulnerability to battle damage because of exposed area, subject to leaks</li> <li>• Logistics requirements</li> <li>• Uncertain protection</li> <li>• Not retrofitable to existing blades</li> </ul>
Mechanical Ice Removal	Use of pneumatically inflated boots to physically break up ice	<ul style="list-style-type: none"> <li>• Low power penalty of activation</li> <li>• Moderate weight penalty</li> <li>• Low cost acquisition</li> <li>• Simple control system</li> <li>• Could be retrofitted to existing blades</li> </ul>	<ul style="list-style-type: none"> <li>• Performance falls off with lower temperature</li> <li>• No development experience on helicopter blades (uncertainty of boot bond in centrifugal force field)</li> <li>• Moderate fair weather power penalty due to increased airfoil drag</li> <li>• Retractability of boot questionable at rotor tip due to 300 "g" field</li> <li>• Severe effect on blade aerodynamics when inflated</li> <li>• Difficult to supply 20 psig air to rotating blade plus vacuum for suction</li> <li>• High maintainability cost</li> </ul>
Air Heated Anti-Icing	Heated air is circulated through the interior of the blade to prevent ice buildup	<ul style="list-style-type: none"> <li>• Good protection</li> <li>• Low weight using bleed air</li> </ul>	<ul style="list-style-type: none"> <li>• High power penalty due to bleed air consumption</li> <li>• High weight penalty if combustion heaters are used</li> <li>• High rotor blade cost due to internal manifolding and high bonding temperatures required</li> <li>• Probable unacceptable thermal stresses</li> <li>• Large rotational seals</li> <li>• Not retrofitable to existing blades</li> </ul>
Liquid Heated Anti-Icing	Ethylene glycol or oil is heated in an engine exhaust heat exchanger and circulated through tubes inside blade leading edge to prevent ice buildup	<ul style="list-style-type: none"> <li>• Competitive weight penalty</li> <li>• Fully evaporative protection</li> </ul>	<ul style="list-style-type: none"> <li>• Leakage into blades and maintenance to avoid leakage</li> <li>• Blade imbalance due to leakage</li> <li>• Vulnerable to battle damage</li> <li>• Not retrofitable to existing blades</li> </ul>
Electrically Heated De-Icing	Electrically heated elements embedded in a plastic laminate and protected by a metal erosion shield	<ul style="list-style-type: none"> <li>• Good performance</li> <li>• Minimum vibration</li> <li>• Best flight characteristics</li> <li>• Low blade drag</li> <li>• Suitable for retrofit to existing helicopters</li> </ul>	<ul style="list-style-type: none"> <li>• Moderate power penalty</li> <li>• Moderate maintenance costs</li> <li>• Moderate weight penalty</li> </ul>



stated in these tables: (1) low temperature icing ( $LWC = 1.0 \text{ g/m}^3$  at  $-4^\circ \text{ F}$ ) and (2) high temperature icing ( $LWC = 2.0 \text{ g/m}^3$  at  $23^\circ \text{ F}$ ).

The design icing conditions specified in AV-E-8593 are, in general consistent with intermittent and continuous maximum design criteria recommended in Figure 12b, and, therefore, represent a valid basis for design. AV-E-8593 does not specify an icing encounter duration for the induction system. However, the 15 minutes icing encounter duration recommended for the severest intermittent icing intensities is well justified even for hover or loiter. Intermittent maximum icing conditions occur only in cumulus clouds, and it is extremely unlikely to expect a pilot to spend a significant amount of time in such a condition, especially considering the dynamic nature of one with very high liquid water content (which is due to a very strong updraft). The need for engine induction system ice protection depends foremost on the induction system configuration and the location and orientation of the EAPS (engine air particle separator). With respect to ice protection requirements, four configurations have been identified:

1. Full Ram Pressure Recovery Duct - In installations where the available engine power margin is moderate, the intake may represent a discrete full ram pressure recovery duct with the EAPS being an integral part of the engine. The internal duct can be protected from snow and ice by either an electrothermal or an engine bleed-air system, with the latter being preferred because of proximity to the engine bleed ports, competitive weight, low maintainability, high reliability and engine/airframe integration considerations. Only in areas remote or inaccessible to any hot air source, or in retrofit installations, is electrothermal anti-icing recommended. Either system can be designed for running wet or evaporative anti-icing. In the running-wet mode, the entire interior duct surface to the engine face is maintained at a temperature just above freezing ( $40^\circ \text{ F}$ ), while in the fully evaporative mode only the water droplet impingement area on the lip is heated to an average temperature in the  $70^\circ$ - $100^\circ \text{ F}$  range. Figures 38 and 39 present typical requirements for electrothermal and hot bleed air anti-icing. Hot bleed air running-wet anti-icing offers several important advantages and, therefore, is more frequently selected:

- There is a large energy saving for running-wet protection (relative to evaporative protection) which is particularly pronounced for short ducts (Figures 38 and 39).

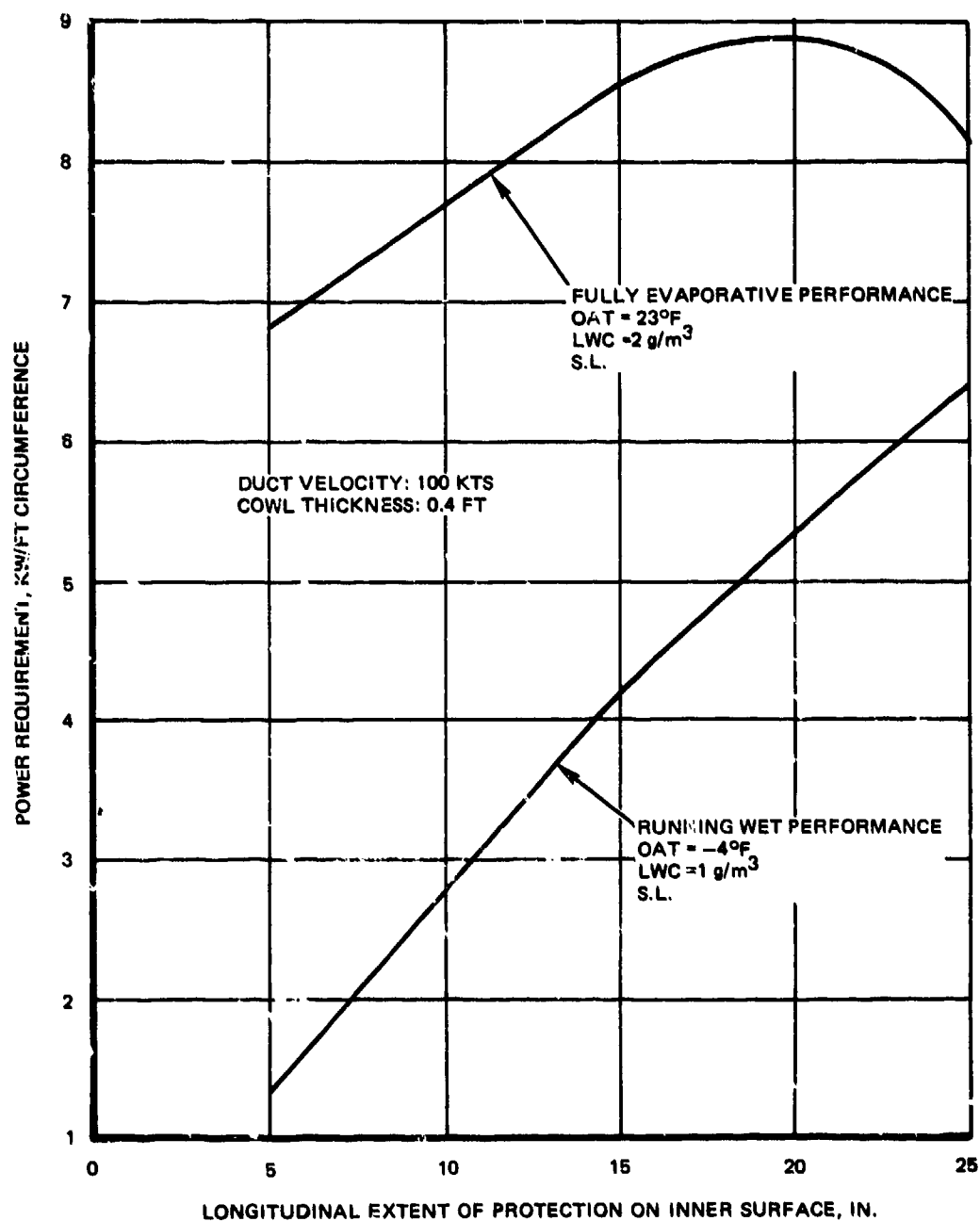


Figure 38. Electrical Anti-Icing Requirements for an Engine Inlet Duct.

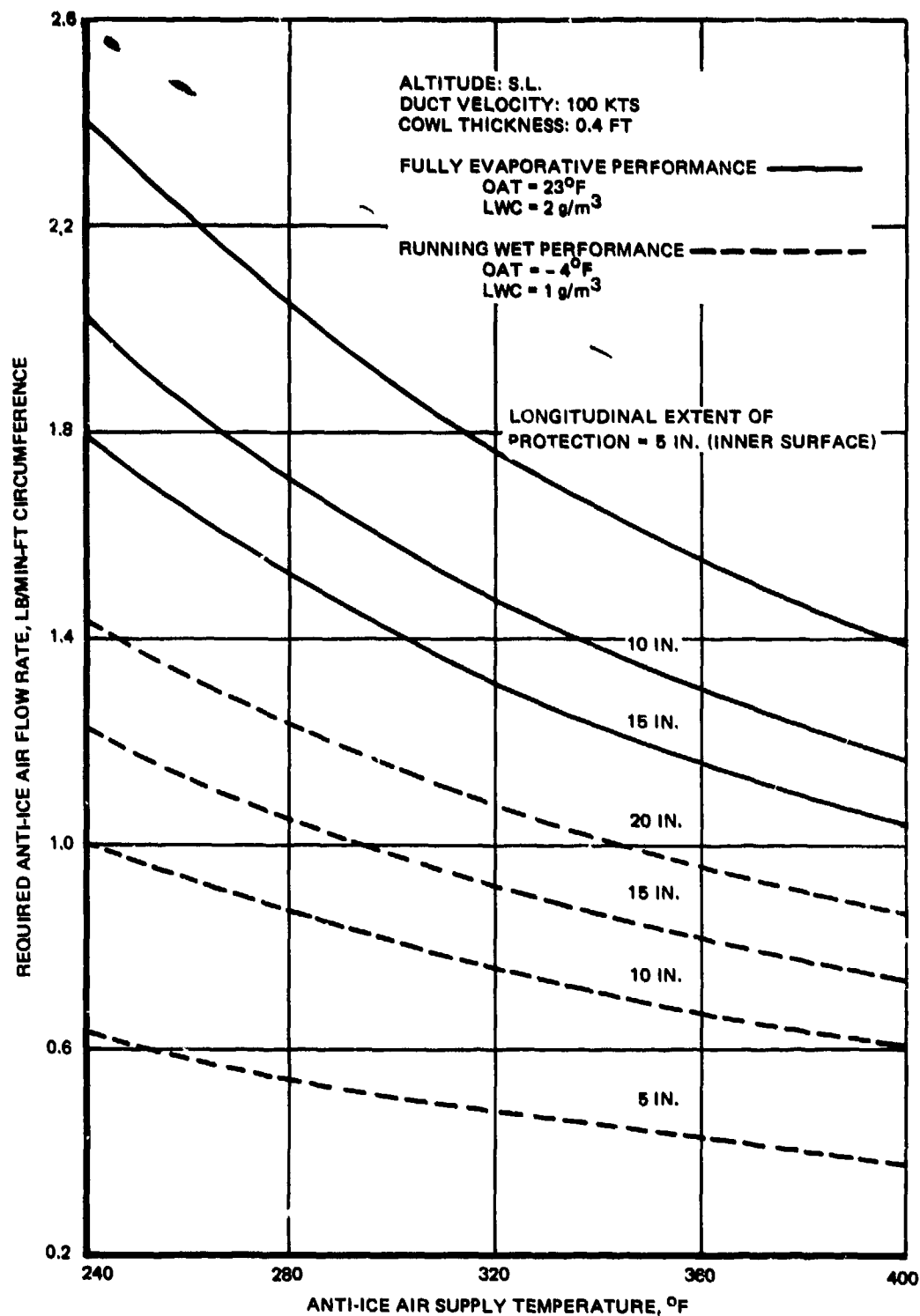


Figure 39. Anti-Icing Requirements of Engine Inlet Duct Using Engine Bleed Air.

- For evaporative protection, the design point is dictated by the evaporative heat loss, i.e., by the maximum LWC which occurs at the highest specified subfreezing temperature. In contrast, the design point for running-wet protection is dictated by the convective heat loss, i.e., by the lowest ambient temperature associated with icing. As a result, the performance of the running-wet system is affected very little, if any, by the degree of icing severity. Conversely, an evaporative system is affected by LWC's higher than those associated with the design point and, under such conditions, theoretically at least, runback may freeze aft of the heated area. As seen in Figure 39, the hot air flow requirements are also inversely related to the heated (longitudinal) length. This occurs since, as the water to be evaporated is a constant independent of the length, the required heat flux ( $\text{BTU/hr-ft}^2$ ) increases with decreasing heated area. This means that the required heat transfer coefficient between the hot air and the duct surface must also increase with decreasing heated length; and this must be obtained by using higher airflow rates.
  - For inlet ducts that feature bends or curves, running-wet heating of the entire surface eliminates the problem of snow that may melt and then freeze, forming ice.
  - The running-wet design with the anti-ice valve fail open requirement (par 3.23.1 of AV-E-8593B) can be met with a conventional aluminum alloy duct structure even on a hot day; evaporative heating, however, may require a high temperature alloy such as steel or titanium.
2. Duct-Plenum-Bellmouth Combination - In this type of installation, the engine is buried in a plenum with an engine inlet bellmouth situated in the plenum chamber. Air may be admitted into the plenum via short bifurcated intake ducts (OH-58) or via a single duct. The EAPS may be either integral with the engine or may be of the multimodule Donaldson type. Engine flameouts due to snow ingestion have proven to be a serious problem with this type of installation. This problem may have been caused by adverse features caused by the retrofit installation of filter panels and by stray heat from the engine into the plenum causing first melting of snow on warm surfaces and then runback and ice formation on cold surfaces. Operational experience has shown that induction system snow ingestion and/or icing can be eliminated by design features which include:

- Ease of accessibility that permits routine inspection of the plenum space behind the EAPS panels, of the engine face, firewall, and of the transmission shaft
  - Heated water drain(s) at the lowest level in the system to rid plenum of moisture
  - Ice protection provisions for the engine bellmouth
  - Filter panels of a simple shape to afford seals along straight lines for easy maintenance
  - A large positive margin for the filter module area over the engine face area with the total passage area of the filter modules being at least three times the engine face area
  - Nonuniform orientation of the filter panels so that no matter what the direction of snow may be due to crosswinds, no more than one-third of the panel would be into wind at any one time
  - Provision of thermal insulation or other means to assure a cold engine bay firewall, if the latter forms a wall of the inlet plenum chamber
  - Elimination of sharp re-entrant corners within the plenum to assure a simple and smooth geometry that will preclude places where snow and runback water might pack
  - Installation of the particle exhaust fan so that its bottom is sufficiently above the floor level to minimize the possibility of flooding
  - A flight station signal light to indicate excess pressure differential across the filter panels
  - Manually or automatically actuated doors to allow airflow to bypass the inlet particle separator system in the event of an excess pressure differential indication.
3. Plenum-Buried Engine with EAPS Panels Forming the Side Walls of Plenum - A typical example of such an engine induction system configuration is found in the CH-54. The tolerance of such an installation to snow and ice is regarded as adequate for all-weather operation due to the following: (1) With the multimodule filter panel surfaces forming a slight angle with the free-stream flow direction, snow and/or ice tends to build up only on the first row of filters, with this buildup shielding the

remainder of the panel; (2) the EAPS airflow area offers a large positive margin for blockage; (3) no matter what the direction of the snow may be, no more than one-third of the total filter area faces into the wind at any time; and (4) efficient purging and drainage of the plenum exists.

4. Side Facing Inlet with Pleated Screens - In this induction system, such as installed on the UH-1, air is admitted into the engine plenum through side-facing fine mesh screens (also referred to as a barrier filter). The fairing holding the barrier filter is so designed as to create a shadow zone at the leading edge of the filter. During hover icing tests at Ottawa and tanker tests at Alaska, it was observed that large areas of the barrier filter can and did become blocked; the shadow zone area, however, was sufficient to preclude any noticeable effects on engine operation. Therefore, unless future data shows otherwise, the pleated screen inlet configuration is considered to be satisfactory for operation under ice and snow conditions.

### 3.4 WINDSHIELD PROTECTION

A simple summation of requirements for the forward transparent areas can be stated as follows: Provide clear viewing-through essential transparent areas for any possible ambient condition, including icing, throughout the entire flight envelope of the aircraft. The three basic types of system used for transparent area anti-icing protection involve hot-air heating, electrical heating by means of a transparent conductive coating or wires, and dispersion of a freezing depressant fluid. The requirements for thermal protection are specified in MIL-T-5842A and for freezing depressant fluid protection in MIL-S-6625A (ASG). Figure 40 is a plot of calculated windshield heat requirements as a function of ambient temperature and altitude, with the velocity of maximum heat requirements a derivative value for each flight condition. These data are compared in Table 13 with the requirements shown in MIL-T-5842A.

The analytical results are more severe than those of MIL-T-5842A. However, the analytical approach is conservative because it is based upon the assumptions of: (1) A fully turbulent boundary layer over the windshield (implying a high heat transfer coefficient), and (2) a fully

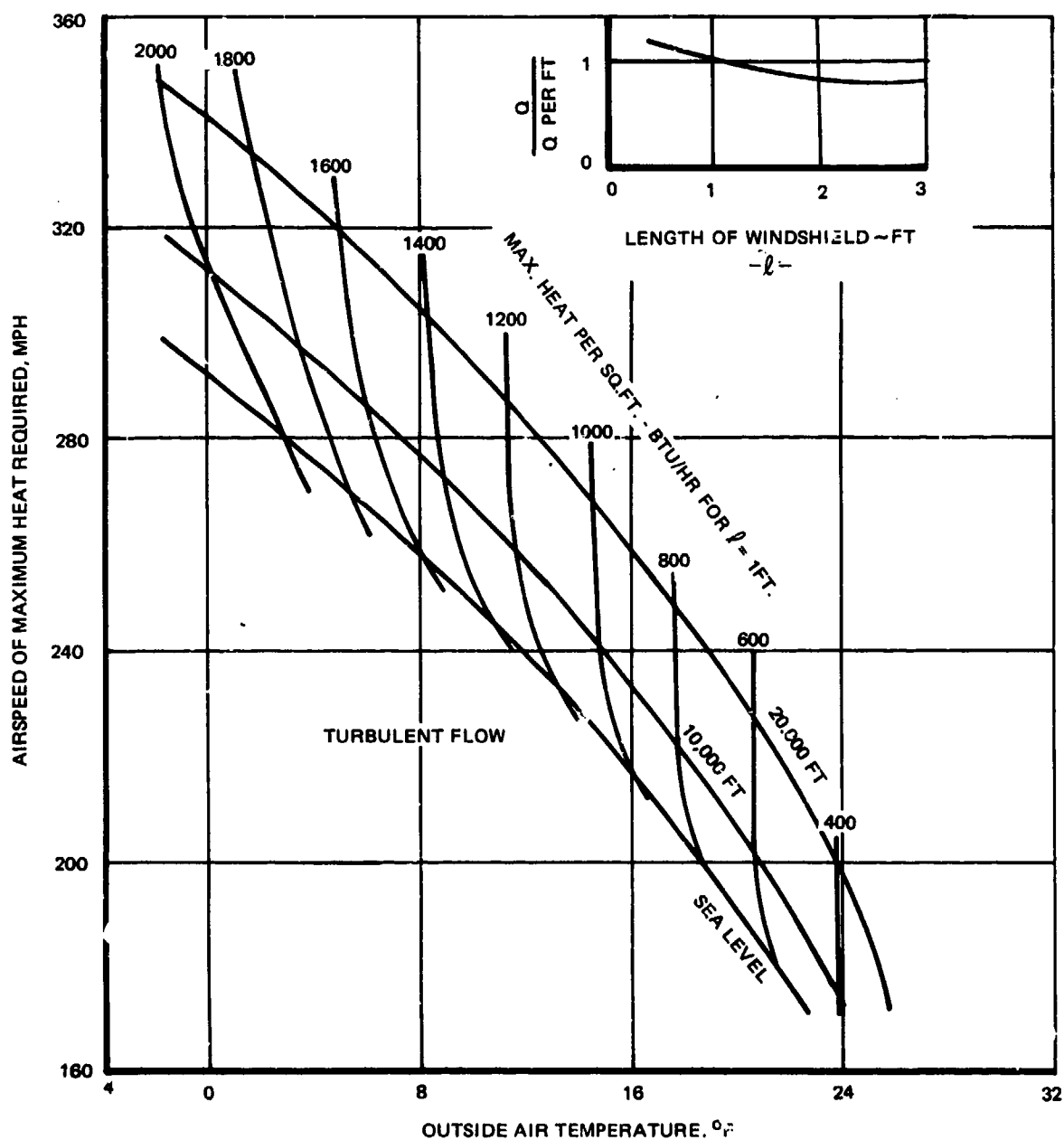


Figure 40. Maximum Heat Required Vs Airspeed and OAT for Windshield Anti-Icing.

TABLE 13. THERMAL WINDSHIELD ANTI-ICING REQUIREMENTS*		
Speed (Knots)	MIL-SPEC <sub>2</sub> Btu/hr-ft <sup>2</sup>	Analysis <sub>2</sub> Btu/hr-ft <sup>2</sup>
100	1,200	1,470
150	1,700	1,950
200	1,900	2,250
250	2,000	2,440
300	2,100	2,370
*Based on -4° F and sea level.		

wetted surface. Also, since service experience has been satisfactory with fixed-wing aircraft and on a limited basis also with helicopters, there is no reason to alter the existing standard. Following is a description of the three candidate systems:

Hot-Air System - Hot air transparent area anti-icing can be obtained from engine bleed air, applied externally via nozzle jet blasts or between two panes of glass. There are, however, very few aircraft which successfully use jet air blasts for windshield anti-icing. There are four principal disadvantages to this type of system:

1. During takeoff and high-speed cruise the high-temperature air from the main bleed-air system creates large thermal stresses in the windshield. The air temperature can be reduced to a usable level with a separate air-to-air heat exchanger, adding weight, cost, and drag.
2. During approach, landing, and slow-speed long-time endurance cruise associated with minimum engine horsepower level, bleed air availability is at its lowest level because the engines are throttled back. This is the time when the need for anti-icing and adequate vision is most critical.
3. The distribution of heat on the windshield surface with a jet blast is highly nonuniform, and only a small area on the lower edge would remain clear during low power conditions.



4. For modern high-efficiency turboshaft engines, inefficient use of bleed air is expensive in terms of power loss and fuel penalty. There is insufficient bleed air from the engine to provide an adequate air jet blast for an anti-icing system. Windshield anti-icing requires 4 lb/min of air at a temperature of 400° F per inch of windshield periphery. In the case of the UH-1, for example, this would require 300 lb/min (5 lb/sec) of bleed air compared to a total T-53 engine flow of 9 lb/sec.

In view of functional requirements as well as the unfavorable impact on the aircraft as a whole, a jet air blast anti-icing system is not recommended. A hot air double pane system suffers from all of the foregoing disadvantages, and, in addition, it is heavier and has optical distortion.

Liquid System - In this system the freezing-point depressant (e.g., glycol, alcohol, etc.) is pumped to the windshield and distributed over the surface in a thin film by the windshield wiper. The system has the following drawbacks:

1. The system has an inherent logistics problem because of storage and replenishment requirements.
2. The system exhibits a marginal visibility recovery capability, i.e., a delay in system activation after encountering icing may affect visibility.
3. The fluid distribution holes are sensitive to clogging, particularly in the dusty environment associated with rotary-wing aircraft operation at or close to the ground.
4. A liquid system will anti-ice but not defog the transparent surface; therefore, a supplemental defogging system is required.
5. The liquid is not compatible with plexiglass.

Electrical Heat System - A survey of modern commercial and military airplanes shows that the overwhelming majority use electrical heat for windshield anti-icing and defogging. Among the major advantages for this method are the following:

1. Simple ON-OFF control switch operation
2. Ability to obtain good control of heat distribution

3. Ability to obtain good temperature control of viewing area
4. Independence of system performance from all aircraft operational modes
5. Clearance of water drops off windshield surface after rain
6. Enhancement of strength of plastic panels due to continuously applied heat
7. Defogging

There are three types of transparent coatings: evaporated gold, tin oxide, and indium oxide. Tin oxide is the most widely used because of its favorable characteristics related to toughness and durability, and also because of its low cost. However, application of tin oxide requires heating of the windshield to "red hot" conditions ( $1000^{\circ}$ - $2000^{\circ}$  F minimum); this precludes the use of chemically tempered glass on the outside because such heating reduces the tempering properties of glass. Therefore, a gold coating is usually applied in conjunction with chemically tempered glass. Indium oxide combines the favorable characteristics of tin oxide and gold, but it is still in the development stage. All coatings require ac power since the resistance is such that 28 volts is inadequate. Wires embedded between windshield laminates can be used with low voltage dc systems but have been used less frequently than coatings because of the adverse impact on optical properties. An electrically heated helicopter windshield would typically consist of an outer 0.10-inch glass ply, an 0.080-inch polyvinyl butyrol (PVB) interlayer, and a 0.10-inch glass interlayer. The coating is applied on the inner surface of the outer ply so that it is as close to the outer surface as possible.

Early windshield heat controllers sensed temperatures by means of a thermistor embedded in the vinyl a short distance behind the heater element. The type used was a disk approximately 0.6 inch diameter by 0.04 inch thick. It had the advantage of a high rate of change of resistance with temperature. As the coefficient of resistance was negative, two or three windshields could be controlled by one controller

by placing a thermistor in each windshield and connecting them in parallel. In the case of an open circuit in either a windshield or a thermistor, the control would still operate satisfactorily with only a slight increase in cutoff temperature.

One disadvantage of the thermistor type of sensor was opaqueness and optical distortion around it. Any current passed through it by the controller causes some self-heating and so compensation is required to avoid a shift in the control point. Another installation difficulty is that the electrical contact to thermistor material has very little mechanical strength and it is necessary to encapsulate the thermistor and leads prior to installation so as to avoid breaking the connections due to elastic flow during windshield lamination.

A more recent technique in windshield control is to use fine resistor wires sandwiched between two plastic sheets. This element has a positive resistance characteristic although its temperature coefficient is very low compared to a thermistor. Also, this element cannot be connected in parallel, for the coldest sensor would then control. Advantages, however, are the simplicity of construction, ease of installation, and the fact that it is nearly transparent. For these reasons, this type of control is now used almost exclusively.

In modern controller design it is normal to use two sensors for control and, sometimes, provide an unused spare to avoid any expensive replacement in case of sensor failure. In a typical mode, each active sensor is connected in a bridge circuit and compared with a standard. The outputs of the two bridges are connected to a comparator and the lower error selected and amplified. The amplified signal is used to switch successive taps on an output transformer so that output is varied gradually until the error-sensed is minimal. This avoids thermal shock and provides overtemperature protection in case of sensor failure. A more economical design is simply to use one sensor (plus a spare) through a bridge circuit to cycle the windshield power on and off (rather than modulate). A solid-state switch may be used to minimize EMI problems.

### 3.5 FUSELAGE NOSE AND RADOME PROTECTION

The ice accretion characteristics on the fuselage nose surface are primarily a function of the shape of the nose. With a blunt hemispherical or ellipsoidal nose radome, such as used in helicopters, flight through supercooled clouds results in an ice formation that is primarily in the forward area, thus providing a large ice-free area on the aft portion of the radome (Figures 41, 42, and 43). It can be seen that for the maximum 40-micron droplet size associated with supercooled icing clouds the impingement limit (Figure 43) is relatively close to the nose stagnation point and affects a frontal area which is only 14 percent of the nose frontal area. Operational experience has shown that the drag increment of such nose ice buildups is well within the positive power margin of existing helicopter engines. Detrimental effects of nose icing, in terms of a speed reduction and/or increased fuel consumption, are hardly detectable. In fact, some drag penalties incurred during normal operation, such as unintentionally opened doors, external armament stores, external rescue gear, etc, are significantly higher than the drag caused by the most adverse supercooled cloud ice formation on the nose. It is estimated that, after an icing encounter duration of 1 hour in a supercooled water droplet cloud of continuous maximum intensity, the drag due to nose icing would not exceed 1.5 percent of the total vehicle drag. Considering ice formations on other exposed surfaces such as light fixtures, antennas, landing skids, main rotor mast, and stabilizer bar, elevator, etc, the total drag penalty would not exceed 5 percent. Thus, ice formed on the nose and other protuberances during supercooled cloud icing encounters does not represent a helicopter safety hazard provided ice shed from the airframe surfaces does not enter the engine or impact upon other rotating components. Keeping ice from entering the engine can be achieved during the design phase by appropriately locating and/or orienting the engine intake.

For large droplet diameters (in excess of 200 microns) typical of freezing rain and drizzle, impingement occurs over the entire nose surface

Reproduced from  
best available copy.

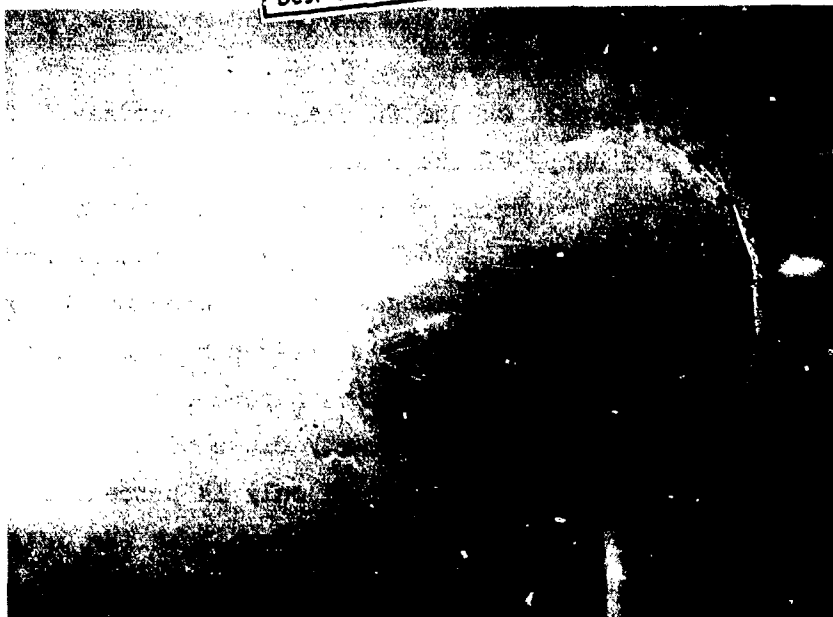


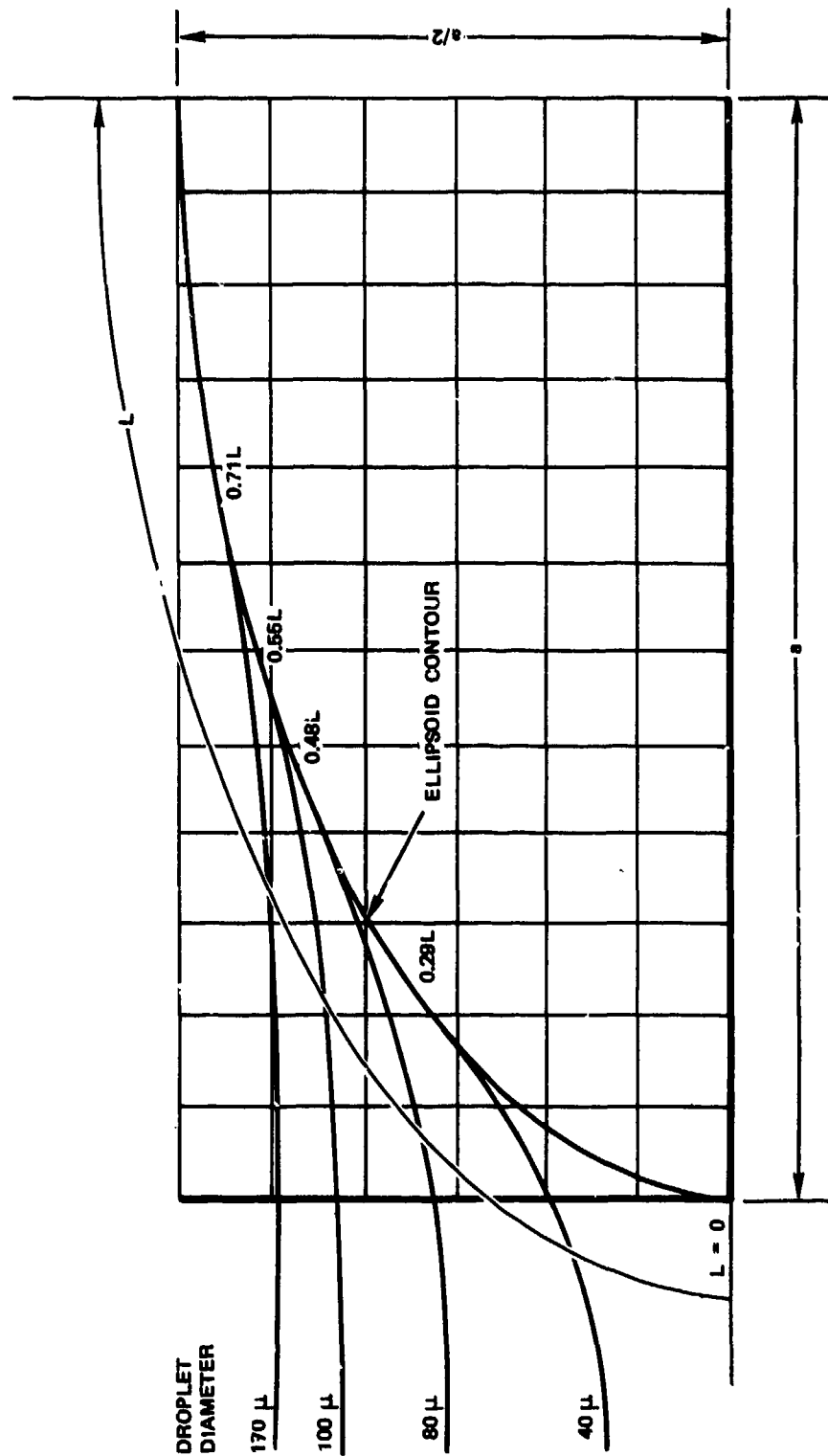
Figure 41. Ice Buildup After 15 Minutes on 1/6-Scale\* Icing Tunnel Model of C-5A Nose Radome - Test 2.\*\*



Figure 42. Ice Buildup After 28 Minutes on 1/6-Scale Icing Model of C-5A Nose Radome - Test 2.

\*1/6 scale C-5 radome is approximately the same size as full size UH-1 nose shape.

\*\*See Table 14.



$s = 30 \text{ IN.} = 2.5 \text{ FT}$

Figure 43. Impingement Limits on Fuselage Nose for Various Droplet Diameters.

and runback freezing may extend on the fuselage aft of the nose (Figure 43). A theoretical extreme may be postulated wherein it is assumed that the nose, under impact of freezing rain or ice, would assume a flat plate shape oriented normal to the free-stream direction. In the case of the UH-1, for example, the resulting nose drag for this geometry ( $C_{D\pi} = 1.0$ ) would add 50 percent to the drag of the clean aircraft. The assumed theoretical extreme yields an overly exaggerated drag value. However, it does point up the potential seriousness of the consequences of a prolonged freezing rain encounter. Of significance are the ice accretion characteristics on the nose, particularly the compatibility of these characteristics with the operational requirements of the nose radar. The X- and  $K_u$ -radar bands are the most commonly used in military as well as in commercial applications. The X-band radar is a forward-looking radar with an 8,000- to 12,000-megahertz frequency; it is located in the nose radome of the aircraft and accomplishes one or a combination of several functions: weather mapping and terrain following, general search and surveillance, and fire control. At the present time there are no helicopters with X-band radar installations, or for that matter with any type of radar. The AAH may be a viable candidate for an X-band radome. The  $K_u$ -band transmission represents a Doppler radar with a 12,000 to 20,000-megahertz frequency; it is a downward looking radar traditionally located on the bottom surface of the fuselage and is used to determine the true ground speed, the sidewise drift, and the altitude of the aircraft. The effect of ice accretion on the radome transmission efficiency is available from C-5A radome tests, the results of which are shown in Table 14. Attenuation of the X-band radar transmission efficiency by icing is less than 20 percent. Installation of a pneumatic deicing boot would cause a similar reduction in efficiency, while freezing depressant anti-icing would cause an average 10-percent reduction in efficiency. Perhaps of greatest significance is the fact that a nose radome ice protection system would permanently affect clear operation as well.

TABLE 14. SUMMARY OF C-5A MODEL RADOME ICING/RADAR TEST RESULTS

Test Condition	Test Description	Minimum Transmission Efficiency, Percent	
		X-Band	K <sub>u</sub> -Band
1a b	Baseline transmission (by definition) Rain	100 98	100 98
	<u>Icing, no anti-icing protection</u>		
2a*	Hold, +25° F	89,84,95	59,63,66
b*	S.L. Cruise, +25° F	69,79,88	69,73
c*	S.L. Cruise, -4° F	89,90,91	96,97
	<u>Scan angle tests with ice buildup</u>		
3a	Hold, +25° F	86	69
b	S.L. Cruise, +25° F	89	86
c	S.L. Cruise, -4° F	91	-
	<u>Melting Ice Effects</u>		
4a*	Hold, +25° F	71,73,79	57,60,77
b	S.L. Cruise, +25° F, 8-minute initial ice buildup	72	60
c	S.L. Cruise, -4° F, 3-minute initial ice buildup	60	63
5*	Glycol spray (4 gal/hr, 15 psig)	91	97
	<u>Glycol spray and icing cloud</u>		
6a	Hold, +25° F 0.2 gal/hr	93	96
b	S.L. Cruise, +25° F 0.3 gal/hr	92	97
c	S.L. Cruise, -4° F 4.0 gal/hr	88	95
7	Glycol deicing	51	63
	Effect of nozzle	98	93
	Effect of nozzle plus lines	97	92
5*	Effect of nozzle, lines and 4 gal/hr flow (15 psig)	85	87
*Repeated tests			



Table 14 shows that ice has a greater effect on  $K_u$ -band transmission than on X-band. However, the location of this type of radome on the bottom of the aft fuselage surface which can be accomplished with only a slight protrusion into the airstream obviates the need for ice protection for such a radar. This location, which is not conducive to severe ice accretion, has been also considered for the advanced attack helicopter and other future models.

It is concluded that in view of the moderate type of ice formation associated with helicopter nose configurations and operational characteristics of the radar involved, as well as the favorable experience in other aircraft having radar, no radome ice protection system is justified.

### 3.6 FLIGHT PROBE PROTECTION

There are two separate specifications for anti-icing of pitot-static pressure sensors. For commercial application FAR 25 intermittent maximum icing conditions specifies  $1.0 \text{ g/m}^3$  at an OAT of  $-22^\circ \text{ F}$  ( $-30^\circ \text{ C}$ ), for military application MIL-P-26292 specifies an LWC of  $1.5 \text{ g/m}^3$  at  $-21^\circ \text{ F}$  ( $-35^\circ \text{ C}$ ) at an altitude of 10,000 ft and a speed of Mach 0.6. The flight criteria (speed and altitude) specified in MIL-P-26292 are commensurate with the performance capability of high-speed fixed-wing aircraft and thus result in heating requirements that are greater than for typical helicopter flight modes.

To maintain an ice-free surface for the specified relatively high LWC values, pitot-static tubes are heated to provide running-wet surface conditions. Figure 44 compares the actual heating intensity on a typical probe with the intensities resulting from MIL-P-26292 requirements. The criteria of a  $40^\circ \text{ F}$  surface temperature and a wettedness factor of unity (ratio of wet-to-dry surface area) tend to maximize the computed heating requirements. Figure 44 shows that for typical helicopter application, the actual applied power intensities provide a positive heating margin

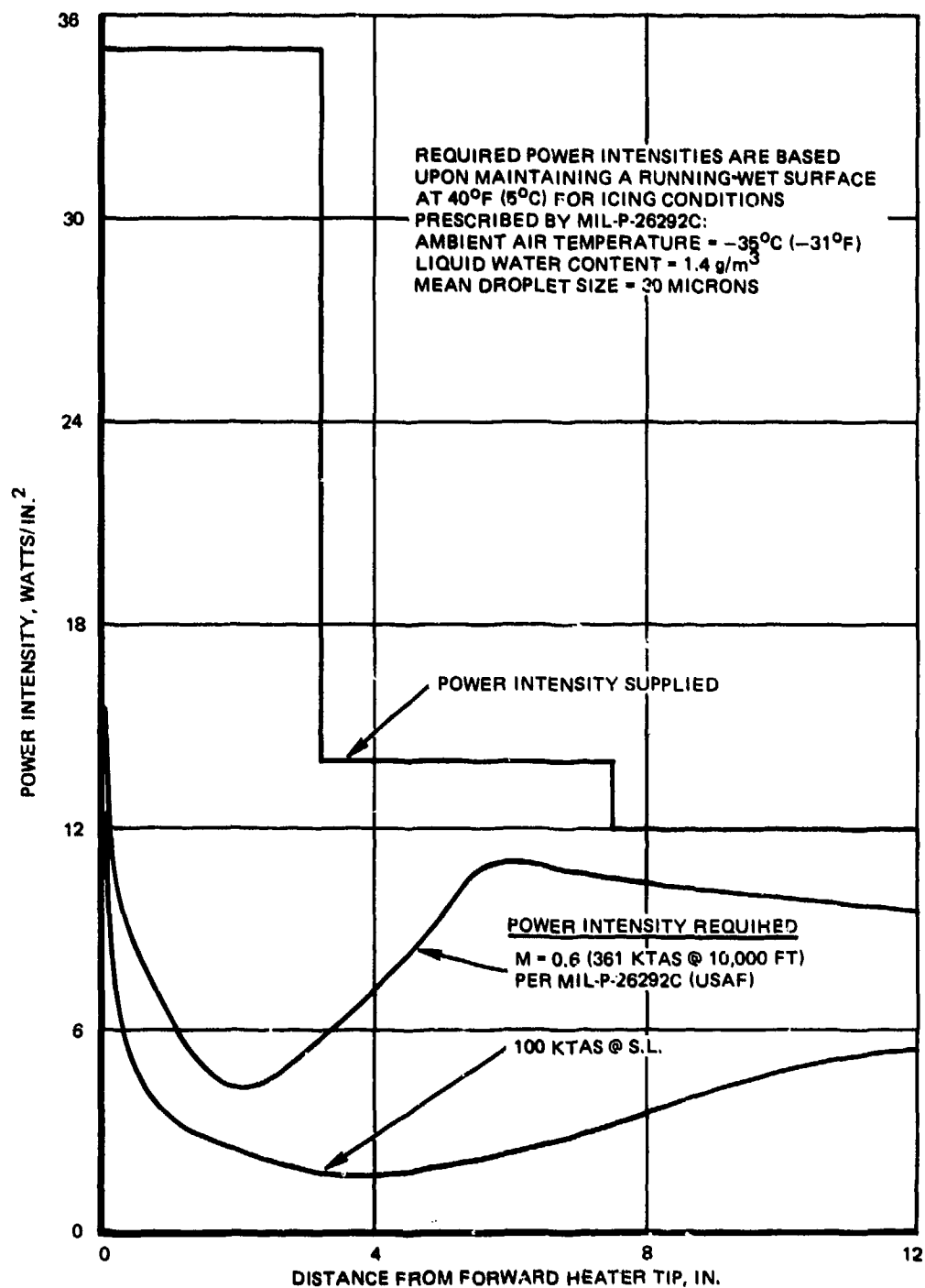


Figure 44. Comparison of Required and Available Anti-Ice Power Intensities For Typical Pitot-Static Tube Heater.

on the order of 200 percent. In this probe, the total peak power consumption for anti-icing is 400 watts, of which 210 watts are allocated to the sensor head and 190 to the mast. The delivered electrical energy is modulated such as to prevent overheating in warm clear ambients.

In summary, the current degree of protection provided for pitot-static probes is more than adequate to meet commercial, as well as military icing criteria. The same conclusion is also valid when applied to freezing rain or drizzle, for freezing rain and drizzle occur at high subfreezing ambient temperatures ( $20^{\circ}$  to  $32^{\circ}$  F). Therefore, the available heating performance margin for freezing rain is considerably greater than for the design icing point.

As far as the two sets of icing design criteria (commercial and military) are concerned, it is recommended that the lower ambient temperature specified by MIL-P-26292 be retained for helicopters. Because of the small dimensions of the probe, protection to  $-31^{\circ}$  F rather than to  $-22^{\circ}$  F requires only an additional 80 watts. Considering that present heating provisions on pitot-static probes are more than adequate to meet the more stringent MIL-P-26292 requirements, the slight power saving for FAR 25 criteria is largely of academic interest. Moreover, the applicable FAR documentation is in the process of being revised, and it is understood that the new requirements will probably be more severe.

### 3.7 WEAPONS AND SENSORS

The copilot/gunner sighting station (CP/GSS) along with the trained gunner is a key element of the fire control system for combat helicopters.

An integral part of the CP/GSS is the sighthead in which are mounted the following sensors:

- Forward Looking Infrared (FLIR) Subsystem
- Laser Rangefinder/Designator (LRD) Subsystem
- TOW IR Tracker and Error Detector

These sensors are installed for viewing through a window, which must be free from optical distortion and kept clear during icing conditions.

Since both window anti-icing and antifogging is required, the thermal type systems have been considered. The methods include hot-air flow on the window and electrical current heating through the window materials. The latter system has been shown to be very suitable for the FLIR subsystem which requires viewing through a germanium window. The intrinsic resistivity of germanium allows the window to be utilized as a heater element. Any distortion is minimized by controlling the surface to a low temperature.

For the visual/laser window, both anti-icing systems considered have disadvantages. This window is made of quartz so that either a conductive coating or a wire mesh is required to transmit electricity. Since light transmission in the visible and the IR range of interest is reduced and some colors are distorted, the conductive coating is unacceptable. The wire-mesh system is practical only if the window strip covered by the laser transmitter may be anti-iced by conduction from the wire mesh on its perimeter.

A hot-air system requires ducting of bleed air or a blower-heater arrangement. The latter is bulky and would require a significant amount of turret volume. A jet pump using bleed air is more amenable to the space available. The hot air may be blown on the outside of the window or channeled through a passage between two panes. The double pane configuration, however, causes optical distortion and adds weight. Blowing on the outside may result in insufficient coverage and temperature stratification if the hot-air distribution is not carefully controlled.

While either the hot air or electrically heated visual/laser window is acceptable for anti-icing, the effect of thermal distortion on scatter, obscuration, distortion, etc., is not known. Light transmission for TV viewing at night is not as critical as for the (CP/GSS) sighthead sensors. Either the hot air or electrothermal anti-icing is considered to be adequate for TV windows.

Since thermal anti-icing of the visual/laser window compromise to some extent the character of the light transmission, a shielding device such as a retractable clam shell should be considered as an alternate. Power for retraction would be designed to overcome the resistance of any ice accumulation, and door actuation would have to be reasonably assured to guard against any failure to open.

Potential weapon icing problems might involve icing of missile launch tubes, gun barrels, fittings and other protruding surfaces. Should such problems be encountered, design of special power-operated collars or enclosures could be considered. These devices are basically within existing technology. An icing tunnel or flight test program would be required, however, to establish actuator forces required to break the ice bond. Frangible heated covers could also be used for rocket launch tubes. While technology is available for the design, an icing tunnel or flight test program would be required to verify the design. A test program to evaluate the effect of accretion on weapons is not within the scope of this contract; however, it is needed to define the problem area, if any.

### 3.8 ICING INSTRUMENTATION

A large number of different types of ice detectors have been developed commercially over the past 25 years. Some types are still in production and are seeing continued active development; some are out of production in the United States (or Canada) but are still being produced in Europe; and some, while still in production, are not really being actively marketed and are not seeing new applications in recent years. Of current interest for helicopter operation are concepts that offer the possibility of indicating icing severity (liquid water content) and/or the presence of icing during the hover mode. The latter capability can be accomplished

by an aspirator-type device (usually by using a small quantity of engine bleed air) to induce the ambient air (cloud) over the sensing surface.

Warning of icing can be accomplished by either a discrete yes/no signal as a minimum requirement, or by an icing rate display of severity levels. The latter could be used as a means of controlling the power input and/or ON and OFF time for electrothermal deicing, commensurate with the icing intensity. A comparative assessment of existing icing meters, as presented below, is based upon the experimental data of Reference (21) and on personal discussions with the various manufacturers.

### 3.8.1 Simple "Hot Rod"

This is the simplest of the ice detection devices and consists of a simple illuminated rod, mounted in front of the windshield, and visually observed by the pilot to detect any evidence of icing. Manual periodic activation of the rod heater affords a rough estimate of the icing severity. The capability of the "Hot Rod" has been extended so that, by the use of two photoelectric devices, an automatic ice warning indication can be given. An infrared light source and detector are spaced apart along the leading edge of an airfoil section, with ice of a predetermined thickness on the airfoil interrupting the light beam. The interruption of the light beam is sensed by the photo detector which is coupled to a relay to operate a circuit controlling a heating element within the sensing probe. This deices the latter and results in the light beam between the light source and detector being reestablished for the next icing cycle. For helicopter application, the detector can be provided with an aspirator-induced airflow. It is claimed that 1972-73 icing trials with a Sea King showed the unit to perform successfully, producing an ice warning signal in advance of other types of detectors.

---

(21) Berry, R. E. and Pardee, J., EVALUATION OF ICING RATE SYSTEMS ON THE SH-3D HELICOPTER, THIRD REPORT (FINAL), Naval Air Test Center Report No. ST-41R-69, 8 July 1969.

### 3.8.2 Ultrasonic System

This system consists of an ice detector head and a console-mounted control box, incorporating an icing signal light, an icing rate indicator, and an event counter. The indicator is capable of exhibiting trace, light, medium and heavy icing rates. The ice detector head contains an icing probe which is set into a resonant axial vibration of 40 kHz by magnetostriction. The probe resonant vibration frequency is a function of its mass. Ice on the probe increases the mass and reduces the frequency. The reduced frequency is compared to a stable reference frequency generated by an oscillator circuit in the detector. The rate of change of frequency is directly related to the rate of ice accretion on the probe and provides the basis for the icing rate indication system which has been developed. The display currently indicates trace light, moderate, and heavy icing.

### 3.8.3 Hot Wire System

This system consists of a detector and meter and/or an icing signal light. It has been developed and produced in the United Kingdom. This system utilizes an inferential technique in which the temperature change, due to the impingement rate of free water on an exposed sensor, is measured against the temperature of a shielded datum sensor which is exposed to the dry component of the airstream. The power differential required to maintain the same temperature on both sensors is indicative of the moisture content of the air and will cause a deflection of the icing rate meter. The unit senses conditions conducive to icing rather than ice accretion, and the indicator displays the LWC in grams per cubic meter.

### 3.8.4 Radioisotope System

This system consists of a detector probe, a remote controller and computer, and a control panel containing a warning light and an icing rate indicator. Radioactive beta particles from a source in the tip of the probe pass in front of an ice accretion surface and into a Geiger-Muller counter. At a preset accretion level, beta attenuation is

sufficient to trigger output circuitry at the controller. The controller then energizes the warning light, which remains "on" until the ice is melted. Icing rate is a function of the time elapsed between the icing cycles. The unit apparently is no longer being marketed in the US, but it has seen wide helicopter application in the USSR.

#### 3.8.5 Differential Pressure System

The pressure differential across two sets of orifices, one iced and one clear, is used to generate a warning signal and to energize a heater to deice the probes. This system has been in existence for 25 years but has earned a poor reputation due to nuisance and false warnings caused by (1) dirt, insects, etc, in the small orifices, (2) freezing of water in the plumbing, and (3) heater burnouts due to high intensity concentration. This technique has not been used in most recent applications (although it is still being produced).

#### 3.8.6 Infrared System

The system is presently in the test evaluation stage. The system contains a probe (heater element) with an infrared emitter and similar detector disposed at right angles to the probe. Occlusion of the IR beam by ice on the probe energizes the heater. An annular ejector nozzle powered by engine compressor bleed air is used to entrain ambient air and thereby induce a constant high velocity airflow over the probe, regardless of the flight mode of the aircraft and the location of the probe. (An aspirator may be used with any of the concepts discussed and has in fact been developed for the ultrasonic type). A modified ice accretion rate indicator has been developed which shows light, moderate, or heavy icing.

#### 3.8.7 Evaluation

According to Reference (21), the ultrasonic system exhibited the best reliability of the systems tested and provided a consistent, rapid warning of entry into icing conditions (1 to 2 minutes subsequent to entry).



However, the degree of severity indication depends upon the location of the probe on the helicopter. The ultrasonic unit was recommended for installation on the SH-3D. The hot-wire inferential system was extremely sensitive, but the icing signal light operation was unsatisfactory. The LWC displayed by the hot-wire inferential meter may be misleading because the unit is calibrated on the ground and there is no allowance made for the altitude effect. (The amount of evaporated moisture on a surface is inversely proportional to the ambient pressure, and this has been brought to the manufacturer's attention.) During the tests described in Reference (21), the radioisotope system was not evaluated for a sufficient period to determine reliability. However, verbal information from the British Ministry of Defense (Mr. Allan Wilson) revealed that, based on their icing trial test results, this system was found to give very satisfactory and reliable performance. Although considered perfectly safe, there is general reluctance to use and handle the system because of the presence of a radioactive source. Also, as noted, there is no marketing effort in the US of the radioisotope system.

The need for an ice detector or icing severity meter is still an open question. On fixed-wing aircraft, the policy has been to provide a unit only if the engine manufacturer requests it. Symptoms of possible icing would be: presence of clouds and outside air temperature below 32° F. In addition, windshield wiper blades have been proven to be sensitive ice catchers. The need for an icing severity signal to modulate rotor blade deicing system performance still needs to be determined from flight test experience. It had been hoped that testing on the UH-1H behind the icing tanker would provide sufficient data on the need for icing severity data in an operational system, but the icing cloud is so thin (the approximate thickness is 5 feet) that the icing severity at the plane of the sensor is materially different from that in the plane of the main rotor. Thus, a final system recommendation will have to be made after sufficient flight experience in natural icing. Experiences with the ice detectors are discussed more completely in Section 5.7 of Volume II.

### 3.8.8 Determination of Droplet Size

Information on the droplet size in supercooled clouds has been obtained by the rotating multicylinder apparatus. The instrument consists of several (in most cases, five) cylinders of different diameters mounted coaxially and rotated slowly with the long axis normal to the wind. The differing catches per unit length are measured, from which the volume-median drop size and an indication of the drop size distribution can be obtained.

Another technique pioneered at the Air Force AEDC wind tunnel involves laser holography. This technique consists in recording on film the interference patterns created when half a laser beam passes through a disturbed (by water droplets) airflow and the other half reaches the same film undisturbed. A 10-Mw laser was used at AEDC to take a hologram of the airflow so that size and distribution of the water droplets could be studied. Still another technique to study cloud and precipitation involves the use of doppler radar. While acceptable for ground laboratory work, the above techniques are less, if at all, suitable for airborne application due to weight, space, and other inherent limitations.

In some cases a large-diameter cylinder with its axis oriented normal to the airstream and longitudinal calibration marks on the cylinder has been used to obtain a rough estimate of the location of the aft impingement limits of the droplets and thus, of the size of the largest drop in the cloud. The median drop is obtained by assuming that its size is half of the size of the largest droplet.

The most commonly used technique to measure droplet size in flight involves microphotography of an oil coated slide after its momentary exposure to the ram stream. A more recent development uses a replicator (Figure 45) which features 35-mm slide frames coated with gelatine. Momentary exposure past an open slot leaves permanent footprints (cavities) in the gelatine substance (Figure 46). In order to capture a true sample, the collection efficiency of the collector (i.e., the fraction of

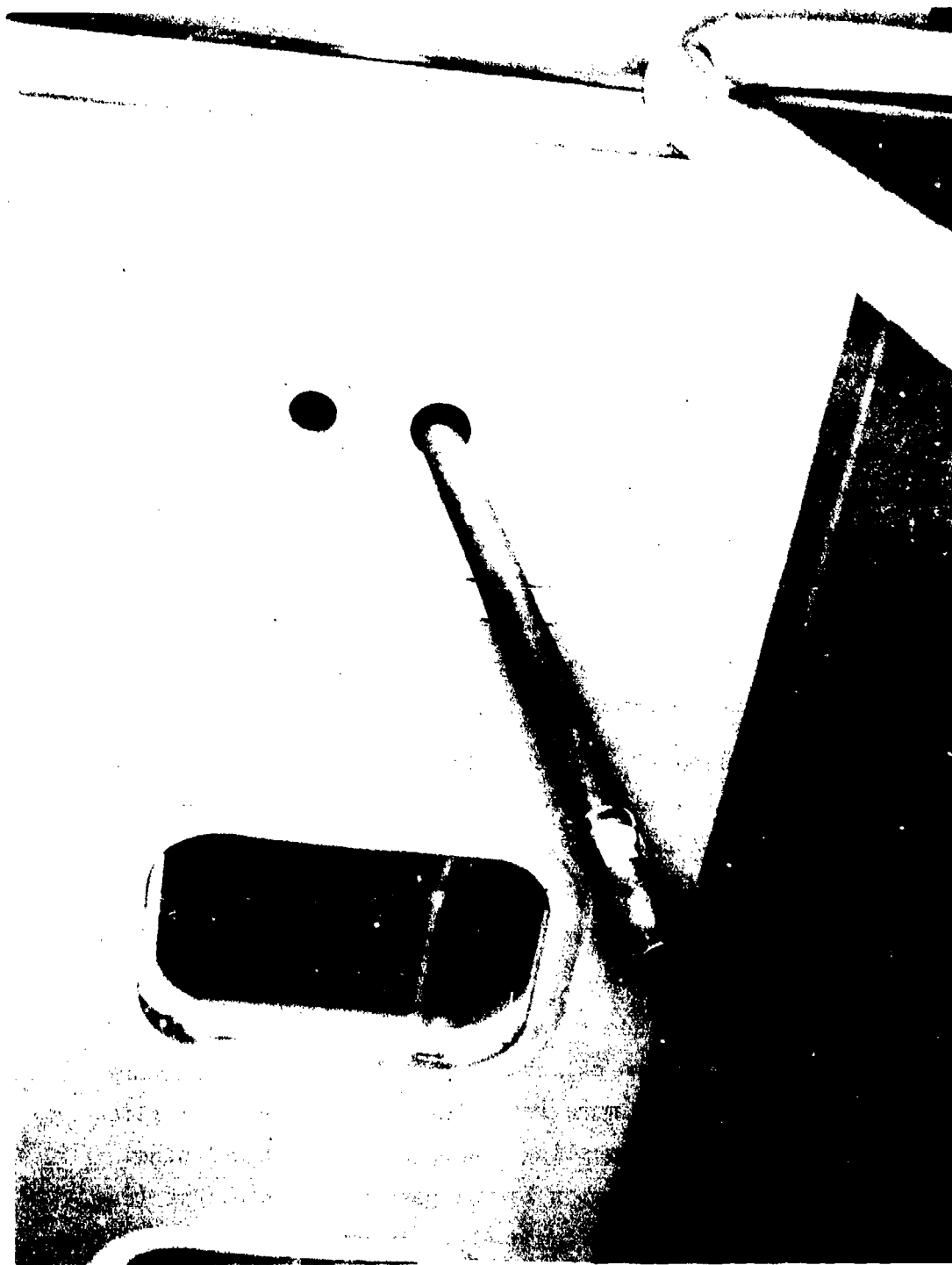


Figure 45. Water Droplet Collection Device.

Reproduced from  
best available copy.

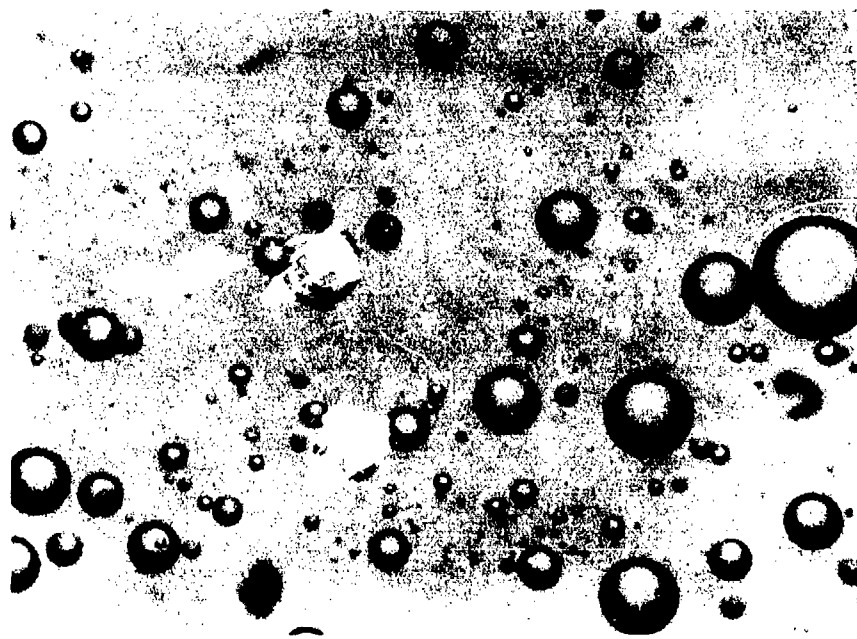
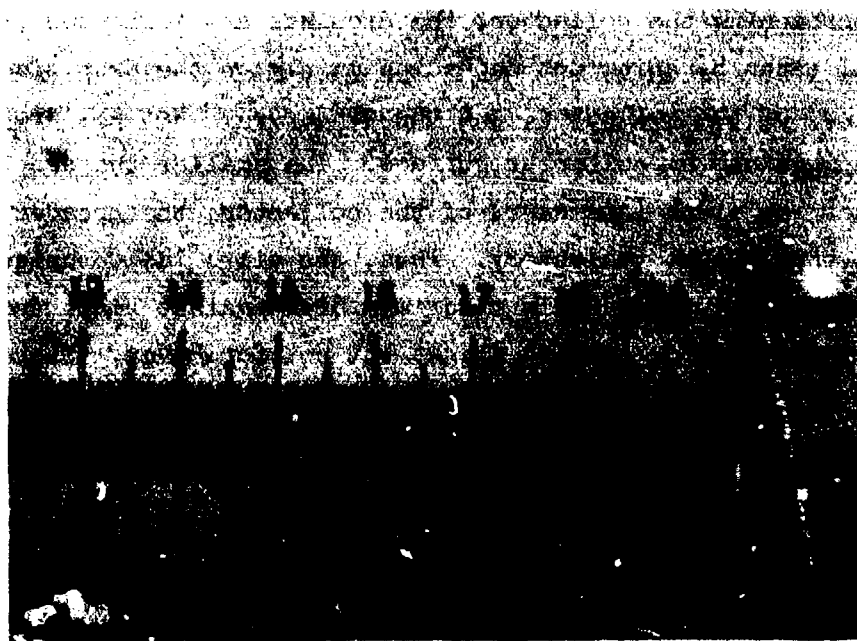


Figure 46. Water Droplet Photomicrograph.

the droplets lying in the projected cross section which actually hit the collector) must be unity for droplets of all sizes occurring in the cloud. On approaching the collector, the droplets are deflected from their original paths by an amount depending mainly on the drop size, the width (diameter) of the collector, and the windspeed. Not all droplets, therefore, impinge on the collector surface. The smaller the droplet and the greater the width (diameter) of the collector, the greater the deflection in the droplet trajectory. Thus, the oil slide technique and the replicator technique result in discrimination against small drops, and are suitable primarily for forward flight but not for hover. There is a real need for flight test instrumentation to accurately measure the drop size in icing conditions but such a device is not necessary for operational aircraft.

## SECTION 4

### SYSTEM TRADE-OFF ANALYSIS

#### 4.1 OBJECTIVES

The trade-off analysis is concerned with the study of application of anti-icing/deicing systems for advanced-type helicopters. To achieve all-weather capability, primary attention is directed in the analysis toward protection of the main and tail rotors and the forward transparent surfaces. One of the objectives, therefore, is to compare and select for each of these components ice protection concepts that will best meet the icing severity criteria previously evolved. This has been done for seven helicopter types.

A second objective is to trade off protection penalties against icing severity or ambient temperature, as appropriate.

It has been concluded in the technology study that snow is not a hazard in properly designed (engine) installations. The special conduction system design features required to achieve an acceptable snow tolerance are discussed in Section 3.3. The penalty associated with incorporation of such design features is insignificant. For the purpose of the trade-off analysis, rotor ice protection concepts include the following:

- Electrothermal cyclic deicing
- Chemical freezing point depressant
- Heated air or liquid anti-icing (three versions)

In comparing these concepts, performance penalties and direct costs have been analyzed. The trade-off parameters that have been generated for each of the above contender systems include the following:

- Performance
- Engine power penalty

- Fuel consumption penalty
- Weight
- Acquisition cost
- Operating cost
- Maintenance cost
- System reliability

The appropriate data shown above have also been reduced to a common denominator that is expressed in terms of cost.

The parameter of droplet size in supercooled water clouds has not been directly analyzed, but the presence of freezing rain and drizzle have been considered since the latter would affect the coverage provided by the ice protection system.

#### 4.2 POSTULATED ADVANCED HELICOPTERS AND THEIR MISSIONS

Seven postulated advanced helicopters have been selected for the trade-off studies to establish the most promising anti-icing/deicing concepts for each type. The helicopter types are defined by the following designations:

1. Light Observation (SCOUT)
2. Armored Aerial Reconnaissance System (AARS)
3. Utility Tactical Transport Aircraft System (UTTAS)
4. Advanced Attack Helicopter (AAH)
5. Light Tactical Transport Aircraft System (LTTAS)
6. Heavy Lift Helicopter (HLH)
7. Very Heavy Lift Helicopter (VHLH)

All the helicopters are powered by turbine engines and have shaft-driven rotors. All except the heavy lift type have the conventional single main rotor/tail rotor. The heavy lift types use tandem rotors.

It is to be emphasized that the weight and cost data which are presented in the following sections are not necessarily to be taken as absolute values but should primarily be considered for comparative purposes since very detailed preliminary designs would have to be conducted for each aircraft to achieve more absolute data.

It should also be noted that the data would be more applicable when included as part of an original helicopter design than as part of a retrofit program.

#### 4.3 SYSTEMS ANALYZED

##### 4.3.1 Rotor Blades

Since blade configuration details were not known in all cases for the seven advanced helicopter types, the analysis of blade ice catch rates was based on an estimate of rotor airfoil chord length and thickness, and rotor tip speed and span. An average 12-percent thick airfoil chord and a solidity ratio of 0.09 were selected as representative of all configurations due to the considerations discussed below.

It is known that existing light helicopters, such as the UH-1, use a symmetrical NACA 0012 airfoil for the rotor blades. Some helicopters may use a 12-percent airfoil which includes camber and may include twist and/or taper along the rotor span. The total water catch varies very little ( $\pm 15\%$ ) for airfoils in the 6- to 16-percent thickness ratio range for a given actual thickness. Therefore, a deviation in the assumed airfoil thickness from its precise value would still provide valid results as far as water catch rates and anti-icing energy requirements are concerned. The chord length for the various helicopter models was derived from a constant value of 0.09 for the rotor disk solidity ratio:

$$\sigma = \frac{NC}{\pi R}$$



where:

$\sigma$  = solidity ratio, dimensionless

N = number of rotor blades

C = chord length, feet

R = rotor radius, feet

Available data shows that the solidity ratio for any rotor system design varies from 0.0875 to 0.0925. It appears, therefore, that a solidity ratio of 0.09 represents a reasonable average value for a four-bladed rotor. The solidity ratio value would affect the water catch rate by less than 5 percent, and the continuous anti-icing energy requirements or freezing depressant fluid requirements would be affected by less than 3 percent. The power density requirements for electrothermal cyclic deicing would not be affected by such a change in the chord length. Consequently, the rotor anti-icing or deicing performance requirements based on the airfoil chord lengths resulting from the 0.09 solidity ratio value and chord thickness of 12 percent provide a valid and rational basis for comparison of rotor protection requirements of the seven helicopter models. While perturbations in the rotor geometry, such as changes in the number of blades, solidity ratio, chord length, etc., may affect the absolute penalty level, the results are unaffected relating to the sensitivity of the penalty changes in meteorological icing parameters since the relative ranking of the various ice protection system in terms of imposed penalties is not affected by any perturbations in rotor geometry.

Rotor rpm values were calculated by using a tip speed of 752 fps for all configurations. This data is necessary to estimate the ice accretion characteristics along the span and the total energy requirements.

It was also necessary to estimate the specific fuel consumption of each of the engines for the seven helicopter models. The SFC values were required to determine the fuel penalties due to the required increased

engine shaft horsepower output caused by the fixed weight of the ice protection system, the additional drag caused by the cyclic intermittent ice accumulation/shedding process of a deicing system, the increase in engine back pressure due to heat exchanger installation at the exhaust, and/or the additional engine power extraction to provide electrical energy for rotor blade deicing.

The above rotor blade configuration data, rpm's, and SFC's were generated for the seven helicopter types and are compiled in Table 15 as the basis for the trade-off analysis results discussed below. Included in this table are additional detail information on size, weight, and performance of each helicopter.

For comparison purposes the analysis is based on icing encounter durations of 1 hour and design mission endurance time for all helicopter types. The penalty trade-off studies for the rotors of the seven helicopter types were based on constant aircraft flight speeds, corresponding to those of the endurance mission. The sensitivity of rotor blade ice protection requirements to speed (between hover and 160 knots) is negligible because the mean rotor velocity is high relative to forward speed. Thus rotor catch and heat transfer are not greatly affected. Approximately 0.5 second additional heat "on" time (5%) is required for electrothermal deicing at 125 knots compared to hover. The chemical system requires only 3 percent more fluid at 125 knots than at hover.

As to the estimate of direct fuel costs due to installation and operation of a rotor blade ice protection system, interpolation of existing data was required. For the various flight regimes associated with forward flight or hover in icing, the required engine hp is usually less than the nominal engine rating at IPR @ SLS. Hence, it is necessary to establish the SFC trend at partial engine power. A review of such SFC trends for several engines has been conducted, and the increase in SFC at partial power is presented in a generalized form in Figure 47, and the data have been applied for the entire range of the engines considered herein.

TABLE 15. CHARACTERISTICS OF FUTURE HELICOPTERS

Characteristics	Unit	SCOUT	AARS	UTDAS	AAH	LTAS	HLH	VHVR
Design gross weight	lb	4,100	10,000	15,400	15,400	58,000	118,000	320,000
Empty weight	lb	2,900	7,000	10,000	11,400	34,000	59,580	180,000
Overall length	ft	43.4	48.4	51.5	51.5	110	162	245
Design mission: endurance (includes reserve)	hrs	2	3	2.3	1.9	2.5	1.75	1.4
Service ceiling	ft	18,000	20,000	20,000	20,000	20,000	15,000	15,000
V-cruise	KTAS	120	140	145	145	150	130	150
V-max	KTAS	145	165	175	175	185	160	170
V-loiter	KTAS	70	70	80	80	85	85	90
Number engines	-	1	2	2	2	2	3	4
Engine shp (IRP @ SLS), each	SHP	550	1,000	1,520	1,540	6,000	8,075	15,000
Specific fuel consumption (IRP @ SLS)	lb/hr/shp	0.56	0.50	0.48	0.48	0.45	0.43	0.40
Main rotor type	-	Single	Single	Single	Single	Single	Tandem	Tandem
Main rotor number of blades	-	4	4	4	4	5	4 each	4 each
Main rotor radius	ft	18	20	25.5	25.5	45	46	70
Main rotor rpm	rpm	400	360	282	282	160	156	103
Main rotor tip speed	fps	752	752	752	752	752	752	752
Main rotor airfoil chord length	in.	15.5	17	22	22	30	38	58
Main rotor airfoil thickness	%	12	12	12	12	12	12	12
Tail rotor number of blades	-	4	4	4	4	5		
Tail rotor radius	ft	3.5	4	5	5	9		
Tail rotor rpm	rpm	2,055	1,800	1,440	1,440	800		
Tail rotor tip speed	fps	752	752	752	752	752		
Tail rotor airfoil chord length	in.	5.4	5	7.7	7.7	10.5		
Tail rotor airfoil thickness	%	12	12	12	12	12		

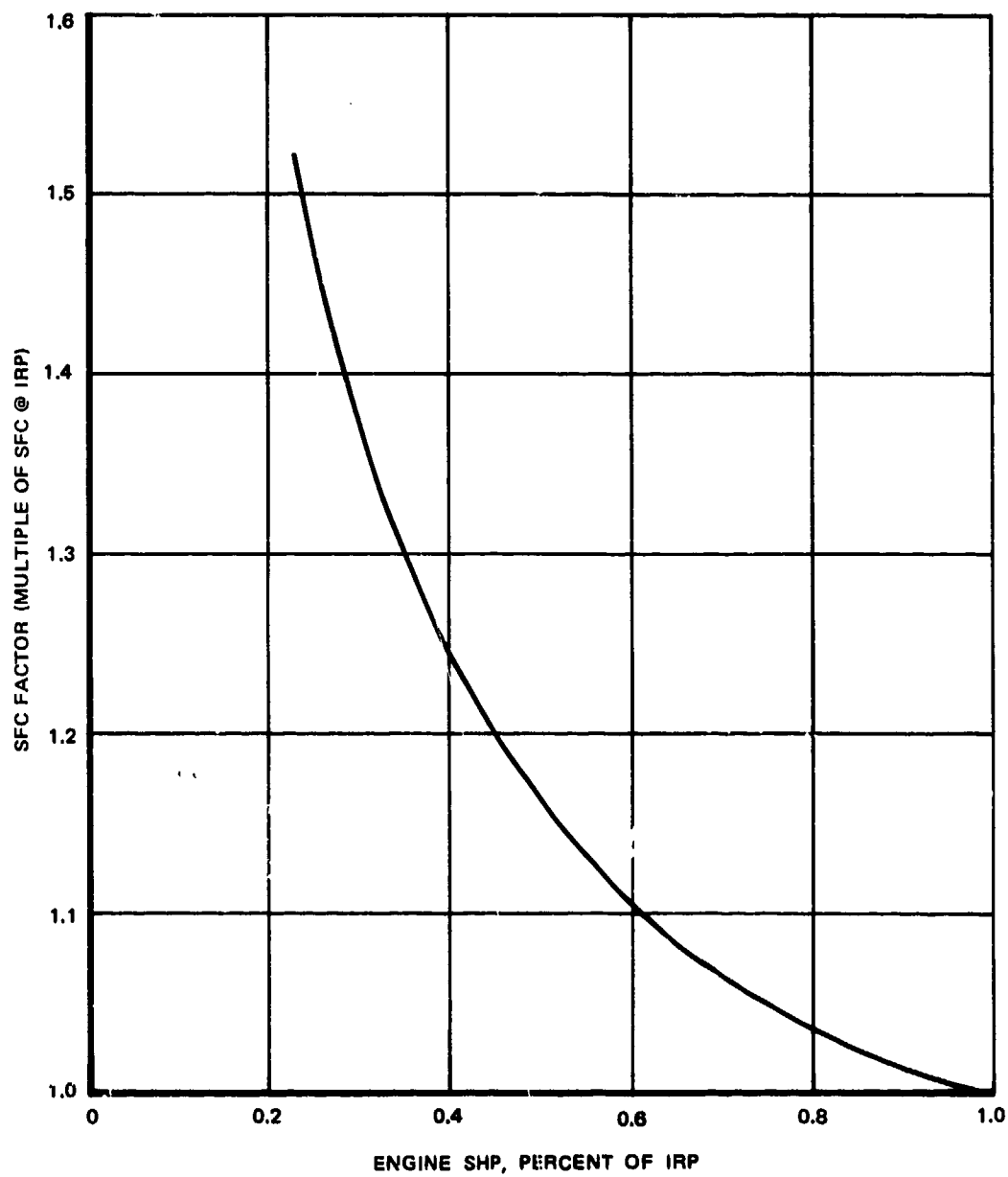


Figure 47. Variation of Engine SFC at Partial Power.

#### 4.3.2 Windshield

Viable anti-icing concepts for the windshield include: (1) the electro-thermal method and (2) the chemical freezing point depressant method. (See Section 3.4.) The power intensity requirement for the electrically heated windshield is based on MIL-T-5842A, "Transparent Areas, Anti-Icing, Defrosting and Defogging Systems, General Specification For." The weights for the liquid system are based on the requirement of MIL-S-6625-A(AKSG), "Spray Equipment, Aircraft Windshield, Anti-Icing." This specification states that "the pump shall be capable of supplying approximately 2 quarts of fluid per square foot of 2/3 of the window area per hour." Also, "the capacity of the fluid tank shall be determined by the following formula:

$$\text{Capacity of tank, gal} = \frac{0.70 AX}{12}$$

where

A = Total area of windshield, square feet

X = Airplane range in hours with full military load"

The weights for the electrothermal system are determined from the power intensity requirement and the windshield area. The power intensity requirement (3.5 watts/sq inch) is based upon a flight velocity of 150 knots. Windshield areas for the seven helicopter models have been interpolated from available data on the basis of vehicle configuration and size.

Tables 16 and 17 present the windshield anti-icing penalties for the seven specified Army helicopters using the liquid freezing depressant and electrical heating systems, respectively. It is seen from Table 17 that the penalty of the windshield anti-icing system featuring a transparent electrically heated coating is about half of the penalty of

TABLE 16. ESTIMATED PENALTIES FOR WINDSHIELD ANTI-ICING-CHEMICAL FREEZING POINT DEPRESSANT SYSTEM

Type of Aircraft	SCOUT	AARS	AAH	UTTAS	LTTAS	HLH	VHLH
Anti-iced area, sq ft	8	10	10	15	18	20	20
Design endurance mission, hr	2.00	3.00	1.90	2.30	2.50	1.75	1.40
Liquid quantity, lb	7.5	14.0	9.0	16.2	21.2	16.5	13.2
Pump and reservoir, lb	3.0	4.0	3.0	4.0	4.5	4.0	4.0
Fittings, line and valve, lb	3.0	3.5	3.0	4.0	4.5	4.0	3.5
Liquid system fixed wt, lb	13.5	21.5	15.0	24.2	30.2	24.5	20.7
Defogging controller and wiring, lb	2.0	2.0	2.0	2.0	2.0	2.0	2.0
Total fixed weight, lb	15.5	23.5	17.0	26.2	32.2	26.5	22.7
Fuel penalty for $\Delta$ shp, lb	6.6	14.2	6.9	12.9	18.3	11.0	7.3
Total penalty, lb	22.1	37.7	23.9	39.1	50.5	37.5	30.0
Shaft-Horsepower Penalties							
Average Mission SFC	0.602	0.545	0.528	0.528	0.487	0.483	0.430
$\Delta$ shp for fixed weight	2.6	5.1	3.3	5.2	8.5	5.7	4.9
$\Delta$ shp for defogging	2.9	3.6	3.6	5.4	6.5	7.3	7.3
Total $\Delta$ shp penalty	5.5	8.7	6.9	10.6	15.0	13.0	12.2

TABLE 17. ESTIMATED PENALTIES FOR WINDSHIELD  
ANTI-ICING-ELECTRICALLY HEATED SYSTEM

Aircraft Type	SCOUT	AARS	AAH	UTTAS	LTTAS	HLH	VHLH
Anti-iced area, sq ft	8	10	10	15	18	20	20
Design endurance mission, hr	2.0	3.0	1.9	2.3	2.5	1.75	1.4
Controller and wiring, lb	4.5	4.5	4.5	4.5	4.5	4.5	4.5
Total fixed weight, lb	4.5	4.5	4.5	4.5	4.5	4.5	4.5
Fuel penalty for $\Delta$ shp, lb	8.9	15.0	9.1	16.3	19.5	14.9	10.7
Total penalty, lb	13.4	19.0	13.6	20.8	24.0	19.4	15.2
Percent of liquid system wt penalty	61.0	50.5	52.5	53.2	47.5	51.7	50.7
Shaft-Horsepower Penalties							
Anti-icing power, kw	4.03	5.03	5.03	7.56	9.06	10.08	10.08
Extracted $\Delta$ hp-elec	6.8	8.4	8.4	12.7	15.20	16.9	16.9
$\Delta$ shp for sys- tem fixed wt, lb	0.5	0.8	0.7	0.7	0.8	0.7	0.8
Total $\Delta$ shp	7.3	9.2	9.1	13.4	16.0	17.6	17.7
SFC	0.602	0.545	0.528	0.528	0.487	0.483	0.43

the liquid system.\* Thus, in addition to the previously listed advantages (Paragraph 3.4), minimum weight is another important advantage of the electrical system which has contributed to its universal acceptance throughout the industry.

#### 4.4 RESULTS - ROTOR BLADES

##### 4.4.1 Evaluation of Systems

The alternate candidate techniques considered in the trade-off study for rotor blade protection of the seven helicopter models include the chemical, cyclic electrothermal, and hot liquid systems. Following are the characteristics and requirements of these systems. The system requirements and penalties are compared in Paragraph 4.4.2.

##### 4.4.1.1 Chemical System

The weight and performance data of the freezing point depressant system for the seven advanced helicopter models are based on the correlation of the theoretical and experimental data as obtained from the Bell UH-1 test data (Paragraph 3.2.2). A mixture of 90-percent ethyl alcohol/10-percent glycerine has been chosen because: (1) this fluid was used in the Bell test program, and (2) it puts the chemical system in a more favorable light since the required expulsion rate is lower than for water-glycol.\*\* Figure 48 shows the chemical system penalties for two sets of criteria related to supercooled cloud protection: (1) the recommended FAR 25 (MIL-E-38453) continuous maximum icing criteria, and (2) the 99th percentile continuous maximum criteria from Figure 10. A typical detailed compilation of the fixed weight and fuel penalty components for the chemical system is shown in Table 18 for MIL-E-38453 criteria. Referring to Figure 48, the MIL-E-38453 conditions correspond to a 15-micron volume median drop size for the maximum water

---

\* Assuming in both cases that a glass or composite laminate is used.

\*\* In addition, a 30-second "on"-30-second "off" duty cycle was assumed for the fluid (based upon Bell experience). Continuous expulsion would double the fluid weights shown in Table 18.



TABLE 18. ESTIMATED WEIGHT AND SHP PENALTIES FOR FLIGHT THROUGH  
ICING - CHEMICAL FREEZING POINT DEPRESSANT SYSTEM FOR  
MIL-E-38453 CRITERIA - 1 HOUR

Type of Aircraft	SCOUT	AARS	UTTAS and AAH	LTTAS	HLH	VHLH
Equipment empty weight, lb	31.0	34.0	43.0	76.0	110.0	164.0
Deicing fluid weight, lb	70.0	85.0	123.0	316.0	460.0	785.0
Fuel penalty for fixed weight, lb	7.0	11.0	14.0	34.0	43.0	69.0
Fuel penalty for $\Delta$ rotor drag, lb	12.0	37.0	54.0	204.0	358.0	933.0
Total penalty, lb	120.0	167.0	234.0	630.0	971.0	1,951.0
Total penalty, per- cent of TOGW	2.92	1.67	1.52	1.09	0.82	0.61
$\Delta$ shp for fixed and fluid weight, lb	11.9	20.3	27.5	70.4	102.4	184.0
$\Delta$ shp for $\Delta$ rotor drag, lb	19.8	68.0	102.0	420.0	741.0	2,170.0
Total $\Delta$ shp penalty	31.7	88.3	129.5	490.4	843.4	2,354.0
Total $\Delta$ shp, percent of reqd shp	8.61	7.01	6.86	6.29	6.15	5.85

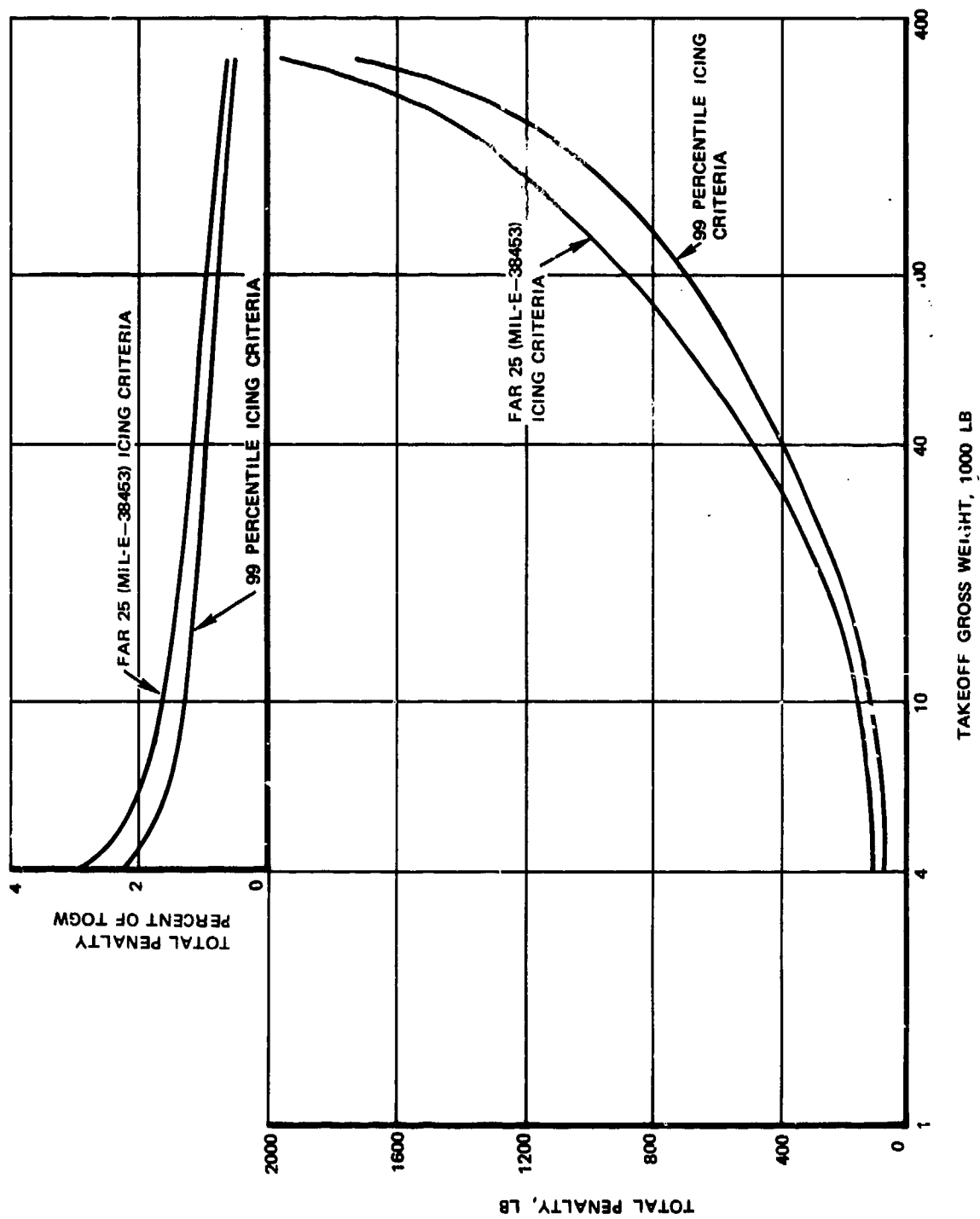


Figure 48. Chemical Freezing Point Depressant Systems Penalty for Two Sets of Icing Criteria.

catch rate; while for the 99th percentile envelope, a 20-micron volume median drop size results in the maximum catch rate. For MIL-E-38453 icing design criteria, a  $0^{\circ}$  F to  $-20^{\circ}$  F OAT design temperature range is applicable, while for the 99th percentile envelope, a  $5^{\circ}$  F OAT design point is appropriate (based upon maximum required fluid expulsion rate). This is illustrated in Figures 49 and 50. The different trends in fluid consumption rates with temperature are caused by the difference in the OAT drop size-LWC relationship in the two sets of criteria. Figure 48 also shows that the (recommended) existing criteria imposes a 20-percent additional weight penalty compared to the 99th percentile criteria.\* The chemical system does not provide a completely clean surface because residual ice is always present. Despite the centrifugal force, experimental evidence found in Reference (22) shows that this problem is still present on rotor blades. Reference (22) states: "A complete shedding of ice from the rotor blades was never achieved with the chemical system. There was always a light residual ice formation remaining on the blades." Therefore, it is necessary to assess a penalty due to rotor blade drag caused by the residual ice. In terms of power, the blade drag penalty is applied to the profile shp component. These shp penalty values in this analysis (Table 18 and Figure 48) are based on an 18-percent increase in the required profile power component. This increment is, perhaps, somewhat optimistic, if it is considered that electrothermal deicers would have an average drag (profile shp) penalty of 12 percent (23) due to ice buildup between deicing cycles. As far as freezing rain protection is

---

\* The 99th percentile criteria, however, are not recommended for adoption since it would leave the Army with a unique specification that is below the requirements of Navy, Air Force, or commercial aircraft and may thus result in an Army design which has no commonality with other service requirements.

(22) Van Wyckhouse, J. F., CHEMICAL ICE PROTECTION FOR HELICOPTER ROTORS AND A COMPARISON WITH THE ELECTRO-THERMAL SYSTEM, from Proceedings of the American Helicopter Society 18th Annual National Forum, Washington, D. C., May 1962.

(23) Bowden, D. T., EFFECT OF PNEUMATIC DE-ICERS AND ICE FORMATIONS ON AERODYNAMIC CHARACTERISTICS OF AN AIRFOIL, NACA TN-3564, February 1956.

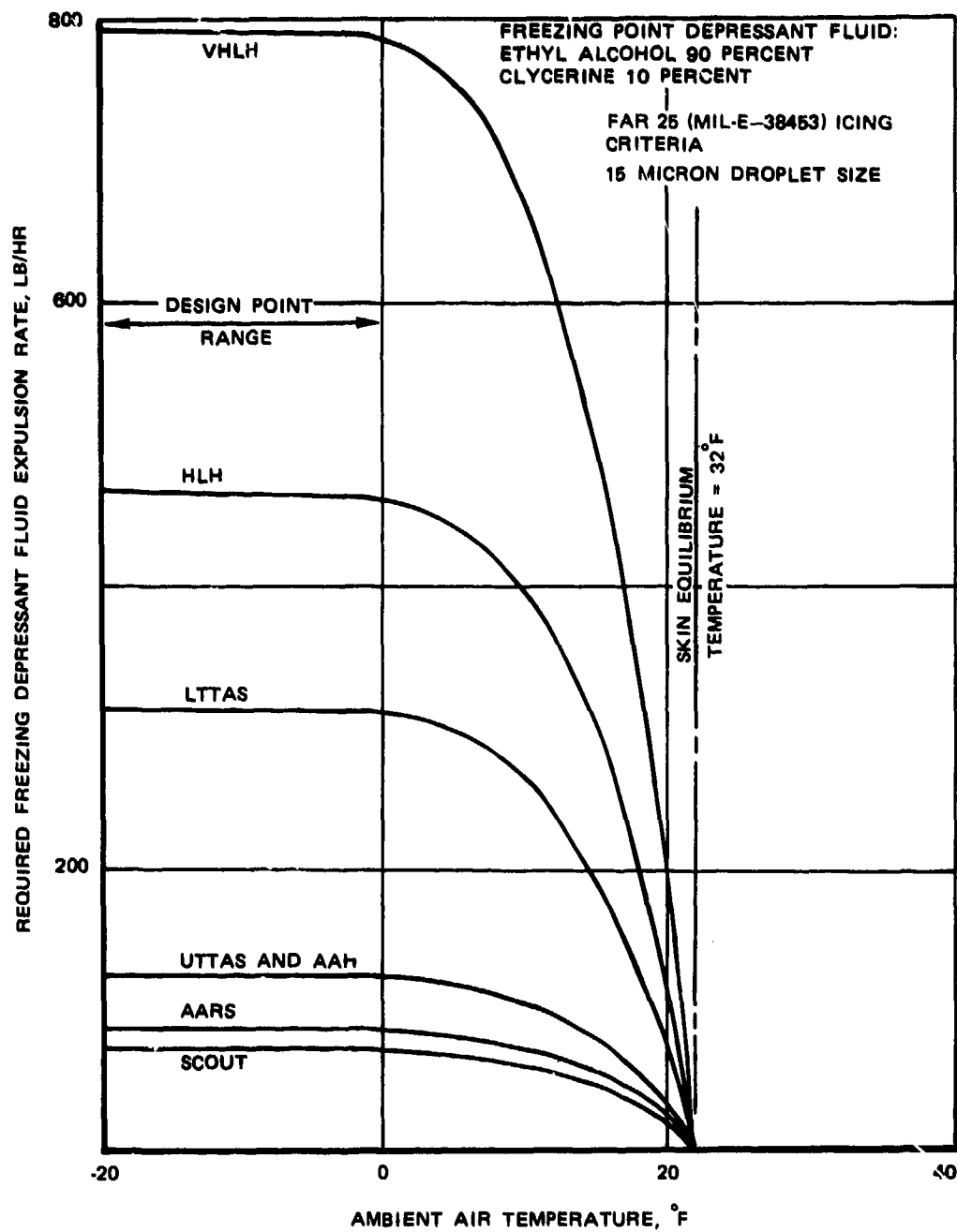


Figure 49. Chemical Freezing Point Depressant Fluid Quantity Required for Rotor Blade Ice Protection as a Function of Ambient Temperature - MIL-E-38453 Criterion.

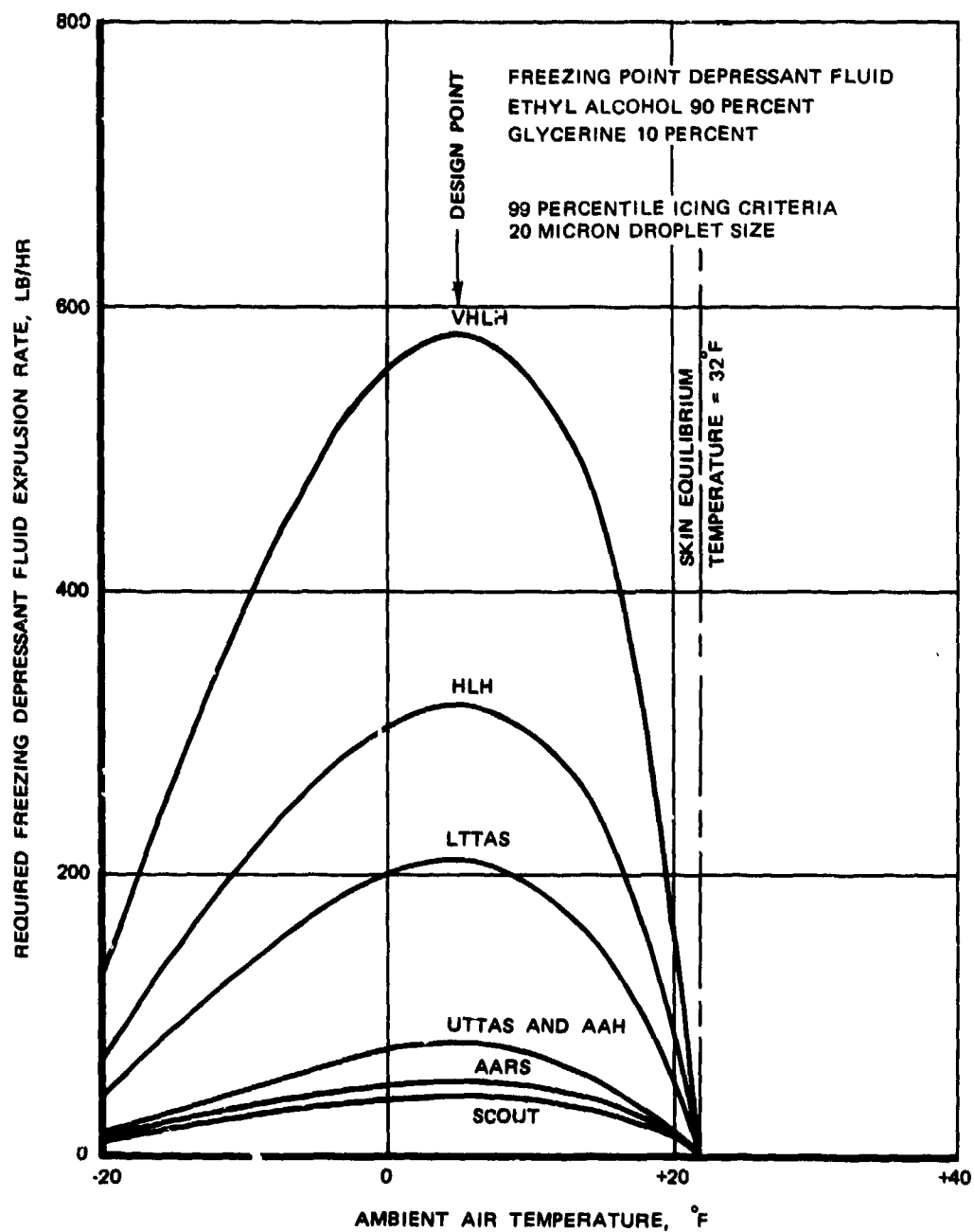


Figure 50. Chemical Freezing Point Depressant Fluid Quantity Required for Rotor Blade Ice Protection - 99th Percentile Icing Criterion.

concerned, the severity of the two criteria (ambient temperature and catch rate) that dictate the freezing depressant consumption rate is not greater for freezing rain than for supercooled clouds. Thus, theoretically, at least, the required freezing depressant fluid expulsion rate for freezing rain protection should be no greater than for stratus cloud protection. The crucial problem relating to freezing rain protection is uniform distribution of the fluid such that it would cover the entire top and bottom surfaces of the blade. Ejection of all the fluid in the leading edge stagnation area and dependence upon the air slipstream to distribute the fluid aft of the leading edge would be unrealistic. The flow field over rotor blade surfaces is governed by the combination of tangential and centrifugal forces. Thus fluid ejected at the leading edge may not reach the trailing edge and may be carried outward toward the blade tip. An experimental program would be required to configure a satisfactory distribution system. The empirical factor of 1.5 applied to the computed expulsion rate to account for distribution inefficiencies (Paragraph 3.2.2) in a supercooled cloud protection system is no longer valid for freezing rain protection. Obviously this factor, and also the system fixed weight, would be higher to cope with both freezing rain and supercooled clouds. Furthermore, the profile drag power penalty due to residual ice would increase for the freezing rain protection system. It is assumed that the system fixed weight penalty would be 50 percent higher than the comparable weight of the stratus cloud protection system and the required profile drag power would increase by 25 to 100 percent compared to a clean blade. These considerations are reflected in Figure 51, which shows the total penalties for freezing rain protection.

#### 4.4.1.2 Electrothermal Deicing

The trade-off analysis for electrothermal deicing for the considered range of helicopter models was based on the optimum number of cyclic zones that is compatible with both the all-solid-state and hybrid power control power technologies. The rotor configuration and electrothermal deicing parameters for the rotor blades of the considered helicopter models are

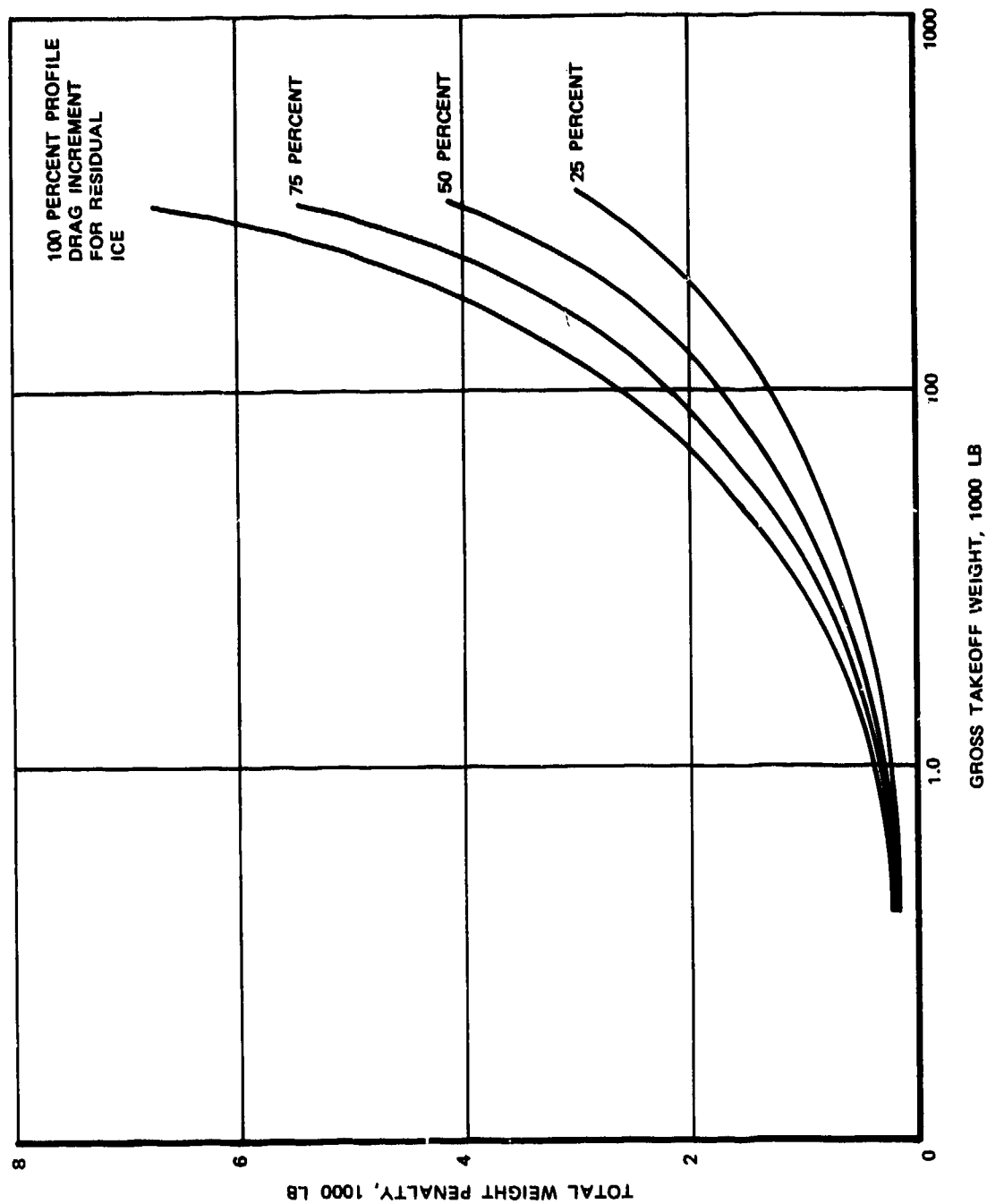


Figure 51. Freezing Rain Protection Penalty (Fixed Weight and Fuel) for Chemical Freezing Point Depressant System - 1 Hour.

shown in Table 19. To comply with requirements related to super-cooled cloud protection, these deicing parameters are based on a  $-4^{\circ}$  F ambient temperature design point, and on 25- and 10-percent chord coverage of the lower and upper blade leading edge surfaces, respectively. As can be seen, the power-off time ranges from 120 seconds for the smallest Scout to 204 seconds for the largest VHIH, reflecting the higher rate of ice buildup on short-chord, small-leading edge-diameter airfoils. The recommended generator ratings (Table 19) and weight and power penalties for electrothermal deicing (Table 20 and Figure 52) account for the intrinsic higher than nominal output of generators under cold air ambient conditions, and also for the fact that the generator is used mostly for functions not related to deicing. Based on these considerations and the weight characteristics of modern high-speed generators, a weight penalty of 0.5 lb per kva of nominal rating is assigned for rotor deicing\*. The profile power penalty due to increased rotor blade drag between shedding cycles constitutes 12 percent of the required profile power. Figure 52 shows a single penalty line for the MIL-E-38453 and 99-percentile icing criteria because the deicing energy requirements depend mainly\*\* on the ambient temperature level and not on the LWC levels, as is the case with the chemical and liquid systems.

Electrothermal protection of the rotor against freezing rain can be accomplished by either one of two candidate techniques. The first technique involves continuous application of heat to the entire blade surface commensurate with running-wet requirements; i.e., the skin

---

\* A modern, high speed generator can be built for a weight of approximately 1 lb per kva. Therefore, 50 percent of the load penalty was charged to the generator with the above premise that the generator would normally be used to supply other loads on the aircraft.

\*\* For aircraft up to the size of LTTAS (~ 60,000 pounds) the number of deicing sequences per cycle (Table 19) - and hence power "off" time per zone and total power requirements - is determined by wiring complexity in the rotor system and not ice buildup rate on the blades. For larger aircraft the LWC would start to affect the total power requirements by establishing the maximum number of allowable zones. The only effect on weight, however, would be through generator size since the other components would be essentially unaffected.



TABLE 19. ROTOR CONFIGURATION AND ELECTROTHERMAL  
DEICING SYSTEM DATA FOR OAT = 4° F

Type of Aircraft	SCOUT	AARS	UTIAS and AAH	LTTAS	HLH	VHLH
<b>MAIN ROTOR</b>						
Number of Blades	4	4	4	5	4 (tandem)	4 (tandem)
Radius, ft	18	20	25.5	45	46	70
Chord Length, in.	15.5	17	22	30	38	58
Protected Surface Length, in. (top and bottom)	6.0	6.6	8.5	11.5	14.6	22.3
Protected Span Length (% Radius)	85	85	85	85	85	85
Heated Area/Blade, sq in.	1,092	1,350	2,198	5,278	6,850	15,922
Total Heated Area, sq in.	4,368	5,400	8,792	26,930	54,800	127,376
Number of Zones/Blade	5	6	4	16	5	6
Deicing Sequences per Cycle	5	6	8	16	20	24
Deicing Order	4 Zones Simult (1 per blade)	4 Zones Simult (1 per blade)	2 Zones Simult (1 in each of 2 Sym Blades)	5 Zones Simult (1 per blade)	2 Zones Simult (1 in each of 2 Sym Blades)	2 Zones Simult (1 in each 2 Sym Blades)
Max ON Time Per Zone, sec	9	9	9	9	9	0
Max OFF Time Per Cycle, sec	120	132	150	174	186	204
Average Power Intensity, watts/sq in.	16	16	16	16	16	16
Max Main Rotor Power, kw	14.0	14.4	17.6	26.4	43.9	84.9
<b>TAIL ROTOR</b>						
Number of Blades	4	4	4	5	-	-
Radius, ft	3.5	4	5	9	-	-
Protected Surface Length, in	2.4	2.7	3.4	4.6	-	-
Protected Span Length (% Radius)	85	85	85	85	-	-
Heated Area/Blade, sq in.	85	108	172	422	-	-
Total Heated Area, sq in.	340	432	638	2,110	-	-
Number of Zones/Blade	1	1	2	3	-	-
Deicing Sequences per	1	1	2	3	-	-
Deicing Order	All Blades Simult	All Blades Simult	All Blades Simult	All Blades Simult	-	-
Max ON Time Per Zone, sec	9	9	9	9	-	-
Max OFF Time Per Cycle, sec	60	66	75	87	-	-
Average Power Intensity, watts/sq in.	20	20	20	20	-	-
Max Tail Rotor Power, kw	6.9	8.6	6.9	14.1	-	-
Recommended Generator Rating, kva	15	15	20	30	40	75

TABLE 20. ESTIMATED WEIGHT AND SHP FOR FLIGHT THROUGH ICING -  
ELECTROTHERMAL DEICING SYSTEM - 1 HOUR

Type of Aircraft	SCOUT	AARS	UTTAS and AAH	LTTAS	HLH	VHLH
Total fixed weight, lb	106.8	114.8	142.3	202.3	264.3	356.8
Fuel penalty for fixed weight, lb	7.3	9.7	11.2	16.5	17.8	24.2
Fuel penalty for electric power, lb	14.1	13.1	15.6	21.5	35.5	61.2
Fuel penalty for $\Delta$ rotor drag, lb	7.9	24.7	35.8	136.7	238.6	622.3
Total penalty, lb	136.1	162.3	204.9	377.0	556.2	1,064.5
Total penalty, percent of TOGW	3.32	1.62	1.33	0.65	0.47	0.33
$\Delta$ shp for fixed weight, lb	13.0	19.6	23.5	36.7	41.5	60.5
$\Delta$ shp for electric power, lb	23.4	24.1	29.5	44.2	73.6	142.3
$\Delta$ shp for rotor drag, lb	13.2	45.4	67.9	280.8	493.9	1,447.2
Total $\Delta$ shp penalty	49.6	89.1	120.9	361.7	609.0	1,650.0
Total $\Delta$ shp, percent of reqd shp	13.48	7.07	6.41	4.64	4.44	4.10

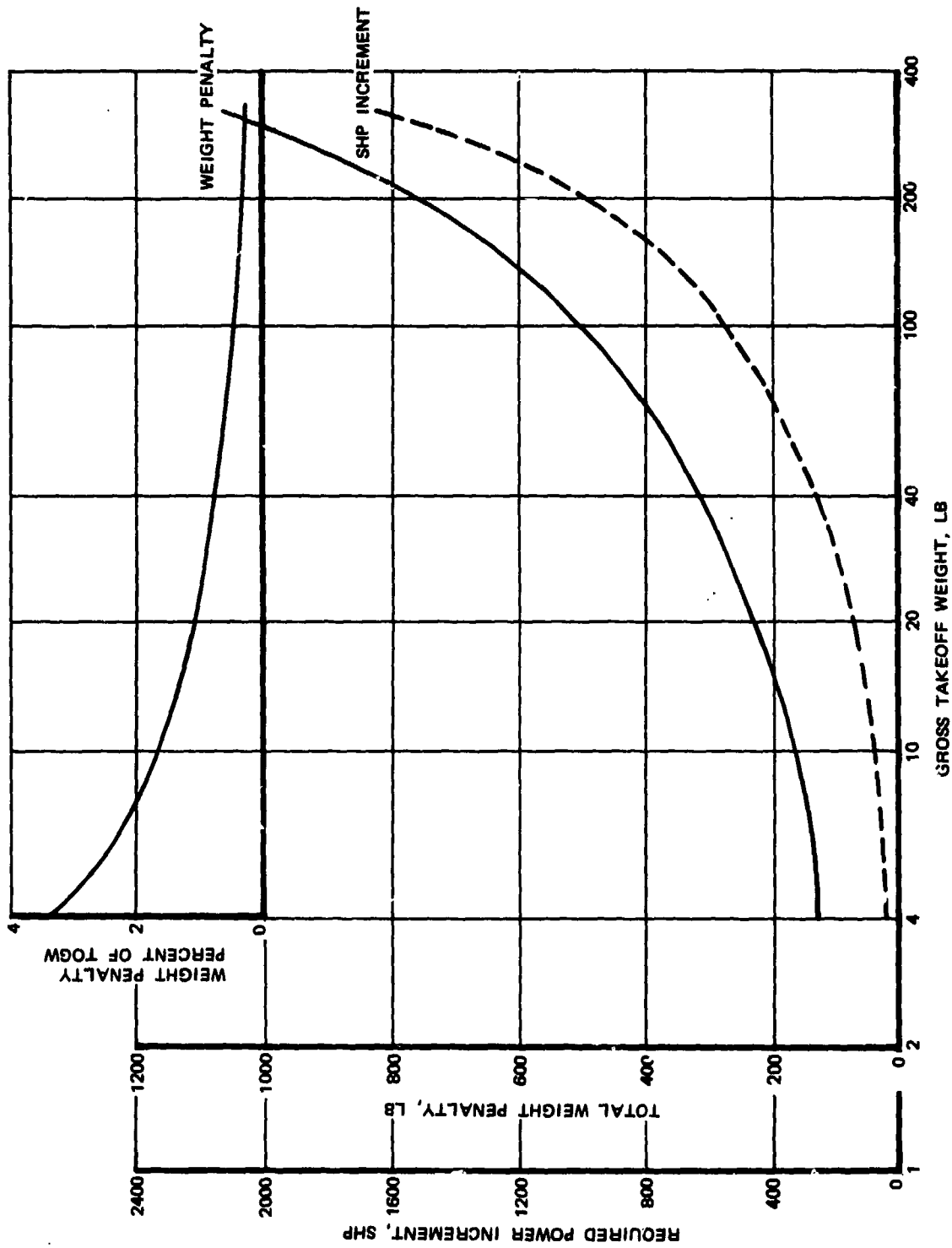


Figure 52. Total Weight and SHP Penalties for Electrothermal Deicing System During Flight Through Icing for 1 Hour.

equilibrium temperature would be maintained just above freezing ( $38^{\circ}$  F in this case) on a  $-4^{\circ}$  F icing day\*. The second technique involves cyclic electrothermal deicing for the entire chordwise extent of both blade surfaces. For the purpose of the analysis, the cyclically deiced area is divided into two major zones to conserve power (not to be confused with the large number of cyclic zones). One major zone is associated with the leading edge area normally protected against stratus cloud icing. Power requirements for individual cyclic elements in the leading edge area are based upon the design criteria for stratus cloud protection ( $-4^{\circ}$  F OAT). The second major zone, aft of the leading-edge zone, extends to the rotor blade trailing edge and covers most of the surface. Power requirements for individual cyclic elements in the second zone are based on freezing rain design criteria ( $14^{\circ}$  F OAT). The dual-zone concept requirements are reflected in Table 21. To achieve minimum power consumption, the number of cyclic elements in each of the major zones was increased by reducing the heat on time per element and correspondingly increasing the power density. As can be seen in Table 21, the total power per element in both major zones is maintained at a constant level by increasing the cyclic element area in the aft zone.

A comparison of the rotor power requirements for running-wet anti-icing and cyclic deicing is shown in Figure 53. The comparison is based on  $-4^{\circ}$  F design icing criterion. Figure 53 shows the power required for deicing only, and does not include power penalties for the increased aircraft weight and drag. The power demand for running-wet anti-icing is 10 times the power demand for cyclic deicing. Based on these excessive power requirements, electrothermal running-wet anti-icing was not considered any further in the trade-off studies.

---

\* While freezing rain requires protection only to  $+14^{\circ}$  F, the entire blade has to be heated for "normal" icing conditions to prevent runback refreezing.

TABLE 21. ROTOR ELECTROTHERMAL FREEZING RAIN DEICING SYSTEM DATA

Type of Aircraft	Scout	AARS	UTAS and AAR	LITAS	HLH	VHLH
Number of Blades	4	4	4	5	4 (tandem)	4 (tandem)
Radius, ft	18	20	25.5	45	46	70
Chord Length, in.	15.5	17	22	30	38	58
Zone 1 - L.E. PROTECTION DATA FOR SUPERCOOLED CLOUDS						
Chordwise Surface Length, in. (top and bottom)	6.0	6.6	8.5	11.5	14.6	22.3
Span Length (% Radius)	85	85	85	85	85	85
Heated Area/Blade, sq in.	1,092	1,350	2,198	5,278	6,850	15,522
Rotor Heated Area, sq in.	4,368	5,400	8,792	26,390	54,800	127,376
Number of Zones/Blade	10	11	15	24	12	14
Max ON Time per Zone, sec	4	4	4	3	3	3
Average Power Intensity watts/sq in.	32	32	32	36	36	36
Area per Zone, in. <sup>2</sup>	110	123	147	240	570	1,140
Zone 2 - PROTECTION AFT OF L.E. FOR FREEZING RAIN						
Chordwise Surface Length, in. (top and bottom)	26.0	28.4	36.8	50.5	64.4	97.7
Span Length (% Radius)	67	67	67	67	67	67
Heated Area/Blade, sq in.	3,650	4,425	7,308	17,715	23,076	53,352
Rotor Heated Area, sq in.	14,600	17,700	29,232	88,575	184,608	426,816
Number of Zones/Blade	17	18	25	37	20	23
Max ON Time per Zone, sec	4	4	4	3	3	3
Average Power Intensity, watts/sq in.	16	16	16	18	18	18
Area per Zone, in. <sup>2</sup>	220	246	294	480	1,140	2,280
General Data						
Deicing sequences per Cycle	27	29	40	21	64	74
Number of Zones Energized Simultaneously	4 (1 per	4 (1 per	4 (1 per	5 (1 per	4 (1 per	4 (1 per
Duration of One Cycle, sec	120	132	160	183	192	222
Power Req'd, kw	14.1	14.1	18.8	43.2	82.0	164.0
Recommended Generator Rating, kva	15	15	20	40	75	150

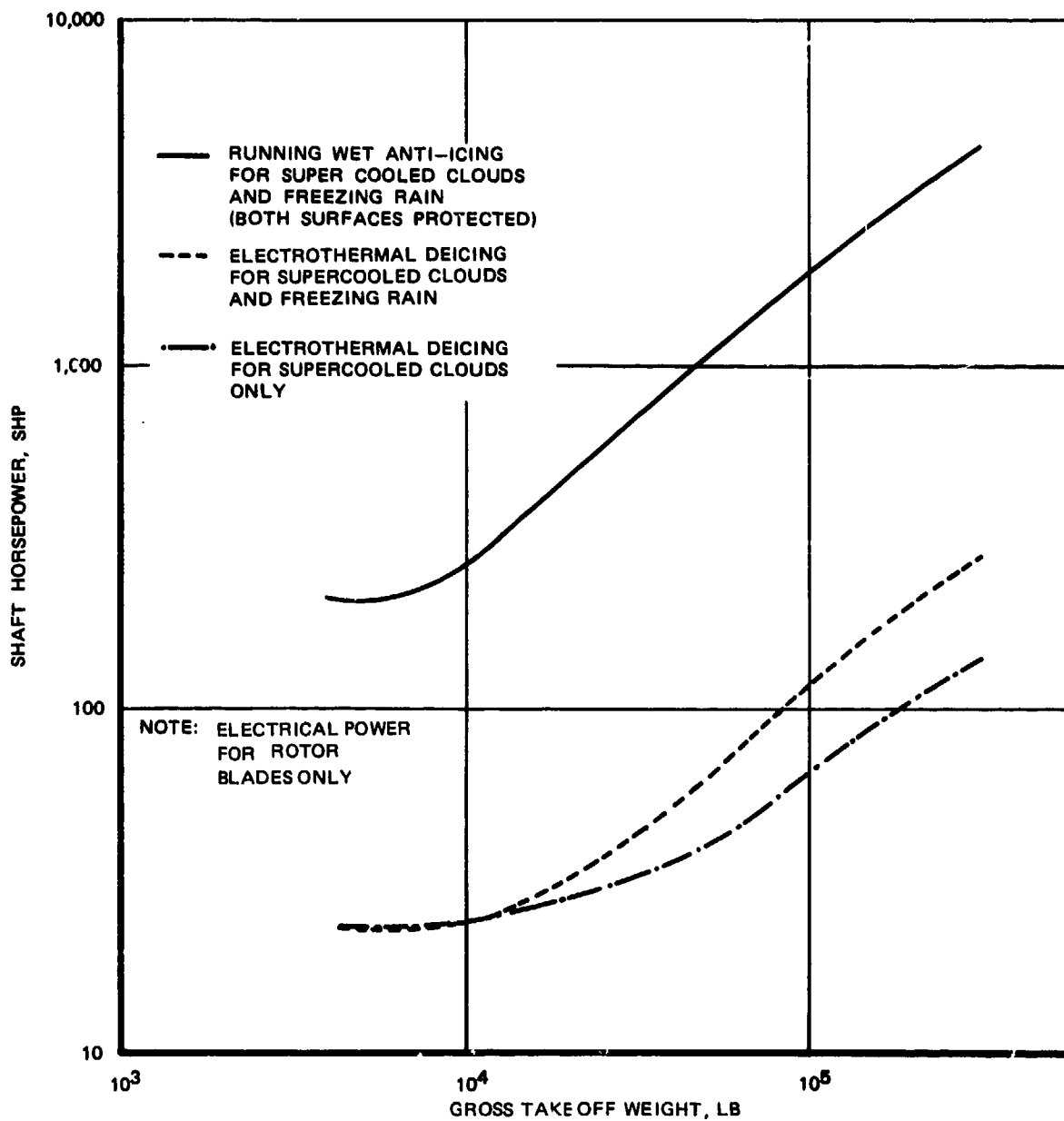


Figure 53. Comparison of Power Extraction Requirements for Electrothermal Ice Protection.

Figure 53 shows that for the smaller helicopters the power demand for a cyclic deicing system for freezing rain protection can be comparable to that of the conventional supercooled cloud deicing systems, provided the large number of cyclic elements could be accommodated in the timer and power controller. For the heavier vehicles, the increasingly larger required power margins for freezing rain protection compared to power requirements for stratus cloud protection (Figure 53) are caused by the larger deiced surface areas and the fact that the number of cyclic zones on the larger aircraft is governed by the required duration of one complete cycle. The estimated weight and power penalties for electrothermal freezing rain deicing are tabulated in Table 22. The generator penalty is based upon the same criteria as for stratus cloud protection, i.e., 0.5 lb per kva of nominal rating, and the drag penalty is based upon a 16-percent increase in the required profile power (compared to 12 percent for electrothermal cyclic ice protection).

#### 4.4.1.3 Liquid-Heated Blades

For fully evaporative performance, such as offered by this system, the heating requirements are based upon the maximum catch rate, i.e., LWC values that result from a skin equilibrium temperature of  $32^{\circ}$  F along the entire rotor span. Variation of the ambient temperature and LWC along the rotor span commensurate with this criterion results, for a given condition, in a total heat load that is higher than required. However, the  $32^{\circ}$  F skin temperature criterion assures that local heating rates are adequate for evaporative performance at any point along the rotor blade span for any ambient temperature of the icing envelope. The design criteria for evaporative anti-icing are shown in Figure 54 for the FAR-25 (MIL-E-38453) and 99th percentile envelopes.

The three principal variations in applying the liquid-heated blade technique (Paragraph 3.2.3) are due to differences in the rotating seal arrangements. However, the system components are very similar and, thus, the weight penalties of the three variations are not appreciably different. Figure 55 shows the weight penalties for the integrated transmission lub/

TABLE 22. ESTIMATED WEIGHT AND SHP FOR FREEZING RAIN  
PROJECTION - ELECTROTHERMAL DEICING FOR 1 HOUR

Type of Aircraft	SCOUT	AARS	UTTAS and AAH	LTTAS	HLH	VHLH
Total fixed weight, lb	214.3	233.3	311.8	624.8	1,011.8	1,982.3
Fuel penalty for fixed weight, lb	15.7	21.2	27.3	55.3	76.9	144.7
Fuel penalty for elect. power, lb	14.2	12.9	16.6	35.3	66.4	118.3
Fuel penalty for $\Delta$ rotor drag, lb	10.6	33.0	47.8	132.3	318.1	829.7
Total penalty, lb	254.8	300.4	403.5	897.7	1,473.2	3,075.0
Total penalty, percent of TOGW	6.21	3.00	2.62	1.55	1.25	0.96
$\Delta$ shp for fixed weight	26.2	38.9	51.7	113.7	159.1	336.6
$\Delta$ shp for elec power	23.6	23.6	31.5	72.4	137.5	275.0
$\Delta$ shp for rotor drag	17.7	60.5	90.5	374.4	658.6	1,929.6
Total $\Delta$ shp penalty	67.5	123.0	173.7	560.5	955.2	2,541.2
Total $\Delta$ shp, percent of reqd shp	18.34	9.76	9.21	7.19	6.96	6.32



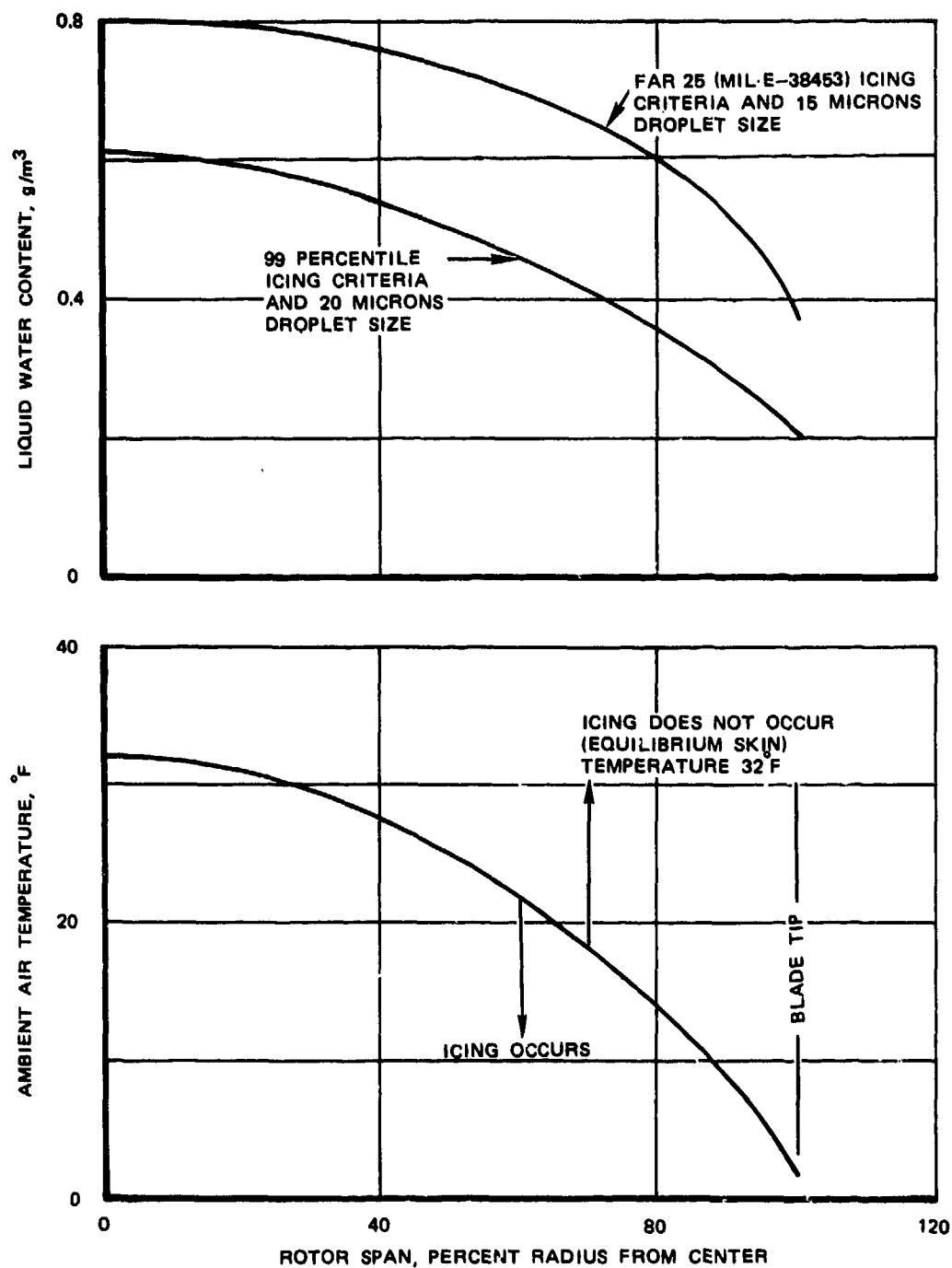


Figure 54. Ambient Icing Design Temperatures and Liquid Water Content-Fully Evaporative Performance.

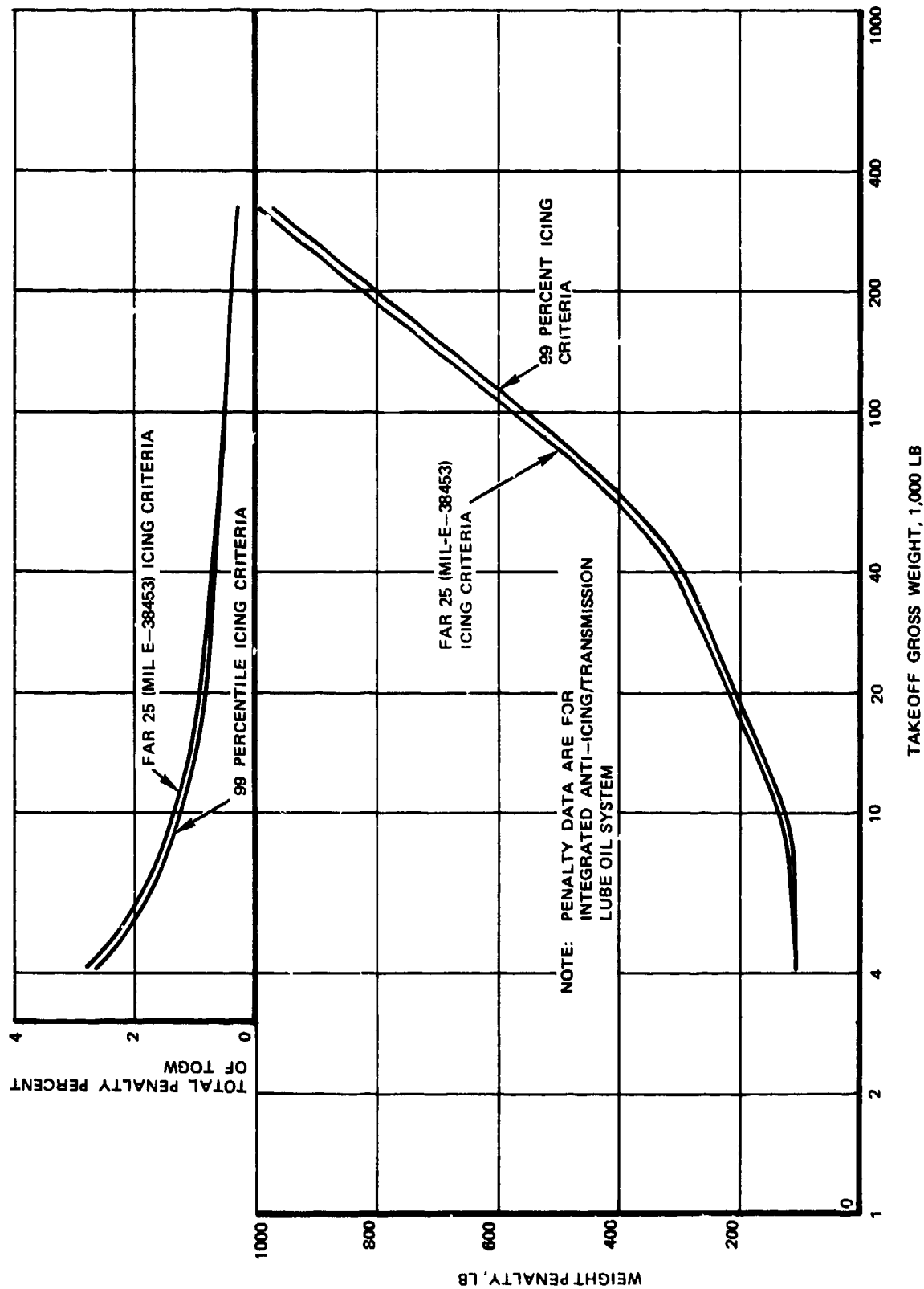


Figure 55. Liquid-Heated Skin Evaporative Anti-Icing System Penalty for Various Icing Criteria.

anti-icing system for the two icing design criteria and Table 23 shows a detailed tabulation of component weights and fuel penalty data for this system based on MIL-E-38453 criteria. The penalties are based upon protecting 10 percent of the chord on the upper surface and 25 percent of the chord on the lower surface.

As far as freezing rain protection is concerned, use of liquid-heated blades would require installation of liquid-flowing tubes on both blade surfaces up to the very trailing edge of the blade to assure running-wet conditions over these surfaces. This would impose severe blade balancing requirements. For example, in the case of the smallest helicopter (Scout), an additional 0.465 lb/in. of counterbalance weight would have to be placed forward of the 25 percent chord point to balance the anti-icing tubes. This weight, together with the fuel penalty it imposes, would amount to approximately 600 lb for the Scout or a 15 percent increase in its TOGW. Not included in this weight penalty is the additional hub and retention system weight required to cope with the higher centrifugal force of the heavier blades. Even for the heaviest vehicle, the VHLH, the penalty (not including the additional hub and retention system weight) would be about 18,000 lb (5.5 percent of the TOGW). A review of Figures 51 and 53 reveals that the equivalent penalties for chemical or electrothermal freezing rain protection systems are lower by a factor of 3 when compared with the above quoted values for the liquid system. It is concluded, therefore, that liquid-heated blades for freezing rain protection are neither practical nor competitive.

#### 4.4.2 Weight and Vehicle Performance Penalties

Comparisons of weight and horsepower penalties incurred during 1-hour flight through icing for the considered rotor protection systems are shown in Figures 56 and 57, and for freezing rain protection systems in Figures 58 and 59. In establishing the freezing point depressant system penalties for freezing rain, it is necessary to make an assumption regarding the effect on blade drag of incomplete removal of ice over the

TABLE 23. ESTIMATED WEIGHT AND SHP PENALTIES FOR FLIGHT THROUGH  
ICING - INTEGRATED TRANSMISSION LUBE OIL/ANTI-ICING  
SYSTEM - EVAPORATIVE PERFORMANCE FOR MIL-E-38453  
CRITERIA FOR 1 HOUR

Type of Aircraft	SCOUT	AARS	UTTAS and AAH	LTTAS	HLH	VHLH
Total fixed weight, lb	98.5	114.4	159.2	342.1	546.3	862.0
Fuel penalty for fixed weight, lb	7.2	10.6	13.9	30.3	41.4	62.9
Fuel penalty for engine backpressure, lb	7.9	8.6	11.9	27.6	44.9	65.9
Total penalty, lb	113.6	133.6	185.0	400.0	632.6	990.8
Total penalty, percent of TOGW	2.77	1.34	1.20	0.69	0.54	0.31
$\Delta$ shp for fixed weight	12.0	19.5	26.3	62.2	85.8	146.3
$\Delta$ shp for engine backpressure	13.1	15.8	22.6	56.8	92.9	153.2
Total $\Delta$ shp penalty	25.1	35.3	48.9	119.0	178.7	299.5
Total $\Delta$ shp, percent of reqd shp	6.82	2.80	2.59	1.52	1.30	0.74

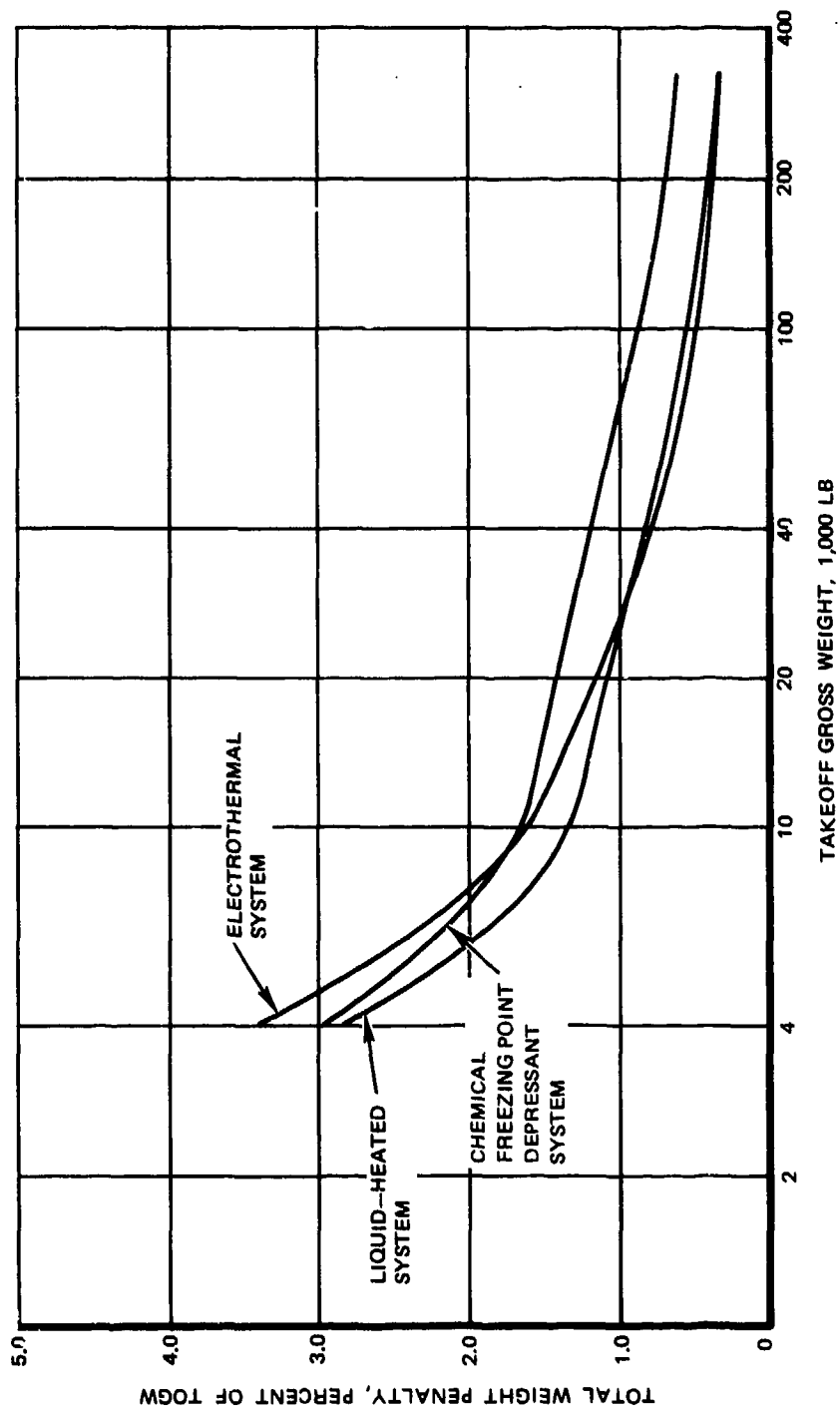


Figure 56. Comparison of Weight Penalties for 1 Hour Flight Through Icing - MIL-E-38453 Criteria.

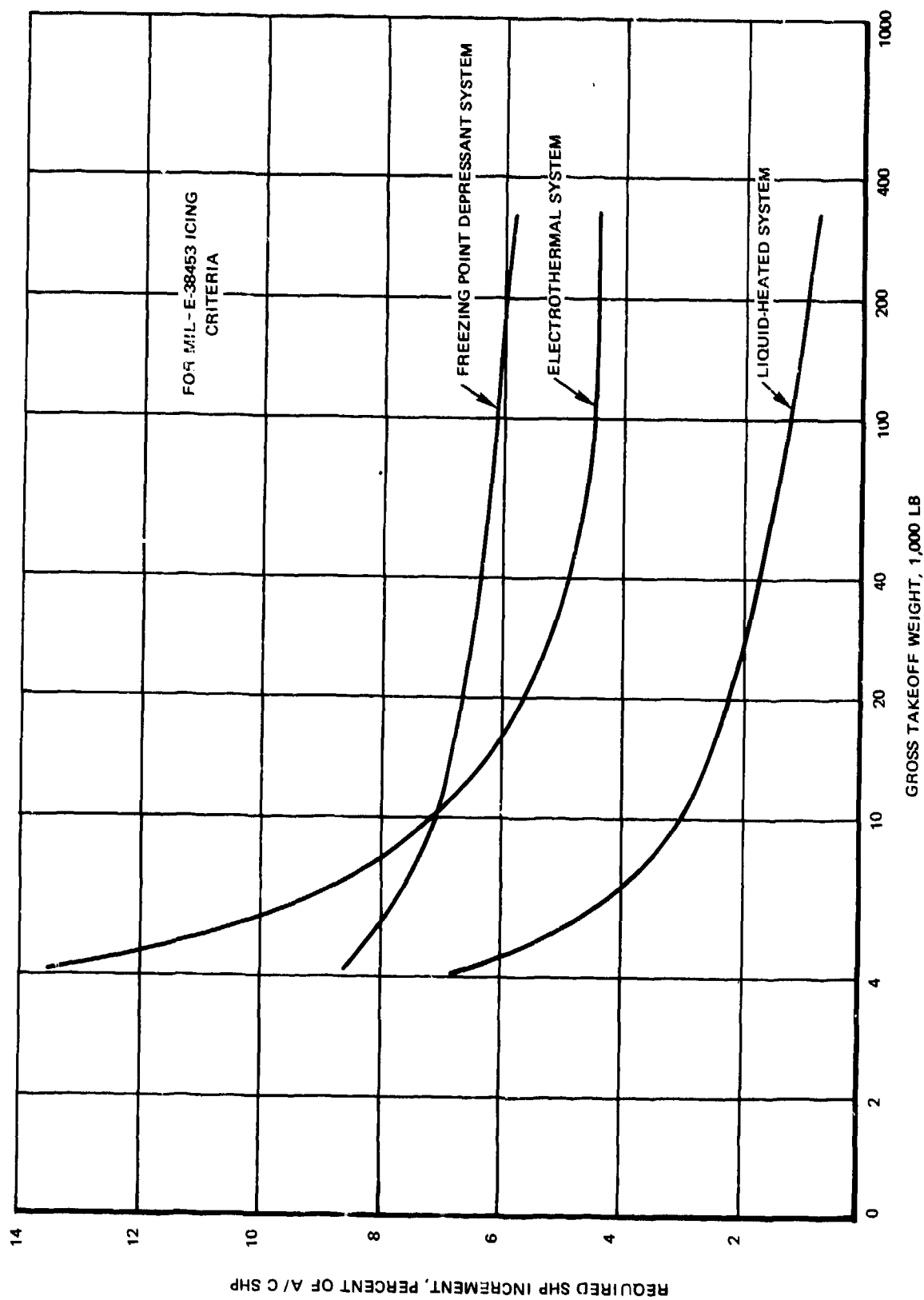


Figure 57. Comparison of SHP Requirements for Flight Through Icing.

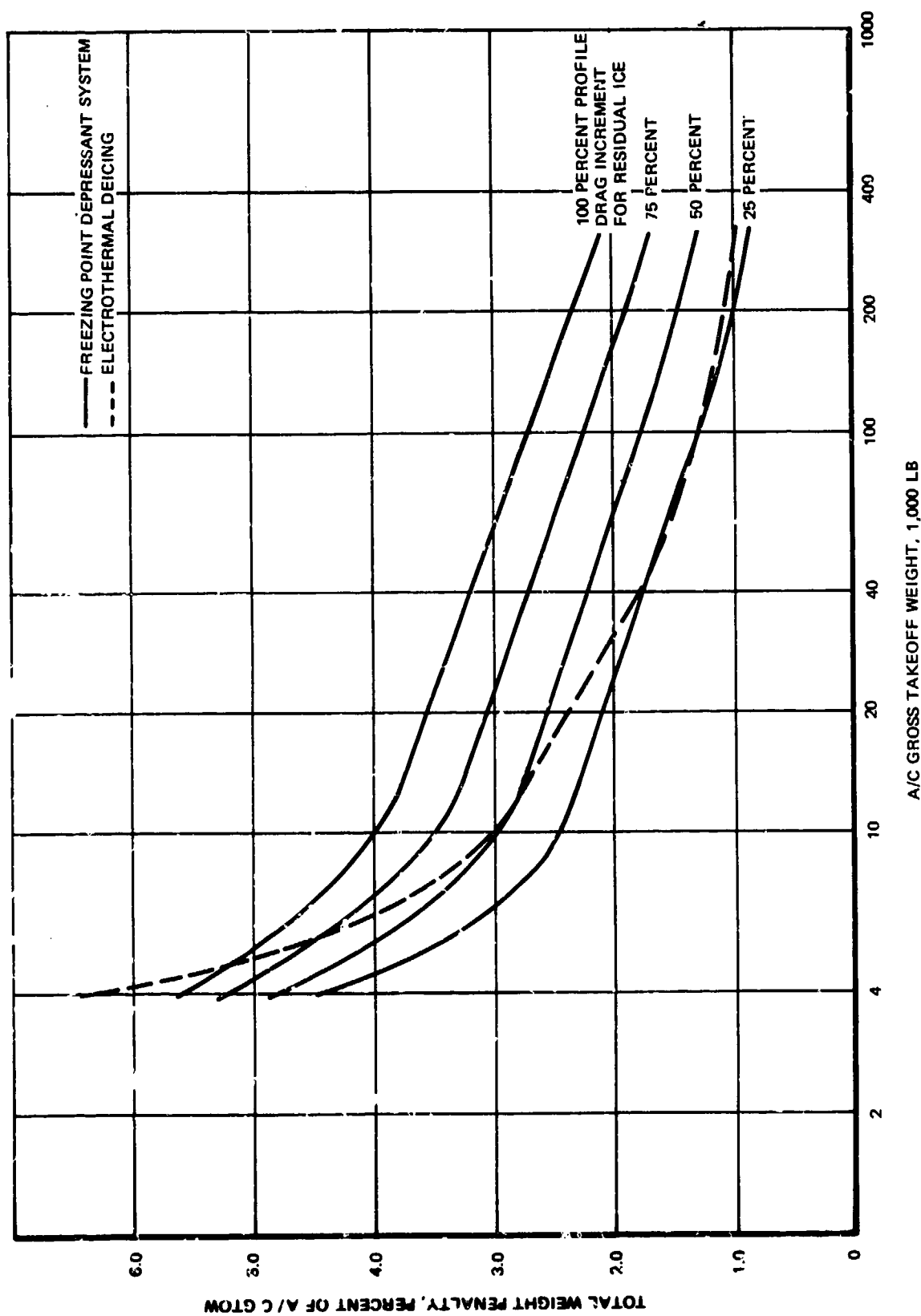


Figure 58. Comparison of Weight Penalties for 1-Hour Flight Through Freezing Rain.

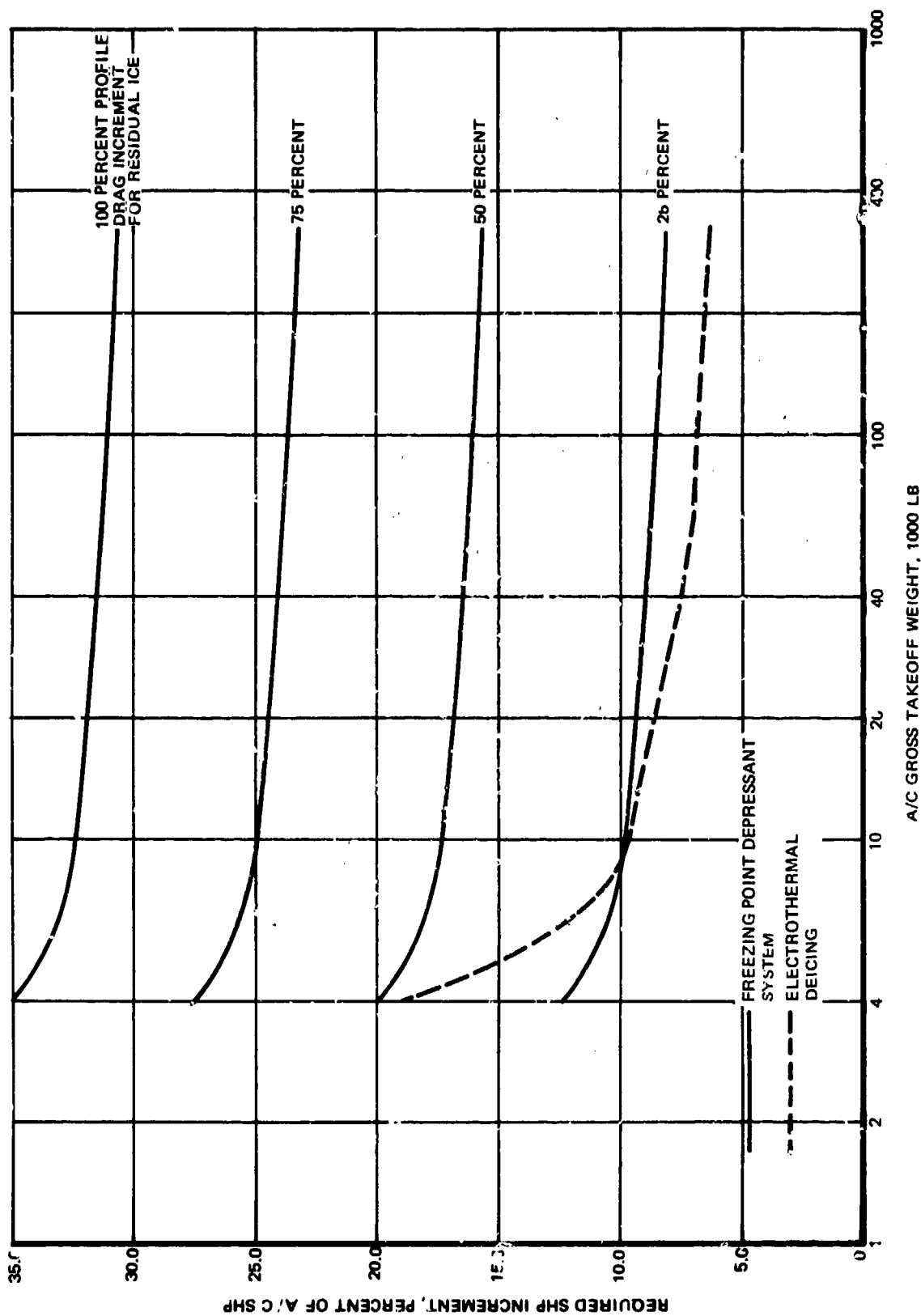


Figure 59. Comparison of SHP Requirements for Flight Through Freezing Rain.



blade. Since there is no experimental data, the data are presented parametrically for increases between 25 and 100% of the profile drag. For the electrothermal system, a drag penalty of 16 percent was assumed. In examining these figures the most significant factor is the overall trend of these penalties regardless of the ice protection technique. The relative penalty, in terms of weight or horsepower percentage increments, rises as the aircraft TOGW is reduced.

Perhaps a more valid comparison than is obtained from considering the penalties for flight through icing is a comparison based on a weighted average of the penalties incurred during clear (non-icing weather) and icing weather. Considering the chemical freezing point depressant system, the expendable fluid need not be carried on board during the summer and, thus, the weight of the hardware alone and the associated fuel penalty need to be applied for two-thirds of the flight-hours (summer) and the full penalty, including the fluid, for one-third of the flight-hours (winter). The fuel penalty due to the increased profile drag is applicable only for the duration of actual icing encounters, ie, for 10 percent of the time for adverse geographical regions. Considering the liquid-heated blade system, the engine backpressure penalty would apply for only 10 percent of the time; similarly, for the electrothermal deicing system the electrical power and airfoil drag penalties due to icing would apply for only 10 percent of the time. Table 24 presents the actual penalty components and the prorated weighted average penalties as obtained from the actual weights based upon above stated ground rules. Figure 60 presents the trend of the average weighted penalties with the aircraft TOGW.

It is noted that for penalties based on flight through icing conditions alone, the advantage of the chemical freezing point depressant system over the electrothermal shows up for a narrower vehicle range (Figure 56), than for penalties based upon average weighted values (Figure 57). This is due to the fact that the penalty for the chemical system during the summer (two-thirds of flight-hours) is greatly reduced, and this is reflected in the results of the average weighted penalty analysis.

TABLE 24. WEIGHTED AVERAGE PENALTIES FOR MIL-E-38453 ICING CRITERIA						
1. Chemical Freezing Point Depressant System - One-Hour Fluid Supply						
Type of Aircraft	Scout	AARS	UTTAS AAH	LTTAS	HLH	VHLH
1. Summer equipment weight, lb	31.0	34.0	43.0	76.0	110.0	164.0
2. Summer fuel penalty due to equipment, lb/hr	2.2	3.1	3.6	6.6	8.3	11.9
3. Winter equipment weight, lb	101.0	119.0	166.0	392.0	570.0	949.0
4. Winter fuel penalty due to system weight, lb/hr	7.0	11.0	14.0	34.0	43.0	69.0
5. Icing drag fuel penalty, lb/hr	12.0	37.0	54.0	204.0	358.0	933.0
Weighted average penalty, lb	59.3	71.8	96.5	217.3	319.0	549.5
2. Liquid-heated Blades (System No. 3)						
1. System fixed weight, lb	98.5	114.4	159.2	342.1	546.3	862.0
2. Fuel penalty due to system weight, lb/hr	7.2	10.6	13.9	30.3	41.4	62.9
3. Engine backpressure fuel penalty, lb/hr	7.9	8.6	11.9	27.7	44.8	65.9
Weighted average penalty, lb	106.5	125.9	174.3	375.2	592.2	931.5
3. Electrothermal Deicing						
1. System fixed weight, lb	106.8	114.3	142.3	202.3	264.3	356.8
2. Fuel penalty due to system fixed weight, lb	7.3	9.7	11.2	16.5	17.8	24.2
3. Electrical power fuel penalty, lb/hr	14.1	13.1	15.6	21.5	35.5	61.2
4. Icing drag fuel penalty, lb/hr	7.9	24.7	35.8	136.7	238.6	622.3
Weighted average penalty, lb	136.1	162.3	204.9	377.0	556.2	1064.5

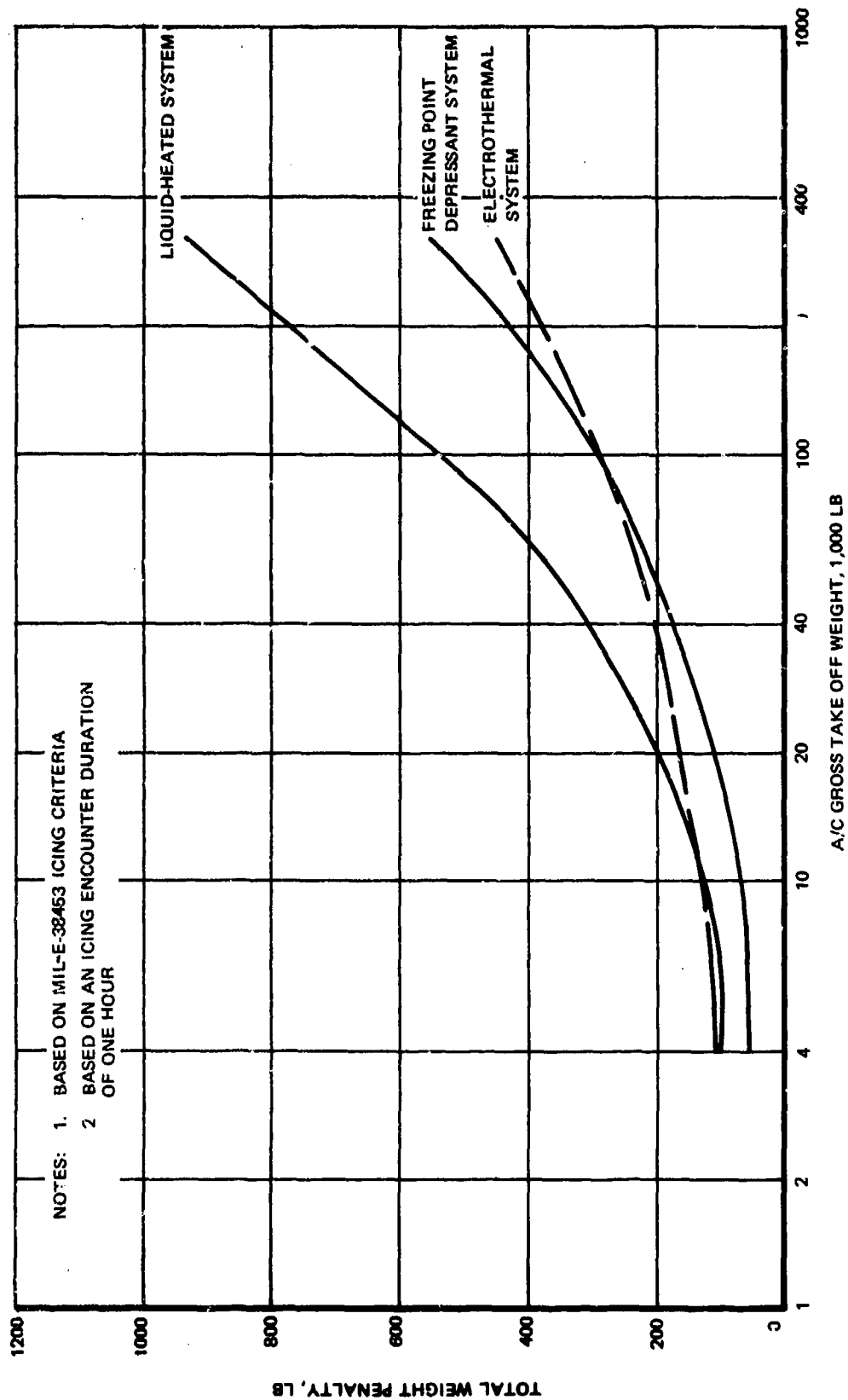


Figure 60. Comparison of Weighted Average Penalties for Flight Through Icing.

#### 4.4.3 Cost Comparisons

Cost trade-off studies were conducted by using 1973 dollars to provide a comparative ranking of each system under consideration and to assist in assessment of possible penalties to be incurred due to selection of a system on a technical or least risk basis rather than lowest estimated cost.

Five basic types of anti-icing/deicing systems were examined. These systems shall be referred to by the designators indicated below for this section of the report.

<u>Designator</u>	<u>System</u>
A	Chemical Freezing Point Depressant
B <sub>1</sub>	Liquid Heated Rotor Blades Utilizing Engine Exhaust Waste Heat, Liquid Rotary Seal System for Water - Glycol
B <sub>2</sub>	Liquid Heated Rotor Blades Utilizing Engine Exhaust Waste Heat, Rotating Heat Exchanger
B <sub>3</sub>	Liquid Heated Rotor Blades, Utilizing Engine Exhaust Waste Heat, Integration of Rotor Anti-icing with Transmission Lubrication
C	Electrothermal

Various production quantities from 100 to 1,500 aircraft were included, based on vehicle type and estimated requirements.

Ninety-six sets of calculations were involved in the process of preparing recurring cost estimates. This coupled with the limited data available during the preliminary design phase necessitated the use of parametric cost estimating techniques.

The overall results of these cost trade-off studies are summarized in Table 25. These costs include the recurring production costs, maintenance, and fuel penalty costs for 10 years on a per aircraft basis. These costs are then multiplied by 200 aircraft to provide a basis for comparison.

TABLE 25. COST SUMMARY - 200 AIRCRAFT PROGRAM

System Designator	A	B <sub>1</sub>	B <sub>2</sub>	B <sub>3</sub>	C
Scout - Prod. Cost per A/C	8,511	17,366	15,893	16,169	17,177
- Maint. Cost per A/C - 10 yrs	1,014	1,366	1,210	1,014	1,288
- Fuel Penalty Cost per A/C - 10 yrs	1,068	1,267	1,556	1,355	2,010
Total per A/C - 10 yrs	10,593	19,999	18,659	18,538	20,475
X 200 A/C = Grand Total \$	2,118,600	3,999,800	3,721,800	3,707,600	4,095,000
Cost Ranking	1	4	3	2	5
AARS - Prod. Cost per A/C	9,332	20,303	18,796	18,605	17,749
- Maint. Cost per A/C - 10 yrs	1,170	1,632	1,404	1,170	1,482
- Fuel Penalty Cost per A/C - 10 yrs	2,488	1,714	2,176	1,856	3,072
Total per A/C - 10 yrs	12,990	23,695	22,376	21,631	22,303
X 200 A/C = Grand Total \$	2,598,000	4,739,000	4,475,200	4,326,200	4,460,600
Cost Ranking	1	5	4	2	3
UTAS and AAH - Prod. Cost per A/C	11,528	28,600	25,567	25,824	24,402
- Maint. Cost per A/C - 10 yrs	1,444	1,950	1,756	1,444	1,872
- Fuel Penalty Cost per A/C - 10 yrs	3,450	2,348	2,832	2,457	3,902
Total per A/C - 10 yrs	16,422	32,898	30,155	29,725	30,176
X 200 A/C = Grand Total \$	3,284,400	6,579,600	6,031,000	5,945,000	6,035,200
Cost Ranking	1	5	3	2	4
LITAS - Prod. Cost per A/C	19,490	62,143	58,461	55,175	43,937
- Maint. Cost per A/C - 10 yrs	2,848	3,900	3,472	2,926	3,706
- Fuel Penalty Cost per A/C - 10 yrs	11,514	5,255	6,609	5,433	9,524
Total per A/C - 10 yrs	33,852	71,298	68,542	63,534	57,167
X 200 A/C = Grand Total \$	6,770,400	14,259,600	13,703,400	12,706,800	11,433,400
Cost Ranking	1	5	4	3	2
HLH - Prod. Cost per A/C	27,998	97,628	92,736	87,894	69,410
- Maint. Cost per A/C - 10 yrs	5,032	6,826	6,084	5,110	6,474
- Fuel Penalty Cost per A/C - 10 yrs	20,075	7,342	9,373	7,755	15,019
Total per A/C - 10 yrs	52,605	111,796	108,193	100,759	90,903
X 200 A/C = Grand Total \$	10,521,000	22,359,200	21,638,600	20,151,800	18,180,600
Cost Ranking	1	5	4	3	2
VHLH - Prod. Cost per A/C	41,448	153,592	145,252	138,578	131,121
- Maint. Cost per A/C	11,038	15,054	13,378	11,194	14,278
- Fuel Penalty Cost per A/C - 10 yrs	51,876	11,066	14,049	11,761	34,660
Total per A/C - 10 yrs	104,362	179,712	172,679	161,533	180,057
X 200 A/C = Grand Total \$	20,872,400	35,942,800	34,535,800	32,306,600	36,011,400
Cost Ranking	1	4	3	2	5
Note: Costs are expressed in 1973 dollars					

It is emphasized that all cost data represent estimates for comparative system rankings and should be used in this context only due to the preliminary design level of available information and omitting elements which are common to all systems.

The cost ranking in Table 25 rates the alternate systems from one to five beginning with the least cost. These results indicate that system A (chemical freezing point depressant) has the lowest cost for all types of vehicles. The relative ranking varies somewhat for the other systems from vehicle to vehicle. System C (electrothermal deicing) is ranked two or three for each vehicle except the smallest (Scout) and largest (VHLH).

Table 26 indicates the individual percentages of production, maintenance, and fuel costs that are shown in Table 25. Production cost is the biggest item in every case except one, followed by fuel and maintenance. The one exception is system A for the VHLH vehicle where fuel is the biggest item followed by production cost.

Table 27 summarizes the recurring production costs for various aircraft quantities. The column titled "Composite Learning Curve" reflects the overall learning from one quantity to another. This composite learning curve ranges from 87 to 94 percent. This variation is caused by the individual contributions of labor and material to the total and their separate learning curves.

The following results based on a quantity of 200 aircraft are indicated on Table 27.

- System A (chemical freezing point depressant) is the least expensive followed by System C (electrothermal cyclic deicing), except for the Scout.
- The dollars per pound of systems' empty weight remain fairly constant through the range of aircraft types except for System C. This exception is caused by the costs for the rotor blade deicing elements.
- The relative ranking of systems in order of least to most costly remains almost constant regardless of aircraft type.

TABLE 26. COST BREAKDOWN BY PERCENTAGE - 200 AIRCRAFT PROGRAM					
	A	B <sub>1</sub>	B <sub>2</sub>	B <sub>3</sub>	C
SCOUT - Prod. Cost	80	87	85	87	84
- Maint. Cost - 10 yrs	10	7	7	6	6
- Fuel Penalty Cost - 10 yrs	10	6	8	7	10
Total	100	100	100	100	100
AARS - Prod. Cost	72	86	84	86	80
- Maint. Cost - 10 yrs	9	7	6	5	6
- Fuel Penalty Cost - 10 yrs	19	7	10	9	14
Total	100	100	100	100	100
UTTAS and AAH - Prod. Cost	70	87	85	87	81
- Maint. Cost - 10 yrs	9	6	6	5	6
- Fuel Penalty Cost - 10 yrs	21	7	9	8	13
Total	100	100	100	100	100
LTTAS - Prod. Cost	58	87	85	87	77
- Maint. Cost - 10 yrs	8	6	5	4	6
- Fuel Penalty Cost - 10 yrs	34	7	10	9	17
Total	100	100	100	100	100
HLH - Prod. Cost	53	87	86	87	76
- Maint. Cost - 10 yrs	9	6	5	5	8
- Fuel Penalty Cost - 10 yrs	38	7	9	8	16
Total	100	100	100	100	100
VHLH - Prod. Cost	40	85	84	86	73
- Maint. Cost - 10 yrs	10	9	8	7	8
- Fuel Penalty Cost - 10 yrs	50	6	8	7	19
Total	100	100	100	100	100

TABLE 27. ANTI-ICING/DEICING TOTAL COST SUMMARY - SYSTEMS BY AIRCRAFT TYPE AND PRODUCTION QUANTITIES

A/C Type	System	100	Aircraft Quantity and Cost by System						Composite Learning Curve
			200	400	500	600	1,000	1,500	
Scout	System A		\$ 8,511	\$ 7,677		\$ 7,249			90
	B <sub>1</sub>		17,366	15,111		14,010			88
	B <sub>2</sub>		15,893	13,836		12,996			87
	B <sub>3</sub>		16,169	14,212		13,220			88
	C		17,177	15,967		15,329			93
AARS	System A		9,332	8,421					90
	B <sub>1</sub>		20,303	17,137					88
	B <sub>2</sub>		18,796	16,363					87
	B <sub>3</sub>		18,605	16,346					88
	C		17,749	16,503					93
UTIAS and AAH	System A		11,528		\$ 10,076		\$ 9,150	\$ 8,666	91
	B <sub>1</sub>		28,600		24,173		21,427	20,020	89
	B <sub>2</sub>		25,567		21,317		18,995	17,315	88
	B <sub>3</sub>		25,824		21,792		19,295	18,015	89
	C		24,402		22,252		20,798	20,011	94
LTTAS	System A		19,490		17,034		15,469		91
	B <sub>1</sub>		62,143		52,524		46,559		89
	B <sub>2</sub>		58,461		48,740		41,764		88
	B <sub>3</sub>		55,175		46,562		41,227		89
	C		43,937		40,324		37,843		94
HLH	System A		27,918	25,260					90
	B <sub>1</sub>		97,628	85,869					88
	B <sub>2</sub>		92,736	80,750					87
	B <sub>3</sub>		97,894	77,218					86
	C		69,410	65,170					94
VHLH	System A	46,165	41,448						90
	B <sub>1</sub>	175,550	153,592						88
	B <sub>2</sub>	167,701	145,252						87
	B <sub>3</sub>	158,571	138,578						87
	C	139,263	131,121						94



Table 28 indicates the major component groups of each system and ranks them in order of the most to least costly as they contribute to the total cost based on 500 scout type aircraft. These major component groups may contain a number of items or components and generally follow the breakdowns of the systems weight statement. Major component groups whose cost is less than \$500 are not included in Table 28.

The first step in conducting cost analyses of the five alternate anti-icing/deicing systems was to determine which elements and areas of cost could be estimated for parametric application to the seven basic types of helicopters (i.e., Scout, AARS, etc). The three basic areas of cost are:

- Development Costs
- Acquisition Costs
- Operation and Maintenance Costs

After review of the problems involved in estimating the development costs from the preliminary design data available, including engineering design, development, testing, tooling, and documentation, it was decided to exclude development costs. There is no historical basis for these data, and generation of new data would have involved a disproportionately large effort.

An evaluation of acquisition costs indicate that the recurring production costs could probably be the most meaningful for development of parametric cost data. This includes manufacturing and quality assurance (QA), labor for fabrication, assembly, and installation of each proposed system. Labor includes direct labor, overhead, and general and administrative costs. Also included are raw materials such as tubing, wire, sheet metal, etc; vendor-supplied major equipment such as deicer timers, heat exchangers, rotary seals, valves, fittings, relays, etc.

Preliminary design data in the form of estimated weights that are broken down into subgroups and components as well as all available schematics, diagrams, layouts, drawings, and technical descriptions

TABLE 28. MAJOR COMPONENT GROUP COST RANKING

	A	B <sub>1</sub>	B <sub>2</sub>	B <sub>3</sub>	C
1	Ice Detector	Blade Tubing	Blade Tubing	Blade Tubing	Generator
2	Lines & Fittings	Pump	Heat Exchanger	Pump	Rotor Blade Deicing Elements
3	Machining Grooves in Blades	Rotary Seal Assembly	Ice Detector	Heat Exchanger	Power Controller
4	Fluid Pump & Reservoir	Heat Exchanger	Pump	Ice Detector	Slip Rings
5	Gages	Ice Detector & Panel	Exhaust Ducts & Valves	Exhaust Duct & Manifold	Ice Detector
6	Main Rotor Slinger Ring	Teflon Hose			Wiring
7	Main Rotor Slinger Ring	Exhaust Duct			Icing Rate Sensor
8	Electrical Components	Electric Units			
9	Tail Rotor Slinger Ring	Brackets, etc.			

were reviewed to generate preliminary parts lists for each system. The basic cost data for production labor and materials was prepared for each alternate system based on the preliminary parts lists. Wiring and plumbing requirements were also estimated. Material estimates were based on raw material requirements for fabrication of detail parts, catalog prices for some components, vendor estimates for major equipment items, and rough order of magnitude (ROM) estimates based on similarity with other items.

Production labor was estimated for fabrication of detailed parts, assembly, installation, and checkout in the aircraft for each alternate system for a vehicle of the Scout type. Production labor was estimated by using time standards and maintenance installation data as well as ROM individual estimates based on experience where data was not available.

The basic production labor and material costs for each type of anti-icing/deicing system based on a Scout vehicle were used to derive parametric dollars per pound for application to the other vehicle types. The material costs for sliprings and rotor blade heating elements are based on ROM estimates from suppliers and not parametric dollars per pound.

Basic costs were developed based on the cumulative average of 500 aircraft, and learning curves applied to arrive at the appropriate cost for alternate quantities of each type of vehicle. A worksheet showing the application of this technique for the electrothermal System C is shown in Table 29. Included are learning curve (LC) calculations, to arrive at the cumulative average (CA) cost per aircraft (A/C), Quality Assurance (QA), and profit factors.

Additionally, it should be noted that recurring sustaining engineering and tooling costs were not included in these costs. These would normally be estimated as a percentage of production costs, so their exclusion does not affect the relative ranking of these estimates.

TABLE 29. ANTI-ICING/DEICING SYSTEM ELECTROTHERMAL (INCLUDES GENERATOR) COST ICING  
SUMMARY - AIRCRAFT TYPE AND PRODUCTION QUANTITIES

A/C Type →	Scout		ARS		UTIAS & ARH		LITAS		HLR		VHLR	
	400 600		200 400		1,000 1,500		500 1,000		200 400		100 200	
A/C Quantities	Mat'l	Labor	Mat'l	Labor	Mat'l	Labor	Mat'l	Labor	Mat'l	Labor	Mat'l	Labor
Basic Cost C.A. @ 500 A/C	8,494	1,462	141	149	60	10	184	249	66	10	326	441
Systems Empty Weight (lbs)	60	10	10	10	10	10	10	10	10	10	10	10
1973 Dollars Per Pound	8,494	1,462	9,956	8,940	11,040	1,840	12,880	17,430	19,560	3,260	26,460	4,410
C.A. Cost @ 500 A/C	1,200	1,200	1,200	1,200	1,400	1,400	1,400	1,800	2,000	2,000	2,500	2,500
Sliprings	2,817	2,817	2,817	2,817	5,673	5,673	5,673	17,054	32,792	32,792	76,222	76,222
Motor Blade Heat Elem. Installed Cost	12,511	1,462	3,973	12,957	18,113	1,490	19,593	33,794	57,612	105,182	105,182	105,182
Subtotal C.A. Cost @ 500 A/C	12,511	1,462	3,973	12,957	18,113	1,490	19,593	33,794	57,612	105,182	105,182	105,182
15% Labor							276	374				
Subtotal Cost							20,229	36,658				
*Cost x 1.10 = Total Incl. 10% Profit							22,252	40,324				
L.C. Factor @ 100 A/C											1,124	1,652
C.A. Cost @ 100 A/C											115,225	7,285
C.A. 15% Labor												1,653
Subtotal Cost												136,603
*Cost x 1.10 = Total Incl. 10% Profit												139,263
L Curve Factor @ 200 A/C	1,069	1,333	1,069	1,333	1,069	1,333	1,069	1,333	1,069	1,333	1,069	1,333
C.A. Cost @ 200 A/C	13,374	1,949	15,323	13,851	19,363	2,453	21,816	36,126	58,102	4,346	112,446	5,879
C.A. 15% Labor	292	292	292	292	292	292	368	406	652	652	882	882
Subtotal Cost	15,615	17,117	15,615	16,135	22,184	22,184	22,184	39,543	63,100	63,100	119,201	119,201
*Cost x 1.10 = Total Incl. 10% Profit												131,121
L.C. Factor @ 400 A/C	1,016	1,073	1,016	1,073	1,016	1,073	1,016	1,073	1,016	1,073	1,016	1,073
C.A. Cost @ 400 A/C	12,711	1,569	14,280	13,164	17,749	240	24,402	55,222	55,222	55,222	55,222	55,222
C.A. 15% Labor	235	235	235	235	235	235	235	235	235	235	235	235
Subtotal Cost	14,515	17,117	14,515	16,135	22,184	22,184	22,184	39,543	63,100	63,100	119,201	119,201
*Cost x 1.10 = Total Incl. 10% Profit												131,121
L.C. Factor @ 600 A/C	.947	.944	.947	.944	.947	.944	.947	.944	.947	.944	.947	.944
C.A. Cost @ 600 A/C	12,345	1,380	13,728	12,345	17,207	1,478	17,685	32,104	34,103	34,103	34,103	34,103
C.A. 15% Labor	207	207	207	207	207	207	222	222	222	222	222	222
Subtotal Cost	13,925	15,329	13,925	15,329	17,414	1,685	17,907	34,326	34,326	34,326	34,326	34,326
*Cost x 1.10 = Total Incl. 10% Profit												37,843
L.C. Factor @ 1,000 A/C												
C.A. Cost @ 1,000 A/C												
C.A. 15% Labor												
Subtotal Cost												
*Cost x 1.10 = Total Incl. 10% Profit												
L.C. Factor @ 1,500 A/C												
C.A. Cost @ 1,500 A/C												
C.A. 15% Labor												
Subtotal Cost												
*Cost x 1.10 = Total Incl. 10% Profit												
L.C. Factor @ 2,000 A/C												
C.A. Cost @ 2,000 A/C												
C.A. 15% Labor												
Subtotal Cost												
*Cost x 1.10 = Total Incl. 10% Profit												

It was necessary to establish certain ground rules and assumptions in order to perform the cost tradeoff studies. Some of these are listed briefly below

- These are rough order of magnitude (ROM) estimates for Engineering Planning purposes only and should not be used for costing.
- An 80-percent learning curve was used for production labor.
- A 95-percent learning curve was used for production materials.
- A quality assurance factor of 15 percent of production labor was used.
- Nonrecurring development costs are not included in this study.
- All costs are stated in terms of constant 1973 dollars.
- A profit factor of 10 percent was applied to production costs.
- Production manufacturing lot release size was 15 aircraft.
- Sustaining engineering and tooling costs were not included.

Maintenance costs shown in Table 25 were developed on the basis of maintenance man-hours per flight-hour (MMH/FH) for real time for a 10-year period of 3,600 flight-hours. A labor rate of \$13.00 was assumed.

Fuel costs for the total flight-hours for 10 years (3,600) were broken down in non-icing conditions (2,400) and icing conditions (1,200). This means that during the four winter months of the year the ice protection equipment was assumed carried complete on the aircraft even though operation time is only 10% of the total flight-hours.

Fuel penalties indicated in Table 25 associated with the alternate anti-icing/deicing systems were calculated for each vehicle type.

Fuel costs are based on JP-4 fuel at 25 cents per gallon or 3.82 cents per pound.

The purpose of these trade-off studies was to provide cost guidance in the selection of the anti-icing/deicing system that best meets overall system requirements. The costs generated in this study for the selected

system would differ, if studied at a later date, for a number of reasons including:

1. Trade-off costs are in constant 1973 dollars.
2. A detail design would exist where only conceptual design data was available for the study.
3. More detailed and complete parts list would be available.
4. Specifications would be available for each vendor-supplied major component, and they could quote more realistically.

#### 4.4.4 Reliability and Maintainability Comparison

The systems have also been compared as to the maintenance man-hours per flight-hour (MMH/FH) required for the advanced helicopter configurations. The results are listed in Table 30.

The increase in MMH/FH from Scout to VHLH is due to the fact that blade area is increasing and the larger blades will require added handling, additional equipment to conduct inspections and make repairs, larger exposed areas to erosion, etc. The other elements of the ice protection system will remain basically the same. A step change occurs for the HLH and VHLH systems because these heavy lift helicopters use tandem rotors instead of the conventional single main rotor/tail rotor systems.

Figure 61 graphically presents the increase in MMH/FH as a function of heater element area and blade size for the electrothermal deicing system. Main rotor blades which are similar, such as those used on the Scout and AARS, will have a maintenance requirement which is linear with blade area and result in 0.0001 MMH/FH per square foot of heater element area, but the factor for the VHLH increases 20 percent to 0.00012 MMH/FH. This 20-percent number was verified by a time line labor analysis for several sizes of heater elements and blades. The smaller tail rotor blades remain linear at 0.0001 MMH/FH. The MMH/FH numbers are "touch time" not "real time" numbers for engineering analysis because of the disparities in the reporting of real time hours. However, a factor of 3 is usually applied to touch time to obtain real time.

TABLE 30. MAINTENANCE MAN-HOURS PER FLIGHT-HOURS (TOUCH TIME) FOR ANTI-ICING/DEICING SYSTEM							
							Total Maintenance Time for 3600-Hour Life
	Rotary Glycol	Rotary Ht Exch	Lube Oil	Chemical Freezing Pt Depst.	Electrothermal	Electrothermal	
						Touch Time (total hr)	Real Time (total hr)
SCOUT	0.0097	0.0086	0.0071	0.007	0.0092	33.12	99.36
AARS	0.0116	0.0099	0.0083	0.0082	0.0106	38.16	114.43
UTIAS	0.0139	0.0124	0.0104	0.0102	0.0132	47.52	142.56
LTTAS	0.0278	0.0247	0.0207	0.0204	0.0264	95.04	285.12
HLH	0.0487	0.0432	0.0365	0.0388	0.0461	165.96	499.83
XHLH	0.1072	0.0953	0.0798	0.0787	0.1016	365.76	1,097.28

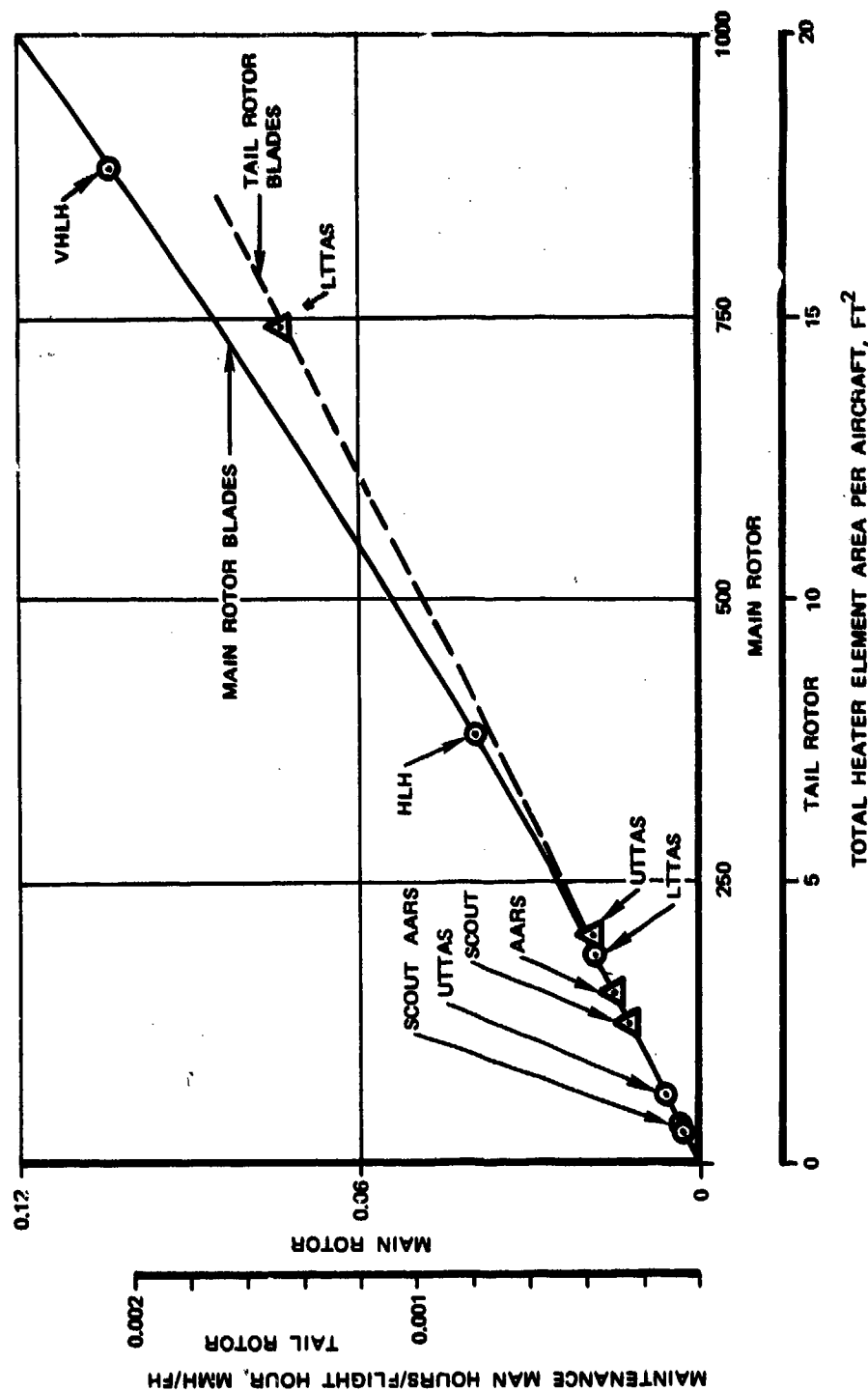


Figure 61. MMH/FH Vs Total Heater Element Area, Main and Tail Rotor Blades.



The bases for the above predictions were:

Life	- 3,600 flight-hours or 10 years
System "on" time	- 10 percent or 360 hours
Exposure	- Juneau winter Dallas summer

It is noted that the electrothermal system has a relatively high number compared to other types of ice protection systems. However, when multiplied by the normal helicopter life of 3,600 hours, none of the systems indicate excessive maintenance costs.

System reliability is not a strong function of vehicle size since the components involved are similar but only different in capacity and power requirement. An indication of reliability is the mean time between failures (MTBF). MTBF hours for the systems being compared are applicable to all the advanced helicopter configurations. These hours are summarized in Table 31.

For the electrothermal cyclic deicing system two sets of reliability and maintainability (R&M) parameters are presented. If the R&M data for electrothermal deicing includes the generator and its voltage control system, the overall system is penalized to the extent that its R&M lag behind those of the other candidate systems. However, such an assumption is not realistic because the generator is generally required for other functions, regardless of ice protection requirements. Table 30 shows that the R&M of an electrothermal deicing system with a hybrid controller is superior to that with an all-solid-state controller, and also compares favorably with the other candidate systems.

#### 4.4.5 Effect of Icing Severity on System Design Requirements

The system design severity trade-offs are confined to electrothermal and chemical deicing systems only since the weight and cost studies do not show any advantage for the liquid-heater blade and its application potential is limited. As pointed out earlier, electrothermal deicing design requirements are sensitive to the OAT, but not the LWC. If the encountered LWC is considerably greater than specified by the design

TABLE 31. ROTOR ICE PROTECTION RELIABILITY COMPARISON

SYSTEM	MTMA (1) HRS	MTUR (2) HRS	MTBF (3) HRS
Chemical Ice Depressant	644	2247	4049
Liquid-heated Rotor Blades:			
1. Rotary Water-Glycol Seals	533	1675	5464
2. Rotating Heat Exchangers	243	1150	3003
3. Modified Transmis- sion Oil Lub. System	647	2652	7353
Electrothermal Cyclic Deicing			
Including Generator and Supervisory Panel			
All-Solid State System	388	1279	2740
Hybrid System	451	1375	2932
Excluding Generator and Supervisory Panel			
All Solid State System	546	2127	4115
Hybrid System	659	2347	4484
(1) Mean time between maintenance actions			
(2) Mean time between unscheduled removals			
(3) Mean time between failures			

criteria, the only noticeable effect would be a slightly larger than optimum ice buildup thickness between shedding cycles. However, the ability to shed this ice with a given energy applied for a given duration would not be impaired as long as the ambient temperature remains within the design envelope. Figure 62 presents the variation of the electrothermal deicing system total weight and horsepower penalties as a function of the ambient temperature. The  $-4^{\circ}$  F OAT icing design point specified in AV-E-8593 for engine installations also represents a valid criterion for rotor electrothermal deicing systems, particularly on small helicopters which exhibit a greater sensitivity to a change in the ambient icing temperature (Figure 62). Thus,  $-4^{\circ}$  F is recommended as the minimum design icing temperature for helicopters since it also meets the 99th percentile criterion.

The total weight penalty of a chemical deicing system depends primarily upon the quantity of the required expendable liquid freezing depressant. This quantity is a function of both the ambient temperature and the LWC. The required fluid expulsion rate reaches a peak value at an ambient temperature of  $0^{\circ}$  F for MIL-E-38453 icing criteria (Figure 49) or  $5^{\circ}$  F for the 95th percentile icing criteria (Figure 50). Protection to ambient temperatures higher than  $-4^{\circ}$  F is not acceptable because it would exclude a universally accepted part of the icing envelope and protection to lower temperatures than  $0^{\circ}$  F would not produce any further weight penalty. Therefore variation of the chemical system weight with ambient temperature is largely of academic interest. The quantity of required freezing depressant is directly proportional to the LWC value. Figure 63 shows the impact of a variation in the LWC values upon the weight of the chemical system.

Perhaps the most important parameter that determines the weight penalty of the chemical system is the anticipated maximum duration of an icing encounter. The amount of fluid carried on board must be sufficient to cope with the longest encounter. There is no existing military specification related to the required duration of chemical system protection

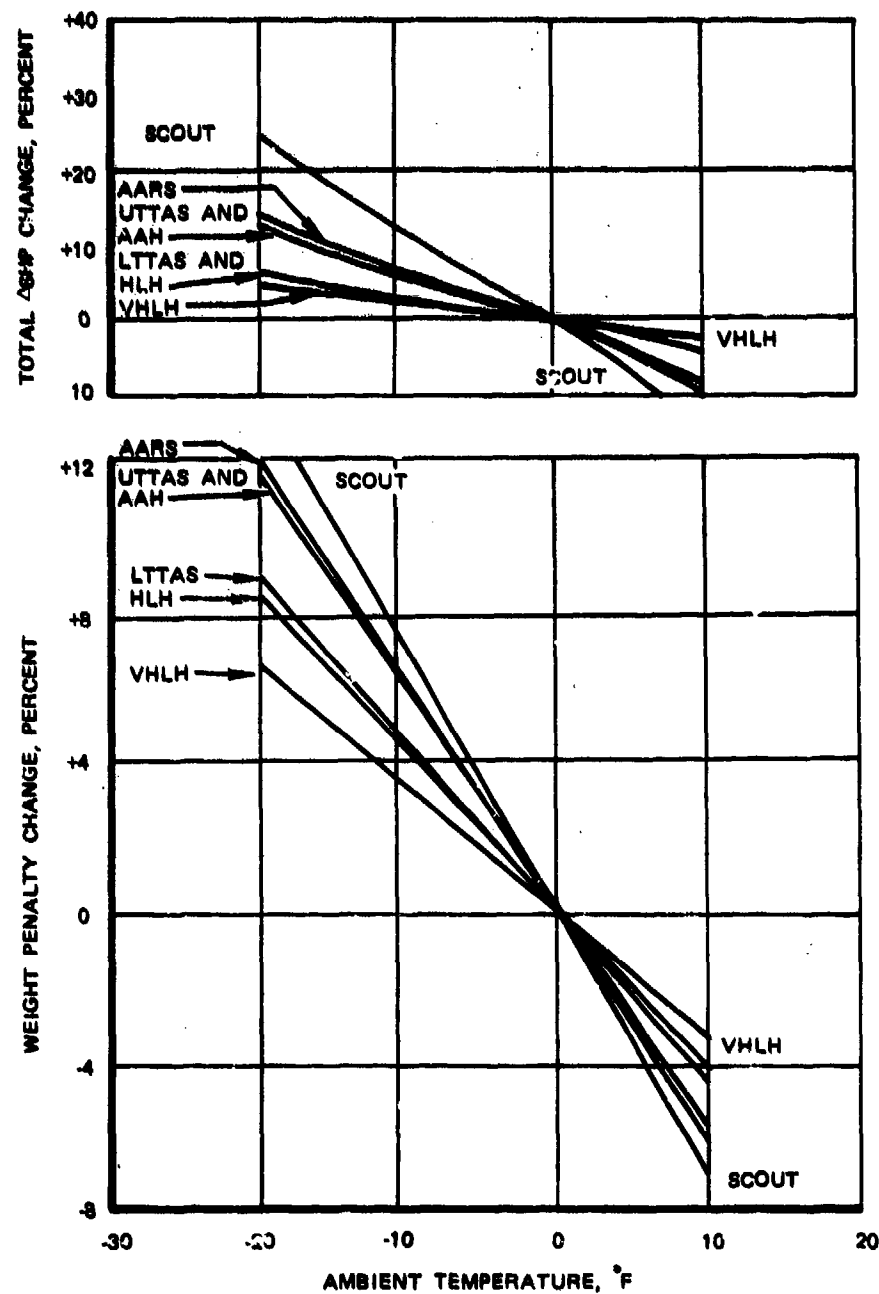


Figure 62. Weight and SHP Penalty Change With Temperature for the Electrothermal System.

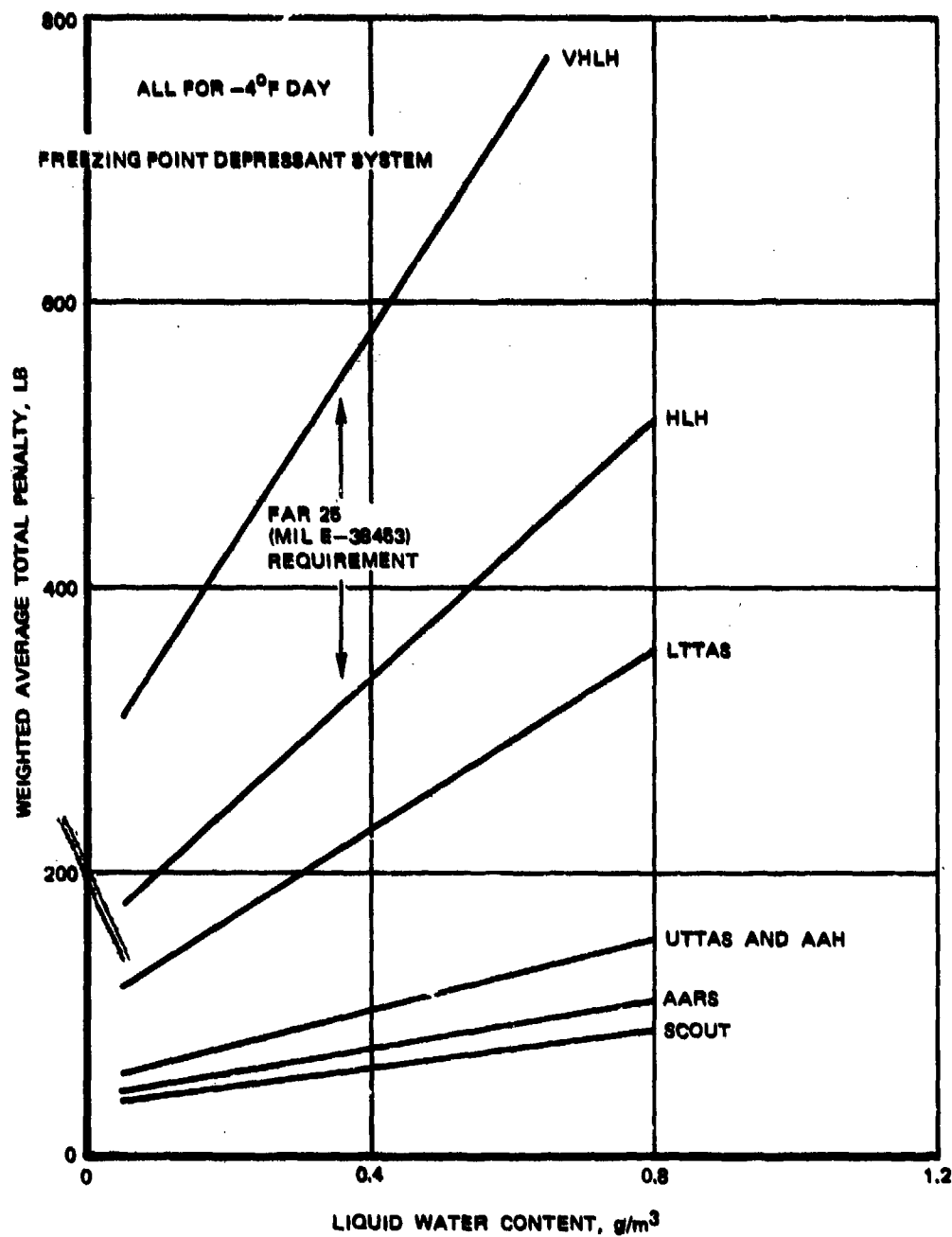


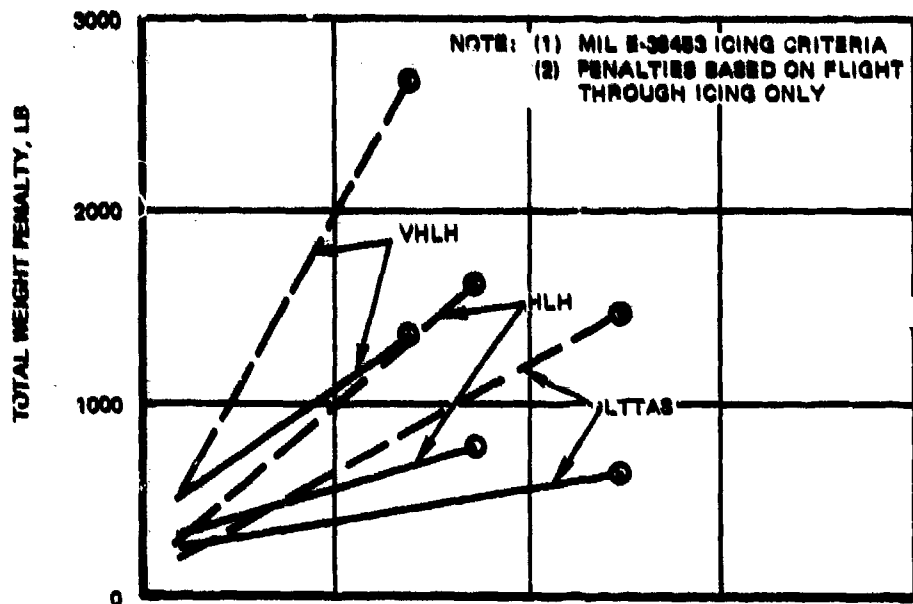
Figure 63. Weighted Average Total Penalty With LWC for the Chemical Freezing Point Depressant System.

for airframe components but future specifications should consider the maximum icing encounter duration. For the purpose of comparing relative penalties for vehicles of different size, the presented tradeoff data were based on a 1-hour encounter duration. However, for windshield anti-icing, MIL-S-6625(ASG) provides a formula for the required fluid capacity that is based on the airplane range in hours with full military load. Therefore, in comparing the chemical system with the electrothermal, it is necessary to evaluate the penalties as a function of time. Such a comparison is provided in Figures 64 and 65. Figure 64 shows that on the basis of flight time in icing equal to the maximum mission duration the electrothermal system is lightest. (The variation in weight with deicing time for the electrothermal system is due only to the fuel penalty attributable to carrying the system weight and to compensate for the drag increase due to ice buildup between deicing cycles.) Comparison of Figure 65 with Figure 60 shows that for an icing encounter based on the endurance mission duration rather than on a 1-hour duration, the year-round average weighted penalty advantage of the chemical system over the electrothermal is greatly minimized, and in the case of the heavier aircraft the electrothermal system is clearly superior. Based on a 1-hour icing encounter the electrothermal rotor deicing system penalty is least for aircraft with TOGW's in excess of 85,000 lb (Figure 60), while based on mission duration, the year-round electrothermal system penalty is least for aircraft with TOGW's in excess of 16,000 lb (Figure 65).

#### 4.4.6 Trade-off Study Conclusions and Recommendations

The trade-off studies have resulted in the following important conclusions and recommendations:

1. The final contenders for rotor blade ice protection are the chemical and electrothermal deicing systems.



————— ELECTOTHERMAL SYSTEM  
 - - - - - FREEZING POINT DEPRESSANT SYSTEM  
 ○ END POINT CORRESPONDS TO DESIGN MISSION ENDURANCE

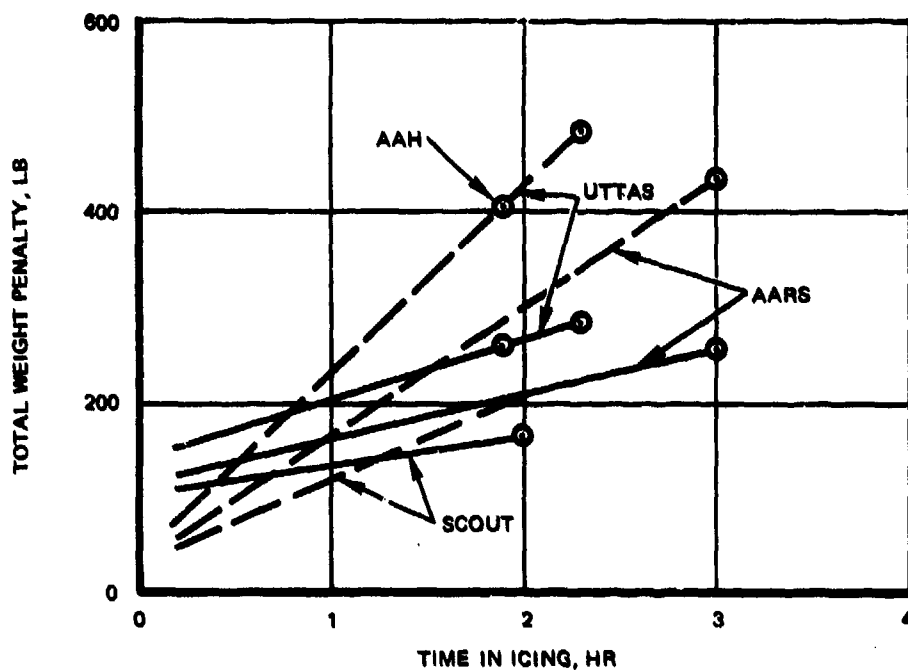


Figure 64. Flight Through Icing Weight Penalty Vs Ice Encounter Duration.

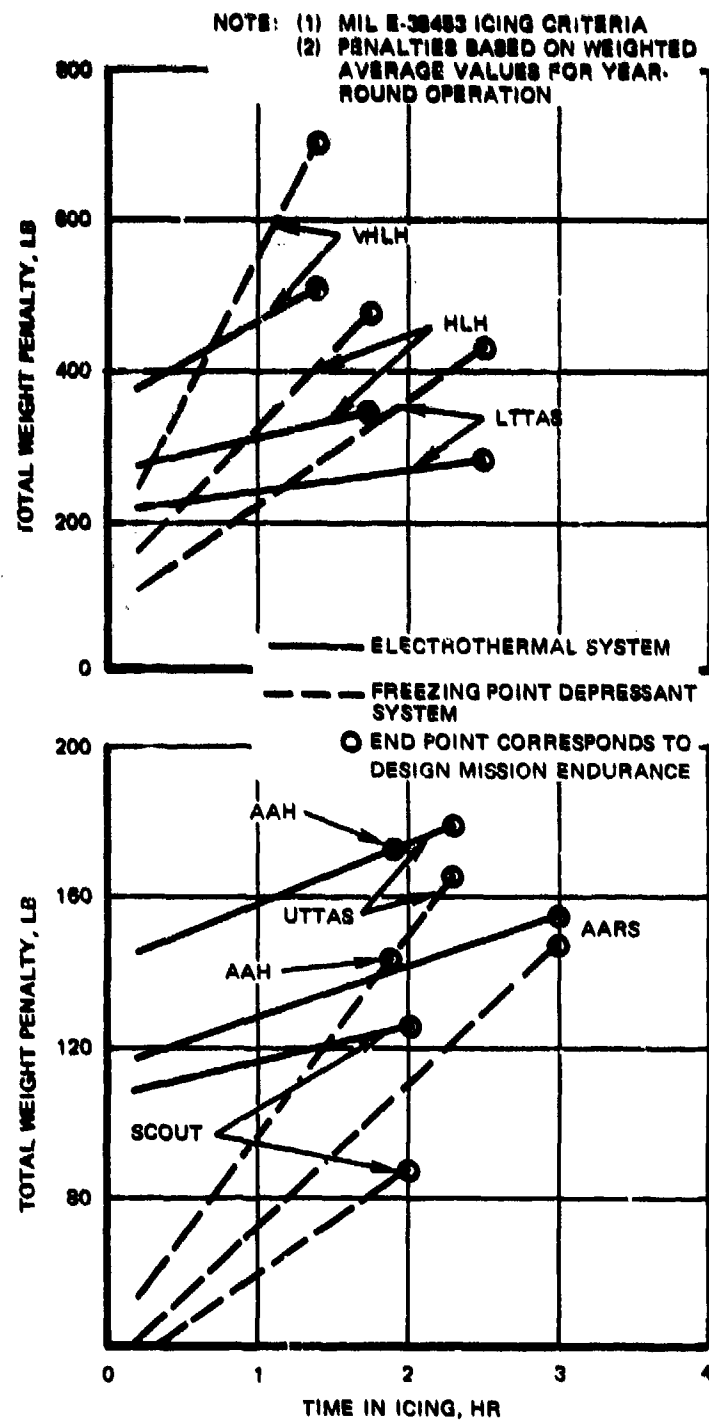


Figure 65. Average Weight Penalties for Year-Round Operation.



2. It is recommended that electrothermal cyclic deicing be used for advanced Army helicopters. Although the chemical system appears to offer the minimum cost approach, other considerations such as questionable ice protection performance, high vulnerability to battle damage, long development span required to achieve a good fluid flow distribution for each individual application, and required logistics support are factors that put the electrothermal cyclic deicing system in first place.
3. For electrothermal deicing the governing criterion is the lower extreme of the temperature envelope, i.e.,  $-4^{\circ}\text{F}$  OAT, and the maximum LWC values, whether based upon MIL-E-38453 or 99th percentile criteria, are of secondary importance. The LWC values do not dictate the power and weight requirements but figure only in determining the duration of the deicing cycle.
4. For chemical systems, use of the 99th percentile criteria results in a slight weight saving compared to the use of MIL-E-38453 criteria. This weight saving is most pronounced for the smallest Scout aircraft (on the order of 0.5 percent TOGW) and is insignificant for the larger vehicles. Considering that the lighter the aircraft the greater its sensitivity to icing, the very modest penalty increment associated with application of the more severe MIL-E-38453 icing criteria is well justified even for light aircraft.
5. Based on the foregoing, MIL-E-38453 icing design criteria down to  $-4^{\circ}\text{F}$  OAT are recommended for helicopter rotor ice protection. Although some slight weight savings might accrue with use of the (lower) 99th percentile criterion as compared to the mil spec, it is recommended that the mil spec severity level be used for Army helicopters since the resulting design will be compatible with the other military services and also with civil (FAA) requirements. If, however, the use of a chemical freezing point depressant system or an advanced concept is selected for use on an aircraft which will be for the sole use of the Army, then the less severe 99th percentile criterion envelope could be used.
6. For helicopters with a TOGW in excess of 16,000 lb, electrothermal deicing of the rotor blades represents the lightest technique. For helicopters lighter than 16,000 lb, the chemical deicing system may be considered because it is both lighter and cheaper. However, because of other reasons (Section 3.2.2) chemical deicing is not recommended even for light helicopters.
7. The primary meteorological criterion for freezing rain protection is the lower ambient temperature extreme of the freezing rain envelope. Review of available data indicates that this

extreme is  $14^{\circ}$  OAT. As pointed out earlier, the lowest temperature represents the governing criterion for electrothermal deicing. For chemical deicing the onboard fluid quantity required is governed by conventional stratus cloud protection criteria and not by freezing rain requirements. Proper distribution of the fluid over the blade surface is the greatest problem in providing for freezing rain protection.

8. In the case of the electrothermal system, it is impossible to accommodate the projected number of cyclic zones for freezing rain protection. A smaller number of zones would impose considerably greater power and weight penalties than shown herein. In the case of the chemical system, nonuniform distribution of the fluid over the blade surface would increase the potential for vibration, unsymmetric loads, and drag due to residual ice formations. Proper fluid distribution may require a special distribution system aft of the 25-percent chord station, which, in turn, would require an additional balance weight at the leading edge.
9. Provision for complete freezing rain protection for the rotor blades might still not eliminate the safety hazard associated with flight through such conditions. This hazard may still exist due to icing on fuselage surfaces, tail surfaces, landing skids or gear, and other surfaces normally not affected by stratus cloud icing.
10. Freezing rain protection for rotor blades is therefore, not justified in view of (a) the high weight and/or power penalties involved, (b) the hazard of even such greater penalties, (c) the possibility of a remaining flight safety hazard even if full protection is provided, (d) the partial protection against freezing rain provided by conventional coverage based on stratus cloud protection, and (e) the relatively low probability of encountering severe freezing rain.

## SECTION 5

### ADVANCED ELECTROTHERMAL DEICING SYSTEM DEVELOPMENT

The conclusion was made from the trade-off studies and the technology evaluation that the electrothermal cyclic deicing concept is the system which should be developed and applied to a broad class of helicopters. The technology study also showed that this concept could be retrofitted to existing aircraft in the inventory. The component that is most critical to a successful application - and that is not state of the art for helicopter application - is the rotor blade deicer heater blanket. This section, therefore, describes the work which has been accomplished to obtain components and designs which will be satisfactory for operational usage with an illustrative application for the UH-1H helicopter. A complete description of the UH-1H rotor blade modification to incorporate an ice protection system for flight testing is contained in Section 2 of Volume II.

#### 5.1 HEATER DEVELOPMENT

As a first step, an experimental program was established to evaluate candidate heater boot materials, configuration, and assembly processes. The results of this task are presented along with a description of the procedures used for assembling the blade heater, the installation on a (UH-1H) rotor blade, results of structural testing, and an analysis of structural requirements for the UH-1H.

The development program focused on the etched foil concept described in Paragraph 3.2.1.1. The particular feature of the concept which has been judged to be superior is the etched foil heating element encapsulated between plies of tough, resilient insulation material. The material and fabrication technology established for application of this concept to the P-3 empennage was used as a base for developing an improved system

designed to meet the more stringent requirements of a rotor blade installation. The first phase of the development work covered:

1. The evaluation of advanced insulation materials to compare dielectric strength and fabricability
2. The evaluation of hard epoxy and soft rubber interlayer materials used to bond deicing boots to rotor blades

The load transfer behavior of these layers was also evaluated.

To guide material and process selection and development, qualitative requirements for each major material and component of the heater assembly were established.

The requirement for a very thin material introduces a need for high dielectric strength insulation materials and laminating adhesives to prevent electrical dielectric failure in service. Concomitant dynamic moments and centrifugal force loading of rotor blades dictate that all adhesives, insulations, heating element, and erosion shield materials in the heater boot laminate resist these loadings without fracture or delamination and consequent electrical failure. Further, these materials must not degrade excessively in chemical environments (high humidity, etc.) or long time cyclic loading (fatigue) as encountered in service. In order to resist the loads encountered, the heater boot laminate must have adequate interlaminar bond strength. This strength consists of three components: peel, tension (perpendicular to plane of laminate), and shear (parallel to plane of laminate). All laminae must also be capable of resisting maximum strain imposed by rotor blade loading without fracture or delamination.

The basic configuration evaluated is depicted on blade-heater installation drawings, illustrated by Figure 66. The variations in configurations together with tests performed are described in Table 32. Therefore, both nickel and stainless steel erosion shield materials were evaluated in material configurations under test on this program.

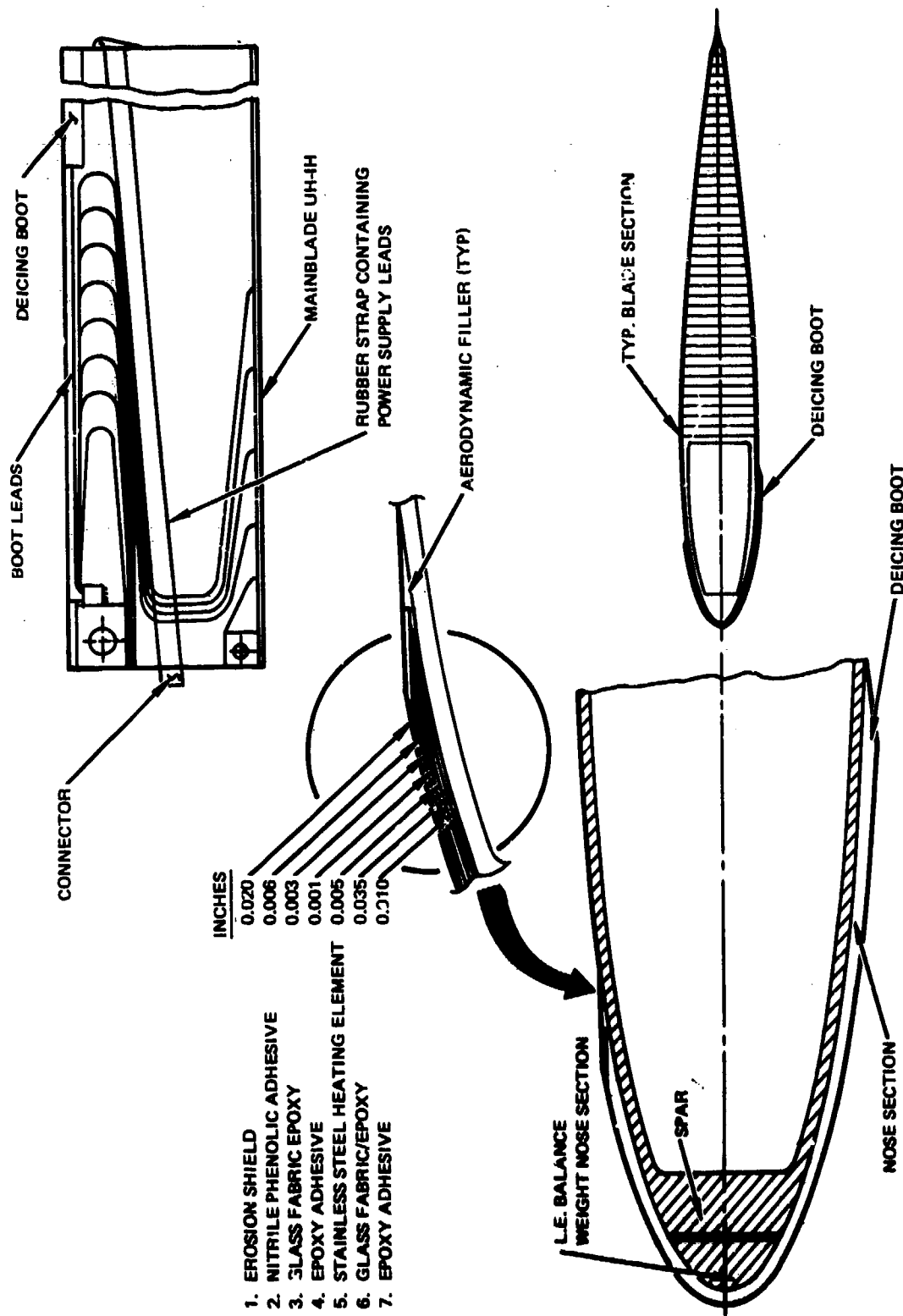


Figure 66. Main and Tail Rotor Blade Deicing Installation for UH-1H.

**TABLE 32. SUMMARY OF TESTS - DEICER BOOT CONFIGURATION**

TABLE 32. SUMMARY OF TESTS - DEICER BOOT CONFIGURATION		
Configuration		Tests
Configuration 1		
Nickel	0.020	Dielectric Strength  Resistance - megohms Breakdown - 1250 volts  Heat Test-Seconds To Melt 150°F Tempilaq.  20 watts/sq in. 15 watts/sq in. 10 watts/sq in.
Nitrile Phenolic Adhesive	0.006	
Glass Fabric/Phenolic	0.004	
Nitrile Phenolic Adhesive	0.001	
Tedlar	0.002	
Nitrile Phenolic Adhesive	0.001	
Stainless Steel	0.005	
Glass Fabric/Epoxy	0.005	
Configuration 2		
Nickel	0.020	Bond Strength  Peel-lb /in. Failure Location  Tensile-psi Failure Location  Shear-psi Failure Location
Nitrile Phenolic Adhesive	0.006	
Glass Fabric/Polyimide	0.005	
Nitrile Phenolic Adhesive	0.001	
Stainless Steel	0.005	
Glass Fabric/Epoxy	0.005	
Configuration 3		
Nickel	0.020	Average Values
Epoxy Adhesive	0.006	
Glass Fabric/Epoxy	0.003	
Epoxy Adhesive	0.001	
Stainless Steel	0.005	
Glass Fabric/Epoxy	0.005	
Configuration 4		
Hardback		Tension Cycling test Humidity tolerance test  For configurations 4 and 5, material thicknesses between the heater element and the shield are the same as in configuration 3.
Shield (both nickel and steel)		
Selected Heater Laminate		
Epoxy Adhesive		
2024T3 Aluminum		
Epoxy Adhesive		
Selected Heater Laminate		
Shield		
Configuration 5		
Softback		
Shield		
Selected Heater Laminate		
Nylon Rubber Interlayer		
Modified Epoxy Adhesive		
2024T3 Aluminum		
Modified Epoxy Adhesive		
Nylon Rubber Interlayer		
Selected Heater Laminate		
Shield (both nickel and steel)		
Configuration 6		
Hardback - Same materials and stacking order as Configuration 4 above except shields are fabricated from 020 electroformed nickel only.		Fatigue tests
Configuration 7		
Softback - Same materials and stacking order as Configuration 5 above except shields are fabricated for 0.020 electroformed nickel only.		

The candidate types of insulation materials between the erosion shield and the heating element selected for evaluation and comparison are:

- Tedlar film plus one ply of 108 style glass fabric impregnated with nitrile phenolic resin (Configuration 1)
- Two plies of 106 style glass fabric impregnated with polyimide resin or equivalent (Configuration 2)
- Two plies of 106 style glass fabric impregnated with epoxy resin or equivalent (Configuration 3).

These materials were selected because of superior dielectric strength, toughness, and ductility. System No. 1 is basically the same as that used in P-3 empennage leading edges except that Tedlar film was added to the laminate to improve dielectric strength and resistance to moisture penetration. The Tedlar film is a polyvinylfluoride compound which is a good dielectric, is free of porosity and pin holes, and is available in a bondable grade. The glass/polyimide material has excellent dielectric strength, heat resistance, and stability and may be fabricated essentially void-free. The glass/epoxy material is also a good dielectric material and it has outstanding toughness, ductility, and amenability to fabrication of void-free laminates.

These systems were evaluated by testing in laminates simulating deicing boot construction to determine:

- Dielectric strength and thermal conduction qualities of insulation
- Interlaminar bond strength in tension, peel, and shear

Two concepts for attaching the heater boot to the blade were evaluated. These concepts involve the transfer of loads between the heater boot and the rotor blade. The concepts are designated as hardback and softback. The hardback consists of a layer of a glass fabric epoxy laminate and nylon fabric reinforced epoxy adhesive, and the softback a layer of

rubber plus the epoxy adhesive. The epoxy/glass fabric laminate has a relatively high shear modulus when compared to that of the rubber material. The rubber selected for the softback was ethylene propylene terpolymer (Epcar). Both materials were selected for ductility and stability over a temperature range of  $-67^{\circ}$  to  $+200^{\circ}$  F with good weathering and fluid resistance.

All test specimens were fabricated using essentially the same methods, assembly sequence, and procedures as those used for fabrication of flight hardware. The basic fabrication sequence is:

1. Bond stainless steel foil to glass fabric/epoxy backing.
2. Etch the required heater element pattern on the stainless steel foil using a photochemical method.
3. Bond the heating element to the nickel or stainless steel erosion shield material.
4. Laminate and bond glass/fabric epoxy to the heating element in the "hardback" configuration. In the case of the "softback" configuration, Epcar rubber was bonded to the heating element in this step.
5. Bond the finished heater boots with epoxy adhesive to aluminum which simulates the blade surface.

Figure 67 is a photograph of a typical buildup.

Standard dielectric strength and bond strength tests were run on the three insulation configurations (Table 33). In addition, the same insulation systems were tested functionally for heating capability. In this test, a heating element segment representative of that to be used on blades was fabricated and laminated in a flat condition with the selected insulation system. Tempilaq was applied to the surface representing the erosion shield. This is a coating designed to melt at a specified temperature. The element was energized, and the time to melt the Tempilaq was recorded. Any cold spots are indicated by lack of melting in the required time. After this test, the selected insulation laminates were bonded to 2024T3 aluminum plate which represented the basic blade aluminum D-spar thickness. Both the hardback and softback



Reproduced from  
best available copy.

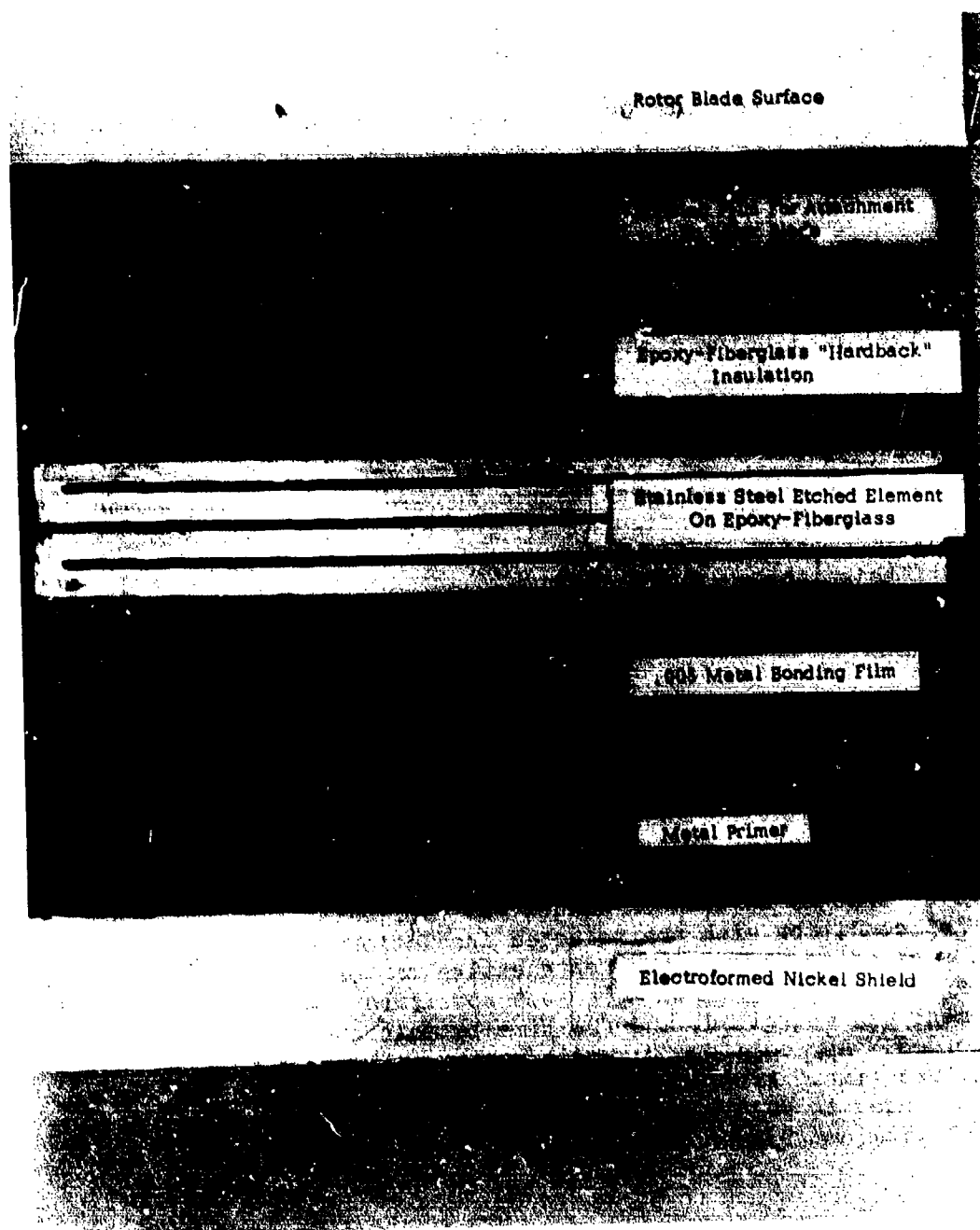


Figure 67. Photo of Rotor Blade Deicer Laminate.

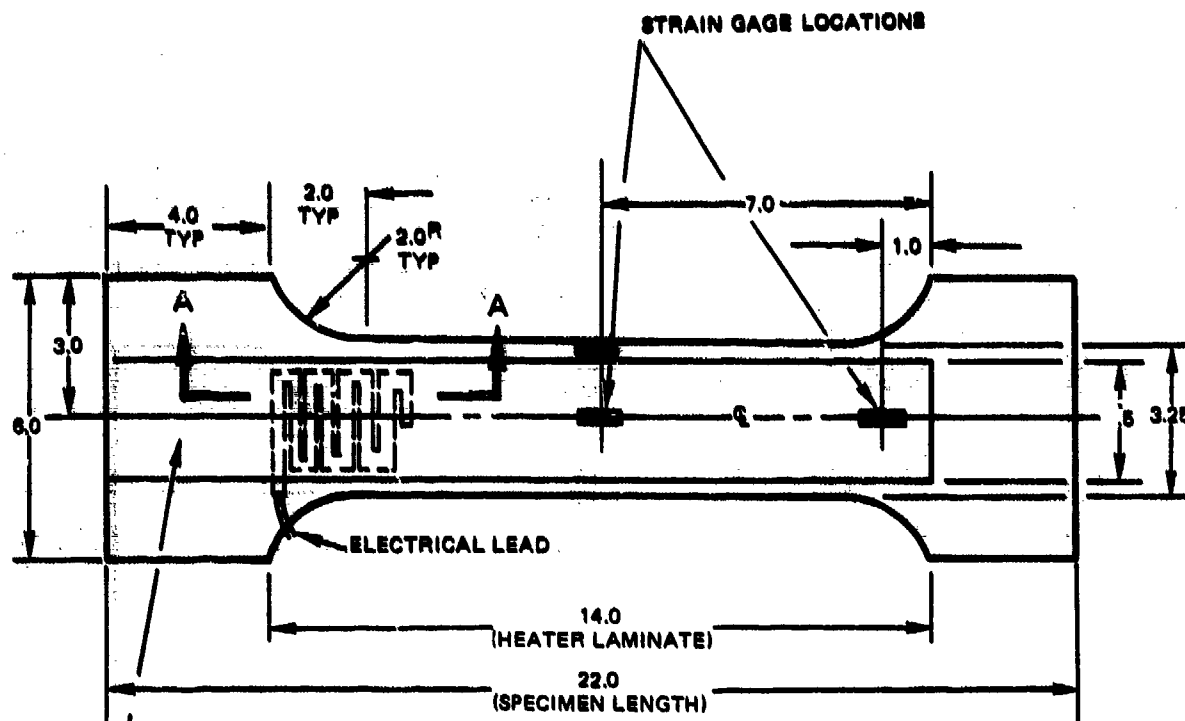
TABLE 33. DATA SUMMARY - TESTS OF HEATER BOOT CONFIGURATIONS

Test	Configuration 1			Configuration 2			Configuration 3		
	Mickel	0.020	0.006	Mickel	0.020	0.006	Mickel	0.020	0.006
<u>Dielectric Strength</u> Resistance - megohms Breakdown - 1250 volts  <u>Heat Test-Seconds To Melt 150°F Temp/Inq.</u> 20 w/sq in 15 w/sq in 10 w/sq in	Nitrile Phenolic Adhesive	0.006	0.004	Nitrile Phenolic Adhesive	0.006	0.004	Epoxy Adhesive	0.006	0.004
	Glass Fabric/Phenolic	0.004	0.001	Glass Fabric/Phenolic	0.004	0.001	Glass Fabric/Phenolic	0.004	0.001
	Nitrile Phenolic Adhesive	0.001	0.002	Nitrile Phenolic Adhesive	0.001	0.002	Epoxy Adhesive	0.001	0.002
	Tedlar	0.002	0.001	Stainless Steel	0.002	0.001	Stainless Steel	0.002	0.001
	Nitrile Phenolic Adhesive	0.001	0.005	Glass Fabric/Epoxy	0.001	0.005	Glass Fabric/Epoxy	0.001	0.005
<u>Bond Strength</u> Peel-lbs/in. average Failure Location  Tensile-psi average Failure Location  Shear-psi average Failure Location	Stainless Steel	0.005	0.005	Glass Fabric/Epoxy	0.005	0.005	Glass Fabric/Epoxy	0.005	0.005
	Glass Fabric/Epoxy	0.005	0.005						
	OK - No Breakdown	250		OK - No Breakdown	1000		OK - No Breakdown	800	
	6.4			6.4			6.4		
	7.2			7.2			7.2		
<u>Bond Strength</u> Peel-lbs/in. average Failure Location  Tensile-psi average Failure Location  Shear-psi average Failure Location	13.0			12.5			12.9		
	5			5			19		
	Tedlar to Glass/Phenolic			Stainless Steel to Glass/ Polyimide			Stainless Steel to Glass/ Epoxy		
	2740			1178			2816 Plus*		
	Tedlar to Glass/Phenolic			Stainless Steel to Glass/ Polyimide			Test Block to Glass/Epoxy		
<u>Bond Strength</u> Peel-lbs/in. average Failure Location  Tensile-psi average Failure Location  Shear-psi average Failure Location	2758			803			2718 Plus*		
	Tedlar-Cohesion			Stainless Steel to Glass/ Polyimide			Test Block to Glass/Epoxy		
*Actual strength greater due to failure of test block									

approaches (Figures 68 and 69) were tested. After subjecting these specimens to tension cycling (simulating centrifugal force cycling), fatigue loading (constant amplitude), and moisture tolerance testing, the complete laminate material array was selected for design of flight test blade articles.

The purpose of the tension cycling test is to evaluate the load transfer characteristics and fatigue characteristics of representative heater boot configurations when subjected to centrifugal force loading. The centrifugal force is primarily generated by the erosion shield from the blade rotational speed. This force (load) is transferred from the erosion shield to the basic blade structure through the heater boot interlayers. The load transfer occurs near the blade root where the erosion shield terminates. The test specimen configuration for this test is shown on Figure 68. In order to insure the application of load into the erosion shield representative of the centrifugal force loading, the erosion shield and appropriate filler material extends into the test fixture grip length on one end as shown in Figure 68). Since the centrifugal force loading is a constant value during rotor operation the repeated loading (cyclic fatigue) applied in this test is representative of stop-start-stop type of load application including power-off overspeed. The loading to be applied is based on a centrifugal force stress of 13,500 psi (as exists at R.S. 80 on the UH-1H rotor blade at 324 RPM) in addition to 2,000 psi to cover blade bending loads. With an assumed design life in this system of 5,000 hours and assuming four stop-start cycles per hour, the application of 20,000 cycles is required for one lifetime.

The purpose of the fatigue test was to evaluate the fatigue behavior of representative heater boot configurations when subjected to rotor blade fatigue loadings. The rotor blade fatigue loadings are those due to centrifugal force and blade dynamic moments (chordwise bending and beamwise bending). The test specimen configuration for this test is shown in Figure 69.



ELECTROFORMED NICKEL OR STAINLESS STEEL AND APPROPRIATE FILLER MATERIAL TO EXTEND INTO GRIP LENGTH ON ONE END ONLY

0.020 ELECTROFORMED NICKEL  
OR 0.020 STAINLESS STEEL

SELECTED HEATER LAMINATE

HARDBACK OR SOFTBACK INTERLAYER

0.20 2024-T3 ALUMINUM

HARDBACK OR SOFTBACK INTERLAYER

SELECTED HEATER LAMINATE

0.020 ELECTROFORMED NICKEL  
OR 0.020 STAINLESS STEEL

SECTION A-A

NOTE: ALL DIMENSIONS  
IN INCHES

Figure 68. Tension Cycling Test Specimen.

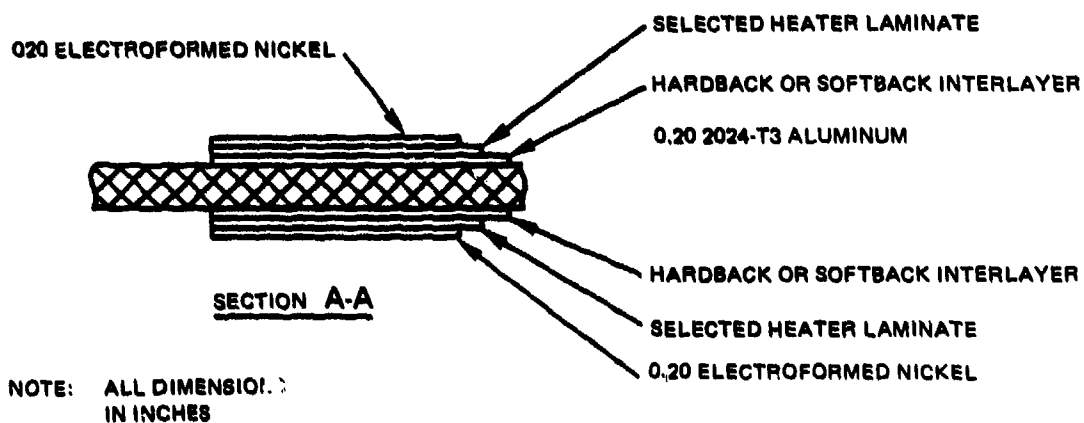
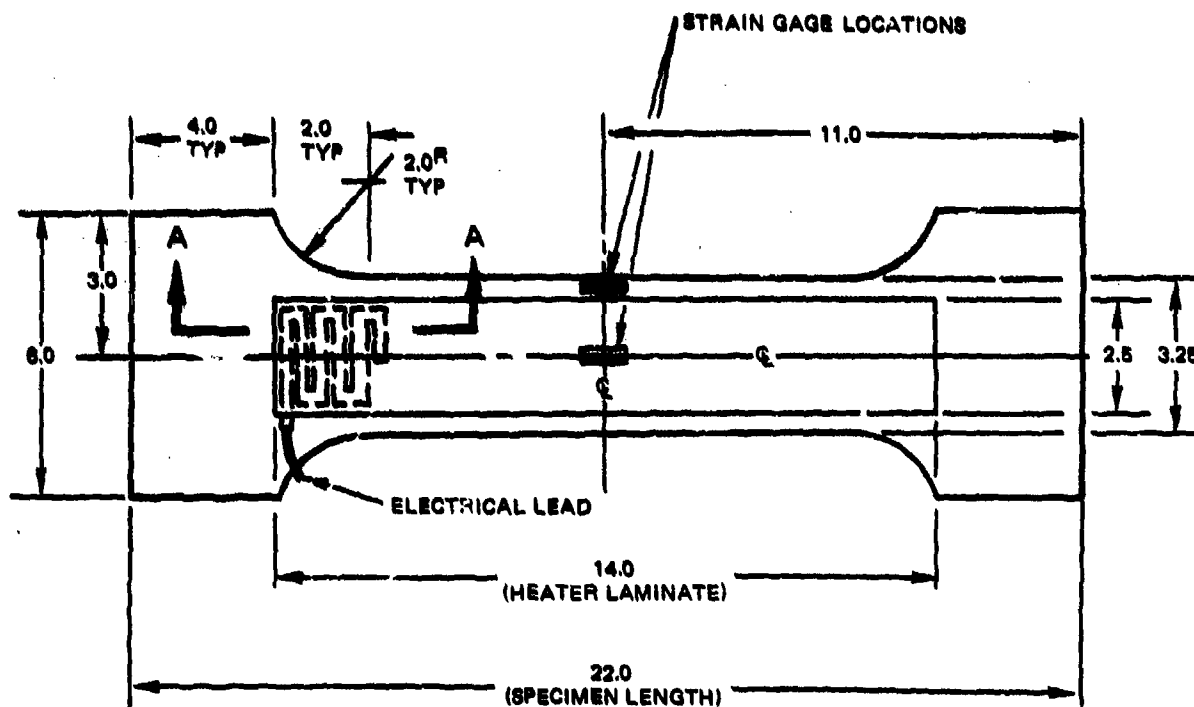


Figure 69. Fatigue Test Specimen.

## 5.2 DEVELOPMENT TEST RESULTS

### 5.2.1 Preliminary Screening

Results of material screening tests are summarized in Table 33.

Examination of these data shows that all configurations are essentially equivalent in dielectric strength. Although there is a considerable difference in the insulation resistance, any value over 10 megohms is considered adequate for this application.

All configurations were also essentially equivalent in heating efficiency as determined by the tempilaq heat test. In bond strength, however, the epoxy system (Configuration No. 3) appeared to be superior since all peel, tensile, and shear test results were higher than for the other configurations.

Based on these results, Material Configuration No. 3 was selected for incorporation in structural test specimens to be evaluated by tension cycling and fatigue tests. During subsequent work in constructing the structural test specimens ("dogbones"), problems were encountered with voids in the adhesive bond line next to the erosion shield. This was attributed to overheating the epoxy adhesive (which has a cure temperature of 250°F) by curing the assembly at 350°F. As a result Configuration No. 3 was modified to substitute nitrile phenolic (350°F cure temperature) for the epoxy adhesive.

### 5.2.2 "Dogbone" Tension Cycling and Fatigue Test

The results of the tension cycling and fatigue tests are given in Tables 34 and 35 for the selected configuration. From the results shown in Tables 34 and 35, the deicer boot configurations tested demonstrated satisfactory fatigue characteristics in that there were no fatigue failures either in the erosion shield material or in the heater laminate. In addition, the test results indicate that the deicer boot (erosion shield) is fully effective in contributing to the overall stiffness of the basic blade and in supporting its share of the load. Continuity of the etched foil heating element was verified throughout

TABLE 34. DEICER BOOT DEVELOPMENT TEST RESULTS

TABLE 34. DEICER BOOT DEVELOPMENT TEST RESULTS						
Specimen No		Shield Material	Loading Range	Reqd No Load Cycles	No of Load Cycles Applied	Comments
Figures 68 & 69			Lb			
TENSION CYCLING	3A*	NICKEL	0-13,000	80,000	80,000	NO FAILURES ↑
	3B	NICKEL	0-13,000	80,000	80,000	
			0-15,700	-	320,000	
	5A*	STAINLESS STEEL	0-13,800	80,000	80,000	↓
			0-17,000	-	250,000	
	5B	STAINLESS STEEL	0-13,800	80,000	80,000	NO FAILURES
**FATIGUE	1A*	NICKEL	11,000 - 14,400	$10^6$	$10^6$	NO FAILURES
	1B	NICKEL	11,000 - 14,400	$10^6$	$10^6$	NO FAILURES
	1C	NICKEL	11,000 - 14,400	$10^6$	$10^6$	NO FAILURES
<p>*ALL 'A' SPECIMENS WERE STRAIN GAGED AS SHOWN IN FIGURES 68 AND 69</p> <p>**10,000 LOAD CYCLES OUT OF EVERY 100,000 LOAD CYCLES WERE APPLIED AT 160° F.</p>						

TABLE 35. HEATER BLANKET STRESS DISTRIBUTION BASED ON STRAIN GAGE MEASUREMENTS

TENSION CYCLING TEST SPECIMEN											
Spec No	Unfield Back- ing Matl	E (Shield Matl)	Load- ing P	*Calc Stress		Measured Strain			**Measured Stress		
				f <sub>Al</sub> (1)	f <sub>Shield</sub> (2)	e <sub>Al</sub> (1)	e <sub>Shield</sub> (2)	e <sub>Shield</sub> (3)	f <sub>Al</sub> (1)	f <sub>Shield</sub> (2)	f <sub>Shield</sub> (3)
		PSI	Lb	PSI		Micro Inches			PSI		
3A	Nickel Hard	29x10 <sup>6</sup>	13,000	13,930	38,610	1,220	1,334	1,120	12,810	38,690	32,500
5A	Stain- less Steel	27x10 <sup>6</sup>	13,800	15,200	39,120	1,435	1,310	960	15,070	38,740	25,920
FATIGUE TEST SPECIMEN											
1A	Nickel Hard	29x10 <sup>6</sup>	14,400	15,480	42,760	1,292	1,428	-	13,560	37,470	-
<p>*CALCULATED STRESS <math>f_{Al} = P/A</math> WHERE A = EQUIV AL AREA = 0.93 IN<sup>2</sup> SPEC 1 &amp; 5 = 0.907 IN<sup>2</sup> SPEC 3</p> <p><math>f_{Shield} = f_{Al} \times \frac{E_{Shield}}{E_{Al}} = 10.5 \times 10^6 \text{ PSI}</math></p> <p>**MEASURED STRESS, F = Ee</p>											



the tests by measuring the electrical resistance of the element through the electrical leads provided on each test specimen. Continuity of the laminate bond within the heater boot configuration was verified throughout the tests by taking both static and dynamic strain gage readings for any indication of load shifting. Additional load cycles were applied to one of the tension cycling test specimens at a loading (centrifugal force) representative of maximum design limit rotor speed (356 rpm, 5 percent above maximum operating speed) to further substantiate the fatigue characteristics of the heater boot configurations. These load cycles were applied to the test specimens after the completion of the required number of load cycles representative of normal rotor speed as shown in Table 34.

The load transfer characteristics and structural effectivity of the heater boot configurations were determined through the use of the strain gages mounted on the test specimens as shown in Figures 68 and 69. The strain gage measurements recorded for each of the specimens strain gaged specimens associated with the tension cycling tests (Specimens 3A and 5A) demonstrated the load transfer characteristics of the heater boot configurations. In these tests, load was also introduced into the heater boot by extending the boot (erosion shield) into the loading grip at one end of the specimen. With this arrangement, the loading was transferred from the shield material to the main body of the specimen through the heater boot laminates (Figure 68). The specimen backing material (epoxy adhesive with a relatively high shear modulus) transferred most of the load in the shield material in the last inch of the heater boot as indicated by Strain gage No. 3 in Table 35. The high shear modulus of the backing material permitted the shield material to be fully effective with the main body of the specimen (aluminum) as demonstrated by the agreement of the calculated stresses with the measured stresses.

The strain gaged specimen associated with the fatigue tests (Specimens 1A) demonstrated the structural effectivity of the nickel erosion shield. In this test, load was applied only to the main body of the test specimen (aluminum), and any load introduced into the heater boot nickel shield was via shear through the heater boot laminates (Figure 69). The nickel erosion shield was fully effective in picking up the test loadings. The results of this test are also applicable to a stainless steel erosion shield since the deicer boot laminates would be the same for each configuration.

#### 5.2.3 Coupon Tests From Rotor Blade

A production sample of an entire UH-1H main rotor blade was then sectioned at various points between Stations 87 and 176 (Figure 70). Coupons in replicate were cut from the root end, center and tip stations. These were tested to determine flatwise tensile strength and shear strength of the weakest ply in the laminate. Results of these tests are given in Tables 36 and 37. Table 36 results indicate that the shear strength in the deicer boot is lowest in the area of copper wire braid conductors at the trailing edge of the boot on upper surface, but there is sufficient strength in the non-braided area to carry all the load even if the strength in the braided area were reduced to zero. Table 37 shows that the flatwise tensile strength of the boot installation is sufficiently high so that stress levels are satisfactory.

In addition to the coupon testing just described on sections of the rotor blade, coupon tests were also conducted on flat samples of the deicer boot laminate made at the same time each of the production parts (3 blades) were made. Both shear and tensile (pull) tests were run. The results of those tests are shown in Table 38.

Fatigue tests were also conducted on coupons cut from a sample production blade. The first of these specimens was subjected to over 40,000 stop-start cycles (6,000-hour life) with no bonding delamination. The load

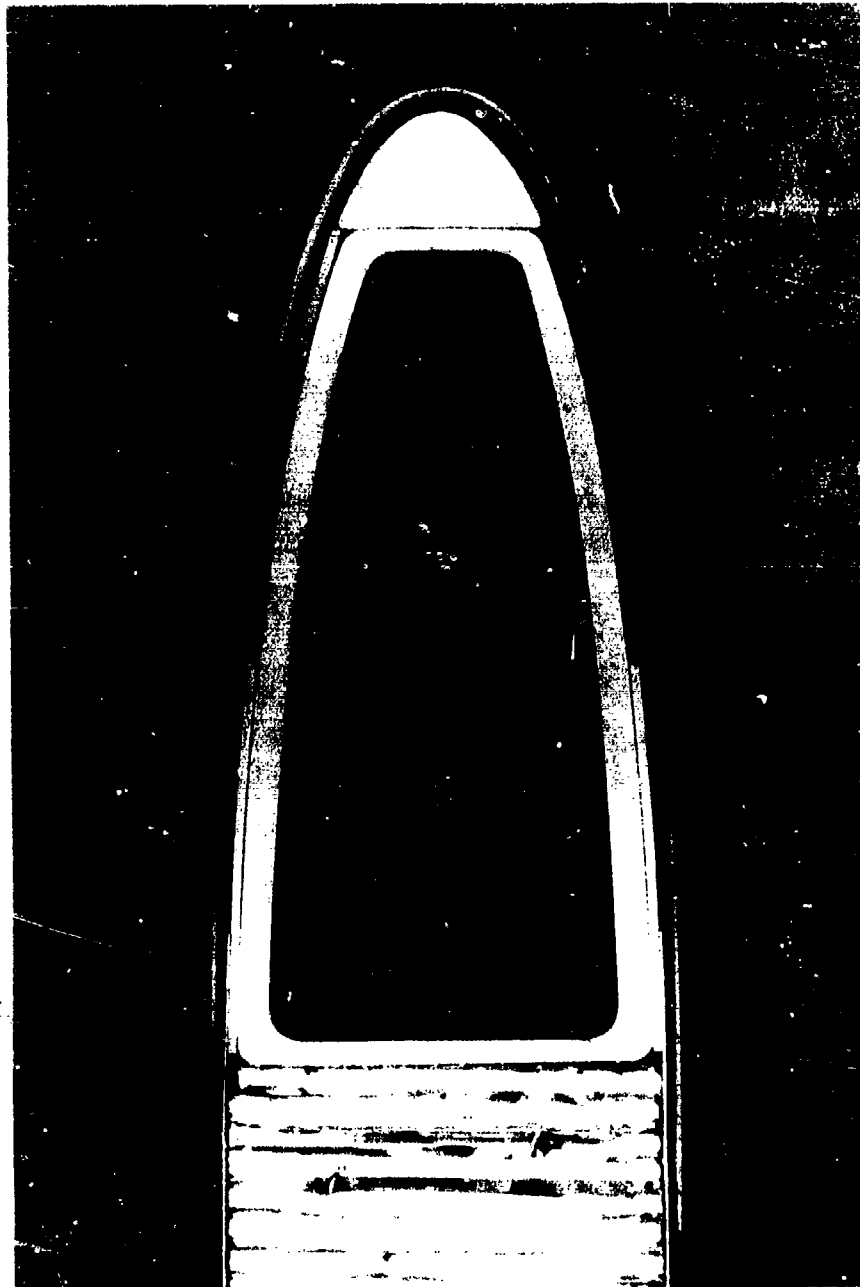


Figure 70. UH-1H Main Rotor Blade Cross Section Showing Installed Deicer Boot.

TABLE 36. SHEAR STRENGTH OF COUPONS CUT FROM MAIN ROTOR TEST BLADE

Blade Location (Sta No)	Shear Strength PSI	Plane of Failure in Laminate
87 - 97	3058	Element to Shield
87 - 97	2874	Element to Shield
87 - 97	2699	Element to Epoxy/Glass
87 - 97	2893	Element to Epoxy/Glass
87 - 97	1709	Conductors to Epoxy/Glass
87 - 97	1740	Conductors to Epoxy/Glass
166 - 176	2450	Boot to Blade
166 - 176	2614	Boot to Blade
166 - 176	2215	Element to Epoxy/Glass
166 - 176	2606	Element to Epoxy/Glass
166 - 176	1270	Conductors to Epoxy/Glass
166 - 176	2474	Conductors to Epoxy/Glass

TABLE 37. FLATWISE TENSILE STRENGTH OF COUPONS CUT FROM MAIN ROTOR TEST BLADE

Blade Location (Sta No)	Flatwise Tensile Strength (PSI)	Type of Failure
105 - 120	>1820	Load Block Bond
87 - 105	>1813	Load Block Bond
140 - 158	>1986	Load Block Bond
105 - 120	>1445	Load Block Bond
105 - 120	>1686	Load Block Bond
140 - 158	>1635	Epoxy/Glass to Epoxy Glass

TABLE 38. ROTOR BLADE DEICER BOOT PRODUCTION COUPON TESTS

Part	Tensile Strength (PSI)	Shear Strength (PSI)
MAIN ROTOR BLADE TEST PART	2,006	3,290
FLIGHT BLADE OUTBOARD SECTION		
S/N #1	2,730	5,000
#2	3,130	4,275
#3	2,555	4,000
INBOARD MAIN ROTOR BLADE		
S/N 002	2,153	3,816
003	2,420	3,405
004	2,460	2,575
TAIL ROTOR BLADE		
S/N #1	2,000	2,620
#2	2,220	3,290
#3	2,140	3,225

applied included centrifugal force load for maximum overspeed power-off rpm, and also a 1.28 factor to provide for the conductor bond area being assumed ineffective. After application of the stop-starts, the specimen was tested to maximum load (max speed Vne at low rpm). The load included the effect of centrifugal force and bending. These loads also included a 1.28 factor. One hundred ninety-eight thousand (198,000) cycles were applied (73 hours of maximum load, conservatively equivalent to 1500 flight hours) with no delamination. The aluminum blade spar failed due to artificially induced bending and a sharp cut.

A second specimen completed 37,000 stop-start cycle and over 2,000,000 cycles of the maximum cyclic loads of the same magnitude and load spectrum as the first specimen with no delamination. The specimen failed in the aluminum spar at the loading grip.

A third specimen was cut from the undamaged end of the first specimen reported above. This specimen was subjected to 65,690 cycles of stop-start load up to 64,000 lb producing 1,570 lb/in. in the 0.030-inch-thick shield with no bonding delamination. Failure took place in the aluminum spar. The load matches the calculated maximum overspeed blade shield loading of 1,570 lb/in. including centrifugal force, bending loads, and also a factor to account for the conductor bond area being assumed ineffective.

#### 5.2.4 Further "Dogbone" Tests

Additional tests were then run on the tension cycling development test specimen (Figure 68). Stop-start loads were increased from 17,000 lb to 21,000 lb for 20,000 cycles and to 25,500 lb for an additional 2,700 cycles. Some delamination then occurred. The increase in load was to cover the change in design erosion shield thickness from 0.020

to 0.030 which had occurred after the initial development tests. The specimen was then used for a delamination rate test. Increased stop-start loads of 27,000 lb and 29,500 lb were applied. The increase in load was to cover the condition where the conductor bond area is failed and assumed ineffective. The average rate of delamination was found to be 1 inch in 3,000 equivalent flight hours of stop-starts. A total of 72,500 cycles of 27,000 lb and with over 6,000 cycles at a maximum of 29,500 lb was applied. The results of the delamination test are shown in Figure 71. The maximum average stress in the first inch of bond for the delamination tests can be determined as follows (Seventy-four percent of the shield load is carried in the first inch.):

At 27,000 lb, load in shield = 1,580 lb per inch

At 29,500 lb, load in shield = 1,730 lb per inch

The average bonding stress for the two loads is:

<u>Load</u> <u>(lb)</u>	<u>Bond</u> <u>Stress</u>
27,000	1,100 psi
29,500	1,300 psi

#### 5.2.5 Bonding Strength Analysis

Strength criteria were then developed to compare with the test results. This was done by an analysis which determined the bond strength requirements along the rotor blade. This analysis determined that the normal bond stress at the blade root (the region of maximum stress) would be 855 psi for normal rotor operating speed (324 rpm) and 920 psi for maximum rotor overspeed (339 rpm). Even assuming that the bond strength in the conductor area were zero, the maximum overspeed stress would be 1,140 psi, which results in a static safety factor of approximately 2 at

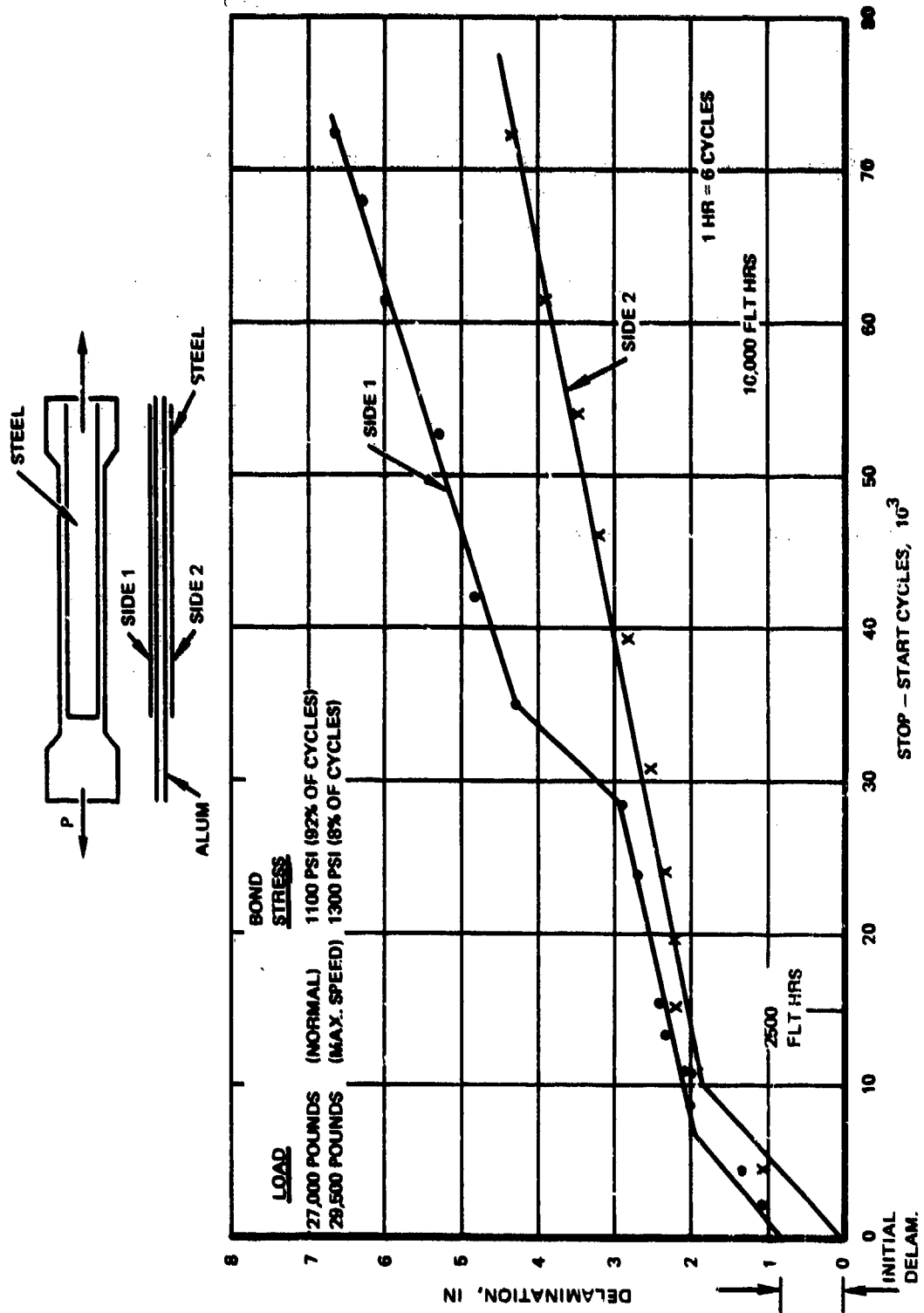


Figure 71. Bond Delamination Progression.

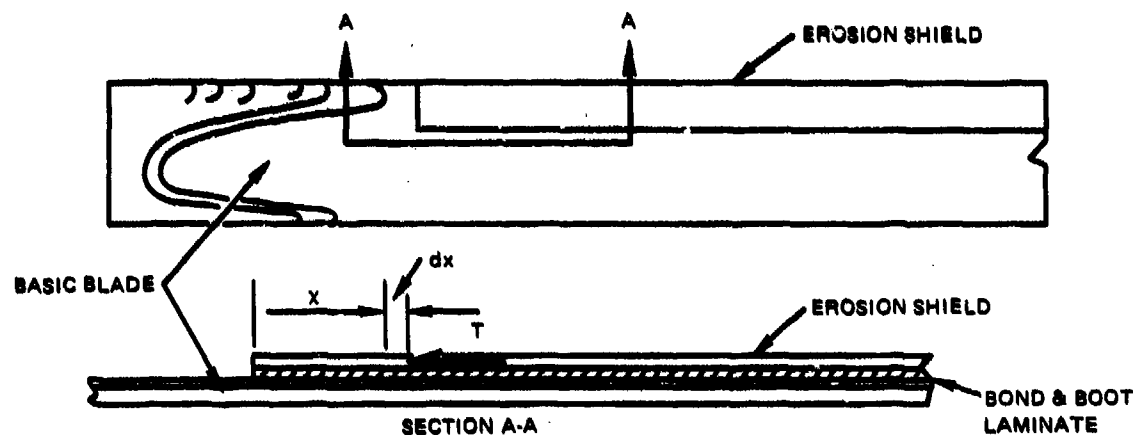


the blade root. The calculated stress of 1,140 psi at overspeed with the conductor area ineffective is below the 1,300 psi applied in the delamination test.

The maximum shear stresses in the erosion shield bonding occur in the inboard end of the shield within the first few inches. The reason for this is that the primary load on the shield is from centrifugal force which builds up from the tip to a maximum at the root. At the point where the shield ends at the blade root, the local bond area must transfer all the shield load to the basic blade, as shown in the analysis to follow. Outboard of this local load transfer area the bond stresses are very low (approximately 6 psi). Here the bond area is large and the only load it receives is the load transfer required to give consistent strains between the basic blade and the erosion shield.

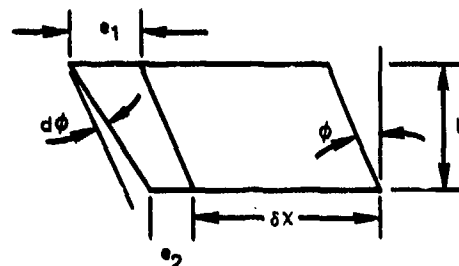
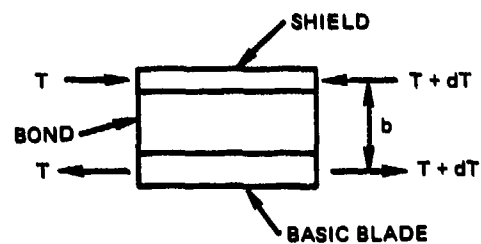
Due to the stiffness of the erosion shield relative to the basic blade, it tries to carry its share of the total blade load in as short a distance as possible. This share of the overall blade centrifugal and bending loads is a direct function of its longitudinal stiffness,  $EA$ , and bending stiffness,  $EI$ , relative to the total stiffness of the basic blade and deicer boot.

While the tension load at the inboard end of the shield must be zero, the distance from the inboard end to the location where the full tension load exists establishes the bonding shear stress. The shorter the distance the smaller the shear area transferring the load, hence the higher the bonding shear stress. This distance is dependent on the shear stiffness of the bond and local structure and the longitudinal stiffness of the shield and basic blade. (The lower the shear stiffness the lower the bonding stress.) This basic shear lag problem can be represented as shown in Figure 72.



LET  $T$  = LOAD (LB) IN SHIELD AT  $x$  FROM THE FREE END.  
 = LOAD GIVEN UP BY BASIC BLADE.

THE EQUILIBRIUM OF THE ELEMENT  $dx$  IS AS FOLLOWS



- $A_1$  = AREA OF SHIELD PER INCH OF WIDTH
- $b$  = THICKNESS OF SHIELD
- $E_1$  = MODULUS OF ELASTICITY OF SHIELD
- $A_2$  = AREA OF BASIC ALUMINUM BLADE PER INCH OF WIDTH
- $E_2$  = MODULUS OF ELASTICITY OF BASIC BLADE
- $e_1$  = LONGITUDINAL STRAIN OF SHIELD
- $e_2$  = LONGITUDINAL STRAIN OF BLADE
- $G$  = SHEAR MODULUS
- $q$  = SHEAR STRESS

Figure 72. Rotor Blade Shear Transfer.

The incremental shear strain  $d\phi$

$$d\phi = \frac{e_1 - e_2}{b}$$

$$e_1 = -\frac{T}{A_1 E_1} \frac{dx}{dx} \quad e_2 = \frac{T}{A_2 E_2} \frac{dx}{dx}$$

$$\frac{d\phi}{dx} = -\frac{T}{b} \left( \frac{1}{A_1 E_1} + \frac{1}{A_2 E_2} \right) \quad (1)$$

Also shear strain  $\phi = \frac{\text{shear stress}}{\text{shear modulus}}$

$$\phi = \frac{q}{Gt} \quad t \text{ in this case is equal to 1 inch}$$

$$\phi = \frac{dT}{dx G} \quad q = \frac{dT}{dx}$$

$$\frac{d\phi}{dx} = \frac{d^2 T}{dx^2 G} \quad (2)$$

equating (1) and (2)

$$\frac{d^2 T}{dx^2 G} = -\frac{T}{b} \left( \frac{1}{A_1 E_1} + \frac{1}{A_2 E_2} \right)$$

$$\text{Set } \frac{G}{b} \left( \frac{1}{A_1 E_1} + \frac{1}{A_2 E_2} \right) = \mu^2$$

$$\text{then } \frac{d^2 T}{dx^2} + \mu^2 T = 0$$

If P equals the end load at some finite distance from the end and if the shield is relatively long, i.e., L is large and the end load  $T = 0$  when  $x = 0$ , then the solution from the equation for buildup of end load is as follows

$$\text{end load in shield} \quad T = P (1 - e^{-\mu x})$$

The shear flow  $q_x = \mu P e^{-\mu x}$

where T equals end load at station x

$$= \frac{G}{b} \left( \frac{1}{A_1 E_1} + \frac{1}{A_2 E_2} \right)^{1/2}$$

With this solution applied to the end of the erosion shield in order to determine end load buildup and bond shear, it is necessary to determine the modulus of the bond laminates and the effective shear depth b. Insofar as the modulus of the bond is very low in the transverse direction, the effective shear depth can be assumed equal to the total bond and filler depth. The buildup of end load was measured during development tests on a dog bone. The results from strain gages No. 2 and 3 (see Table 35) give the load P at some distance from the end and the load T at 1 inch from the end.

The stress measured at gage No. 3 was 960 psi, and the stress measured at gage No. 2 was 1,310 psi.

$$\text{This ratio} = \frac{960}{1,310} = .73 \text{ (also equals the load ratio).}$$

The ratio can be related to the equation

$$T = P (1 - e^{-\mu x})$$

$$(1 - e^{-\mu x}) = .73, \text{ when } x = 1.0$$

thus

$$\mu = 1.3$$

and

$$2 = \frac{G}{b} \left( \frac{1}{A_1 E_1} + \frac{1}{A_2 E_2} \right)$$

On the development tests with the 0.020 inch erosion shield,

$$A_1 E_1 = 2.5 (.020) \times (27) (10^6) = 1.350 (10^6)$$

$$A_2 E_2 = 3.25 \left( \frac{.20}{2} \right) (10^7) = 3.25 (10^6)$$

$$b = \text{bond laminate thickness} = .060 \text{ inch}$$

thus,

$$G = \frac{1.7 \times .060 \times 10^6}{1.04} = 0.098 \times 10^6$$

By using this test value of G, the distribution for the existing shield (0.030 stainless and the increased bond thickness  $b = 0.090$ ) can be determined.

$$T = P (1 - e^{-\mu x})$$

$$\mu^2 = \frac{G}{b} \left( \frac{1}{A_1 E_1} + \frac{1}{A_2 E_2} \right)$$

$$A_1 E_1 = .030 (27) (10^6) = 0.81 (10^6)$$

1-inch width

$$A_2 E_2 = .25 \times 10^7 = 2.5 (10^6)$$

at

$$x = 1 \text{ inch}$$

$$T = 0.74P$$

Since the buildup of end load on the development test shield is essentially the same as for the blade shield (0.74 versus 0.73), they can be compared directly on a basis of total end load in the shield.

The maximum tensile stress in the erosion shield is 38,500 psi.

The load in a 1-inch width would be:

$$\text{Load in shield} = 38,500 (.03) = 1,155 \text{ lb}$$

$$\text{Load in aluminum} = .25 (38,500) \frac{(10^7)}{27 \times 10^6} = 3,565 \text{ lb}$$

$$\text{Total load} = 4,720 \text{ lb}$$

The stress in the bond at the root = .74 (1,155) = 855 psi (324 rpm).

The stress at overspeed (power off 339 rpm) =  $31,800 \left( \frac{339}{324} \right)^2 + 6,700 = 41,500 \text{ psi}$

The stress in the bond at the root (R.S. 83) will be  $41,500 (.030)$   
 $(.74) = 920$  psi.

This is conservative because the oscillatory loads go down as the rpm goes up.

The main rotor deicer has all the conductors in the upper surface towards the trailing edge as shown in Figure 73. There are 12 conductors covering a width of approximately 3 inches. If this area is assumed ineffective, then the load in the shield will be transferred to the non-conductor area. The additional shear deflection in the shield will spread the area over which the shield load is transferred into the aluminum as shown in Figure 74. The dotted line shows the planform effectiveness of the shield, and shear lag analysis shows this line to be at  $40^\circ$ .

The effective width =  $(6.42 - 3.0) + 1 (\tan 40^\circ)$  1 inch from the end =  $3.43 + .84 = 4.27$  inches.

The increase in bond stress if the conductor area were ineffective would be

$$\frac{4.27}{3.03} = 1.24$$

The bonding stress away from the root is very low. Although the maximum acceleration at the tip of the rotor = 925 g's, a 1-inch square of shield would have an inertia force applied =  $.030 (.286)(925) = 7.9$  psi. The total load on the bond between the basic blade and the shield would be approximately 6 psi including the centrifugal force transfer.

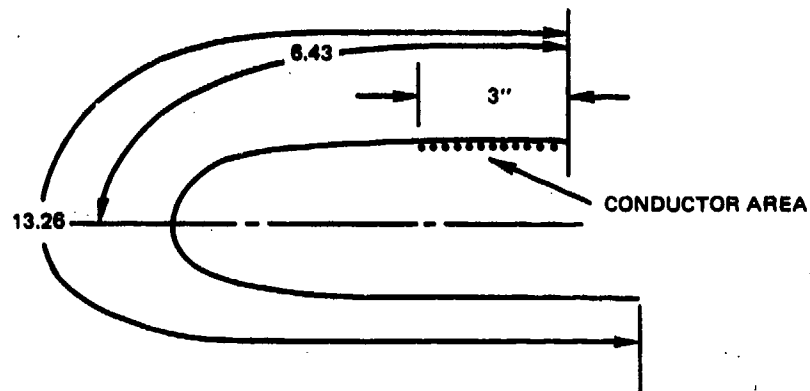


Figure 73. Location of Main Rotor Conductors.

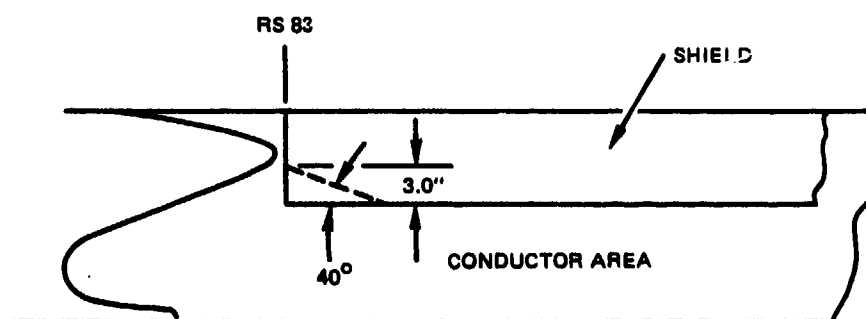


Figure 74. Rotor Blade Shear Transfer Area.



### 5.3 MATERIALS AND PROCESSES

The primary materials selected for construction of heater boots and bonding of boots to rotor blades are listed in Table 39. These materials were selected on the basis of structural static and fatigue tests previously described and/or proven performance in similar applications.

The insulation system selected for use on blades was the hardback configuration described in the previous section. The hardback configuration was selected in preference to the softback based on results of the tension cycling and fatigue tests on "dogbone"-type specimens. Strain measurements made during these tests indicated that more load was transferred into the erosion shield through the hardback configuration. This is desirable to avoid a significant change in dynamic characteristics of the blade caused by addition of the heater boots. The softback design does have some advantages, however, for the root end of the boot and a composite design may, in fact, be optimum.

Although data previously presented on erosion characteristics of erosion shield materials indicated that electroformed nickel was optimum, 301 half-hard stainless steel was selected for the outboard main rotor shield demonstration program. This was done because of cost and schedule considerations. The startup nonrecurring costs for fabricating erosion shields of electroformed nickel for three test rotor blades were judged to be excessive for an experimental program. Electroforming tanks long enough for the blade were not available, and the time required to fabricate these tanks would also have had an unfavorable impact on program schedule. The clad 7075TC aluminum was selected for inboard rotor erosion shields since erosion is negligible in this area, and the material is readily formable.

Electroformed nickel was selected for tail rotor erosion shields since this material is preferred. In this case, cost was not a significant factor in selection because of the small size of hardware involved.

TABLE 39. MATERIAL CONFIGURATION SELECTIONS

BASIS: TEST AND/OR PROVEN PERFORMANCE

Heater Installation Component	Selection
Erosion Shield	<p>Main Rotor Outboard - 0.030 Inch 301-1/2 Stainless Steel</p> <p>Main Rotor Inboard - 0.016 Inch 7075T6 Clad Aluminum</p> <p>Tail Rotor - Electroformed Nickel Tapered 0.030 - 0.010 Inch</p>
Adhesive	0.005 Inch Nitrile Phenolic Film Adhesive
Insulation	0.005 Inch Glass Fabric/Epoxy
Heating Element	0.005 Inch 301 Stainless Steel
Insulation	0.040 Inch Glass Fabric/Epoxy (8 Plies Fabric, 0.005 Thick)
Conductors	0.025 x 0.120 Inch Copper Wire Braid
Adhesive	0.010 Inch AF126 Film Adhesive
Blade Cavity Filler	0.010 Inch Style 181 Glass Fabric/Epoxy
Adhesive	0.010 Inch AF126 Film Adhesive

The adhesive used for bonding the heater boot to the actual flight blades was AF126 instead of the FM137, which was used for bonding simulated boots to aluminum in previous development tests (Figures 68 and 69). These adhesives both cure at 250° F and performance properties are essentially equivalent. The AF126 adhesive was selected for use in actual hardware to obtain a higher quality bond under production conditions and a pressure constraint of 35 psi maximum on the blades. The AF126 has more flow than the FM137 under these conditions, and this normally can be expected to result in a more void-free bondline between mating parts where some mismatch exists. In addition, the AF126 adhesive is currently used for bonding standard erosion shields to blades during overhaul (with good service history) in accordance with Reference 24. This reference is also followed with respect to preparing surfaces of the "D" spar for bonding. This entails leaving the FM1000 adhesive intact on surfaces to which the standard erosion shield was originally bonded.

In order to develop and prove detail tooling, fabrication processes, and quality control procedures, one complete heater boot installation on a scrap main rotor blade was fabricated and evaluated by nondestructive and destructive testing. This work was done prior to fabricating three flight test blade assemblies required for the flight test program described in Volume II. The procedure which was developed for fabrication of heater boots and installing them on rotor blades is described below. Methods and tooling used for each operation are discussed, together with in-process controls of critical operations employed to assure quality.

## 1. Manufacturing Plan

The fabrication methods, process, and manufacturing sequence developed for all heater-boot installations can be summarized as:

### A. Fabrication of Heater Boots

- (1) Form erosion shield of applicable material.
- (2) Bond stainless steel (for elements) to glass/epoxy (350° F, 100 psi).
- (3) Etch element pattern (photo chemical process).
- (4) Bond element and conductors to erosion shield (strong back tool - 350° F, 100 psi).
- (5) Laminate eight plies glass/epoxy to erosion shields (350° F, 90 psi).

### B. Preparation of Rotor Blades

- (1) Remove existing erosion shields.
- (2) Fill erosion shield cavity - laminated glass/epoxy and adhesive) special tool - 250° F, 35 psi).
- (3) Fill doubler area with epoxy and fair to match boot.

### C. Bonding of Boots to Blades

- (1) Perform "verifilm" check.
- (2) Lay up adhesive film on blade.
- (3) Mate boot and bond in special tool (250° F, 35 psi).

## 2. Master Templates

One of the primary problems in bonding heater boots to rotor blades is contour dimensional control of fabricated heater boots. This is required to assure mating of the boot with blade surfaces to which it is bonded. Improper mating could result in

excessively thick or thin adhesive bondline and/or voids. Therefore, master templates for main and tail rotor blade leading-edge airfoil surfaces were fabricated to serve as a common dimensional reference for forming erosion shields, preparation of blade surfaces, and for all laminating and bonding tools.

Master templates for main and tail rotor blade constant section leading edges were developed and fabricated based on loft contour data. Templates for leading edges of the inboard section of the main rotor blade (in blade doubler area) were developed from a blade model (with faired doublers) at three stations to provide dimensional control of inboard heater boots and installation in this area (Station 24.5 - 83.0). These master templates were used for dimensional control of all forming, laminating, and bonding tooling in the program.

### 3. Forming of Erosion Shields

#### A. Main Rotor Outboard

This shield was formed of .030 inch 301-1/2 hard stainless steel. It was formed by a process combining brake and stretch forming. The leading edge radius was formed over a die in a power brake. Contour forming was accomplished by stretch forming over a form block. Final straightening was done by stretching in a spanwise direction.

#### B. Main Rotor Inboard

This shield was formed from .016 inch 2024T3 clad aluminum sheet by roll forming in sheet metal rolls.

#### C. Tail Rotor

Tail rotor shields were constructed of electroformed nickel. This process consisted of electrodepositing nickel from a chemical bath on a form block having a conductive surface. Control of tapered thickness (0.030 inch at leading edge to 0.010 inch at trailing edge) was achieved by strategic placement of electrodes relative to the part in conjunction with suitable current density in the plating bath.

#### 4. Fabrication of Heater Elements

Heater elements were fabricated by a previously developed proprietary process essentially as follows:

- A. Bond 0.005 inch 302 stainless steel foil to cured glass/epoxy sheet 0.005 inch thick with nitrile phenolic adhesive. In this process, the stainless steel must be carefully cleaned and etched prior to bonding. Bonding is done in an autoclave at 350° F, 100 psi. Peel test coupons are fabricated simultaneously for process control.
- B. The required element pattern is then etched in the stainless steel by selective masking of element ribbons with a photo-resist coating in a chemical bath. The photo-resist coating is then removed and element ribbons are carefully inspected by optical means for evidence of any burrs or spurs which might penetrate the thin insulation layer between element and erosion shield during later pressure bonding operations.

#### 5. Fabrication of Heater Boot Assemblies

Fabrication operations and controls used for all heater boots are:

- A. Prepare erosion shields for bonding by cleaning and etching in chemical baths appropriate for the material involved (i.e., stainless steel, nickel, and aluminum).
- B. Brake-form leading edge radius of heating elements to match radius of erosion shields.
- C. Lay up heating elements in erosion shields using a nitrile phenolic film adhesive (0.005 inch thick). This is done under clean room conditions to avoid contamination with any foreign material such as dust, oil, metal particles, etc.
- D. The heating element is then bonded to the erosion shield in an autoclave at 350° F and 100 psi. A "strongback" tool is employed which applies mechanical pressure at the zero-percent line of the leading edge to assure mating of heater element and erosion shield before autoclave bag pressure is applied.

- E. Make soldered connections of braided copper wire conductors to heating elements and adhesively bond conductors to glass fabric/epoxy backing adjacent to heater elements. Conductors must be properly spaced and located.
- F. Laminate eight plies of prepreg glass fabric/epoxy (0.005 inch per ply) over heating elements inside of erosion shield. In the area of braided wire conductors at aft edge of heater boots, three plies of glass/epoxy were used as backing because of conductor thickness (0.025 inch) equivalent to five plies of glass over heating elements. This is necessary to maintain a smooth inside contour for mating with rotor blades. This operation was accomplished by laying up the glass/epoxy on a glass-fabric-reinforced plastic male tool. The laminate was then preformed, densified, and "tacked" to the erosion shield assembly by placing the erosion shield/element assembly over the glass laminate on the tool. A vacuum bag was placed over the assembly and vacuum pressure was applied at room temperature for several hours. The uncured assembly was then transferred from the male mold to the "strongback" tool previously used for bonding heating elements to the erosion shield. Mechanical pressure was again applied at the zero-percent line leading edge. A pressure bag was then installed and the assembly placed in an autoclave and cured at 350° F and 90 psi pressure. Suitable bleeding techniques were employed to assure removal of air resulting in a laminate essentially void-free. All cure cycles including time, temperature, and pressure were monitored and recorded by means of suitable instrumentation.
- G. Process control samples were processed along with parts through all fabrication stages. Shear and tensile tests were then performed on coupons made from these samples (Table 38).
- H. Inspection of completed heater boots and in-process inspection, in addition to normal dimensional checks, included the following:
- (1) Visual inspection of entire inner surface for evidence of any excessive voids in the laminate. Since the glass/epoxy insulation laminate is translucent, any gross voids are readily apparent.

- (2) The dielectric strength of insulation between the heating element and erosion shield was made at the assembly stage when elements were bonded to shields. Thereafter, only resistance of the insulation between elements and shields was determined by repeated medium voltage tests. In the dielectric strength test, no breakdown is permitted when insulation is subjected to 1,200 volts ac, 60 Hz for 1 minute. In the resistance test, minimum permitted insulation resistance is 3 megohms (actual values ran as high as 200 megohms). The resistance of heater elements is also checked immediately after elements are fabricated to meet established limits for each element.
- (3) Completed heater boots were (coin) tap tested to detect any gross voids between the heater element and the erosion shield which are not discernible by visual means.
- (4) The final acceptance test for heater boot assemblies consisted of a heating efficiency test. In this test, a "Tempilaq" coating which melts at 150° F is applied to all exterior surfaces of heater boot erosion shields. Heater element segments are then energized and the time to completely melt the coating is recorded. Hot spots are indicated by fast melting and cold spots by slow melting. Acceptance requirements specify a maximum time for complete melting with no evidence of excessively hot or cold spots. Excessively cold spots usually indicate voids in the bond line between the heating element and the erosion shield. Hot spots indicate thin spots in insulation or local high resistance in heater elements.

The completed main rotor heater boot assembly is shown in Figure 75.

#### 6. Preparation of Rotor Blades for Installation of Heater Boots

Prior to installation of heater boots, a considerable amount of work was required to modify balance weights, remove existing erosion shields, and apply fairing compound in the inboard



doubler area. All blade modifications were done in accordance with standard Army Depot Maintenance and Repair Documents<sup>(24)</sup> and<sup>(25)</sup> where applicable requirements exist. These tasks consist of:

- A. Removing balance weights.
- B. Removing existing erosion shields by peeling off strips with a special tool which operates on the principle of a large sanding can opener (most of the old FM-1000 adhesive remains adhered to the blade spar after this operation).
- C. Lightly sanding the old adhesive surface. The whole surface is then cleaned with methyl-ethyl-ketone, and any bare metal spots are coated with an adhesive primer (Minnesota Mining EC2320 or equivalent). Any cavities are filled with epoxy putty and sanded smooth.
- D. Filling in the leading-edge cavity (approximately 0.020 inch deep) formerly occupied by the erosion shield with one ply of epoxy film adhesive and one ply of glass fabric/epoxy prepreg. A caul sheet\* is then placed over the layup with suitable bleeder and parting film in place. Then the blade is placed in a special bonding tool (Figure 76) and the adhesive-prepreg laminate cured and bonded to the blade at 250° F and 30 psi for 90 minutes (plus heatup and cool-down to 160° F).
- E. Lightly sanding the glass fabric/epoxy surface on the blade leading edge after curing in order to match the contour check templates (Figure 77).
- F. Smoothly fairing the leading edge of the inboard doubler area of the main rotor blade (Sta 245 - 83.0) by filling with epoxy compound and sanding the surface to match contour templates.

(24) Army Document DMWR 55-1560-198 "Depot Maintenance Work Requirements for Main Rotor Blade," 15 March 1971.

(25) Army Document DMWR 55-1560-200 "Depot Maintenance Work Requirements for Tail Rotor Blade," 1 December 1965.

\* A caul sheet is a piece of carefully formed sheet metal placed next to the laminate but under the pressure bag. Its purpose is to maintain a smooth surface during cure.



Figure 75. Main Rotor Blade Deicer Blanket.

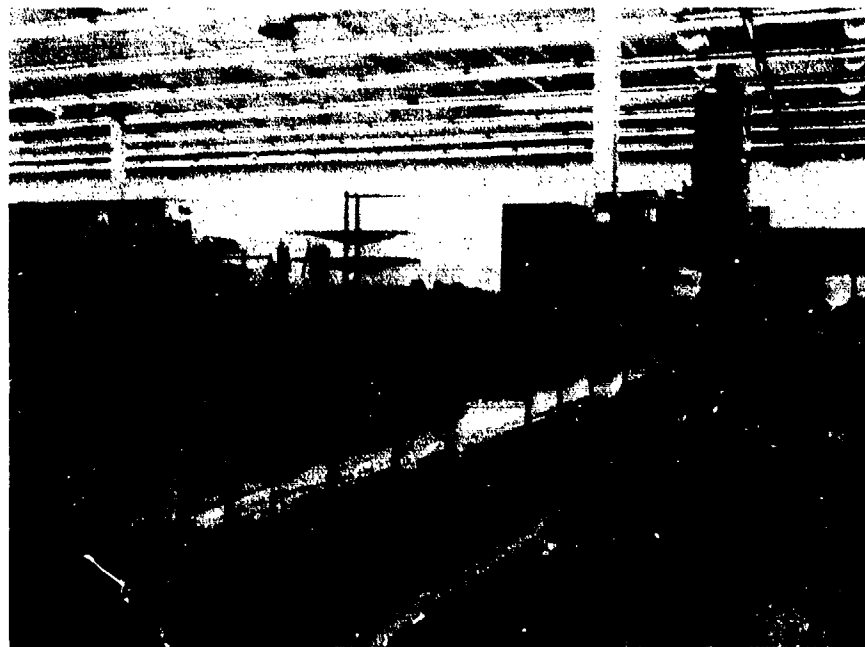


Figure 76. Main Rotor Deicer Bonding Tool.

- G. Removing fixed tip weight at Sta 275.0 - 280.0 on the main rotor blade by cutting holes in the blade, prying out the weight, and then repairing by replacing core and skin with adhesive bonded patches (Figure 78).
- H. Removing 20 inches of the brass nose block weight on the main rotor blade just inboard of the blade tip and replacing with an aluminum piece having the same cross section. This weight is bonded in place at the same time the glass/epoxy and adhesive filling the erosion shield cavity is cured in the bonding tool (Figure 78). The change in balance bar material is made in order to minimize the change in blade dynamic response due to the additional weight of the heater boots.

#### 7. Bonding of Heater Boots on Blades

- A. After the blade surface is prepared to receive the heater boot, a "verifilm" check is made to determine that mating of the boot with the leading edge of the blade is within required dimensional tolerances to achieve an acceptable bond. In this check, epoxy adhesive film representative of the material to be used for final bonding is sandwiched between two plies of Teflon film 2 mils thick. This sandwich film is then laid in place between the blade and the boot. The assembly is then placed in the bonding tool and a complete cure cycle is simulated using 250° F and 30 psi for 90 minutes. The cured adhesive/Teflon sandwich is then removed, and thickness measurements of the film are made at periodic intervals in a spanwise direction. Any required corrections to blade contour are then made to maintain a bondline thickness of 0.010 to 0.020 inch.
- B. After the "verifilm" check, a surface peel ply of nylon fabric is removed from the heater boot. The blade surface is solvent cleaned and adhesive film is laid in place. The boot is then placed on the blade, and the assembly is placed in the bonding tool using application of mechanical pressure (prior to the application of bagging pressure) to assure mating at the leading-edge radius. Bonding is done at 250° F and 30 psi for 90 minutes. Time, temperatures and pressures are monitored and recorded by suitable instrumentation.

To provide assurance that adequate strength of the heater boot bonding could be obtained in finished assemblies, several nondestructive test methods were evaluated to detect voids in the bondline.



Figure 77. Blade Contour Check With Template.

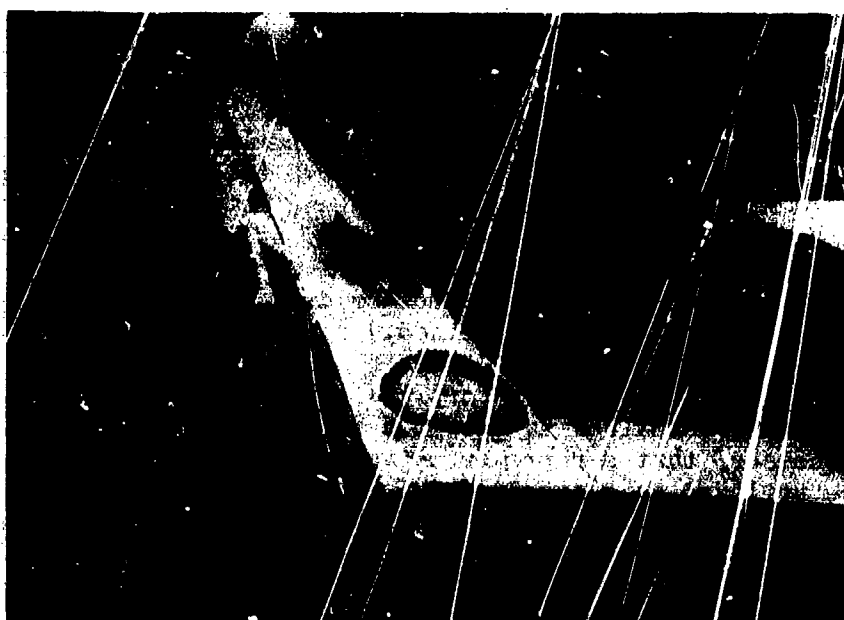


Figure 78. Main Rotor Blade Balance Weight, Rework.

Three methods have been considered which are listed and described below in order of increasing sensitivity:

1. Hand Tapping

This method consists of tapping bonded surfaces with a suitable tool such as a coin or small plastic hammer. A trained inspector can detect voids by a variation in sound detected by the human ear.

2. "Contact" Ultrasonic (Pulse Echo)

Contact ultrasonic inspection is a procedure that requires hand placement of the transducer (ultrasonic energy emitting element) in intimate contact with the part being inspected. Since ultrasonic energy is readily dispersed in air, it is necessary to "couple" (contain) the sound by use of light oil between the transducer and the part. It is necessary to move the transducer by hand from point to point, because the area being inspected at any one contact point is the area immediately under the transducer and is restricted by the size of the transducer, which is usually 1/2 to 1 inch in diameter.

3. "Through-transmission" Ultrasonic

"Through-transmission," as referred to herein, is a procedure that requires at least two transducers. One is placed on one side of the part to emit sonic energy, and the other is placed on the opposite side of the part to receive the transmitted energy. Evaluation of the bond line/lines is usually a function of energy absorption in the bond line. Comparison is made with energy response from known (purposely produced) discontinuities which have been manufactured for this purpose. This method is usually accomplished by immersing the part being inspected in water. (Care must be exercised to prevent water from entering the blade or deicer installation, as this is a problem with this method.)

In order to properly interpret indications of abnormal structure or bond lines as detected by these methods, it is necessary that a representative part incorporating known flaws be utilized as a standard. In this program a UH-1H main rotor test blade was constructed which incorporated known voids (Teflon disks) of various sizes, locations and depths, in the deicer boot laminate. This section of blade was inspected by using the three methods described above with the objective of detecting all known voids. Variations in the ultrasonic

methods such as energy frequency and intensity were explored to determine best techniques. The known voids were detected by the "through-transmission" method, and calibration standards were established for machine settings. After tests on the standard part were completed, all flight rotor blades were inspected by the "through-transmission" method ("C" scan) to determine extent and location of detectable flaws (Figure 79). No significant flaws were detected. It should be noted that the area around the copper braid conductors on upper blade surface was detected as showing "voids" which are inherent on the copper braid and as previously discussed do not present a problem.

#### 5.3.1 Nondestructive Test Methods - Conclusions and Recommendations

Analysis of results of the limited nondestructive testing trials performed in this program leads to the following conclusions:

1. The hand tapping method is capable of detecting voids in deicer boot laminates if there is a substantial air gap such as exists in the majority of real voids. "Tight" voids with no air gap such as implanted Teflon disks used in the test blade are not readily detectable by hand tapping. It was established that "real" voids near the exterior surface of the boot can be readily detected, provided they are not too small. Minimum detectable size in relation to depth below the surface was not established in this program since the tapping method was not sensitive enough to pick up implanted Teflon disks in the test blade. "Real" voids in "dogbone" test specimens were detectable at maximum depth. These were approximately 1 inch in diameter. "Real" voids exposed by destructive sectioning near the surface of the boot on the test blade were detected by hand tapping.
2. The ultrasonic pulse-echo equipment that was used to scan the test blade was judged to be comparable to hand tapping in effectiveness. This equipment could not detect implanted voids but did detect "real" voids near the surface of the deicer boot as evidenced by destructive sectioning.
3. The "C" Scan, "through-transmission" method done with the blade submerged in water was found to be very effective. Using this method, implanted Teflon disks down to 1 inch in diameter were detected at all depths in the boot laminate. "Real" voids were also detected including porosity.

Reproduced from  
best available copy.



Figure 79. "C" Scan Test Signature.

It is recommended that deicer boot installations be ultrasonically inspected by using the "C" Scan, "through-transmission" system as part of a production process. Since the normal "C" Scan "through-transmission" equipment is not portable, its use would be restricted to factory or depot repair operations. Therefore, a "through-transmission" ultrasonic inspection method utilizing contact scanning crystals needs to be investigated since this equipment would be portable.



## SECTION 6

### PROGRAM CONCLUSIONS AND RECOMMENDATIONS

This section is a brief overview of the technology phase of this contract. The conclusions and recommendations resulting from the flight test program are contained in Volume II.

With respect to meteorological design criteria and systems technology (Volume I), the following conclusions and recommendations are made:

1. For supercooled water droplets - which represent the normal icing situation, it is recommended that aircraft with all weather missions be designed to operate under meteorological conditions contained in the existing military specification (Mil-E-38453) except that the minimum design temperature should be  $-20^{\circ}\text{C}$  ( $-4^{\circ}\text{F}$ ) instead of  $-30^{\circ}\text{C}$  ( $-22^{\circ}\text{F}$ ) because of the lower altitudes (below 10,000 feet) at which helicopters normally operate. The volume median diameter of supercooled droplets encompasses the range of 10-40 microns. In this range, ice accretion is limited to the leading edge area of rotor blades and other aerodynamic surfaces (to approximately 20 percent chord), windshields, and the nose region of the fuselage.
2. Airframe components requiring protection against supercooled droplets include the windshield, the rotor system (main and tail blades), and pitot systems.
3. Flush engine inlets may not require protection, but insufficient flight experience under prolonged exposure to moderate or heavy icing exists to establish a final conclusion. Full ram scoops will require ice protection, as will all engines.
4. Freezing rain encompasses supercooled water droplet diameter in the hundreds of microns (to approximately 1200 microns), but liquid water content in the atmosphere is low. It primarily occurs at temperatures just below freezing and has not been observed at temperatures below  $-10^{\circ}\text{C}$  ( $14^{\circ}\text{F}$ ). Ice accretion with these large droplets extends over a much larger area of the helicopter, impinging over 2 - 5 times more of the rotor blade chord than the small droplets, and also covering the entire frontal area of the fuselage. For these reasons, protection against freezing rain imposes weight, performance, and cost penalties which are unacceptable. In addition, severe freezing rain, which would represent the critical aircraft safety problem, occurs very infrequently (perhaps one storm in 10 years).

5. Snow has not been found to be an operational problem with a properly designed aircraft. If care is not taken, however, snow in engine inlets can melt and then refreeze and become an engine FOD problem.
6. Electric heat is recommended for windshield anti-icing, and recommended energy levels are provided.
7. Electrothermal cyclic deicing is very effective for main and tail rotor blade protection, with a typical protected area being 10% of chord on the upper surface and 25% of chord on the lower surface. Protection of the entire rotor span is recommended.
8. An electroformed nickel erosion shield, tapered from 0.030 inches at the leading edge to 0.010 inches at the aft edge is recommended for best erosion protection and minimum weight; and an etched foil heating element design is recommended for best thermal efficiency, long life, and repairability.
9. Electrothermal cyclic deicing is compatible with both all-metal and composite blade designs, and can be easily retrofitted onto existing blades. Careful control of assembly procedures, tooling, and proper bonding materials are mandatory to assure a rotor blade of reliable quality. The rotor blade deicer is, in fact, the key technology component in the development of an advanced rotor blade deicing system.
10. A hybrid solid-state/electromechanical timer control/power distribution system has been found to provide a light-weight and flexible design. Full protection and cockpit warning can be provided for open circuits, short circuits, phase unbalance and timer malfunction.

## SECTION 7

### REFERENCES

1. Werner, J. B., ICE PROTECTION INVESTIGATION FOR ADVANCED ROTARY-WING AIRCRAFT, Lockheed-California Company USAAMRDL Technical Report 73-38, Eustis Directorate, US Army Air Mobility Research and Development Laboratory, Fort Eustis, Virginia, August 1973, AD 769062.
2. Bennett, I., GLAZE, ITS METEOROLOGY AND CLIMATOLOGY, GEOGRAPHICAL DISTRIBUTION, AND ECONOMIC EFFECTS, Technical Report EP-105, US Army Quartermaster Research and Engineering Center, Natick, Massachusetts, March 1959.
3. Byers, H. R., GENERAL METEOROLOGY, McGraw-Hill, New York, New York, 1944.
4. Federal Aviation Regulation Part 25: AIRWORTHINESS STANDARDS; Transport Category Airplane Appendix C
5. MIL-E-38453 (USAF) Amendment 1, ENVIRONMENTAL CONTROL, ENVIRONMENTAL PROTECTION, AND ENGINE BLEED AIR SYSTEMS, AIRCRAFT AND AIRCRAFT LAUNCHED MISSILES, GENERAL SPECIFICATION FOR dated 4 May 1967.
6. ARMY AVIATION - GENERAL PROVISIONS, AR 70-38 (Army Regulations), 12 September 1969.
7. Marshall, J. S. and Palmer, W., THE DISTRIBUTION OF RAINDROPS WITH SIZE, J. Meteor., 1948, pp. 165 - 166.
8. Sekhon, R. S. and Srivastava, R. C., SNOW SIZE SPECTRA AND RADAR REFLECTIVITY, J. Atmos. Sci., 27, March 1970, pp. 299 - 307.
9. Lewis, W. and Perkins, P. J., A FLIGHT EVALUATION AND ANALYSIS OF THE EFFECT OF ICING CONDITIONS ON THE ZPG-2 AIRSHIP, NACA Technical Note 4220, Washington, D. C., April 1958.
10. Anonymous: HYDROMETEOROLOGICAL LOG OF THE CENTRAL SIERRA SNOW LABORATORY, Department of Army, Corps of Engineers, 1946-47 to 1951-52.
11. Riordan, P., EXTREME 24-HOUR SNOWFALLS IN THE UNITED STATES: ACCUMULATION, DISTRIBUTION, AND FREQUENCY, Special Report ETL-SR-73-4, US Army Engineers Topographic Laboratories, Fort Belvoir, Virginia, January 1973.
12. Lewis, W. and Bergrun, R., A PROBABILITY ANALYSIS OF THE METEOROLOGICAL FACTORS CONDUCIVE TO AIRCRAFT ICING IN THE US, NACA Technical Note 2738, Washington, D. C., July 1952.

13. Schmitt, George F., Jr., RAIN EROSION BEHAVIOR OF GRAPHITE AND BORON FIBER REINFORCED EPOXY COMPOSITE MATERIALS, AFML-TR-70-316, March 1971.
14. Lapp, R. R., et al., A STUDY OF THE RAIN EROSION OF PLASTICS AND METALS, WADC-TR-185, Part II, May 1955.
15. Weaver, James H., ELECTRODEPOSITED NICKEL COATINGS FOR EROSION PROTECTION, AFML-TR-70-11, July 1970.
16. Weaver, J. H., ELECTROPLATED NICKEL RAIN EROSION RESISTANT COATING, AFML-TR-67-356, January 1968.
17. U. S. Army Report TC REC-TR-62-111, HELICOPTER ROTOR BLADE EROSION PROTECTIVE MATERIALS, December 1968.
18. Morris, J. S. and Wahl, N. J., SUPERSONIC RAIN AND SAND EROSION RESEARCH: EROSION CHARACTERISTICS OF AEROSPACE MATERIALS, AFML-TR-70-265, November 1970.
19. J. R. Garrison, "Load Level Test of UH-1D Helicopter in 48 Foot Diameter Main Rotor Configuration" Bell Report 205-099-049, April 27, 1964, Volumes I-IV.
20. J. R. Garrison, "Structural Demonstration of 48 Foot Diameter Rotor on a UH-1D Helicopter" Bell Report 205-099-058, May 13, 1964, Volumes I-IV.
21. Berry, R. E. and Pardee, J., EVALUATION OF ICING RATE SYSTEMS ON THE SH-3D HELICOPTER, THIRD REPORT (FINAL), Naval Air Test Center Report No. ST-41R-69, 8 July 1969.
22. Van Wyckhouse, J. F., CHEMICAL ICE PROTECTION FOR HELICOPTER ROTORS AND A COMPARISON WITH THE ELECTRO-THERMAL SYSTEM, from Proceedings of the American Helicopter Society 18th Annual National Forum, Washington, D. C., May 1962.
23. Bowden, D. T., EFFECT OF PNEUMATIC DE-ICERS AND ICE FORMATIONS ON AERODYNAMIC CHARACTERISTICS OF AN AIRFOIL, NACA TN-3564, February 1956.
24. Army Document DMWR 55-1560-198 "Depot Maintenance Work Requirements for Main Rotor Blade," 15 March 1971.
25. Army Document DMWR 55-1560-200 "Depot Maintenance Work Requirements for Tail Rotor Blade," 1 December 1965.